Gravity Surveying, Potential-field Modeling, and Structural Mapping and Analysis of the Howley Basin, western Newfoundland

By

Linden Ernst

A Thesis submitted to the school of Graduate Studies

in partial fulfilment of the requirements for the degree of

Master of Science

Department of Earth Sciences

Memorial University of Newfoundland

2018

Abstract

The northeast trending Cabot Fault transects western Newfoundland. Early Carboniferous, possibly late Devonian, activation and continued strike-slip movement throughout the late Paleozoic has led to the deposition of non-marine, fluvial and lacustrine facies, in an isolated sedimentary basin in western Newfoundland, the Deer Lake Basin. The Howley Basin is the northeast depocenter within the Deer Lake Basin. It is separated from the Humber Basin depocenter to the west by a northeast trending, elongated ridge of inverted older Carboniferous sedimentary units.

Active oil seeps, bitumen in shallow drill core, organic rich lacustrine shales and mudstones, porous sandstones, and a large negative gravity signal over the Howley Basin make it an attractive hydrocarbon exploration target. Poor exposure, limited shallow drilling along the margins, and a lack of high-resolution geophysics leaves much of the Howley Basin's internal stratigraphy and structure unknown. Integration of potential-field geophysics and detailed structural mapping and analysis is used to asses the Howley Basin's structure and hydrocarbon potential.

A large lake overlies most of the Howley Basin. Full coverage of gravity surveying required acquisition of gravity stations over the lake. A Ground Penetrating Radar was used in conjunction with the gravity survey to determine the bathymetry of the lake and was used to remove the anomalous mass of the water column in the complete Bouguer gravity anomaly. Gravity data collected in this study was combined with reprocessed pre-existing gravity datasets. A high-resolution aeromagnetic survey and the gravity data was used to model the Howley Basin. Interpretations show that the basin

forms an asymmetric half-graben deepening to the east, reaching a depth of 4.3 km, well into the predicted oil window.

Structural mapping of the Howley Basin revealed that the basin has been affected by episodes of transtension and transpression throughout the Carboniferous and likely continuing into the Permian. Hydrocarbon maturation is predicted to have peaked in the late Pennsylvanian to early Permian. Late-stage transpressional inversion of the Howley Basin is interpreted to have been focused on its margins, potentially creating large wavelength structural traps in the center of the basin.

Acknowledgements

I would like to acknowledge NALCOR Energy and the Petroleum Exploration Enhancement Project for providing the funding for this project. Many of the fine Faculty members and staff of the Earth Science Department of Memorial University of Newfoundland assisted with the completion and improvement of this thesis, most notably, Dr. Chuck Hurich for constructive discussions, and Peter Bruce for help with software. Thank you, Gerry Kilfoil of the Newfoundland and Labrador Geological Survey, for teaching me a tactful method of combining aeromagnetic surveys of different acquisition parameters. Thank you to my father, Bill Ernst, for his help trudging geophysical equipment through bogs. Much gratitude is given to Calvin and Patsy Samms, of Howley Newfoundland, for the lovely accommodation, fantastic meals, humor, and expert knowledge of the area. A very special thank you must be given to Dr. Alison Leitch, a passionate educator, scientist, and hard worker, for her compassion and persistence throughout the thesis completion process. I would like to also thank Dr. Tom Calon for his help improving the manuscript and sharing his wisdom in structural geology.

Table of Contents

List of Tables

List of Figures

List of Abbreviations

APC – Antenna Phase Center

BBL – Baie Verte-Brompton Line

CFS –Cabot Fault System

CGSN – Canadian Gravity Standardization Network

CGSN – Canadian Gravity Station Network

CGVD28 – Canadian Geodetic Vertical Datum of 1928

CSRS – Canadian Spatial Reference System

DEM – Digital Elevation Model

DoD – United States Department of Defence

DOP – Dilution of Precision

DVL – Digital Video Logger

GLONASS – Global Navigation Satellite System

GPR – Ground Penetrating Radar

GPS – Global Positioning System

GRS80 – Geodetic Reference System 1980

GSC – Geologic Survey of Canada

NLGS – Newfoundland and Labrador Geologic Survey

NRCan – Natural Resources Canada

PDZ – Principle deformation zone

RTK – Real Time Kinematic

SHMM – Slant Height Measure Mark

TCH – Trans Canada Highway

PPP – Precise Post Positioning

Chapter 1: Introduction

The Carboniferous Deer Lake Basin is a fault-dominated, non-marine, onshore basin in west-central Newfoundland (Figure 1.1; Hyde et al., 1988). Alluvial to lacustrine sedimentary units of the basin unconformably overlay Proterozoic gneiss and plutonic rocks, and allochthonous Ordovician shelf and rise rocks of the Humber margin to the west, and are in fault contact with Ordovician to Silurian igneous rocks of the Notre Dame arc to the east (Figure 1.1, 1.2; Hyde, 1982). Thus, the tectonic contact between these two crustal blocks, the Baie Verte-Brompton Line (BBL; Williams and St-Julien, 1982), lies beneath the basin. The Deer Lake Basin is transected by two disjunct north-northeast trending fault-bounded elongated prominent ridges (Fisher Hills and Birchy Ridge; Figure 1.1) of Tournaisian rocks that separate two low-lying depocenters underlain by Viséan to Westphalian rocks (Hyde, 1982): the Humber Basin to the west and the Howley Basin to the east (Figure 1.1). This study focuses on Howley Basin.

The Howley Basin is overlain by a large lake (Sandy Lake; Figure 1.1), thick spruce forests and bogs, and large accumulations of glacial till. Exposure within the basin is extremely sparse and typically only small sections of outcrop are separated by large distances. Minor shallow drilling within the basin has been confined to its margins, leaving its internal stratigraphy unknown. The basin is accessible by a network of forest service roads, an abandoned railway, and by traversing small streams where the majority of exposure is.

The Carboniferous strata within the Deer Lake Basin have been of economic interest since the discovery of coal in 1838 (Hayes, 1949). Howley's (1879-1909) coal

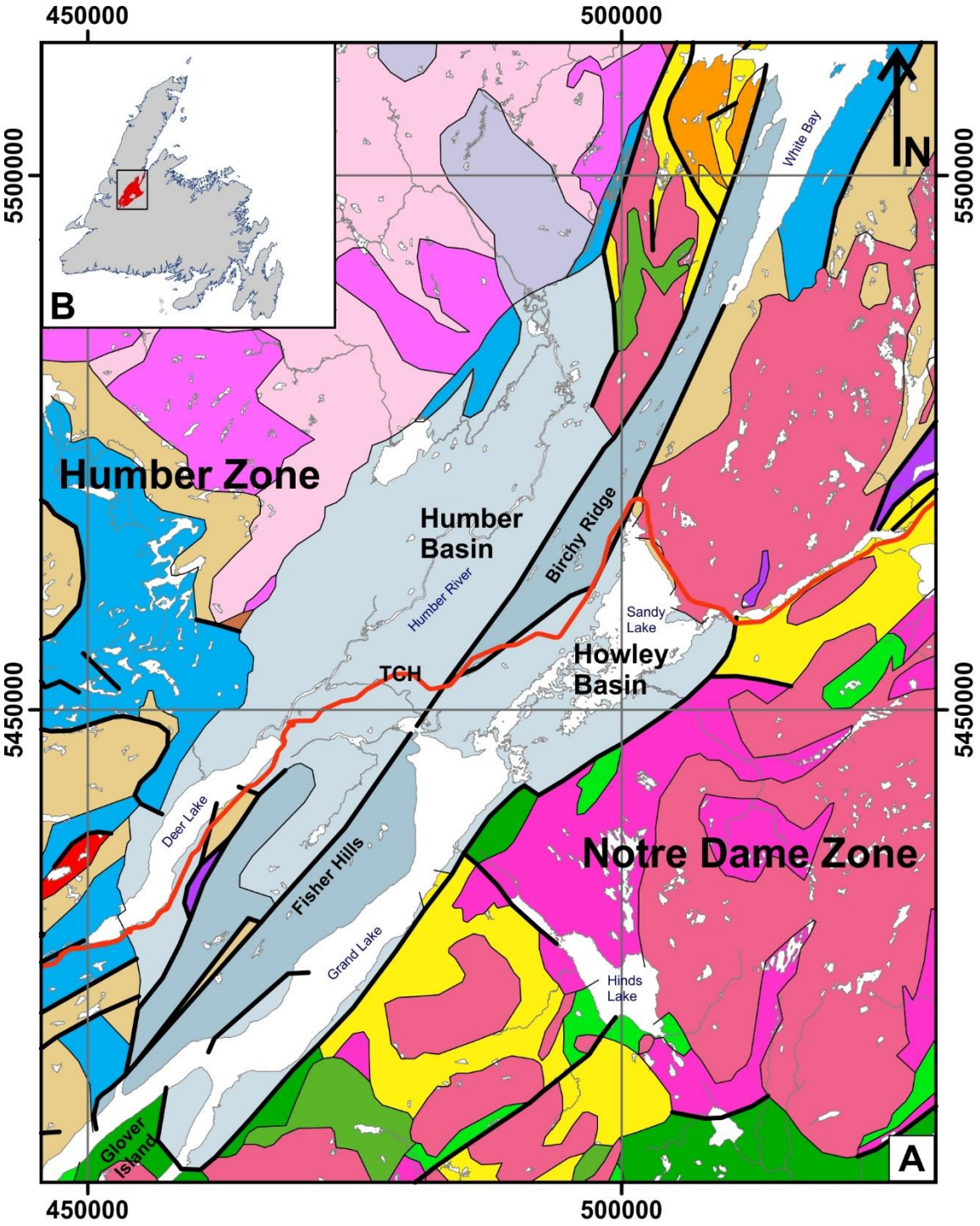

Figure 1.1: A) Overview geological map of the Deer Lake Basin, showing locations of major geologic subdivisions. Maps scale 1:600,000. Geologic legend given on Figure 1.2. Trans Canada Highway (TCH) shown. Modified from Colman-Sadd et al., 2000. **B)** The island of Newfoundland showing location of map. Carboniferous rocks of the Deer Lake Basin in red.

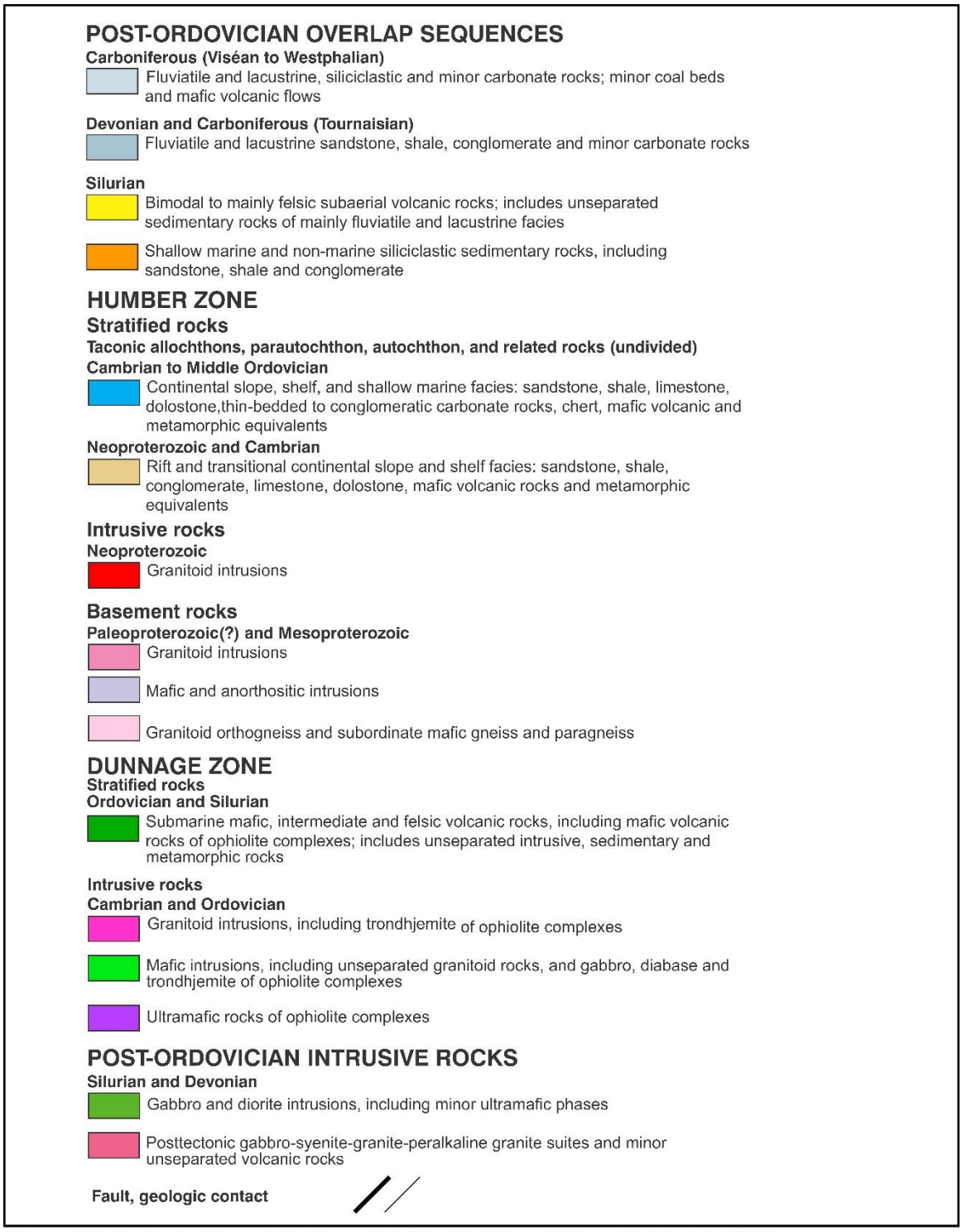

Figure 1.2: Geological legend for Figure 1.1. Modified from Colman-Sadd et al., 2000.

exploration efforts for the Newfoundland and Labrador Geological Survey (NLGS) resulted in trenching and testing the near-surface stratigraphy along the eastern margin of the Howley Basin by sinking boreholes (Murray and Howley, 1881, 1918). Hatch (1921), for the Reid Newfoundland Company, followed up Howley's discovery of coal showings and intersections by extending a boring operation into the west-central Howley Basin, to maximum depths of approximately 150 m. Intermittently, between 1898 and 1920 small-scale underground coal mining was conducted by the Reid Newfoundland Company and the Anglo Newfoundland Development Corporation within the Howley Basin (Hayes, 1949).

Bitumen seeps have been recognized and exploited by early residents of the area (Hyde et al., 1994). Langdon (1993) reported on the bitumen seeps primarily occurring at unconformable boundaries between Carboniferous and pre-Carboniferous rocks, both west and east of the Tournaisian ridges. Hatch (1919) produced geological maps of the Deer Lake Basin, outlining the shale series, and sampled and tested their volatiles and oil yields. His results showed that the greatest yields came from shales exposed on the southern shoreline of Grand Lake, near Glover Island (Figure 1.1). These outcrops have since been flooded by the construction of a dam on Grand Lake. Between 1917 and 1919, one of three wells drilled in the Humber Basin (maximum depth 231 m) encountered over-pressurized gas (Landell-Mills, 1954). Another two of four wells (maximum depth 848 m), drilled in 1955-1956 by Claybar Uranium and Oil Ltd. and Newkirk Mining Company in the Humber Basin, encounted gas (Langdon, 1993). In 2000, Deer Lake Oil and Gas Ltd. drilled three oil exploration wells in the Humber Basin (one reaching a

depth of 1879 m), with minor gas showings (Mukapahydhay, 2009, quoted from Burden et al., 2014).

Extensive uranium exploration in the Deer Lake Basin in the late 1970s by Northgate Exploration Ltd., Shell Resources Ltd., and Westfield Minerals, resulted in 150 shallow drill holes (Deveraux et al., 2009), primarily on prospects in the Humber Basin. Of this exploration effort, only 5 holes were collared in the western margin of the Howley Basin reaching a maximum depth of 77 m (O'Sullivan, 1979a, b, c). Throughout the 2000s a very focused uranium exploration in the northeast Humber Basin by a joint venture between Altius Resources Inc. and JNR Resources Inc., resulted 78 high-density very shallow drill holes, as well as geochemical surveying and airborne magnetic and radiometric (Deveraux et al., 2009). Spruce Ridge Resources Ltd., over the same period, also conducted geochemical and airborne magnetic and radiometric surveys in the northwest Humber Basin (Froude and Metsaranta, 2009).

Palynological, thermal maturation, and Rock-Eval studies of outcrop and core samples show lacustrine rocks of Tournaisian age are over-mature, and lie in the dry gas zone, whereas Viséan lacustrine oil shales are marginally mature to under-mature, with an oil window depth of 2-3 km (Barss, 1981, Macauley 1984: Hyde et al., 1988; Kalkreuth and Macauley 1989; Hamblin et al., 1997). Langdon (1993) showed that Viséan to Westphalian arkosic sandstones have good effective porosity and are prospective reservoirs. Langdon and Abrajano (1994) performed geochemical studies on bitumen found in core of Westphalian sandstones in the Howley Basin and concluded it had migrated from Viséan lacustrine oil shales.

Baird (1960) produced geological maps of the region for the Geological Survey of Canada (GSC). Popper (1970) determined that structures he observed in the Fisher Hills were of dextral strike-slip origins. Hyde (1982), completed the most extensive field mapping project of the Carboniferous rocks in the Deer Lake Basin to date, and his stratigraphic and sedimentology reports are the most comprehensive available (e.g., Hyde 1978, 1979, 1984, 1989, 1995; Hyde et al., 1988).

Weaver's (1967) regional gravity survey, and Miller and Wright's (1984) focused gravity survey over the Deer Lake Basin both showed a large negative gravity anomaly over the Howley Basin. Weaver (1967) suggested the Howley Basin was 5 km deep, and Miller and Wright proposed that it was 1.5 km deep. Wiseman, in Langdon (1993), modeled the Howley Basin to potentially reach a maximum depth of 4 km. Most of the few seismic surveys have been limited to the Humber Basin. An experimental refraction survey is reported by Miller and Wright (1984). Wright et al., 1996 interpreted a 12 km long seismic reflection line to show that Viséan units reached a depth of 2.5 km and were cut by normal and reverse faults. A recently acquired seismic survey traversed the eastern Howley Basin and its eastern bounding fault, and has been interpreted to show strongly deformed Viséan and Westphalian formations reaching a depth of 1.5 km (Vasquez, 2017).

Despite the Howley Basin's large low gravity anomaly (Weaver 1967; Miller and Wright, 1984) presumably associated with a deep sedimentary pile and greater burial depths, potentially being underlain by lacustrine source rocks (Hamblin et al., 1997) and known good reservoir sandstones (Langdon, 1993), with migrated bitumen intersected in

core (Langdon and Abrajano, 1994; Hamblin et al., 1997), it has received no hydrocarbon exploration. A lack of exposed bedrock outcrops, limited shallow drilling, and basin-wide seismic reflection surveys, leaves internal stratigraphy, structures, and development of the Howley Basin unknown.

This study is a multidisciplinary approach combining structural geology and potential-field geophysics to evaluate the deformational history, depth, and internal stratigraphy of the Howley Basin with a focus on the potential for the basin to produce, migrate, and trap hydrocarbons. Detailed structural field mapping of known exposures and suspect areas of new outcrops was completed to analyze the structural styles and relationships of stratigraphic units within the basin. Acquisition and processing of a new high-density gravity survey was combined with pre-existing datasets and publicly available high-resolution aeromagnetic surveys to assist with delineating structural trends and build a 2½ D geophysical forward model of the Howley Basin.

Chapter 2: Geological and Geophysical Background

2.1 Regional Geology and Tectonics

The geology of the island of Newfoundland can be separated into lithotectonic elements consisting of Early Paleozoic ribbon-shaped microcontinents and suprasubduction-zone oceanic terranes (Figure 2.1) that were accreted onto the eastern Laurentian margin in successive orogenic cycles in the Early to Late Paleozoic closure of the Iapetus Ocean. These microcontinents evolved, some as composite terranes, on either side of Iapetus Ocean, outboard of the Laurentian (Dashwoods- basement to obducted oceanic tracts and Notre Dame arc) or Gondwanan (Ganderia, and Avalonia) continental masses (Figure 2.1), prior to docking with Laurentia. Accretion of the continental lithosphere of these microcontinents produced the most profound orogenesis in the Newfoundland Appalachian orogeny (van Staal and Barr, 2012).

Going from present day west to east, and in order of time, the accretion of Dashwoods is attributed to the most significant phase of the Early-Middle Ordovician Taconic orogenic cycle, Ganderia to the Silurian Salinic orogeny, and Avalonia to the Early Devonian Acadian orogeny. Newfoundland was positioned in the hinterland of, and was largely unaffected by, the subsequent accretion of the peri-Gondwana Meguma microcontinent (Middle Devonian to Late Carboniferous Neoacadian orogeny), and the terminal collision between composite Laurentia and Gondwana (Carboniferous-Permian Alleghanian orogeny), which were major mountain building events further south in the Appalachian mountain belt (see van Staal and Barr, 2012, and references therein).

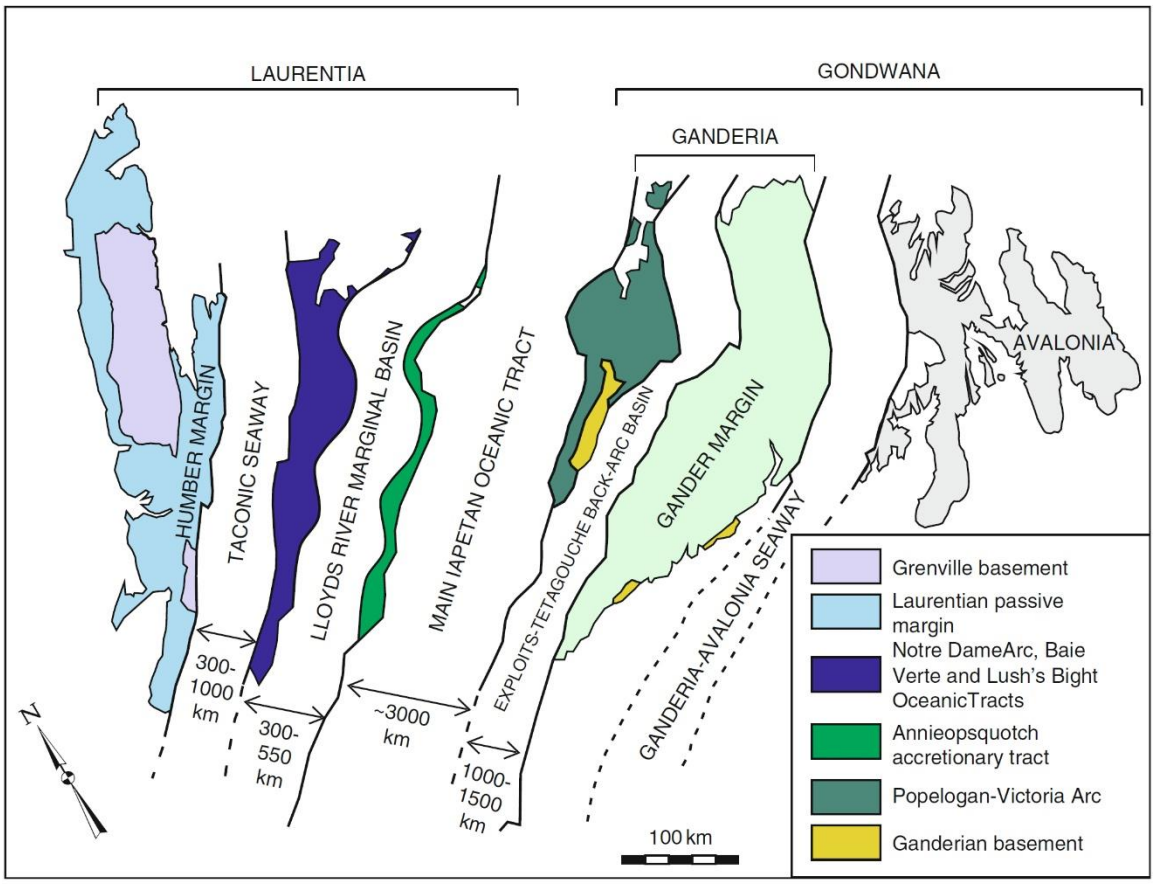

Figure 2.1: Lithotectonic elements of Newfoundland expanded to show seaways that occurred outboard of Laurentia and Gondwana (from Zagorevski and van Staal, 2011).

However, in Newfoundland, pre-existing weak tectonic lineaments were reactivated as dextral strike-slip faults during these later orogenies (Waldron et al., 2015).

The tectonstratigraphic zones proposed by Williams (1979), and subzones (Williams et al., 1988; Williams, 1995; Figure 2.2), have recently been refined with the aid of deep crustal imaging of the LITHOPROBE East project (e.g., Quinlan et al., 1992; Waldron and Stockmal, 1994; Waldron et al., 1998; Hall et al., 1998; van der Velden et al., 2004), which suggests that some zones are rootles allochthons that cannot be extended

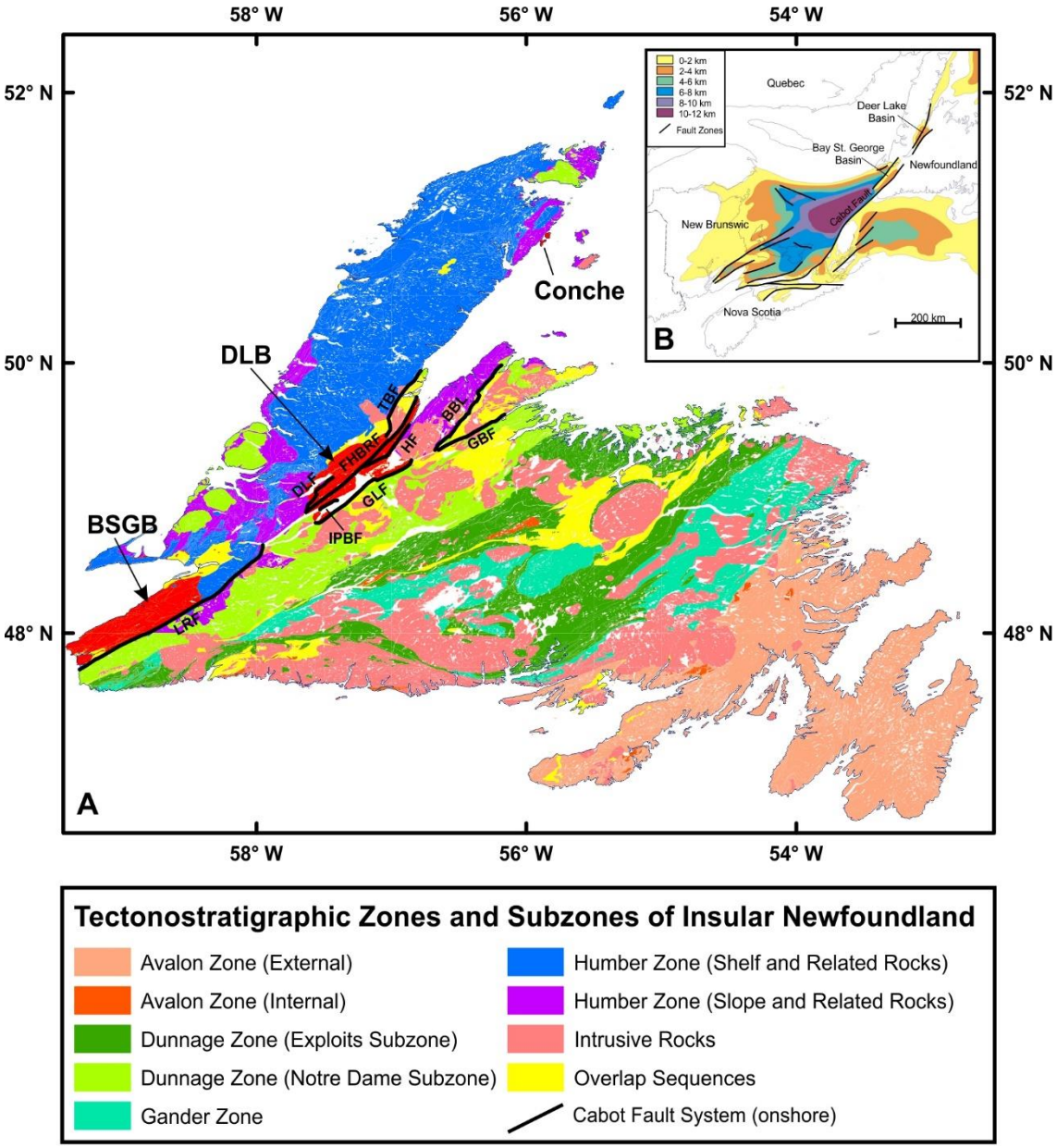

Tectonostratigraphic Zones and Subzones of Insular Newfoundland

- Avalon Zone (External)
- Avalon Zone (Internal)
- Dunnage Zone (Exploits Subzone)
- Dunnage Zone (Notre Dame Subzone)
- Gander Zone
- Humber Zone (Shelf and Related Rocks)
- Humber Zone (Slope and Related Rocks)
- Intrusive Rocks
- Overlap Sequences
- Cabot Fault System (onshore)

Figure 2.2: A) Geological map of tectonostratigraphic zones and subzones of Newfoundland, showing the locations of major onshore Carboniferous basins in western Newfoundland (red) and onshore extensions of the Cabot Fault System (after Williams et al., 1988; Williams, 1995). Abbreviations: Bay St. George Basin (BSGB); Deer Lake Basin (DLB); Baie Verte-Bromton Line (BBL); Deer Lake Fault (DLF); Fisher Hills - Birchy Ridge Fault (FHBRF); (Green Bay Fault (GBF); Grand Lake Fault (GLF); Hampden Fault (HF); Island Pond Brook Fault (IPBF); Taylor's Brook Fault (TBF). **B)** Regional isopach map of Upper Paleozoic strata in the Maritimes Basin, with major fault zones (from Lavoie et al., 2009).

to depth. Instead, van Staal and Barr (2012) propose lithotectonic elements compose the building blocks of the geology of Newfoundland. However, the tectonstratigraphic zones of Williams (1988) hold true as a good first-order subdivision of rocks at the surface. A comparison of the two terminologies used to subdivide the geology of Newfoundland follows.

The Humber zone (Williams, 1979) or Humber margin (van Staal and Barr, 2012), is a Cambro-Ordovician passive margin built on the eastern edge (present coordinates) of Laurentia. The Notre Dame subzone (Williams et al., 1988) is now described as several peri-Laurentia suprasubduction-zone oceanic tracts obducted onto the Dashwoods microcontinent (van Staal and Barr, 2012) with an additional three phases of overprinting magmatic activity (the Notre Dame arc). The Exploits subzone (Williams et al., 1988) has been divided into the peri-Gondwana Victoria arc and Tetagouche-Exploits back arc basins. The Gander and Avalon zones are redefined as accreted composite peri-Gondwanan microcontinents, Ganderia and Avalonia, respectively (Williams et al., 1988; van Staal and Barr, 2012; Figures 2.1 and 2.2). These tectonostratigraphic zones or lithotectonic elements are separated by predominately northeast-trending throughgoing sutures, which are marked by ductile and/or brittle fault zones that were reactivated in subsequent orogenic events. Post-tectonic igneous activity or sedimentation have indiscriminately intruded or overlapped the sutures zones (Figure 2.2).

This dissertation is concerned with the formation and geometry of the Howley Basin, which is situated along the suture zone between the Humber zone and Notre Dame subzone. The BBL, a narrow structural zone characterized by discontinuous ophiolite

complexes, separates the Humber and Notre Dame subzones (Williams and St. Julien, 1982; Figure 2.2). The BBL was developed during the Taconic orogeny but has had a long-lived polyorogenic displacement history lasting possibly into the Permian (Waldron et al., 2015). Following Brem (2003), the term Cabot Fault System (CFS) will be reserved for brittle Carboniferous movements, which have reactivated and crosscut the BBL in Newfoundland (Figure 2.2).

The following sections are a brief overview of the Lower to Middle Paleozoic development of the geology of western Newfoundland and Upper Paleozoic geology in Atlantic Canada. These sections are particularly relevant to this study because the Humber zone, and potentially the Notre Dame subzone, form the basement to the Howley Basin, and several lines of evidence suggest a cogenetic evolution for a series of Upper Paleozoic basins in Atlantic Canada.

2.1.1 Development of Lower to Middle Paleozoic Geology in Western Newfoundland

Humber Margin

The Humber margin records the generation and closure of the Cambro-Ordovician Taconic Seaway (Zagorevski and van Staal, 2011; van Staal and Barr, 2012). Following Neoproterozoic rifting of Rodinia, a passive margin developed on Mesoproterozoic Grenvillian basement along the eastern edge of Laurentia (present coordinates). Early Ordovician tectonic loading of the then advancing composite Dashwoods microcontinent created a westward migrating peripheral bulge followed by a foreland basin (Knight,

1991). Middle Ordovician docking of the Dashwoods block produced westward trusting of siliciclastic slope and rise rocks over platform carbonates as imbricated thin-skinned duplexes, the uppermost of which carried ophiolites of the Bay of Islands Complex (Cawood and Shur, 1992). The Silurian Salinic orogeny further imbricated the duplexes with westward displacement and exposed metamorphosed and deformed platform rocks in the eastern Humber margin (Cawood et al., 1994). Acadian deformation in the Early Devonian resulted in thick-skinned westward thrusting at the orogenic front (Cawood and Williams, 1988; Waldron and Stockmal, 1991, 1994).

Dashwoods Microcontinent

The Notre Dame subzone of Williams et al. (1988) is a composite terrane of Early Paleozoic obducted oceanic tracts (Lushs Bight, Baie Verte) and pulses of arc and non-arc magmatism (Notre Dame arc; Whalen et al., 2006; van Staal et al., 2007; Figure 2.3). The Dashwoods microcontinent, of Mesoproterozoic Grenvillian crust, is inferred from isotopic data and zircon inheritance of Ordovician arc plutons and volcanics to underlie all of these terranes (van Staal et al., 2007).

A Lower Cambrian transgressive sequence in the Humber margin is regarded as a rift-drift transition that is thought to represent rifting of part of the St. Lawrence promontory to create the ribbon-shaped Dashwood microcontinent (Waldron and van Staal, 2001). It is postulated that this was facilitated by an inboard ridge jump of the main Iapetus tract (van Staal et al., 2007), creating a narrow spreading seaway, the Taconic Seaway (Zagorevski and van Staal, 2011; van Staal and Barr, 2012; Figure 2.1), rifting

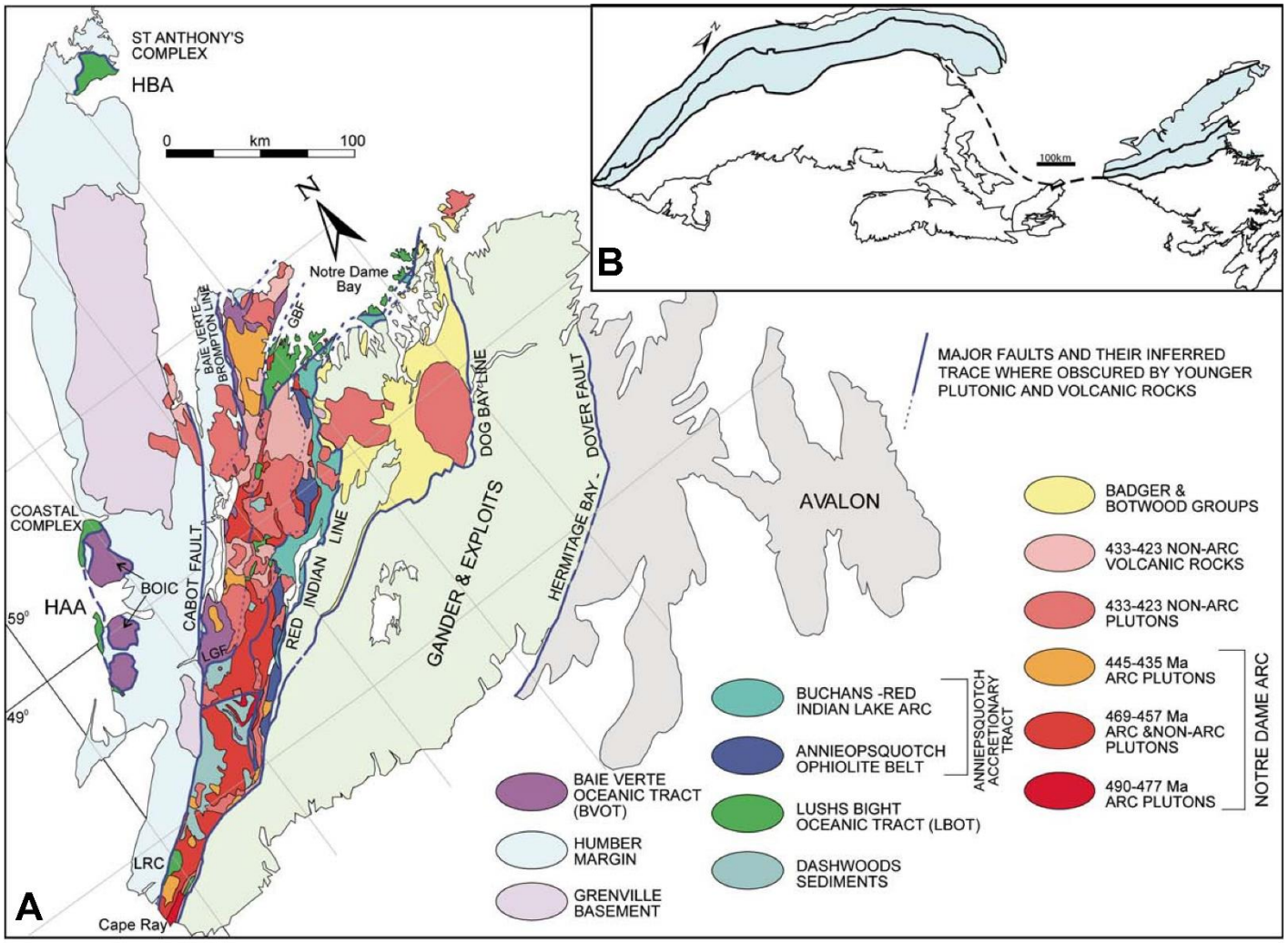

Figure 2.3: A) Tectonostratigraphic zones and subzone of Newfoundland with detailed distribution of the various ophiolitic, sedimentary, and plutonic rocks in the Notre Dame subzone and related regions. Abbreviations: Bay of Islands complex (BOIC); Green Bay Fault (GBF); Humner Arm allochthon (HAA); Hare Bay allochthon (HBA); Little Grand Lake Fault (LGF); Long Range mafic-ultamafic complex (LRC). **B)** Taconide zone of northen Appalachians. From van Saal et al., 2007.

Dashwoods from Laurentia. Paleomagnetic data and fossil evidence show that Dashwoods never traveled very far from the Laurentian margin. Following rifting, a complex series of subduction-related processes between the Late Cambrian to Middle Ordovician led to the accretion of suprasubduction zone oceanic tracts and associated arc rocks and cover sequences onto the Dashwoods microcontinent. This was accompanied by two pulses of arc magmatism. All Ordovician igneous activity is bounded to the west by the BBL, and to the east by the Red Indian Line (Figure 2.3). A final episode of non-arc magmatism in the Early Silurian indiscriminately intrudes and overlaps tectonic boundaries (see van Staal et al., 2007; van Staal and Barr, 2012 and references therein for further details on the development of the Notre Dame arc; Figure 2.3).

2.1.2 Overview of Upper Paleozoic Geology in Atlantic Canada

Upper Paleozoic sediments are widespread throughout the Maritime Provinces of Atlantic Canada, both onshore and offshore, unconformably overlying all of the terranes assembled during the Neoacadian and earlier (Gibling et al., 2008; Figure 2.2 B). These sediments are preserved in series of variably connected or isolated depocenters (basins in their own right), collectively known as the Maritimes Basin (Roliff, 1962; Williams, 1974; Bradley, 1982). The greatest accumulation of sediments in the Maritimes Basin, up to 12 km deep (Sanford and Grant, 1990), occurs along a relatively narrow, northeast-trending, fault-bounded and fault-dominated, central region (Figure 2.2 B). Flanking the thick, highly deformed central region, are relatively thin, and mildly deformed platformal areas (van de Poll et al., 1995; Figure 2.2 B).

Although presently isolated, the Deer Lake Basin lies along strike of the northeast-trending principal deformation zone (PDZ), the CFS, and is considered a constituent of the Maritimes Basin (Hyde, 1988; Langdon, 1996; Figure 2.2). The existence of common stratigraphic elements within the "subbasins" of the broader Maritimes Basin (Figure 2.4), suggests basin-wide events controlled subsidence and deformation throughout their evolution. Tectono-stratigraphic sequence stratigraphic interpretations of industry and academic seismic surveys in the Gulf of St. Lawrence have greatly improved understanding of the interplay and timing of faulting and subsidence within the Cabot Fault region (e.g., Langdon and Hall, 1994; Langdon, 1996, and many others).

The term 'Maritimes Basin' encompasses all post-Acadian sedimentation in the Canadian Appalachians, ranging in age from Early- to Mid-Devonian to Early Permian. However, because of the diachronous nature of orogenesis in an oblique collision zone with promontories and reentrants, post-Acadian deposition in their respective areas may be coeval with or even older than Acadian events elsewhere. Early- to Mid-Devonian alluvial to lacustrine strata associated with thick volcanic successions and intrusions occur in small, poorly exposed, and structurally complex areas in Nova Scotia and southern Quebec. Deposition may have been in small fault-bounded basins developed along reactivated Acadian tectonic lineaments, but limited exposure and lateral extent has precluded definitive models for this period of basin formation (see Gibling et al., 2008).

By the Late Devonian and into the Early Mississippian, deposition of thick alluvial to lacustrine sediments (Horton Group and equivalents; Figure 2.4) into linear,

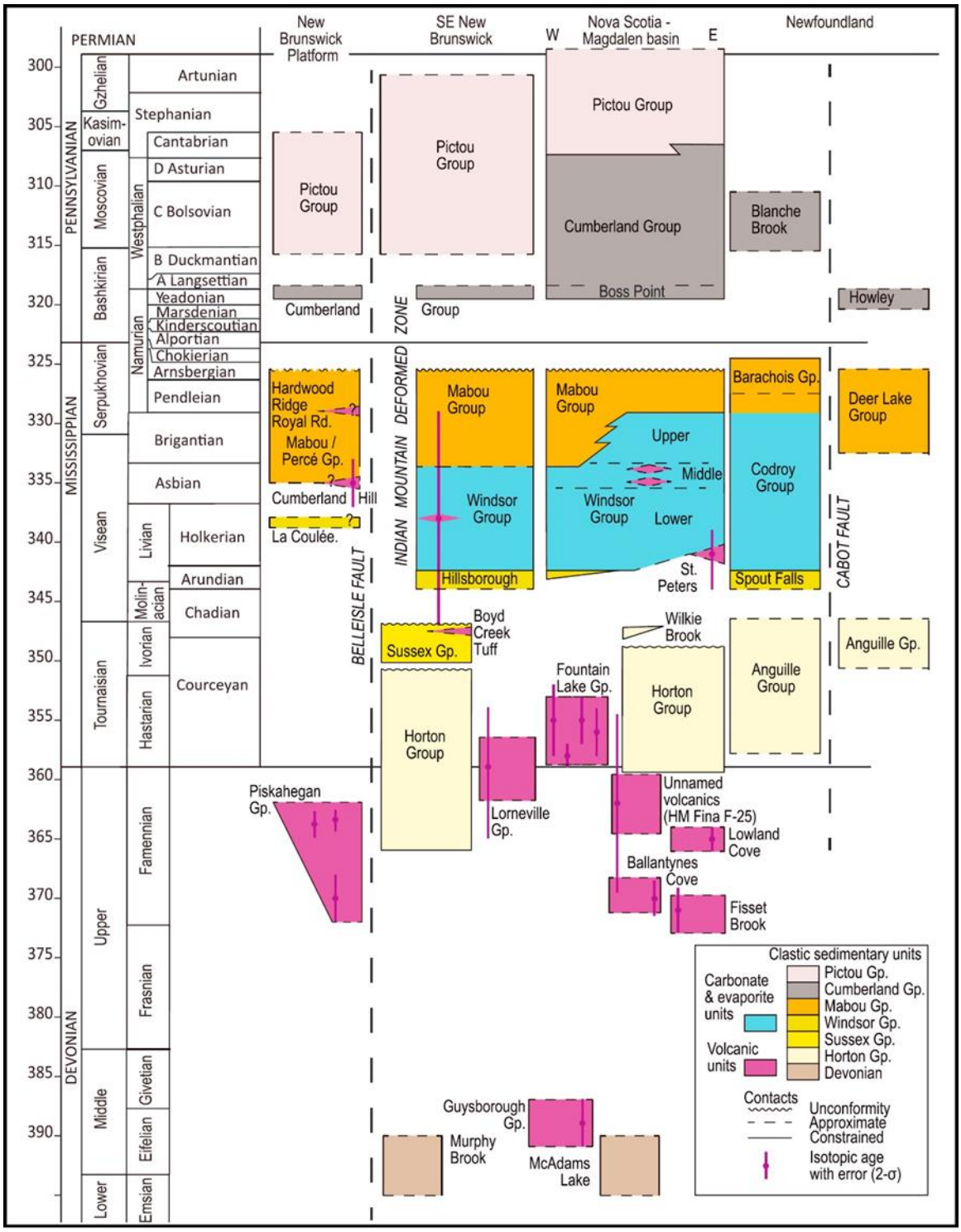

Figure 2.4: Regional chronostratigraphic chart for post-Acadian group-level stratified units in the Maritimes Basin, and selected formations. Abbreviation: Group (Gp.). Lithostratigraphic names without designation are formation-level. From Waldron et al., 2015 and references therein.

northeast- and east-trending, fault-bounded basins was widespread across the Maritimes Basin. Thick, dark oil shales across the region, with a common Tournaisian age, indicate subsidence was extremely rapid and outpaced sediment supply (Gibling et al., 2008). Topmost Anguille strata in the Bay St. George Basin and Horton strata in the Gulf of St. Lawrence overstep bounding faults and onlap basement, suggesting that a period of thermal subsidence followed initial rifting (Hall et al., 1992; Durling and Marillier, 1993; Gibling et al., 2008). Seismic profiles over Horton basins show several kilometers of strata, typically in half-grabens, with basin-bounding faults linked to Acadian thrusts in extension (Marillier et al., 1989; Gibling et al., 2008). Waldron et al. (2015) propose that there was substantial dextral displacement along regional northeast-trending faults during this time period, and Anderson et al. (2000) showed that the Ming's Bight Group, within the BBL/CFS on the Baie Verte Peninsula in northern Newfoundland, was exhumed in a dextral transtensional regime in the Middle to Late Devonian. These conclusions suggest that dextral lateral motion along releasing bends or offsets in pre-existing weak northeast-trending tectonic lineaments may have contributed to localized subsidence during the Late Devonian (e.g., Langdon and Hall, 1994; Langdon, 1996).

Inversion and a sedimentary hiatus succeeded Horton Group deposition followed by a change in sedimentation throughout the Viséan (Figure 2.4). The Mid-Viséan basal Windsor Group (in part Deer Lake Group equivalent) and Horton Group contact is an angular unconformity at numerous localities across the region and marks the change to an open-marine sequence of laminated bituminous limestone and shale deposited in a relatively deep reducing environment. Thick sulfate and chloride evaporite conformably

overlie basal Windsor units, indicating that subsequently much of the basin experienced restriction of oceanic connection in an arid environment. The Windsor Group occupies a large area and is seen to overstep basin boundaries and onlap basement, implying a near-simultaneous marine inundation into a region below sea-level (Schenk et al., 1994; Gibling et al., 2008). Accommodation space for Windsor Group has been attributed to thermal subsidence (Pascucci et al., 2000), however, locally thickened strata and coarse conglomerates within fault-bounded basins implies tectonic activity during Windsor Group deposition (Waldron and Rygel, 2005; Gibling et al., 2008).

The Upper Viséan to Lower Namurian Mabou Group rocks conformably overlie Windsor Group strata (Figure 2.4) and are up to 1 km thick. The Mabou Group marks the change to non-marine deposition, transitioning from gray shallow lacustrine facies to red playa and floodplain deposits. A wide distribution of the Mabou Group and onlapping stratigraphic relationships with pre-Carboniferous sediments suggests that thermal subsidence controlled deposition, however, local conglomerates within the group have been interpreted to imply tectonic activity during this period (Knight, 1982; St. Peter, 1993).

The Mabou Group is capped by a regional unconformity that cuts down into older units at numerous locations (Langdon and Hall, 1994; Langdon, 1996; Pascucci et al., 2000; Figure 2.4). An angular discordance and sedimentary hiatus implies that it represents a long-standing subaerial erosional surface. Gondwanan glaciation has been proposed for lowering of base-level at this time (Gibling et al., 2008); however, most

authors attribute regional exhumation to tectonism related to the onset of the Alleghenian orogeny (e.g., Langdon and Hall, 1994; Langdon, 1996).

By the Early Pennsylvanian, basal Cumberland Group (Figure 2.4) were being deposited into rapidly subsiding active extensional basins along major fault zones (Cabot, Hallow, and Cobiquid-Chedabucto Fault Zones), throughout the Maritimes Basin. Alternating and coeval braided-fluvial, lacustrine and floodplain deposits with abrupt changes in paleoflow directions, stratal thickening, synsedimentary deformation structures (Waldron, 2004), and exposed syndepositional faults (Plint, 1985), all point to pronounced intermittent tectonism during this period of deposition (Gibling et al., 2008). Transpressional and transtensional structures developed over this period attest that the Alleghanian compression in the southern U.S. Appalachians manifested as predominately dextral strike-slip in character over the Maritimes Basin.

The Upper Cumberland Group and Pictou Group (Figure 2.4) reflect a period of regional thermal subsidence following the tectonism of Early Pennsylvanian. A single basin, fed by a large river system with headwaters in the Appalachian Mountains to the southwest, is envisioned to cover much of the Atlantic Provinces during this time. Subsidence was slow and changes in facies are coincident with Milankovitch cycles (Gibling et al., 2004).

Transpressional deformation affecting Permian strata has been observed in several basins (Pascucci et al., 2000; Gibling et al., 2002; Waldron, 2004), indicating that tectonic activity had resumed in the Maritimes Basin.

Shortly after the assembly of Pangea, rifting along the Gondwanan, and the then composite Laurentian suture zone, led to the opening of the Atlantic Ocean in the Mesozoic. Pre-existing east-west-trending faults were reactivated as sinistral trantensional structures (Waldron et al., 2015), and regional exhumation and erosion removed considerable thicknesses of Permian to Carboniferous cover (Ryan and Zentilli, 1993).

2.2 Geology of the Deer Lake Basin

The Deer Lake Basin is an elongated, northeast-trending, distensive depocenter paralleling the CFS in west-central Newfoundland. Within the basin, the CFS is represented by a series of parallel or sub-parallel steep north-northeast trending faults (Map A). Intermittent dextral strike-slip displacement along the CFS throughout the Carboniferous is thought to be the predominant mechanism for subsidence and subsequent inversion of the basin, creating a tectonically active intermontane valley into which detritus from nearby pre-Carboniferous highlands were deposited. Post-tectonic thermal subsidence, changes in paleoclimate, and an evolving dynamic drainage system may have influenced depositional environments throughout the basin's history (Hyde, 1995; Hyde et al., 1988; Langdon, 1996).

Three gross intervals of sedimentation are preserved in the Deer Lake Basin. They are represented by the Tournaisian Anguille Group, the Viséan Deer Lake Group, and the Westphalian Howley Formation (Figure 2.5; Hyde, 1995). Faults, unconformities, varying degrees of deformation, and palynological breaks separate and define these units. Deposition is postulated to have continued into the Permian, but exhumation and erosion

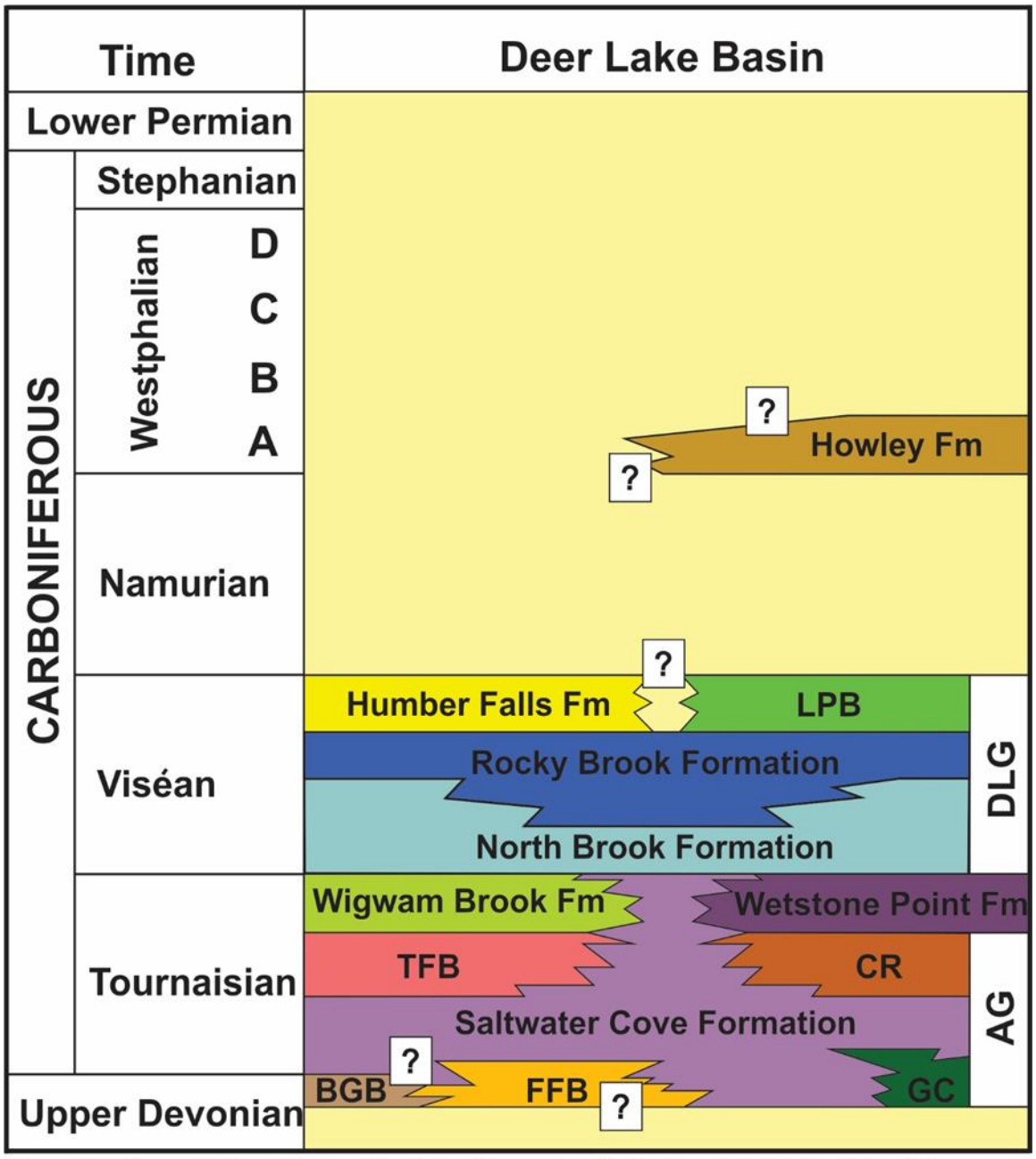

Figure 2.5: Chronostratigraphic chart for Carboniferous strata in the Deer Lake Basin. Abbreviations: Anguille Group (AG); Deer Lake Group (DLG); Blue Gulch Brook Formation (BGB); Cape Rouge Formation (CR); Forty-five Brook Formation (FFB); Gold Cove Formation (GC); Little Pond Brook Formation (LPB); Thirty-fifth Brook Formation (TFB). Modified from Hyde (1989).

have since removed 1-2 km of strata, possibly including Permian cover (Hamblin et al., 1997). All of the sediments preserved in the Deer Lake Basin are non-marine, indicating the basin was topographically high enough or was isolated from regional Viséan marine transgression by surrounding topography (Hyde, 1984). Geophysical studies (Haworth et al., 1976) and stratigraphical considerations (Hamblin et al., 1995) indicate that the valley basin was open to the northeast into White Bay during the Tournaisian (Anguille deposition), as far as Conche on the Great Northern Peninsula of Newfoundland (Figure 2.2). In Carboniferous units near Deer Lake, clasts which are clearly derived from the south, imply that topography separated the Deer Lake Basin from the Bay St. George Basin for most of its depositional history. And the basal North Brook Formation of the Deer Lake Group, with an inferred lower Viséan age, contain clasts derived from adjacent surrounding highlands with paleoflow indicators that suggest at this time the basin was fed from all directions (Hyde et al., 1994).

Carboniferous strata in the basin are in fault contact with Ordovician to Silurian igneous terranes of the Notre Dame arc along its length to the east, and unconformably onlap Cambro-Ordovician platform carbonates and Precambrian Grenville basement to the west (Hyde, 1982; Map A). Thus, the inferred suture zone between the Humber margin and the Notre Dame arc, the BBL, is buried somewhere underneath the Deer Lake Basin.

A stark contrast in the structure of Carboniferous units is evident throughout the basin. Tournaisian units are highly indurated, tightly folded, frequently internally faulted, and occupy two elongated, northeast-trending disjunct end-on ridges that form a central

spine to the basin, separating the topographically low Humber Basin to the west and the Howley Basin to the east (Map A). On the other hand, the younger strata in the basin (Deer Lake Group and Howley Formation) underlie the topographically low regions to the east and west, and are generally gently folded and less consolidated. Deformation of the Deer Lake Group increases with proximity to faults (Hyde, 1982). The contact between Tournaisian strata and the Deer Lake Group is typically faulted, but an angular unconformity has been inferred in the Fisher Hills Block (Hyde, 1982, 1989; Figure 2.5).

2.2.1 Anguille Group

The Anguille Group is considered the initial basin fill and the first fining-upward megasequence in the Deer Lake Basin (Hyde, 1984, 1988). Palynological evidence and the remains of paleoniscoid fish suggest a Tournaisian age, but basal units are undated and may be as old as Famennian (Hyde, 1995). The Group has been subdivided into the Gold Cove, Saltwater Cove, Cape Rouge, Blue Gulch Brook, Forty-Five Brook, and Thirty-Five Brook Formations (Hyde, 1982, 1984; 1995; Map A; Figure 2.5).

Lithologies of the Anguille Group consist of basal alluvial to fluvial conglomerates and sandstones of varying composition – reflecting proximal sources – in the south, and dolostones in the north. These units grade upwards and are interbedded with dark grey mudstones and grey micaceous sandstones. Higher up in the stratigraphy, pebble to cobble conglomerates are interbedded with dolomitic and micaceous sandstones. Finer-grained calcareous sands and silts with black mudstone are regarded as coeval distal deposits. Coarse-grained sandstone and pebble to coble conglomerates cap

the succession in the south (Hyde, 1984, 1995). An aggregate thickness for the Anguille Group is probably up to 3000 m (Hyde, 1995).

The lithostratigraphy of the Anguille Group has been interpreted to represent the deepening and filling of a narrow lake(s). Alluvial fans formed prograding deltas as the lake(s) deepened with distal turbidites interfingering with deep water lacustrine facies (Hyde, 1984, 1995). An absence of bioturbation, the preservation of organic matter, and the presence of sulfides indicate anoxic bottom conditions within the Anguille lake(s) (Popper, 1970; Hyde et al., 1994); thus, shale rich horizons within the Anguille Group are an attractive hydrocarbon source rocks (Langdon, 1993).

2.2.2 Wigwam Brook and Wetstone Point Formations

The Wigwam Brook and Wetstone Point Formations are both only observed in fault contact with other lithologies, except where the Wigwam Brook Formation nonconformably overlies pre-Carboniferous plutonic rocks in northwestern Birchy Ridge (Smyth and Schillereff, 1982; Hyde, 1982; Map A; Figure 2.5). The Wigwam Brook and Wetstone Point Formations both are characterized by conglomerates, sandstones, intercalated with silt- to- mudstones and thin carbonate beds, reflecting fluvial environments (Hyde, 1995). Both units have been placed stratigraphically between the Anguille Group and Deer Lake Group and are considered time equivalents (Hyde, 1995; Figure 2.5). A well-preserved Late Tournaisian spore assemblage in the Wetstone Point Formation, and sandstone clasts within the Wigwam Brook Formation that are

petrographically similar to Anguille Group sandstone, point to a post-Anguille deposition for both formations (Hyde, 1995).

2.2.3 Deer Lake Group

The Deer Lake Group is widespread in the Deer Lake Basin, occupying the topographically low regions flanking east and west of the ridges underlain by Tournaisian strata, from north Glover Island, Grand Lake, in the southeast (Figure 1.1), to the lower reaches of Taylor's Brook in the northwest (Map A). Based on stratigraphic relationships and microspore analysis the group has been subdivided into the North Brook Formation, Rocky Brook Formation, Humber Falls Formation, and The Little Pond Brook Formation (Hyde, 1982, 1985; Figure 2.5). These units represent a second fining upward megasequence representing the development and filling of an intermontane lake (Hyde, 1988).

North Brook Formation

The North Brook Formation is the most extensive formation, and forms the basal member of the Deer Lake Group (Hyde, 1982, 1989; Map A; Figure 2.5). In the lower part of the formation, massive, thick beds of poorly sorted, pebble to boulder conglomerates are intercalated with coarse arkosic sandstones, interpreted as reflecting paleo-debris flow and alluvial fan settings. These coarse sediments mark the present-day basin margins. This, together with matching clast lithologies to proximal sources, suggests that that present-day basin margins closely represent basin margins during deposition. Coarse lithologies grade upward and basin-inward into finer, red, calcareous

sandstones and mudstones, representing deposition on distal meandering fluvial channels. Rare stromatolitic limestone beds are considered to have been deposited as inorganic precipitates in discrete ponds that formed on alluvial fan and basin floor surfaces (Hyde, 1989). A single occurrence of amygdaloidal basalt is underlain and overlain by North Brook Formation, just east of Deer Lake (Hyde, 1984, 1989, 1995).

Abundant schists, phyllite and quartzite clasts observed in North Brook conglomerates to the south are correlated with Fleur-de-Lys rocks (metamorphosed rift sediments of the Humber margin; Map A; Hibbard et al., 1980) that outcrop further to the south, implying that a topographical high separated the Bay St. George and Deer Lake Basins at the time of North Brook deposition (Hyde, 1984, 1989, 1995). Paleoflow indicators show that during North Brook deposition detritus arrived from all directions, filling the basin center (Hyde et al., 1994). The North Brook Formation has not been dated paleontologically; however, an intertonguing stratigraphic contact with the overlying Rocky Brook Formation, of Viséan age, favors a similar age for the youngest North Brook beds (Hyde, 1989).

Rocky Brook Formation

Lithologies of the Rocky Brook Formation consist of interbedded gray, green and red siltstone and mudstone, red fine-grained sandstone, oölitic and stromatolitc dolostones, and dark brown oil shales (Hyde, 1984; Hamblin et al., 1997). Hyde (1982, 1984; 1995) subdivided the Rocky Brook Formation into two members: the lower Spillway Member, and the upper Squires Park Member (Map A). Stratigraphic

arrangement of the above lithologies is interpreted to reflect the inception, deepening and filling of a paleolake(s) above the North Brook Formation (Spillway Member), followed by another phase of subsidence and filling (Squires Park Member; Hamblin et al., 1997). In both members, periods of basin subsidence and deepening of the lake led to deposition of organic-rich shales in anoxic conditions. These beds are excellent hydrocarbon source rocks (Hamblin et al., 1997).

The Rocky Brook Formation is interpreted to overlie and partly be a distal equivalent to North Brook Formation (Hyde, 1995). It is dated palynologically to be confined to the Late Viséan (Hamblin et al., 1997), providing a time constraint for North Brook deposition. A lack of marine fossils, paleoniscoid fish remains, and the presence of analcime in most lithologies, indicate a lacustrine depositional environment for Rocky Brook Formation (Gall and Hyde, 1989; Hyde, 1995). Rocky Brook Formation is present in both the east and west basins, flanking the Tournaisian ridges, but only the Spillway Member has been recognized in the east (Hyde, 1982). Stratigraphic thickness of Rocky Brook Formation vary significantly throughout the basin (Wright et al., 1996), but reach upwards of 1000 m on Glover Island (Hyde, 1995; Figure1.1).

Humber Falls Formation

The Humber Falls Formation is the upper unit of the Deer Lake Group in the Humber Basin. It is characterized by red, grey and pink arkosic, cross-stratified, sandstone interbedded with grey pebble to cobble conglomerates, and minor red siltstone, in thick fining-upward sequences (Hyde, 1984). The Humber Falls Formation is

interpreted as braided fluvial to alluvial fan deposits that prograded over Rocky Brook lacustrine units as subsidence decreased and sediment input overwhelmed the lake (Hamblin et al., 1997). In the western Humber Basin, basal conglomerates overlie mudstones assigned to the Rocky Brook Formation in a sharp contact that has been regarded as a potential disconformity (Hyde, 1984, 1995). However, spore assemblages reported by Barss (1980) give a Viséan age, similar to underlying Rocky Brook, signifying a rapid facies change (Hyde, 1995). Abundant planar and trough cross-stratification, together with clast lithologies, and a decrease in grain size towards the southwest, indicate a southwesterly dipping paleoslope, with a source to the northeast (Hyde, 1984, 1995). The Humber Falls Formation reaches a maximum thickness of 250 m in the Humber Basin (Hyde, 1995).

Little Pond Brook Formation

The Little Pond Brook Formation is exposed only east of the Fisher Hills structural block, where it outcrops along the eastern and western shores of Grand Lake, north of Glover Island (Hyde, 1982; Map A). Lithologies consist of sandstones, mudstones, and conglomerates that have a gradational contact with the underlying Rocky Brook Formation (Hyde, 1982, 1984; Map A). Previous workers mapped the Little Pond Brook Formation as the Howley Formation (e.g., Belt, 1969; Hyde and Ware, 1981); however, a Viséan-Namurian spore assemblage (Barss, 1981), led Hyde (1982) to map these units as Little Pond Brook Formation. Similar lithologies and time of deposition suggests that the Little Pond Brook Formation is the eastern equivalent of the Humber Falls Formation. As such, a similar depositional environment is interpreted (Hyde, 1995).

Paleoflow indicators in fluvial facies and clasts lithologies point to a western paleoslope. The Little Pond Brook Formation is at least 750 m thick (Hyde, 1995).

2.2.4 Howley Formation

The Howley Formation is the youngest preserved stratigraphic unit within the Deer Lake Basin, with a spore assemblage dated as Westphalian A (Barss, 1981; Hyde, 1995). Thus, a significant time gap separated the Howley Formation from the Humber Falls and Little Pond Brook Formations, and a sedimentary hiatus has been suggested to span most of the Namurian in the Deer Lake Basin (Langdon and Hall, 1994; Figure 2.5). Exposure of the Howley Formation is very sparse and is limited to the western and eastern margins of the northeastern depocenter, the Howley Basin. The Howley Formation is inferred to underlie the center of the basin, but exposure is absent. Along its margins the Howley Formation is inferred to be in fault contact with other Carboniferous and pre-Carboniferous rocks (Hyde, 1982; Map A).

Lithologies of the Howley Formation consist of interbedded gray to red cross-stratified arkosic sandstone, coarse- to- very coarse-grained brown arkose sandstone, pebble to boulder conglomerate, and siltstone. Thin bituminous coal seams are interbedded with pyritiferous and carbonaceous sandstones and siltstones. Carbonate and ironstone nodules, and coalified wood debris are common (Gall, 1984). Conglomerate clasts in the formation indicate highland basement sources to the east and northeast (Gall, 1984). The formation has been interpreted as dominantly fluvial with coal seams, probably forming on a well-vegetated alluvial plain/coal swamp crossed by low to high

sinuosity streams (Belt, 1968; Gall, 1984; Hyde, 1984, 1995). Hyde (1984) calculated a stratigraphic thickness of 3100 m for a section of Howley Formation along the northeast margin, but noted this result was speculative given the lack of exposure and deformed nature of the formation.

2.3 Previous Geophysical Studies and Interpretations

The structure and depth of the Deer Lake Basin has been investigated with geophysical methods from the 1960s to present. Geophysical methods used to investigate the structure of the basin are: ground-based gravity surveying, aeromagnetic surveying, and seismic refraction and reflection surveys. High-resolution seismic surveys have only been collected over and west of Birchy Ridge, to the axis of the Humber Syncline, in the Humber Basin (Wright et al., 1996). The LTHOPROBE East transect crossed the northern portion of the Fisher Hills block, and continued on the eastern side of Grand Lake near Hinds Brook, just south of the Howley Basin (Figure 2.5). This survey was designed and processed for deep-crustal imaging, at the expense of near-surface resolution (Quinlan et al., 1992).

The first geophysical investigation that included data collection over the Deer Lake Basin was a regional gravity survey covering the island of Newfoundland in the 1960s by Weaver (1967). Gravity stations were taken at 13 km mean station spacing, with four stations in the Howley Basin and approximately 30 over the Carboniferous strata in the whole Deer Lake Basin (Miller and Wright, 1984). This dataset showed an anomalous gravity high in the northwestern part of the basin, associated with gabbro and/or diorite in

the Aides Pond area (Baird, 1960; Map A), and an east-west low over sediments in the Howley Basin. Modeling by Weaver (1967) suggested that the gabbro/diorite extends to greater than 6 km and, using a density contrast of -0.06 g cm^{-3} from a Bouguer value of 2.67 g cm^{-3}, modeled sediments in the Howley Basin to reach 5 km in depth.

In 1981 and 1982 Miller and Wright (1984) collected 230 gravity stations over the Deer Lake Basin and adjacent pre-Carboniferous units with a mean station spacing of 2.5 km. Elevation data was obtained using barometric altimeters and psychrometers for temperature and humidity information, that was reported to be accurate to ± 2 m. Positions of gravity stations were located on topographical maps, with an estimated uncertainty of ± 50 m. The resulting uncertainty in the gravity measurements were ± 0.5 mGal (Miller and Wright, 1984). The gravity survey was complimented by an aeromagnetic survey database available in the public domain, and augmented with industry aeromagnetic and land-based magnetic surveys (see Miller and Wright, 1984 for more details). A small (1.5 km in length) preliminary refraction seismic survey was also reported on by the same authors. This survey was shot east-west over a western petal of the Birchy Ridge flower structure, underlain by North Brook and Humber Falls Formation (see Figure 1 of Miller and Wright, 1984).

Miller and Wright (1984) modeled the gravity and magnetic data on a profile that trended northwest-southeast over the Howley and Humber basins, across the southern portion of the Birchy Ridge structure and the northern section of the Humber Syncline (see Figure 1 of Miller and Wright, 1984). The authors removed a fifth-order polynomial trend surface from the Bouguer anomaly map, stating it was the most ‘statistically best-

fitting.' The residual gravity anomaly map was modeled in conjunction with the magnetic data. After placing a mafic-ultramafic unit up to 7 km depth, correlated with rocks of the Long Range Inlier, under the western limb of the Humber Syncline; felsic volcanics up to 4 km deep under the eastern limb; and felsic (?) volcanics up to 4 km depth under the Howley Basin, Miller and Wright (1984) reported a maximum depth of 1.2 km for the Humber Basin and 1.5 km for the Howley Basin (see Figure 6 of Miller and Wright, 1984). It should be noted that Miller and Wright (1984) followed Hyde's (1982) geological interpretation that the Howley Formation rests unconformably on pre-Carboniferous basement throughout the Howley Basin, and as such, used a homogeneous density of 2.37 g cm^{-3} in their modeling. This may be an oversight; basement geology is not constrained, and a fifth-order polynomial would have been influenced by igneous bodies present to 7 km depth, also there exists a distinct possibility that the denser Deer Lake Group rocks constitute a significant volume of sediments within the Howley Basin.

The seismic refraction data was interpreted to show the Deer Lake Group reaching a maximum depth of 250 m, with a westward dip (see Miller and Wright, 1984 for processing parameters and survey logistics). This is likely not an accurate estimation for a maximum thickness of the Deer Lake Group, as the seismic line was shot over a potentially thrust-bounded fault panel underlain by North Brook Formation with expected uplifted basement. Furthermore, the western part of the section was surveyed over the Humber Falls Formation and its sharp lithological contact with the underlying Rocky Brook Formation is suspected to be of high seismic impedance, and produce a refracted wave.

Wiseman in Langdon (1993) used an ‘improved’ gravity data set and aeromagnetics to complete a 2.5-D simultaneous modeling of the Humber and Howley basins. Their imaged profiles show models of the Humber Basin, but do not include the Howley Basin. Instead the authors stated that ‘revised basin profiles’ indicate that the Howley Basin reaches a maximum thickness of 4 km along its eastern margin. It should be noted that the following was not reported in the modeling: processing parameters for potential-field data; sources of their potential-field data, or how it was improved from previous datasets; rock density or magnetic susceptibilities used for modeling; strike lengths used in the 2.5-D modeling; or ties to well data. The lack of details in this report is a serious flaw and undermines its scientific utility.

Wright et al. (1996) reported on a 12 km long seismic reflection survey shot over the east limb of the Humber Syncline, underlain by Rocky Brook and Humber Falls Formations (Map A). This survey was less than 2 km away from the seismic refraction survey of Miller and Wright (1984). Wright et al. (1996) interpreted the depth-migrated profile to show that the Deer Lake Group reached a maximum depth of over 2.5 km towards the center of the syncline (Figure 2.6). A number of high-angle faults are imaged in the seismic data, both normal and reverse, cutting Deer Lake Group sediments (Figure 2.6). Wright et al. (1996) interpreted this fault zone to be an along strike extension of the Fisher Hills block, which developed in the Late Devonian to Early Carboniferous, and continued throughout the whole Carboniferous period. A comparison between this seismic line and that of the LITHOPROBE transect interpreted by Waldron and Stockmal (1994), 10 km to the southwest, shows that Rocky Brook strata thicken to the northeast.

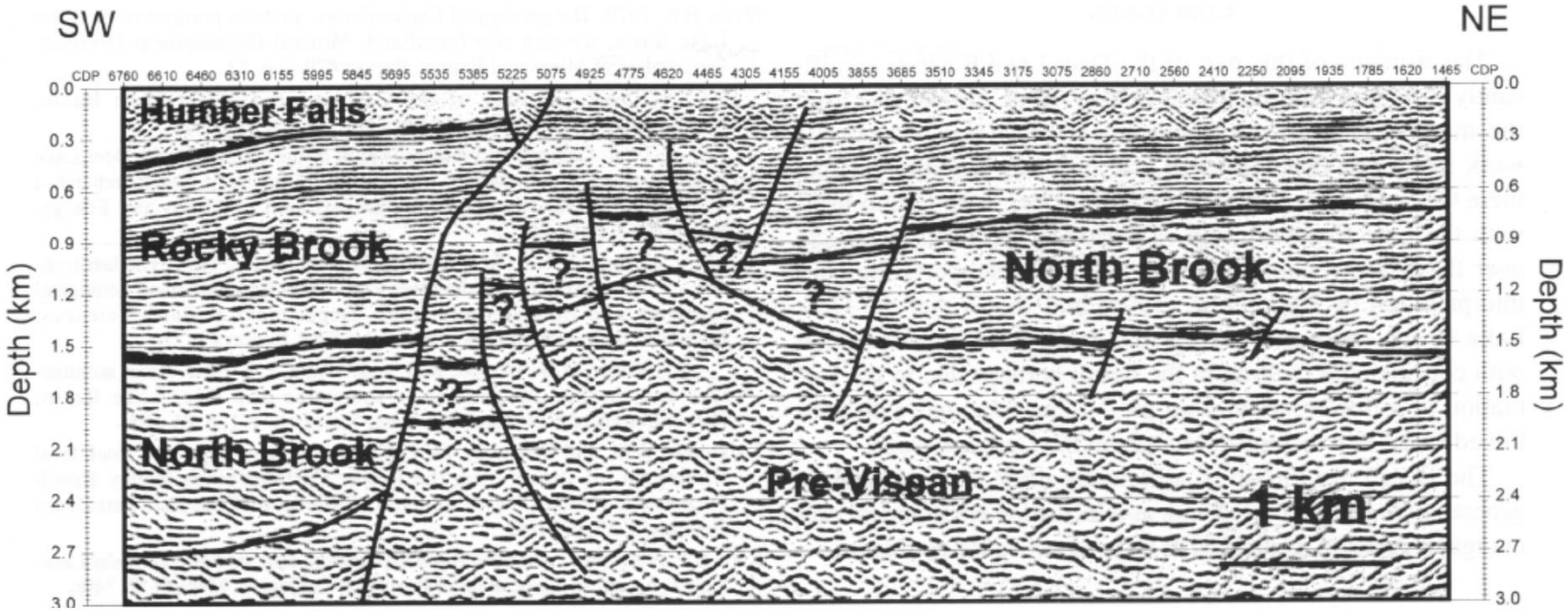

Figure 2.6: Depth-migrated seismic profile west of Birchy Ridge, with Humber Syncline to southwest (location of seismic line given on Map A). Interpretation of Wright et al., 1996 superimposed. See original authors and text for further discussion.

The LITHOPROBE East onshore Vibroseis, Meelpaeg 3 and 4 profiles, transect Carboniferous units of the Deer Lake Basin across the Fisher Hills block and into the Notre Dame arc across northern Grand Lake (Map A). The seismic data from this project has been processed and interpreted by different authors (Quinlan et al., 1992; Waldron et al., 1998; Hall et al., 1998; van der Velden et al., 2004). Seismic acquisition and processing for this project was designed for deep crustal imaging, however, Waldron et al. (1998) and van der Velden et al. (2004) interpret reflections to represent the interface of Carboniferous sediments and basement. Waldron et al. (1998) depicts the Deer Lake Basin as shallow to the west, deepening into a half-graben to the east, with subsidence focused on a steep east facing normal fault, presumably breaching just east of the Fisher Hills block; whereas, van der Velden et al. (2004) shows the Deer Lake Basin to be shallow and symmetrical, with the BBL/CFS vertical on the eastern margin along the Grand Lake Fault. It should be noted that both of these publications focused on deep structure and the architecture of the Deer Lake Basin is only briefly mentioned in text.

2.4 Proposed Basin Evolution Models

Two alternative structural models for the development of the Deer Lake Basin have been proposed: that of flower structures and lateral basins developed from thermal subsidence (Hyde et al., 1988), based on detailed mapping within the basin and regional potential-field geophysics of Miller and Wright (1984); and that of intermittent fault controlled subsidence (Langdon, 1996), primarily extrapolated from tectonic considerations of regional Carboniferous deposition in the Maritimes Basin and geophysical studies therein. Both authors are in agreement that dextral transpressive

movement along the Cabot Fault system produced tight folds within the Anguille Group with axes and second-order faults oriented obliquely to strikes of through-going steep bounding-faults, forming positive flower structures (e.g., Harding, 1985). However, timing, duration, and mechanisms of basin development have been debated (Hyde et al., 1994).

Hyde et al. (1988) proposed that deposition of the Anguille Group followed rifting related to strike-slip faulting in the late Devonian(?) to early Tournaisian. A subsequent dextral transpressive movement along the Cabot Fault System in the Tournaisian uplifted and deformed the Anguille Group. This interpretation is based on sandstone clasts found in the Tournaisian Wigwam Brook Formation that contain the same heavy minerals (epidote and garnet) as is observed in sandstones of the Saltwater Cove Formation, implying that the Anguille Group was uplifted, at least in part, by the Tournaisian. He also interpreted the presence of an angular unconformity of near orthogonal dips between the North Brook Formation and Saltwater Cove Formation in the Fisher Hills block. At this location a greater stratigraphic thickness than vertical thickness of the North Brook Formation is interpreted to reflect offlapping of North Brook strata to have been deposited in a small pull-apart basin, and that deposition occurred during uplift of the flower structure(s). He also pointed to locally derived schist and quartzite clasts in the North Brook Formation to imply uplift to the south before North Brook Formation deposition. Hyde et al. (1988) also interpreted onlapping stratigraphical relationship, combined with matching clasts in Viséan units to proximal sources on the western Humber Basin margin, to indicate no lateral movement since deposition. Viséan Deer

Lake Group sediments unconformably overlying pre-Carboniferous basement on the western margin of the Humber Basin led Hyde et al. (1988) to ascribe post-Tournaisian sedimentation in the Deer Lake Basin to lateral growth by thermal subsidence, combined with normal faulting, east and west of the Fisher Hills and Birchy Ridge structural blocks. This model predicts that the Deer Lake Group and Howley Formation both unconformably overlie pre-Carboniferous basement (i.e., the Deer Lake Group does not underlie the Howley Formation in the Howley Basin).

Alternatively, Langdon (1996) purposed that basin initiation in the Late Devonian-Tournaisian was produced by extensional collapse of an over-thickened crust at the Acadian mountain front, accompanied by dextral transtension along irregular fault traces of the CFS. This produced a distensive east-dipping half-graben into which the Anguille Group was deposited. Continued dextral displacement along shifting faults geometries in the CFS, caused a pulse of regional transpression and inverted the Anguille Group in the Tournaisian. Second-stage expansion of the Deer Lake Basin in the Viséan (Deer Lake Group deposition) is described as resulting from the development of cross-cutting east-west faults with dextral lateral movements, creating right-stepping geometries and pull-apart basins. Continued inversion of the Anguille Group is considered by Langdon (1996) to have occurred in the Namurian to Westphalian. Under a regional transpressive stress field through the Westphalian, active dextral strike-slip fault geometries confined subsidence to the Howley Basin, but produced reverse faulting in the northwestern Humber Basin. Deposition must have continued into the Permian to account

for known burial depths of the Howley Formation, but have since been eroded (see Langdon, 1996 for a full description).

Chapter 3: Structural Analysis of the Howley Basin

The internal structure of the Howley Basin is poorly documented and understood. This is mainly due to extremely sparse exposure, and a lack of detailed structural analysis, seismic reflection geophysics, and deep drilling within the basin. Previous interpretations of the evolution of the Humber and Howley Basins have relied primarily on regional considerations, while mappable structures within the Howley Basin have largely been overlooked (e.g., Hyde et al., 1988; Langdon, 1996; Section 2.4).

The construction of a dam on Grand Lake at the outflow of Junction Brook in 1924 (Howley, 2009) flooded the low-lying topography in the central region of the basin, creating Sandy Lake. Furthermore, much of the basin is covered by thick glacial till, limiting exposures to eroded streambeds along the eastern and western margins of the basin. In fact, there are no bedrock outcrops within the central region of the basin. This is a very limiting factor when attempting to delineate the structural geometry of the basin.

The basin has been explored in shallow drilling programs along its margins during coal exploration in the 19th century, and uranium and asbestos exploration in the late 1970s to early 1980s. Drill logs from these historic drilling operations are reported on, but provide little insight into the structure of the basin (Appendix A).

To date there have been no published detailed cross-sections of the structures within the Howley Basin: Hyde's (1979a, b), Hyde's et al. (1980) and Hyde and Ware's (1981) geological maps documented some macroscopic structures of the basin, but Hyde's regional cross-sections did not contain structural constraints for the overall

architecture of the Howley Basin (Hyde, 1982). Popper's (1970) cross-sections transect Anguille Group members through the Fisher Hills region further south, and the cross-section of Cawood and van Gool (1998) is also located south of the Howley Basin proper. LITHOPROBE East transects that cross the basin have been processed for deep crustal reflections and have poor resolution of the shallow crustal structure (Quinlan et al., 1992; Hall et al., 1998; Waldron et al., 1998; van der Velden et al., 2004).

The following sections describe the structural analytical methods employed in the study, and the mappable structures within the Howley Basin. These structures are documented in a series of detailed geological maps, constrained viable vertical cross-sections, and associated stereoplots for orientations of the various structural elements. In the absence of exposure, digital terrain models (DEMs) (Map B) and aeromagnetic data (Maps C, D) are of great value in delineating structural features and are presented and described throughout this chapter. Derivation of these maps is given in Chapter 4.

3.1 Methods

Geological mapping of the Howley Basin was completed over two field seasons, from August 14th to 22nd, 2012 and August 29th to September 2nd, 2013. These periods were chosen based on low precipitation during the preceding weeks, because most of the outcrops within the basin occur low in streambeds. Increased precipitation at the end of both field trips made continued work unpractical.

Mapping of the Deer Lake Basin by the NLGS by Hyde, in the late 1970s and early 1980s, is the most extensive and detailed report on the surficial structures of the

basin to date. Geological base maps (Hyde, 1979a, 1979b; Hyde et al., 1980; Hyde and Ware, 1981), used for his 1:100,000 compilation map of the Deer Lake Basin (Hyde, 1982), were used to locate known exposures within and east of the Birchy Ridge area. These locations were visited and re-examined for stratigraphic and structural features. Areas of new development since the early 1980s (i.e., new logging roads, clear cuts, and quarries) were explored for new bedrock outcrops.

Some of the outcrops documented on Hyde's maps were not found. This is likely due to erosion and slumping of surficial material into streams with high/steep banks, covering previously exposed sections, or migration of sediments and/or encroaching spruce forests or bogs in the less turbulent, flatter-lying streams. In some instances high water levels of streams prevented examination of documented riverbed exposures.

Exploration for coal in the Howley Basin was a priority for the NLGS between the years of 1879 to 1909 (Murray and Howley, 1881, 1918), and prospective tracts of land within the basin became privately owned, explored, and mined into the 1920s (Hatch, 1921; Hayes, 1949). These earlier efforts in coal exploration and extraction were the most laborious attempts at uncovering the stratigraphy of the Howley Formation, which lies under a thick cover of superficial deposits over much of the basin. Results of boreholes, trenching, and notes on now flooded exposures recorded during these early workings have been integrated into this study because they offer a glimpse into the internal structure and stratigraphy of parts of the basin with no current exposure.

Data obtained in these early coal explorations is difficult to pinpoint onto current maps because most of it is referenced to geographic features in text. To further obscure the accuracy of locating the positions referenced to, rising of the water level in the Grand Lake-Sandy Lake watershed in 1924 (Howley, 2009) has since changed the extent of the water courses in this region. Also, azimuths used to describe geographic features, relative distances between locations of interest, and oriented features are implicitly referenced to magnetic north. All of the above was taken into consideration when attempting to place this data onto the following geological maps and incorporate it into this study.

Locations of exposures studied during this investigation were recorded with a Garmin MAP62® handheld GPS, WAAS (Wide Area Augmentation System) enabled, in NAD83 UTM Zone 21N. Previous geological mapping in the Howley Basin was completed before the wide use of field-based GPS units, and locations of previous field data must have been located by geographic features from topographic maps and air photos. The precise documentation of exposure localities with GPS improves the overall dataset for the Howley Basin. A Freiberg geological compass was used to collect orientation data, and is presented in dip direction/dip amount notation for planar features and plunge-trend notation for linear features. All data were recorded in field notebooks and placed into spreadsheets on a personal computer at a later date.

Geological data collected in this study – and unlocatable, pertinent observations made by previous workers – were overlain onto a newly created digital geological map for the study area (Map A). This map was created from geological data (Newfoundland and Labrador Geological Survey a, b, c) and topographic data (Natural Resources Canada

a) downloaded from the NLGS's Geo Atlas and Natural Resources Canada's (NRCan) web portals, respectively, and reprojected into NAD 83, UTM Zone 21N. Geological units, and locations of contacts and faults, were modified to adhere to field observations and geophysical interpretations. Lithological subdivisions (Map A) of pre-Carboniferous rocks were created by separating units based on their Generalized Unit Name and their Detailed Rock Type, as given in the attributes table associated with the Detailed Geology Layer file available from the GSN's Geo Atlas. This was deemed to be the most useful subdivision of geological units for this study because the Generalized Unit Name groups rocks of similar affinity and the Detailed Rock Type separates rocks based on their overall composition, which can correspond to physical properties of rocks (i.e., magnetic susceptibility and density); this is helpful in delineating units with potential-field geophysics (Chapters 4, 5). Carboniferous strata subdivisions were kept at the greatest detail possible from the same layer file.

Orientation data for locations on Hyde's 1:50,000 geological maps (Hyde, 1979a, 1979b; Hyde et al., 1980; Hyde and Ware, 1981) that were not found during the present study were measured from copies of his paper maps with a protractor relative to the UTM grid and placed onto digital maps. Locations were determined by referencing to geographical features on topography maps of the area. Symbols used to differentiate between data collected during this study and those that have been copied from Hyde's maps are given on Map A.

Detailed geological maps of subareas were created at various scales. These subareas are grouped into the Southeastern Margin (Section 3.2), Northeastern Margin

(Section 3.3), Northern Margin (Section 3.4), Western Margin (Section 3.5), and Birchy Ridge regions (Section 3.6), in order to present all structural geological data collected in the surveyed area (Map A). Each detailed geological map is accompanied by a vertical cross-section and a lower-hemisphere, equal-area stereographic projection plot of orientation data.

Viable vertical cross-sections were constructed for each of the subareas based on considerations of the observed structural styles and orientation patterns. Symbols used in the cross-section design are given on Map A. Cross-section trends were set orthogonal to the beta axis of the corresponding strip map (i.e., average calculated fold axis orientation, based on bedding orientation data). In some instances, however, homoclinal sections gave poorly constrained beta axes, and apparent dips in such sections show values close to true dip if cross-section trends were set slightly oblique to their calculated beta axis. Beta axes and pi girdles were calculated for areas with sufficient bedding orientation data using GEOrient (Holcombe, 2011). For a given cross-section trend, apparent dips of planar features were calculated with GEOcalculator (Holcombe, 2013), with locations projected orthogonally onto the plane of section. Down-plunge projections of stations with bedding orientations were deemed unnecessary for several reasons. The calculated beta axes show low plunges, but somewhat variable trends due to a mild degree of non-cylindricity of the structures, as well as to the inherent inaccuracies of strikes measured on the irregular surfaces of the thick beds. For low plunges of beta axes, the difference in geometry between the constructed fold profile and the vertical section is minimal (Ramsay and Huber, 1987). Variation in trend of calculated beta axes may lead to inappropriate cross-

over of the projection lines for adjacent stations. All stations lie at the bottom of stream beds which have low topographic elevation gradients; also elevation differences between bottom stream bed and top of valley wall are low (<50 m). These aspects have little effect on the construction of the vertical sections, and stations are conveniently projected onto the elevation gradient of topography in the plane of section.

Macroscopic folds have been delineated in a number of subareas, in both the Eastern and Western Margins of the basin. In all cases, folds are characterized by straight limb dip domains with narrow, angular to sub-angular hinge zones. Unfortunately, macroscopic hinge zones are not observed in the field – primarily due to the lack of exposure – with the exception of some larger mesoscopic folds, located in quarry walls of the Anguille Group in the Birchy Ridge area (Map A; Section 3.6). Based on orientation data analysis of bedding in macroscopic folds and observations of fold styles of mesoscopic folds, folding in the study area is considered to be kink-style in nature; polyclinal kink-fold geometries were observed in a few localities. The folds affect well-bedded siliciclastic successions of relatively competent sandstone strata with relatively minor interbeds of shale and siltstone, and in rare localities coal and limestone. Given the mechanical constitution of the folded successions and the kink-style of the folds, it is reasonable to assume that the folds have class 1B (parallel-style) profile properties, and formed by a flexure slip and/or flow mechanism. This mechanism leaves the beds internally unstrained, and maintains orthogonal bed thicknesses throughout folded layers (Ramsay and Huber, 1987; Marshak and Mitra, 1988). In well-constrained observed and constructed fold sections, no evidence for thickening or thinning of beds on opposing fold

limbs has been observed, strengthening the argument that folding is accommodated by flexure slip or flow.

In order to maintain orthogonal bed thickness in cross-sections with kink-style folding, axial planes must form the bisector plane of the bedding planes on the opposing limbs (Marshak and Mitra, 1988). When calculated axial planes for sets of bedding planes with large differences in orientation, with a well-constrained fold axis, are projected into the plane of section, they produce axial planes with apparent dips that are very close the bisectors of the apparent dips of the bedding planes in the section. But, in situations where kink axial planes were calculated for sets of bedding planes with only slight differences in orientation, the results may produce spurious axial planes that can be very different from the bisector of their apparent dips in section; this is primarily due to the poorly constrained beta axis of those planes not accurately representing the fold axis (e.g., Ramsay and Huber, 1987). In the vertical cross-sections presented in this study, axial planes are drawn as the bisectors of the apparent dips of bedding planes because they produce more realistic fold geometries, in keeping with maintaining apparent bed thicknesses. The cross-sections below show viable geometries, in terms of balanced section constructions (Marshak and Mitra, 1988), and are a good first-order approximation of fold style within the study area.

Faulting is common within the Carboniferous strata in the Howley Basin, particularly with increased proximity to basin-bounding faults; however, because of the lack of exposure, it is likely that many faults are not directly observable in outcrop. Their presence and apparent offsets are further obscured by the absence of repeated correlable

stratigraphic sequences. Thus, the presence and frequency, as well as orientation and movement patterns of faults displacing Carboniferous strata are largely unknown. This makes calculating approximate stratigraphic thickness of the Howley Formation speculative. On the assumption that displacements on faults within the Howley Formation are relatively minor, estimates of stratigraphic thicknesses are reported for subareas with homoclinal sections, excluding the documented macroscopic folds.

3.2 Southeast Margin

The Southeast Margin of the Howley Basin extends for 11 km along the eastern shore of Grand Lake where a narrow, up to 1.5 km wide strip, of Howley Formation is exposed to the west of its faulted contact with Silurian mafic and felsic volcanics of the Topsails Igneous Complex along the Grand Lake Fault (Map A). Exposures of the Grand Lake Fault are limited to outcrops in Alder Brook and Coal Brook (Map A), but only strike orientation can be estimated at these locations, based on geomorphic expressions. In other areas, closely spaced outcrops of Howley Formation to the west and pre-Carboniferous igneous rocks to the east, constrain its location. In the absence of exposure, the presence of the Grand Lake Fault is marked by a sharp topographic gradient running along its length (Map B) and a short wavelength, high amplitude magnetic signature present in igneous rocks to the east (Map C). Thus, despite the lack of exposure, the location of the Grand Lake Fault is well defined on the Southeastern Margin of the basin, and has an overall trend of 220°. To the north, the map pattern shows that the Grand Lake Fault has a dextral strike separation of 1.25 km along an inferred southeast-northwest

trending cross-fault (Map A), north of which the basin widens considerably. Presence of the inferred cross fault is well established in physiographic and magnetic expressions (Map B and C), and is tightly constrained by a single outcrop of Howley Formation in its crook, with pre-Carboniferous igneous rocks exposed nearby in the highlands to the northeast and southwest (Hyde and Ware, 1981; Map A).

The best exposed sections of the Howley Formation anywhere in the basin occur along the southeastern margin of the basin, in Alder Brook and Coal Brook (Map A). These brooks flow westward off the Notre Dame arc highlands into northeastern Grand Lake exposing up to 1.5 km long sections of Howley Formation in deeply eroded canyons. Other, isolated, exposures of the Howley Formation along this portion of the basin occur in a couple of other streambeds, road berms, and the northeastern shoreline of Grand Lake (Map A).

The most southerly exposure of the Howley Formation occurs along the northeastern shore of Grand Lake, south of Hinds Brook (Hyde and Ware, 1981; Map A). This location was inspected, and a poorly sorted, sub-rounded, pebble to cobble, polymictic conglomerate bed was observed (Figure 3.1), but active erosion along the shoreline has caused this outcrop to slump off into large boulders, destroying any measurable features.

Hyde and Ware's (1981) map shows that the Howley Formation at this location is dipping very steeply to the northwest (335/71), and they interpreted a curved splay of the Grand Lake Fault to strike parallel to this bedding orientation, separating it from Silurian

Figure 3.1: Photograph of polymictic massive pebble to cobble conglomerate bed of the Howley Formation subcroping at its most southerly exposure along the eastern shore of Grand Lake. Active erosion has caused this once in situ outcrop (Hyde and Ware, 1982) to slump off into boulders. Hammer is 28 cm in length.

felsic volcanics exposed just to the south (Whalen and Currie, 1988; Map A). However, in Hyde's (1982) compilation map this contact is shown as an unconformity. Given the steepness of bedding in the Howley Formation here, this unconformity would need to have been greatly tilted by post-Westphalian faulting or folding that affected both the Silurian volcanics and the Howley Formation. This is an unlikely scenario, and Hyde and Ware's (1981) original interpretation of a faulted contact is favored (Map A).

3.2.1 Hind's Brook

The most southerly *in situ* exposure of the Howley Formation occurs along the northern road berm just northeast of the Hinds Lake Hydroelectric Generation Station (Figures 3.2, 3.3). Here, very coarse to conglomeratic arkosic sandstones with sub-angular clasts dip steeply and young towards the west, as indicated by fining-upwards grading and a sharp contact between a conglomerate and sandstone bed. Bedding shows minor variation in strike and dip, and is treated to represent a homoclinal dip domain (Figures 3.2, 3.3). Further to the southeast, across the Grand Lake Fault, hematized, fractured, amygdaloidal basalt of the Topsails Igneous Complex (Whalen and Currie, 1988) shows faults dipping steeply to the northwest and moderately to the south. Stepped fiber slickenlines on the southerly dipping fault indicate a normal-dextral sense of motion, and the northwestery dipping fault shows dip slip grooves (Figures 3.2, 3.3). Further to the southeast, strongly fractured and chloritized quartz-porphyritic rhyolite, containing thin disjunct quartz ribbons and macroscopic quartz veins dipping moderately steep to the east, is exposed. The contact between basalt and rhyolite at Hind's Brook was not observed and its geometry and orientation are speculative (Figures 3.2, 3.3).

The trend of the cross-section shown in Figures 3.2 and 3.3 is chosen to be perpendicular to the mean strike of the bedding in the Howley Formation, and is slightly oblique to the trend of the Grand Lake Fault.

At Hinds Brook, the Grand Lake Fault was not observed directly; however, outcrop spacing between the Howley Formation and basalts constrain its surface location

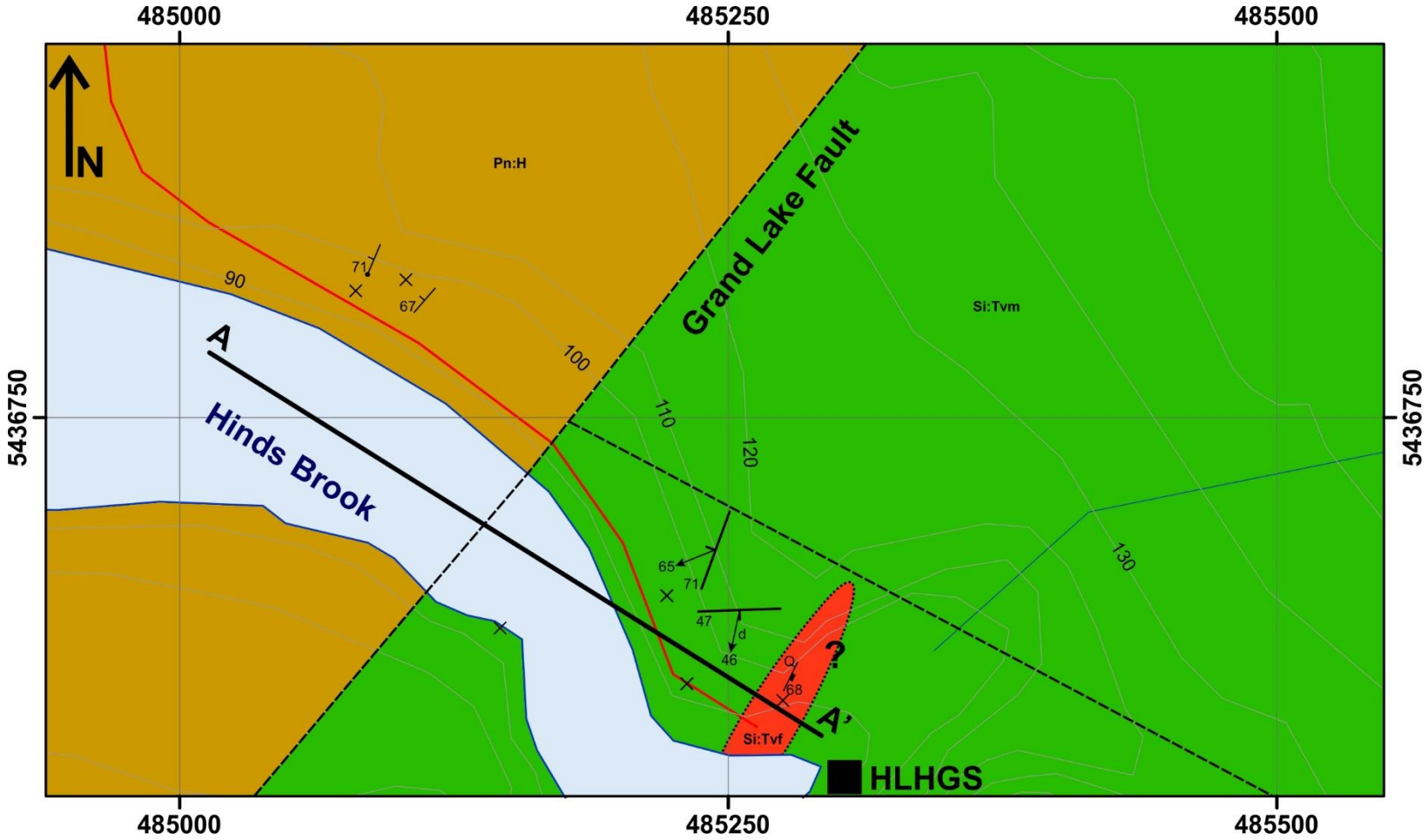

Figure 3.2: Detailed geological map of Hind's Brook showing the location of vertical cross-section A to A', trending at 122°. Location of Hind's Lake Hydroelectric Generation Station (HLHGS) given. Map scale, 1:6,000. Lithological units, map symbols, and location given on Map A.

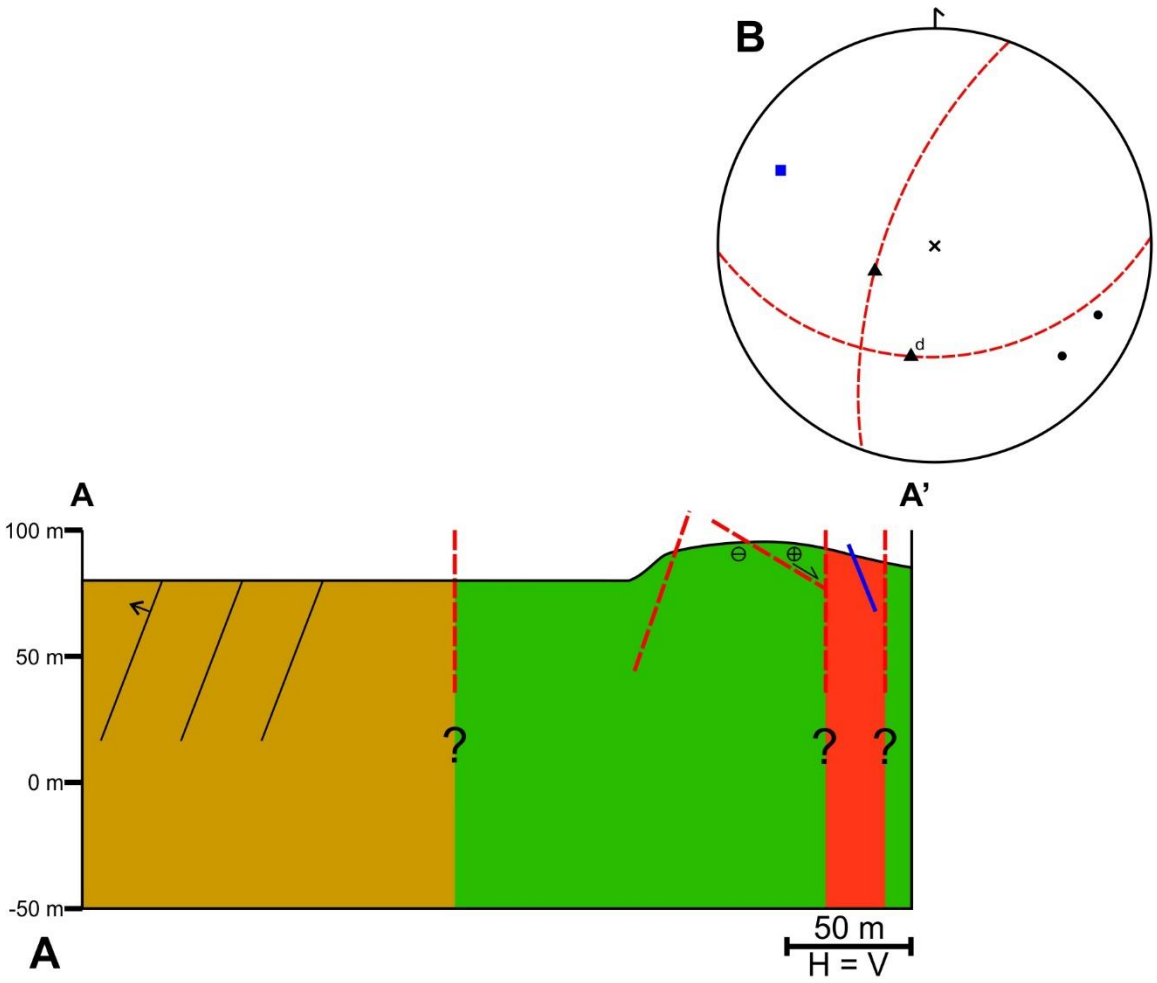

Figure 3.3: A) Vertical cross-section A to A' through Hind's Brook, trending at 122°. Location of cross-section given on Figure 3.2. No vertical exaggeration. Legend for cross-section symbols given on Map A. **B)** Lower-hemispere, equal area stereographic projection plot of structural elements at Hind's Brook; number of poles = 2. Legend for plot symbols given on Map A.

to within approximately 50 meters (Figure 3.2). In order to adhere to field observations, the location of the fault, as given by the detailed faults layer (Newfound and Labrador Geological Survey c), was moved approximately 100 meters to the west. The strike of the fault was adjusted slightly, but kept with the trend of the surrounding topographic gradient (Map B). The dip of the Grand Lake Fault at this location cannot be determined from geological field data, but topography suggests a relatively steep dip.

Approximately three kilometers to the north-northeast from Hinds Brook, a single bedding measurement in a small unnamed brook was recorded by Hyde and Ware (1981), dipping moderately steep to the southeast (Map A). This exposure was sought after, but not discovered during this study. Before the rising of the water level in Grand Lake, Howley (1918a) noted coarse, thick-bedded, friable, gray sandstone and fine conglomerates, characterized by numerous small, white quartz pebbles, outcrop at the mouth of this brook, "dipping S. 10^0 E. at a high angle of inclination." Correcting for the magnetic declination of the era (~30^0 W; Natural Resources Canada b) and assuming a dip of 60^0, this bed has been placed on Map A with an orientation of 140/60, just to the west of the current location of the mouth of this brook (Map A). This location is approximate. Without bathymetry data or a detailed map of this coast before the construction of the dam, it is impossible to accurately determine where the mouth of this stream used to be. Also, a long period of time has passed since Howley's (1918a) observation and the course of this small brook could have changed dramatically since then. Regardless, the moderately to steeply southeast dipping beds in this brook – documented by others – contrast with the steep westerly dips near Hinds Brook (Figure 3.2), suggesting that macroscopic fold(s) are present in the Howley Formation between these two localities (see Section 3.2.4).

3.2.2 Alder Brook

The Howley Formation is relatively well-exposed along Alder Brook in a one kilometer long section from its termination against the Grand Lake Fault in the east, to the eastern shore of Grand Lake in the west (Figure 3.4; Map A). Along Alder Brook the

Howley Formation is dominated by alternating, thick to thin beds of coarse-grained to conglomeratic arkosic sandstones, and fine- to medium-grained laminated, mica-rich, arkosic sandstones, with rare mudstone, shale and thin coal seams. Locally these beds show scouring and grading, and are internally cross-bedded, providing younging criteria, indicating normal way up. There is no clear fining up or down trend in the succession.

These lithologies form a non-cylindrical homoclinal succession that youngs and dips moderate to moderately steep to the southeast (Figures 3.4, 3.5). Minor variations in strike and dip within the succession are regarded as small dip domains that produce calculated axial planes that dip steep to moderately steep to the southwest (Figure 3.5). A beta axis of 40-177 is calculated for bedding planes in Alder Brook (Figure 3.5), but it is poorly constrained due to the lack of opposing fold limbs in the section. There are two aspects to the orientation of the calculated beta axis that raise concerns. The plunge of the axis is unexpectedly steep, especially when compared with fold axes plunges calculated for well-folded sections of the Howley Formation, for example in Coal Brook (see Section 3.2.3). Furthermore, the trend of the calculated beta axis is quite different from that determined for sections showing folds in this area of the basin, and is highly oblique to the basin-bounding fault. This beta axis reflects primarily small-moderate changes in the strike of the beds and is unrepresentative of macroscopic folding in the area A vertical cross-section was, therefore, constructed trending at 123º rather than at 087º (perpendicular to beta axis). This choice of cross-section trend is much more in keeping with the trends of section planes determined for other areas with better constrained

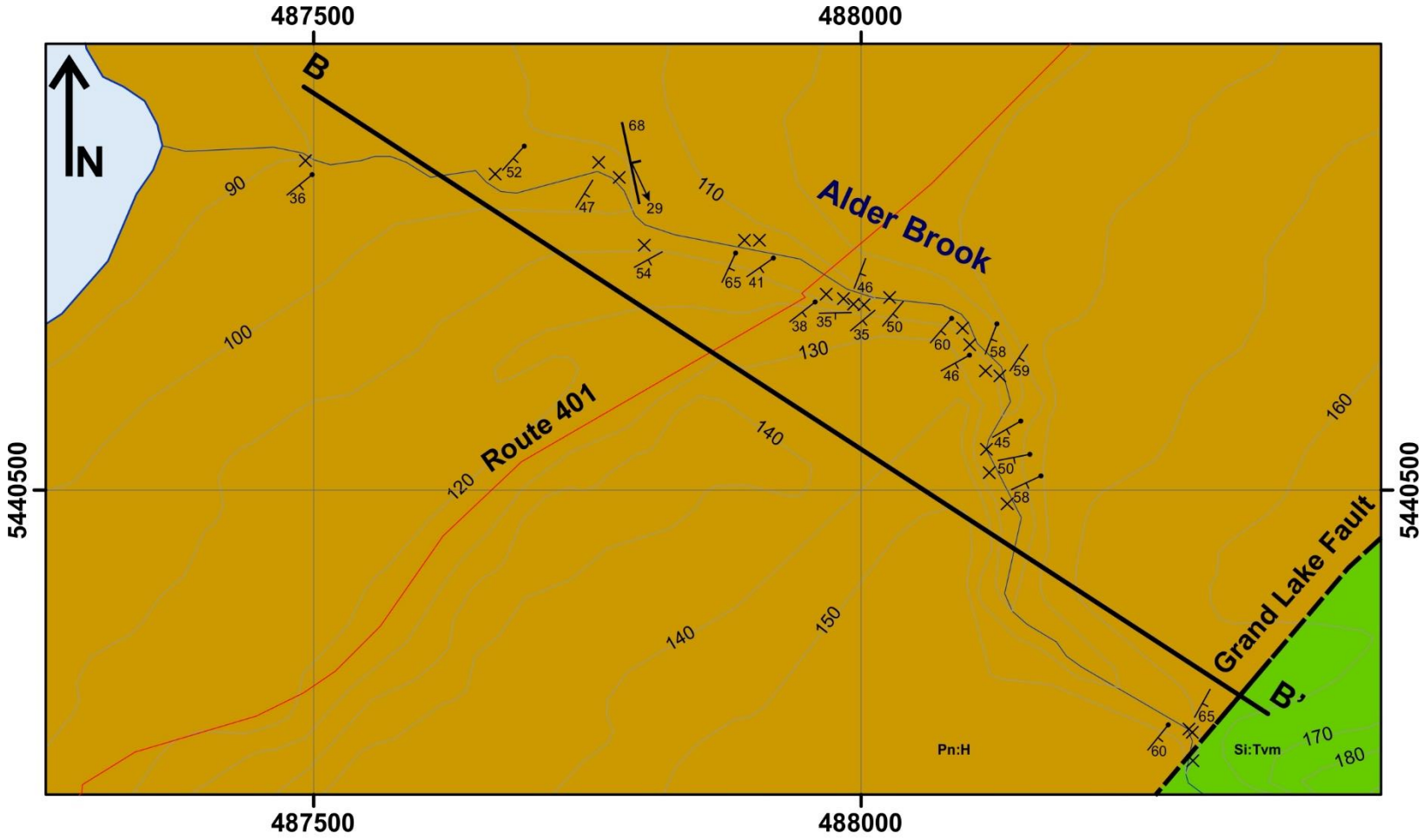

Figure 3.4: Detailed geological map of Alder Brook showing the location of vertical cross-section B to B', trending at 123°. Map scale, 1:6,000. Lithological units, map symbols, and location of map given on Map A.

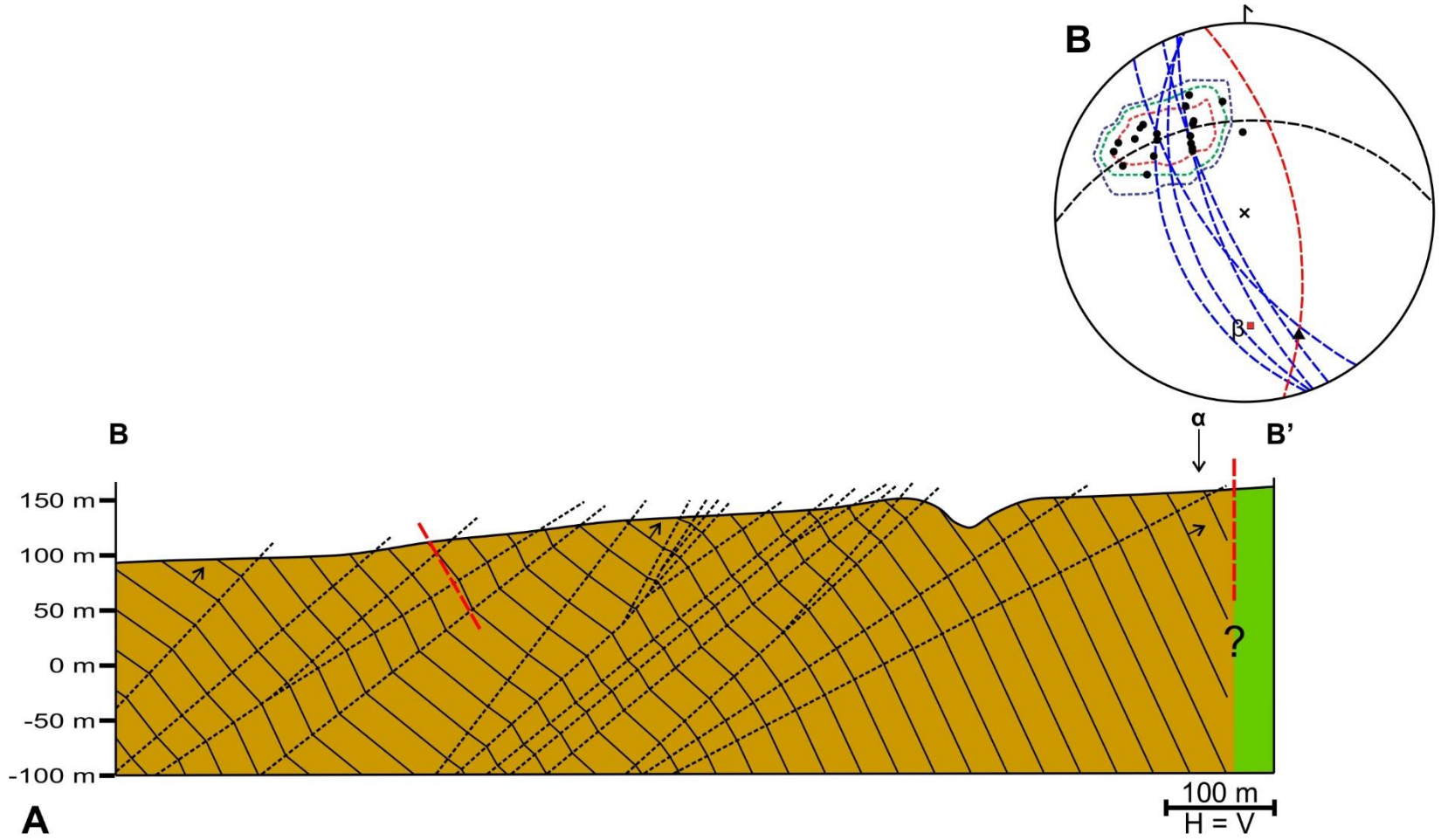

Figure 3.5: A) Vertical cross-section B to B' through Alder Brook, trending 123°. Location of cross-section given on Figure 3.4. No vertical exaggeration. Legend for cross-section symbols given on Map A. **α** marks the location of the projection of the Alder Brook section onto the Coal Brook Section, see Figure 3.7. **B)** Lower-hemispere, equal area stereographic projection plot of structural elements at Alder Brook; number of poles = 20; calculated beta axis is 40-177; calculated girdle is 357/50; contour intervals at 5%, 10%, 20% with a maximum of 30.0%. Legend for plot symbols given on Map A.

structure along the eastern basin margin. It also produces a more viable pattern of apparent dips for bedding in the section than if the section trended 087°.

During an investigation into the structure of the Carboniferous series in the field seasons of 1891 and 1892 (before the raising of the water level of Grand Lake), Howley (1918a) reported: "fine-grained, finely micaceous, greenish-gray sandstone and loose, shaley layers were just protruding above the water surface [near the mouth of Alder Brook], striking up and down the shore in an extremely straight line, dipping to [120^0] between 60^0 and 70^0" (dip azimuth corrected for magnetic declination, 1920; Natural Resources Canada b). This bedding measurement has been approximately placed on Map A; without knowing the exact geography of the eastern shoreline of Grand Lake or the flooded section of Alder Brook before raising of the water level, it is impossible to accurately locate where this observation was made, and therefore it has been omitted from cross-section B to B' (Figures 3.4, 3.5). the measurement is in keeping with other bedding orientations found along this stretch of the shoreline (Map A).

In the northwest part of the section, a moderately steep, east-dipping fault was observed in a coarse arkosic sandstone outcrop with striae on a slikensided surface at 29-155 (Figures 3.4, 3.5), indicating a northwest-southeast directed predominant strike-slip. At the southeast end of the succession, the Grand Lake Fault's location is expected to lay in the streambed between closely spaced outcrops of Howley Formation to the west and Silurian, aphanitic, strongly sheared and hematized amygdaloidal basalt to the east. Although the fault plane is not directly observed, there is a sharp rise in local topography

at this location that trends 220°, and this is regarded as the strike of the Grand Lake Fault in this area (Map B).

Assuming there is no structural repetition or omission of strata within the Alder Brook succession, an estimate for minimum thickness of the Howley Formation along the eastern margin of the basin can be made. Averaging both strikes and dips of all bedding measurements, with assigned equal weights, gives an orientation of 137/50 (dip direction/dip). Using this average strike and dip, anchoring a section perpendicular to strike of bedding at the most northwestern exposure and orthographically projecting the most southeastern exposure into the plane of section, plus correcting for overall change in topography between the two points (a gain of 60 m to the southeast), gives an estimated stratigraphic thickness of approximately 760 meters.

A further 1.5 kilometers to the north-northwest from Alder Brook, Hyde and Ware (1981) documented two exposures of Howley Formation, in an unnamed stream, dipping moderately steep to the east-southeast to southeast (100/41 and 124/42; Map A). These exposures, despite considerable effort, were not located during this study. The beds at these localities have undetermined younging directions; however, considering their moderate east to southeast dips, and their position along strike in between the southeast-dipping and younging homoclinal panel in Alder Brook and the southeast-dipping and younging western fold limb in Coal Brook (see Section 3.2.3), it is likely that these beds represent a continuation of beds between Alder Brook and Coal Brook, implying a southeast younging direction.

3.2.3 Coal Brook

Another 0.5 kilometers to the north-northwest, the Howley Formation is relatively well-exposed for approximately 800 meters along Coal Brook, from where it crosses Route 401 southeastwards to its termination along the Grand Lake Fault (Figure 3.6; Map A). Lithologies exposed along Coal Brook are very similar to those observed in Alder Brook, but structural style is much different. Beds in the southeastern portion of Coal Brook form sub-cylindrical to non-cylindrical, steep to upright folds that trend oblique to sheared and hematized Silurian basalts across the Grand Lake Fault (Figures 3.6, 3.7). The Grand Lake Fault is not directly observable in outcrop, but closely spaced exposures of the Howley Formation to the west and basalts of the Topsails Igneous Complex mark its location, and a sharp rise in topography defines its strike at 220° (Map B).

The folds in the eastern part of Coal Brook define a macroscopic syncline-anticline pair with additional parasitic folds on the eastern limb of the anticline (Figure 3.7). The macroscopic folds are defined by planar, moderate to very steep dipping limb domains with close interlimb angles (48° and 50°). Calculated axial planes for the main kink folds in the east dip steeply southeast (127/76, mean orientation) and are more or less parallel to one another, so that there is no singularity (Marksha and Mitra, 1988) in the kink structure when projected to depth. On the eastern limb of the anticline, near-surface parasitic folds form a gentle (132°) syncline and an open (80°) anticline pair with upright southeasterly and steep northwesterly dipping axial planes, respectively (Figure 3.7). When projected to depth, these folds quickly meet at a singularity, so that at depth

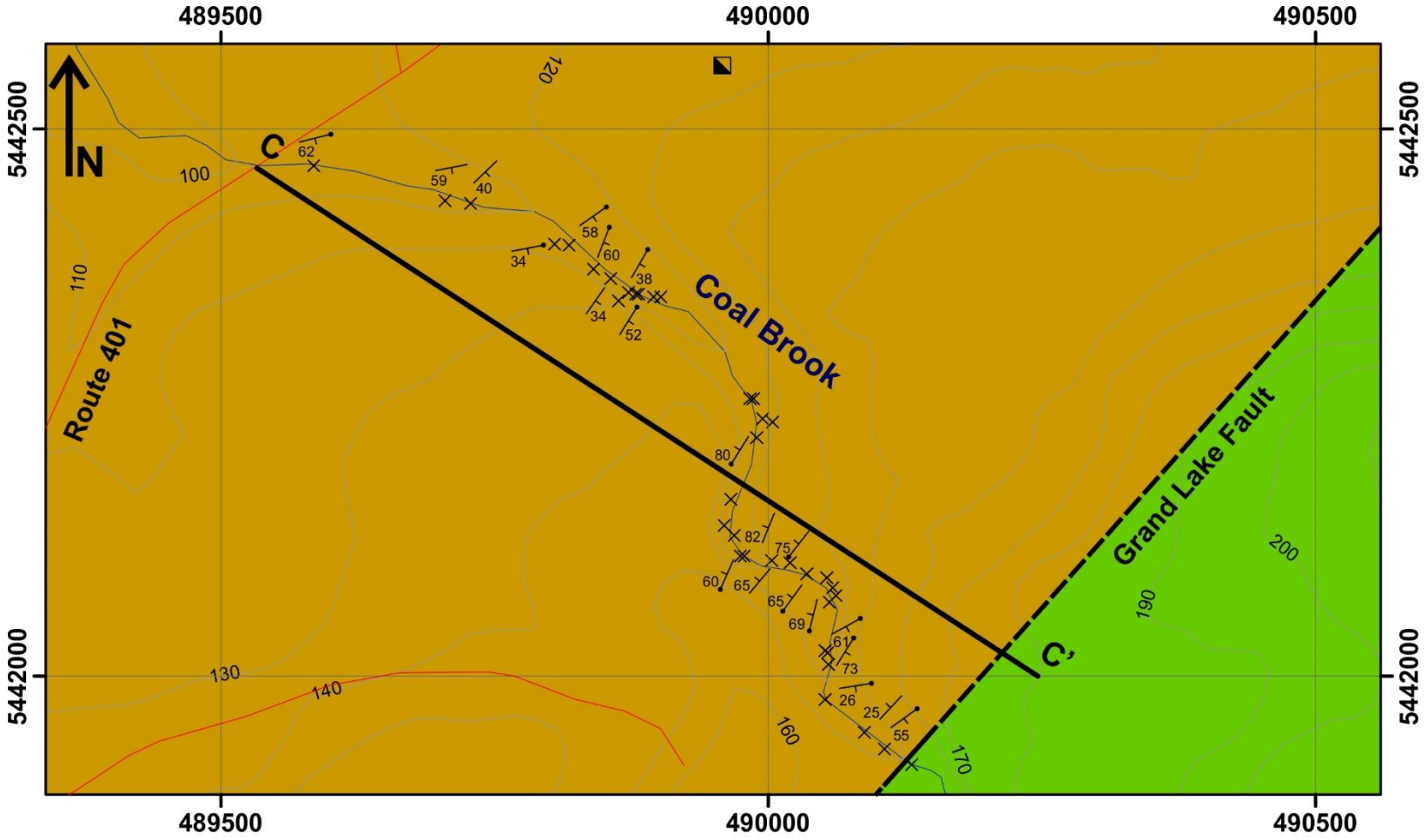

Figure 3.6: Detailed geological map of Coal Brook showing the location of vertical cross-section C to C', trending at 123°. Map scale, 1:6,000. Lithological units, map symbols, and location of map given on Map A.

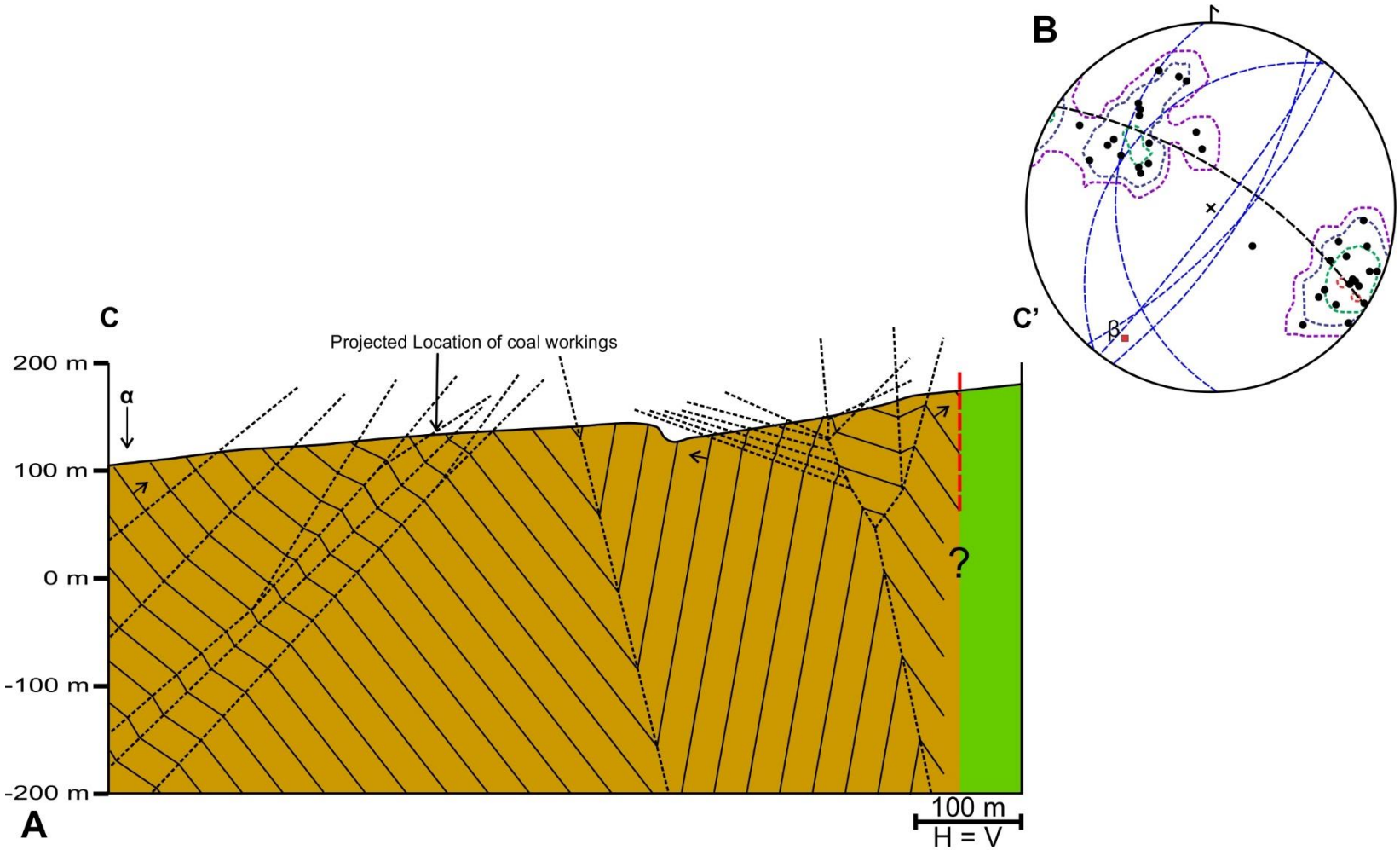

Figure 3.7: A) Vertical cross-section C to C' through Coal Brook, trending 123°. Location of cross-section given on Figure 3.6. No vertical exaggeration. Legend for cross-section symbols given on Map A. **α** marks the location of the projection of the Alder Brook section onto the Coal Brook Section, see Figure 3.5. **B)** Lower-hemispere, equal area stereographic projection plot of structural elements at Coal Brook; number of poles = 35; calculated beta axis is 16-213; calculated girdle is 033/74; contour intervals at 3%, 6%, 12%, 24%, with a maximum of 25.71% . Legend for plot symbols given on Map A.

the eastern limb of the main anticline is solely defined by a single exposure of a moderately southeast dipping bed (Figures 3.6, 3.7).

Bedding in the northwestern section of Coal Brook dips and youngs moderately to steeply to the southeast and south-southeast, forming the western limb of the main syncline (Figures 3.6, 3.7). Slight variations in strikes and moderate variations in dips of bedding close to the hinge of the syncline are interpreted to reflect small dip domains with moderately steep west and southwest-dipping axial planes (Figure 3.7). Further to the northwest, bedding diverges to a more southerly dip direction (Figure 3.6). This compares well with the bedding measurement at the confluence of Coal Brook noted by Hyde and Ware (1981) (see Map A). The steep dips of some of the more southerly dipping beds suggest that they do not represent the strike of a fold hinge, but rather have a more elaborate origin. Coal mining near the intersection of Coal Brook and Route 401, circa 1910, was discontinued because steeply dipping coal measures were offset by faults (Hayes, 1949; Figure 3.6). In re-examination of the workings by the Anglo-Newfoundland Development Co. (Howse, 1947), geologists noted that the faults were near vertical. Thus, the more southerly dips of beds to the northwest likely represent a separate, rotated fault block. Alternatively, the change to more southerly dips in the northwestern section of Coal Brook could be explained by the superimposition of dissipating southeast plunging folds, away from the Grand Lake Fault, onto earlier developed southerly dipping beds. The structural geometry of bedding planes in the western portion of Coal Brook compares very well with that documented for Alder Brook (Figures 3.5, 3.7). The inferred southeast plunging kinks in both areas does not correlate

with the folds in the eastern part of Coal Brook (figure 3.7), and may represent a separate generation of structures.

The pole plot for Coal Brook bedding shows two distinct sub-maxima for moderate to steep southeast dipping beds and steep southwest dipping beds (Figure 3.7). The two pole clusters define high-density maxima which accurately define the calculated best fit pi girdle (033/74) and beta axis (16-213) (Figure 3.7). This beta axis is, however, somewhat skewed by the more southerly dips of bedding towards the northwest. Also, calculated fold axes for the parasitic folds, which are based on single bedding measurements on each of their limbs, give spurious results; axial planes are highly oblique to the master fault trace and fold axis plunge to the north and south. The preferred, and likely the most accurate, mean fold axis for Coal Brook is calculated from averaging strikes and dips of closely spaced bedding measurements nearest to the hinge on either limb of the main syncline (122/46 for western limb and 298/74 for eastern limb). This method gives a fold axis orientation of 04-209.

Folding of the Howley Formation in the southeastern section of Coal Brook likely causes repetition of strata from the west to east, and without recognized unique stratigraphic marker units exposed throughout the fold structure a stratigraphic thickness estimation for the entire section is not feasible. However, in the northwestern section, the moderate to steep southeasterly dipping and younging western limb of the main syncline is very similar in orientation to the homoclinal section through Alder Brook, as noted before (Figures 3.4-3.7). Using the best constrained fold axis, as defined by the syncline in Coal Brook (04-209), to project Alder Brook's homoclinal section into the plane of

Cross-Section C to C', a minimum thickness estimate can be made for both Alder Brook and northwest Coal Brook sections together. This projection puts the most southeasterly outcrop in the Alder Brook section at the most northwesterly outcrop (observed in this study) in Coal Brook, near the intersection of Coal Brook and Route 401 (α in Figures 3.5 and 3.7). The average dip direction and dip for the northwest section of Coal Brook (135/48) is very close to that determined for Alder Brook (137/50), increasing the validity of this construction. Making the same assumptions and using the same methods as was done for Alder Brook, the total minimum stratigraphic thickness of the Howley Formation along the southeastern margin obtained from sections through both Alder Brook and Coal Brook is approximately 990 meters.

3.2.4 Fold Orientation Patterns along the Southeast Margin

The pole plot for bedding within the Howley Formation along the Southeast Margin shows a bimodal population density distribution with two broad sub-maxima for very steep northwest dipping beds and steep southeast dipping beds (Figure 3.8). The broad sub-maxima suggest the presence of an overall non-cylindrical fold geometry, attributed to the minor kink folding of the southeast dipping homoclinal panels in Alder Brook and the west part of Coal Brook (Figures 3.4-3.7). The point maxima in the pole clusters define a gently southwest plunging beta axis (15-213) and a corresponding steep northwest dipping pi girdle (75/033), oriented slightly oblique to the map trace of the Grand Lake Fault along this margin (Figure 3.8).

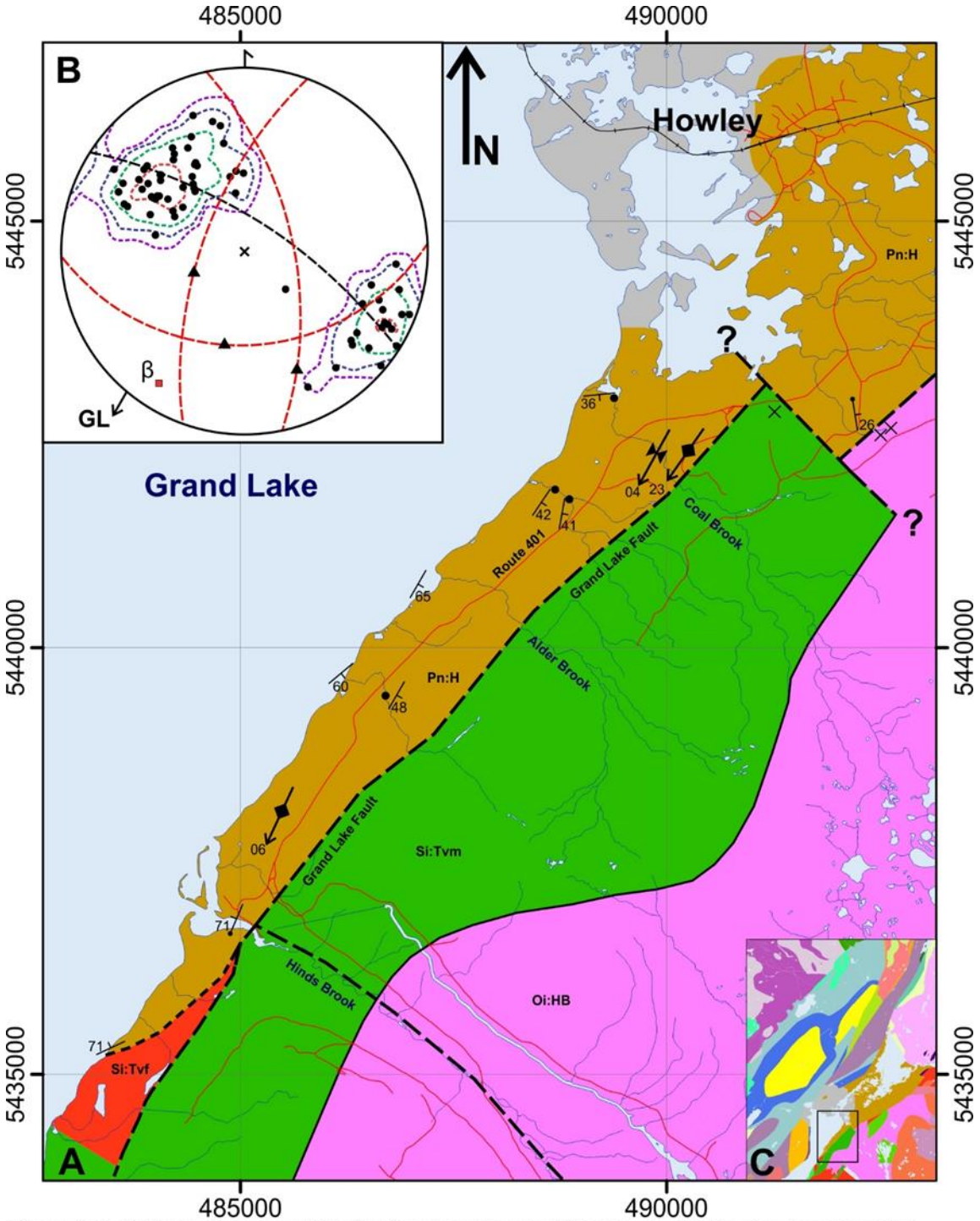

Figure 3.8: A) Geological map of the Southeastern Margin of the Howley Basin, showing calculated fold axes. Lithological units and map symbols given on Map A. Map scale 1:75,000.
B) Lower-hemispere, equal area stereographic projection plot of bedding planes along the South-eastern Margin; number of poles = 62; beta axis is 15-213; pi girdle is 033/75; contour intervals at 2%, 4%, 8%, 16%, with a maximum of 20.97%. Legend for plot symbols given on Map A. Average strike of Grand Lake Fault (GL) at 220^{0}. **C)** Insert showing location of map.

This bedding population distribution stems from a predominance of steep northwest dipping beds in the south and in the eastern section of Coal Brook, and moderate to steep southeast dipping beds in the north and the western section of Coal Brook (Figures 3.4, 3.6, 3.8).

Folding along the Southeast Margin is only relatively well-constrained in the best-exposed section through Coal Brook (Figures 3.6, 3.7). But even here, outcrops do not expose fold hinges and true fold geometries are not fully constrained. The most well-defined fold for the Southeast Margin is that of the macroscopic syncline-anticline pair through Coal Brook (Figures 3.6, 3.7, 3.8). Calculated fold axes for these folds both plunge sub-horizontally to gently to the south-southeast (04-209 for the syncline and 24-215 for the anticline; Figure 3.8).

Another fold in the Southeast Margin is inferred to account for the change in bedding orientations from steep west-northwest dipping and facing beds (293/71) observed near Hinds Brook (Figure 3.8) and the next northerly occurrence of Howley Formation where bedding dips moderately to the southeast (120/48; Figure 3.8). The bedding plane of Howley (1918a; 140/60; Figure 3.8) was not considered as data for interpretation of this fold because of the possibility of a large error in its estimated location. If the two bedding planes (293/71 and 120/48) are projected along the regional beta axis, they are predicted to form an anticlinal fold with an open to close interlimb angle (61°), steeply inclined south-southeast dipping axial plane (116/78), and a sub-horizontal south-southeast plunging fold axis (06-205; Figure 3.8). The geometry of this fold is however very speculative, as it is only defined by a two bedding orientations

separated by several kilometers along strike with no exposure in between. Given the presence of faults observed elsewhere in the limited outcrops available to view, the probability of this fold's continuity over this distance without additional folding and/or faulting is low. But in such a poorly exposed basin, this is the best representation of folding of the Howley Formation, south of Alder Brook.

An alternative view of the stratigraphy and structure of the Southeast Margin of the Howley Basin was presented by Howse and Fleishmann (1982). In their interpretation of the geology of the Southeast Margin of the Howley Basin the stratigraphy of the Howley Formation can be traced along the entire margin (Figure 3.9). They also interpreted that the main syncline in Coal Brook extends south with a faulted (downthrown to the east) curvilinear fold axis, south through Alder Brook, and speculated that it continued north. These features were not observed in the detailed work performed during this study, or documented by Hyde and Ware (1981); the main syncline in Coal Brook was not observed to extend south into Alder Brook. Furthermore, the strikes of beds recorded in this study throughout the map area have significant variations in orientations, whereas the strikes of beds in Howse and Fleischmann (1982) are uncanningly consistent throughout the entire margin (Figure 3.9). Furthermore, the stratigraphy of the Howley Formation was not observed to have the unique stratigraphic succession of marker horizons needed to confidently make correlations between the brook sections throughout the Southeast Margin. In addition, all of the macroscopic fold axes calculated from bedding data collected in this study, combined with those of Hyde and Ware (1981), plunge towards the south-southwest, and are predicted to be truncated by

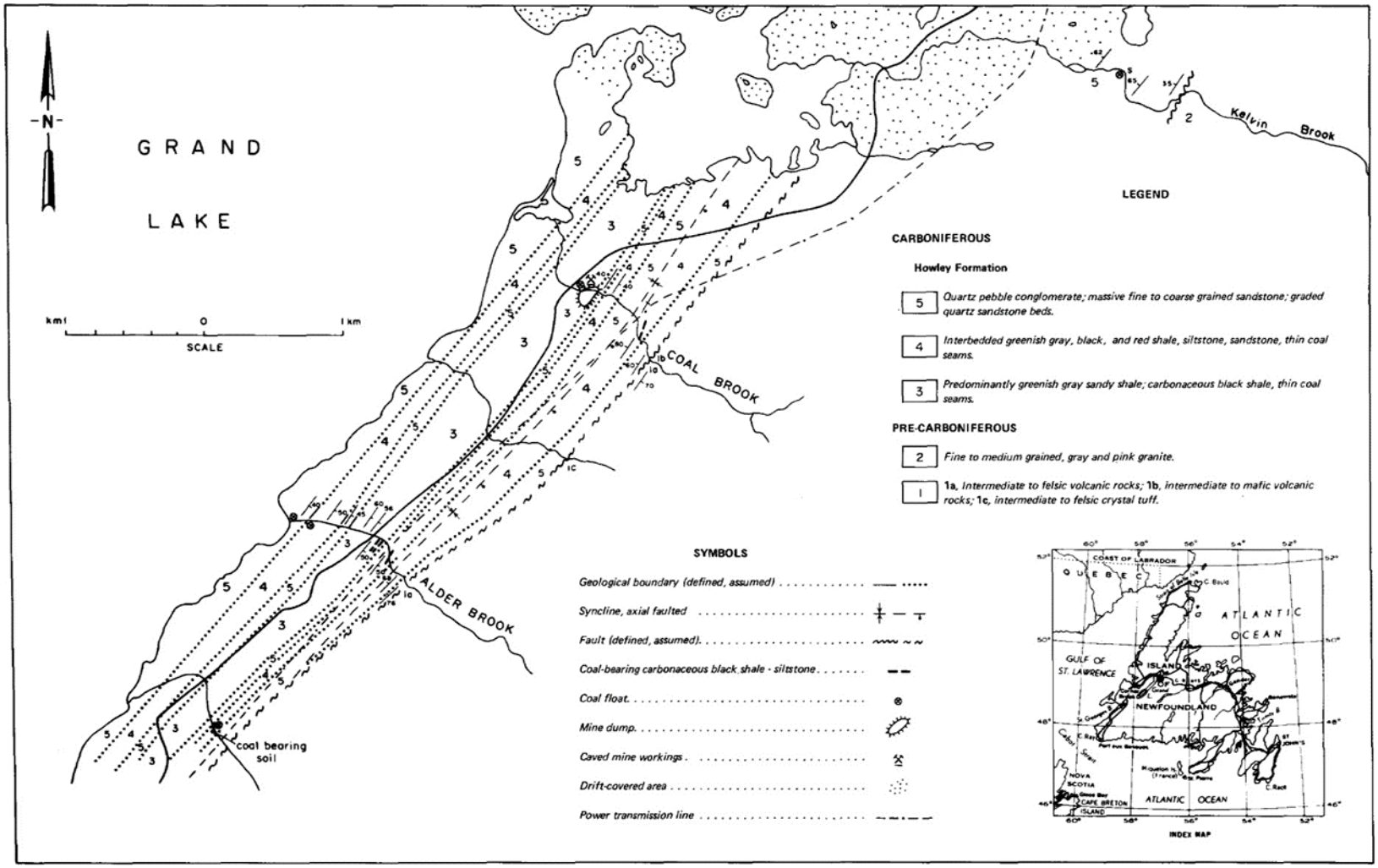

Figure 3.9: Howse and Fleishmann's (1982) geological map of the Southeast Margin of the Howley Basin.

the Grand Lake Fault if projected southwards. This is contrary to the fold pattern inferred by Howse and Fleishman (1982) who trace the syncline in continuity parallel and in proximity to the Grand Lake Fault (Figure 3.9).

All observed and inferred macroscopic folds within the Southeast Margin have steep limbs and open to close interlimb angles that are interpreted to bend as angular kink folds around very steeply inclined southeast dipping axial planes. These are interpreted as contractional folds because such steep bedding dips and close interlimb angles are not predicted for extensional forced folds occurring in the hanging-wall of a listric normal fault (Hardy and McClay, 1999).

The lack of exposure and drilling, or clear geophysical expressions of folds or subsidiary faults in the Howley Formation along the Southeast Margin all make definitive interpretations of stratigraphy and structure difficult. However, given the regional strike-slip nature of the Cabot Fault system (Section 2.1.2), combined with observed oblique slip lineations on subsidiary faults along the fault zone in the map area, and interpreted contractional folds with fold axes making acute angles with the map trace of the Grand Lake Fault (5°-15° to the northwest; Figure 3.8), structures along the Southeast Margin hint at a dextral transpessional event occurring post-Howley Formation deposition (Westphalian A).

3.3 Northeastern Margin

The Northeast Margin, north of the inferred margin-defining cross-fault, extends for 25 km from northeastern Grand Lake to northeastern Sandy Lake (Map A). Along this

margin the Grand Lake Fault separates the Howley Formation to the west from Ordovician and Silurian plutonic and volcanic terrains of the Notre Dame arc to the east. Exposure is extremely poor with the Howley Formation typically occurring as isolated outcrops in streambeds separated by several kilometers along and across strike. The only exceptions are moderately-exposed sections through Kelvin Brook and Northeast Brook (Map A).

The Grand Lake Fault is not observed in outcrop, but its map trace is periodically constrained by closely spaced outcrops of the Howley Formation to the west and Notre Dame arc rocks to the east (Hyde, 1982; Whalen and Currie, 1988; Map A). Between geologically constrained locations, its map trace is well-defined in both topographic (Map B) and magnetic expressions (Map C), with the exception of the area between McGregor Brook and Kitty's Brook where a magnetic low is continuous over the inferred boundary of the fault (Map C). This magnetic low does not correspond to geological boundaries observed at the present-day surface in the Notre Dame arc (Whalen and Currie, 1988), but does have a sharp gradient around its perimeter in all directions, except to the northwest, indicating that it has an upper-crustal source (Map C).

A notable kink in the trace of the Grand Lake Fault occurs in Kelvin Brook, north of which the fault has a more easterly trend (approximately 240°) than seen in the Southeast Margin (Map A). North of Kitty's Brook, three unnamed east-west trending cross faults are interpreted to intersect the Grand Lake Fault and continue into the Notre Dame arc to the east (Hyde, 1982; Whalen and Currie, 1988; Map A). The two more southerly cross faults are interpreted to form a lens-shaped faulted contact around the

Ordovician Hungry Mountain Complex (basement to the Topsails Igneous Suite; van Staal et al., 2007), with Ordovician plutonic rocks and Silurian volcanics to the south and north (Whalen and Currie, 1988; Map A). The most southerly of these two faults has an inferred apparent dextral strike separation of 600 m (Whalen and Currie, 1988; Map A). This offset is however not constrained by bedrock exposures nor is it reflected in magnetics (Map C) or associated with a topographic gradient (Map B), and it is thus considered speculative as to whether the fault has affected the Howley Formation or offset the Grand Lake Fault. Its northerly counterpart is not interpreted to offset the Grand Lake Fault (Whalen and Currie, 1988; Map A). A further 3 km to the north-northeast, a west-northwest trending cross fault is interpreted to offset the Grand Lake Fault with a 1.5 km apparent sinistral strike separation (Map A). To the north of this cross fault, an east-dipping thrust slice of ultramafic rocks is brought to the surface (Adams, 1981; Hyde, 1979b, 1982; Whalen and Currie, 1988; Map A). Adams (1981) has suggested that the Howley Formation unconformably overlies the ultramafics to the west and south. The surficial extent of the ultramafics depicted in Whalen and Curie's (1988) map and the Detailed Bedrock Geology Layer of the NLGS's GeoAtlas is underestimated: exposure of fine-grained serpentinized ultramafics and sericite schist discovered in the berm of a new logging road during this study (not shown on the maps of Hyde, 1979b, 1982, or Whalen and Curie, 1988), extends the strike of the unit by 1.5 kilometers to the northeast (Map A). Intersections of shallow drill holes (Adams, 1981; Map A) in between exposures confirms that the body lies just under the overburden (Section 3.3.5). The ultramafic thrust slice's northwestern faulted boundary has been redrawn along the edge of the large magnetic high associated with it (Map A, C), extending its strike and width, while

adhering to field and drill observations. The magnetic high associated with the ultramafic body extends to the south, beyond the inferred cross-fault, but shows no signs of displacement, suggesting that the presence of this fault may be erroneously interpreted. Notably, there is no constraint by exposures of the Howley Formation on the presence, location, or nature of the northern cross-fault (Hyde, 1979b, 1982; Map A).

The Northeast Margin of the Howley Basin has been explored for coal in the late 19th to early 20th century (Murray, 1918; Hatch, 1921), and less so for uranium and asbestos in the early 1980's (Wilkinson, 1982; Adams, 1981). Coal exploration included testing the near-surface stratigraphy of the Howley Formation by sinking boreholes westwards of the intersection of Goose Brook and the (then) Reid Newfoundland Railway, towards the center of the Howley Basin (Section 3.3.2). Ground-based uranium exploration tested the thick overburden with reverse circulation drilling and geochemical till surveys, but data acquired during these programs are of little use in the structural interpretation of the basin and are not reported on. Three diamond drill holes were situated on the aforementioned ultramafic thrust slice in the northeast corner of the basin in the search for asbestos mineralization, but unfortunately they did not intersect Carboniferous strata (Section 3.3.4; Map A).

Lack of exposure and absence of high-density diamond drilling, or high-resolution geophysics leaves the structure of this part of the basin largely unknown. However, during the 2014 and 2015 field seasons, two seismic lines were collected using the Memorial University of Newfoundland's MUNSIST vibrose source system along logging roads that cross the approximate trace of the Grand Lake Fault and extend to the west,

into the Howley Basin (Vasquez, 2017; Map A). Interpretation of these seismic surveys show the Deer Lake Group to underlie the Howley Formation, together reaching a maximum depth of ~ 1.5 km. Steep to sub-vertical east and west-dipping faults are interpreted in the seismic profiles, with the majority to be isolated in the Deer Lake Group (Vasquez, 2017). Livada (2014) completed a 17 km magnetotelluric survey that transected this part of the Howley Basin (Map A). Results show that the basin is 1-1.5 km deep with Deer Lake formations underling the Howley Formation, but was unable to image mesoscopic structures in the subsurface (Livada, 2014).

The most southerly exposure of the Howley Formation in the Northeast Margin occurs in a logging road berm just north of the boundary-defining cross fault that separates the Southeast Margin and the Northeast Margin (Map A). Here, a single outcrop of poorly indurated, scoured, conglomerate and fine-grained, cross-bedded sandstone show gentle dip and younging direction to the west. Exposure of Silurian mafic volcanics and medium-grained amphibole granite across a narrow valley in the highlands to the east (not shown on the map of Whalen and Currie, 1988), tightly constrains the presence, location, and right-stepping offset geometry of the Grand Lake Fault along this cross-fault (Map A). The Detailed Bedrock Geology Layer (Newfoundland and Labrador Geological Survey a) shows Silurian mafic volcanics occurring where granite was discovered during this study. To accommodate field observations, the strike of the cross-fault was extended to the southeast to the contact between the mafic volcanics and the Ordovician Hinds Brook Granite, and the Hinds Brook Granite is presumed to occupy the area directly to the northeast of the cross-fault (Map A).

3.3.1 Kelvin Brook

The Howley Formation is exposed within a few bends in eastern Kelvin Brook before heavily faulted, fractured, and veined red/pink, locally feldspar and quartz porphyritic rhyolites are encountered to the east of the Grand Lake Fault (Figures 3.10, 3.11). In the west, coarse to very coarse massive arkosic sandstones intercalated with fine-grained sandstones containing abundant coalified plant fossils dip moderately to the southwest. Further east, approaching the Grand Lake Fault, the Howley Formation coarsens to thick scoured beds of poorly sorted, rounded to sub-angular, cobble to boulder polymictic conglomerate beds that young and dip moderate to steeply to the northwest (Figures 3.10, 3.11). These beds are cut by steep to vertical faults with varying strikes (Figure 3.10 – 3.12). Lineations on these faults predominately pitch shallowly (15° to 20°) to the north and east with the exception of a moderately steep pitch (48°) to the northeast on a vertical northeast-southwest striking fault, next to the Grand Lake Fault (Figure 3.10).

In cross-section, bedding is shown to kink around steep southerly and northeasterly-dipping axial planes (Figure 3.11). However, the large contrast in strikes between the most westerly bedding measurement and those to the east suggest that bedding orientations along Kelvin Brook have been affected either by folding and/or rotational faulting (Figure 3.10). Without more data it is difficult to predict any detail of the structure at depth. The small population of bedding measurements in Kelvin Brook produces a moderately west plunging (24-261) calculated beta axis beta and a steeply west-dipping pi girdle (081/66), but these orientations are strongly controlled by the

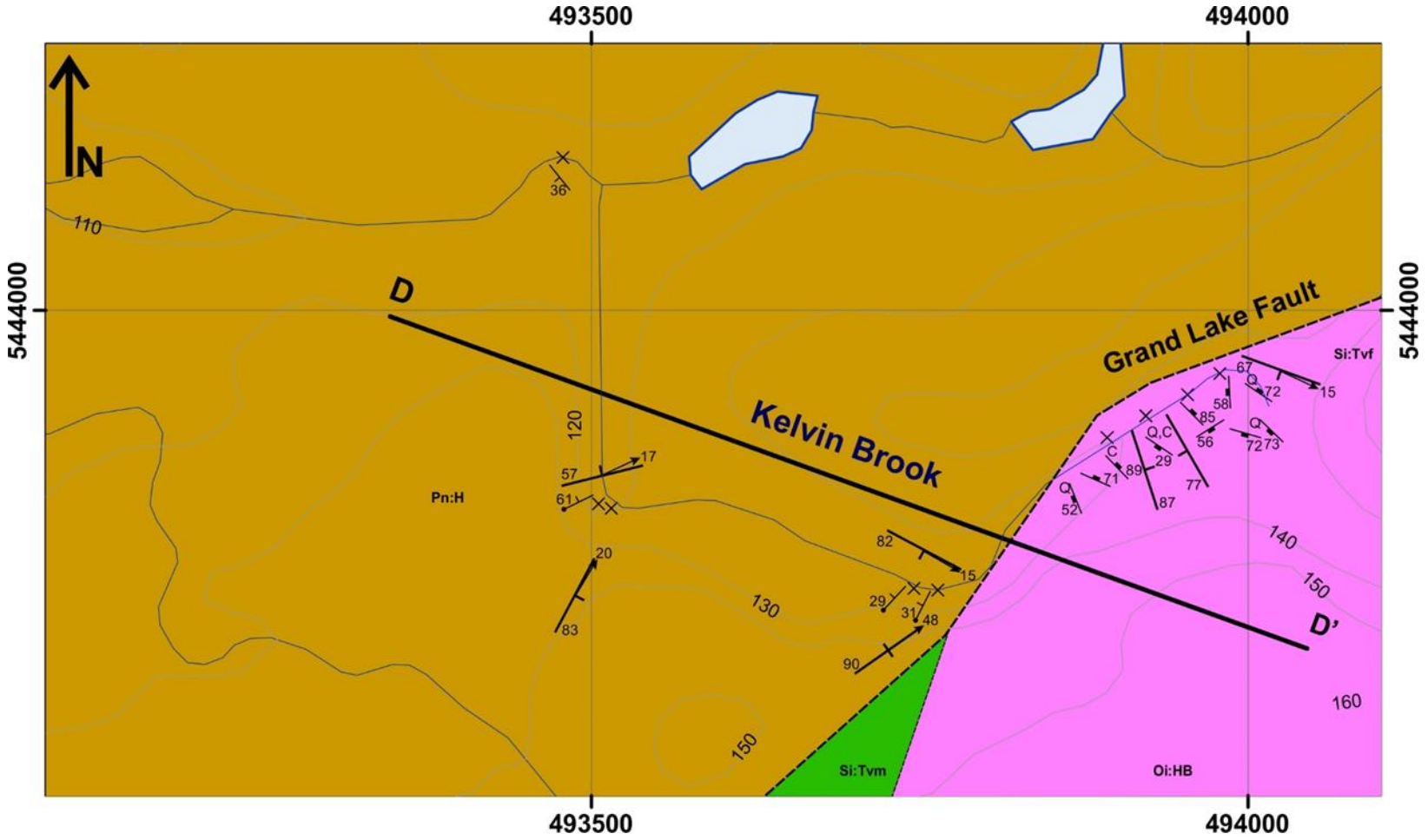

Figure 3.10: Detailed geological map of Kelvin Brook showing the location of vertical cross-section D to D', trending at 110°. Map scale, 1:5,000. Lithological units, map symbols, and location of map given on Map A.

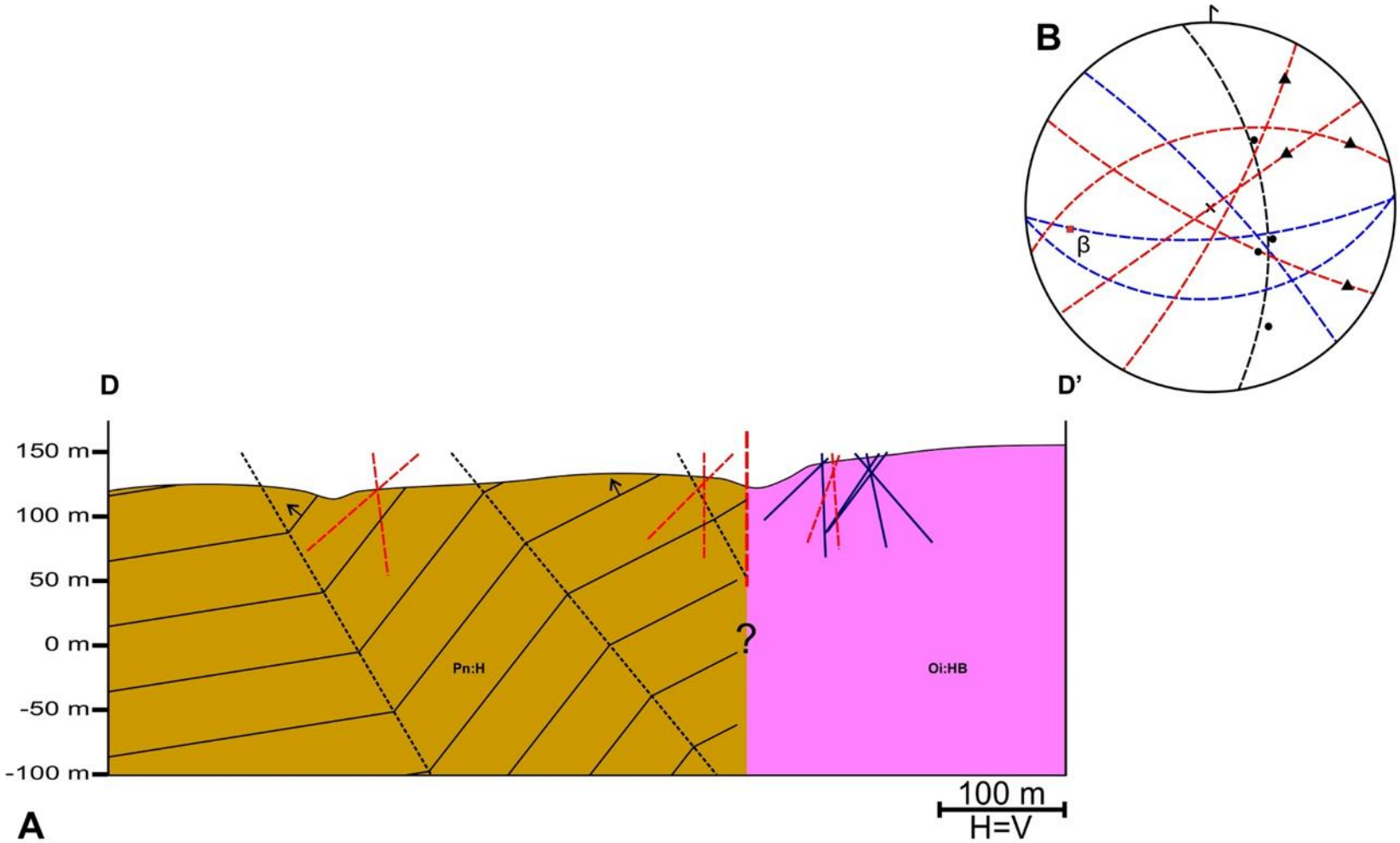

Figure 3.11: A) Vertical cross-section D to D' through Kelvin Brook. Location of cross-section given on Figure 3.10. No vertical exaggeration. Legend for cross-section symbols given on Map A. **B)** Lower-hemispere, equal area stereographic projection plot of structural elements at Kelvin Brook; number of poles = 4; calculated beta axis is 24-261; calculated girdle is 66/081. Legend for plot symbols given on Map A.

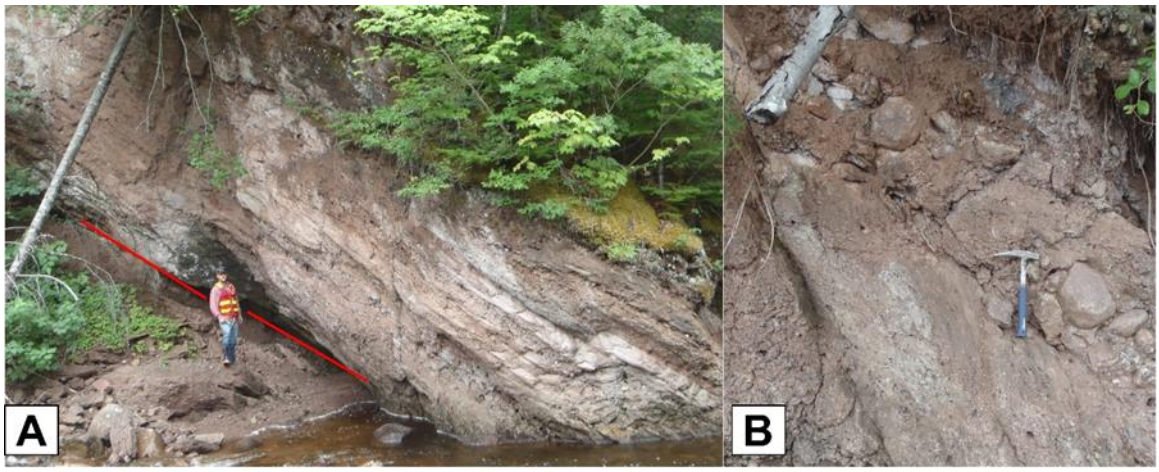

Figure 3.12: A) Photograph looking south towards faulted (red) thick scoured beds of poorly sorted, pebble to cobble conglomerates. Bedding dips moderately to the northwest, fault dips sub-vertically to the southwest. **B)** Close-up photograph of thick scouring conglomerate bed. Hammer is 28 cm in length.

single southwest-dipping bed in the west, and may therefore may not be a true representation of fold orientation (Figure 3.11).

Within 100 m north-northeast further upstream of the last outcrop of Howley Formation in the east, rhyolites are well-exposed in a section of Kelvin Brook, closely constraining the location of the Grand Lake Fault trace (Figure 3.10). The location of the map trace of the Grand Lake Fault needed slight adjustment and the contact between Hind's Brook Granite and Silurian mafic volcanics was moved approximately 100 m to the west to account for field observations (Figure 3.10). Rhyolites exposed along this section are heavily faulted and veined. Quartz and/or carbonate veins and shear fractures predominately dip moderately to very steeply to the northeast and southwest (Figures 3.10, 3.11).

Two boreholes sunk in the field seasons of 1879 and 1893 are quoted as being ¼ of a mile, and the other one 1 ¾ miles up Kelvin Brook, respectively (BH-79-01, BH-93-

01; Howley, 1881, 1918b; Map A; Appendix A). These boreholes were sunk before the raising of the water level of Grand Lake, and since then much of the western extent of Kelvin Brook has been flooded. Before flooding, Kelvin Brook flowed westerly for several miles past its present outflow into Grand Lake, to where it met with, the then called, Sandy Lake River (Howley, 1907). Judging from the descriptions of locations and the pre-flooding map of Howley (1907), these boreholes were actually much further west than what is shown on the maps of Hyde (1978, 1982) and Hyde and Ware (1981). The locations of these boreholes, as shown on Map A, are rough estimates of their locations, but are much closer to their true position than other workers have shown.

The drill log of BH-79-01 (Map A; Appendix A) shows that after 5 m of overburden, alternating, very thick to thin beds of sandstone and shale with intercalated coal persisted to end of the hole at 66 m, dipping northerly at a very low angle (Howley, 1881). The presence of coal in these beds would suggest that BH-79-01 intersected Howley Formation. However, further upstream in the since flooded Kelvin Brook, BH-93-01 (Map A; Appendix A), below 32 m of overburden, intersected alternating very thick to thin beds of shale and sandstone to a depth of 102 m, with an average dip of 50^{o} (undetermined dip direction; Howley, 1918b). The core retrieved from this hole was interpreted to be lower down in the Carboniferous strata than the coal-bearing measures and the succession was considered by Howley (1918b) to be correlable with bituminous shales he had observed exposed in a stream a mile north of Wetstone Point, only a short distance inland from the (then) northwest shore of Grand Lake. Hyde (1982) has since mapped exposures along this section of Grand Lake to belong to the Wetstone Point

Formation (Tournasian conglomerates and sandstones) and Rocky Brook Formation (Viséan mudstones). Thus, it is probable that the bituminous shales described by Howley (1918b), north of Wetstone Point, belong to the Rocky Brook Formation. This location is also where Hatch (1919) calculated the highest oil yields from in the region. Unfortunately the creation of the dam on Grand Lake has flooded this area. Although the presence of these potential source rocks in the borehole near the eastern margin of the basin was of inconsequence to Howley's pursuit of coal, they are significant in evaluating the hydrocarbon potential of this area; if these rocks are Rocky Brook Formation then they would underlie the Howley Formation (at least in part) along the eastern basin margin. This interpretation has not been documented in previous works.

3.3.2 Goose Brook, McGregor Brook, and Kitty's Brook

Proceeding north along the Northeastern Margin there are several isolated exposures of the Howley Formation in brooks that flow from the east into Sandy Lake (Hyde, 1979b; Hyde, 1982; Map A). Despite great effort, none of these exposures were found during this study. All of these outcrops occur close to the assumed and inferred map trace of the Grand Lake Fault with strikes of bedding near parallel to the fault trace (Map A). Dips are shallow to moderately steep and switch between southwest and northeast dip directions. Proximal exposures of igneous rocks of the Notre Dame arc to the east in Goose Brook and Kitty's Brook give a geologically-constrained position of the Grand Lake Fault's map trace along this margin of the basin (Hyde, 1982; Whalen and Currie, 1988; Map A). However, the structure of this part of the basin remains unresolved due to the lack of exposure.

3.3.3 Results of Coal Exploration in the Sandy Lake Area

Construction of the railroad between Kitty's Brook and the Sandy Lake trestle in 1895 revealed lots of coal fragments in gravel cuts, but the lack of exposure in this region left little for interpretation of the geological structure and the lithostratigraphy, including the source of the coal fragments (Howley, 1918c). A gravel cut, about a mile and a half east of Goose Brook, with a greater abundance of Carboniferous fragments in the drift (sandstones and shales rather than the dominant granitic detritus of the highlands to the south and east) prompted Howley to postulate that bedrock lay a short depth underneath the cover and he began removing the overburden (Howley, 2009). He was correct and at a depth of three to four feet uncovered and sunk into a two-foot coal seam, dipping 290/40 (Howley, 1895; Figure 3.13). Further trenching in this area that year, and in 1904, along with a single borehole, uncovered more bedrock and coal seams under a thin interval of overburden. All bedding showed a constant dip towards the northwest, leading Howley (1918d) to believe that the strata were un-faulted or folded in this area. These beds strike somewhat oblique to the beds exposed in proximity to the Grand Lake Fault (Figure 3.13; Map A).

Following this discovery, coal exploration in the basin was focused in the area around Goose Brook, and resulted in numerous boreholes being drilled between the years 1904 to 1921 by Howley (1918d, e, f, g, h, i) on behalf of the NLGS and Hatch (1921) for the Reid Newfoundland Company (Figure 3.13). Core from these operations is not available for inspection, but documented drill logs for most of the holes are attached to the Howley's and Hatch's reports (Appendix A). In lieu of the lack of exposure within

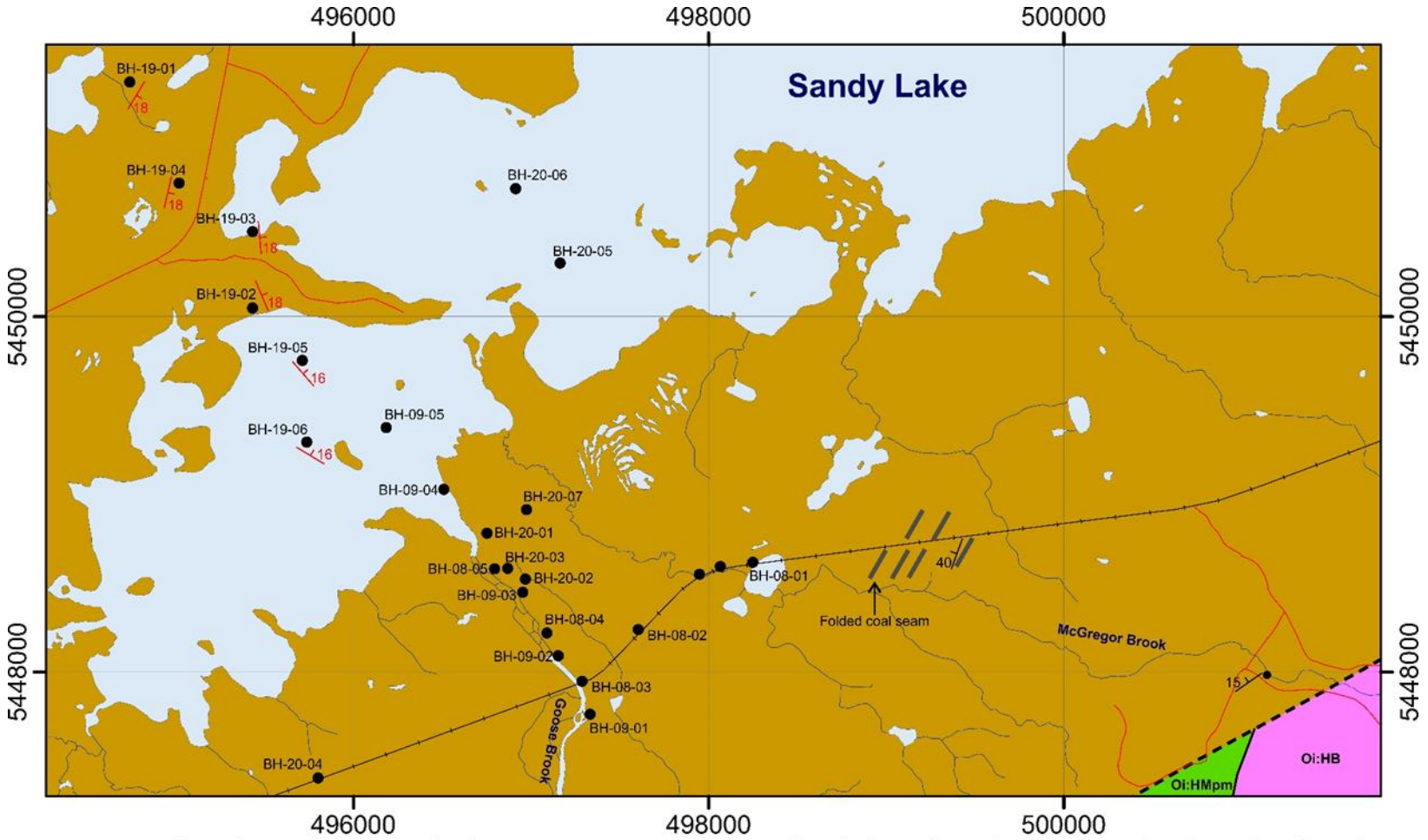

Figure 3.13: Geological map of Goose Brook, showing approximate locations of boreholes and trenches of Howley (1895-1909) and Hatch (1920-1921); see text for discussion. Map scale is 1:37,000. Lithological units, map symbols, and location given on Map A.

this area, these logs provide valuable insight into the near-surface structure and stratigraphy of the Howley Formation towards the center of the basin.

Locations of these exploration sites are given on maps of Hyde and Ware (1981), and Hayes (1949, provided by the Reid Newfoundland Company). However, discrepancies in borehole locations between these two maps prompted an evaluation of their validity. Also, some of the relative distances between boreholes given in the text of the original authors do not coincide with the locations given on the maps of Hyde and Ware (1981) or Hayes (1949).

Accurately locating the positions of these boreholes proved difficult; maps of borehole or trenching locations do not accompany any of the available reports of Howley or Hatch. Instead, the authors give relative distances and azimuths from a landmark or previously sunk borehole. In the case of Howley's (1819c, d, e, f) earlier workings, the descriptions of borehole locations are vague and there are significant discrepancies between descriptions of the same location from different field seasons.

For the boreholes of Hatch (1921), as presented on Figure 3.13, locations were found by using the azimuth and distance between the previous borehole and the next, correcting for the magnetic declination for the area in 1920 (30.78° W Natural Resources Canada b). In his 1920 report, Hatch (1921) referenced the first borehole of the season to mile 354 of the railway. The UTMs of this location (E 0495592 m, N 5447319 m, NAD83 UTM Zone 21N) were found by measuring 1.1 miles westward along the railroad from the Goose Brook Bridge (mile 352.9; T'Railway). In his 1921 report the first

borehole of the season was referenced to the Goose Brook Bridge (E 0497258 m, N 5447930 m, NAD83 UTM Zone 21N). Given the precision of Hatch's (1920, 1921) relative measurements of azimuths and distances between holes (e.g., BH-19-03 is 1475 feet North 13º15' East magnetic of BH-19-02), this method of locating the coordinates of these boreholes must be the most accurate.

The boreholes of Howley, drilled pre-1908, are significantly less precise in their descriptions of borehole locations. Also, drill logs are not appended to his reports on exploration for years prior to 1907. In many instances, Howley started a borehole in one year and would return to that location in a following field season to extend the borehole further. The approximate locations of Howley's boreholes given on Figure 3.13 are labeled by the year they were first reported on, in ascending order.

Within the drill logs of these boreholes the authors, in some instances, give the average dip of bedding relative to (presumably vertical) drill core axis for the entire borehole (Table 3.1; Appendix A). Changes in dip throughout the hole are not stated, leaving the reader to wonder to what extent of variance in dip within the borehole exists. In the reports of Hatch (1921), he also states the dip direction of bedding for the entirety of each borehole, and in several of Howley's reports (1918h, i) he shows changes in dip directions between holes. It is unclear how either of these geologists were able to undoubtedly make conclusions on the strikes of bedding encountered in the boreholes given the technological resources available to them at that time. This is so because strikes of beds cannot be uniquely determined in vertical drill holes based on bedding/core angles alone (Marshak and Mitra, 1988).

Table 3.1 summarizes the results of borehole logs post-1906, with their respected depth of overburden, vertical depth, percentage of shale intersected (overburden omitted), and average dip and speculated dip direction (corrected for magnetic declination) of bedding in core (1919 logs only; Hatch 1921).

Hole Number	Overburden	Vertical Depth	Percent Shale	Avg. Dip/DipDirction
BH-07-01	8.5 m	57 m	77%	N/A
BH-07-02	6.4 m	83 m	71%	N/A
BH-08-01	12.5 m	84 m	66%	N/A
BH-08-02	40.2 m	40.2 m	N/A	N/A
BH-08-03	41.5 m	57 m	N/A	N/A
BH-08-04	5.8 m	159 m	81%	N/A
BH-08-05	11.9 m	140 m	78%	N/A
BH-09-01	39.6 m	39.6 m	N/A	N/A
BH-09-02	16.8 m	110 m	75%	N/A
BH-09-03	21.6 m	121 m	73%	N/A
BH-09-04	29 m	78 m	67%	N/A
BH-09-05	21.3 m	63 m	88%	N/A
BH-19-01	6.1 m	153 m	59%	18/121
BH-19-02	8.2 m	152 m	46%	18/067
BH-19-03	8.2 m	168 m	62%	18/085
BH-19-04	6.4 m	136 m	74%	18/102
BH-19-05	9.1 m	153 m	55%	16/050
BH-19-06	13.7 m	154 m	61%	16/033
BH-20-01	20.7 m	169 m	60%	20/???
BH-20-02	19.5 m	133 m	46%	N/A
BH-20-03	17.6 m	170 m	61%	N/A
BH-20-04	37.2 m	173 m	59%	N/A
BH-20-05	40.8 m	144 m	63%	N/A
BH-20-06	42.4 m	42 m	N/A	N/A
BH-20-07	21.9 m	128 m	72%	N/A

Table 3.1: Summary of coal boring operations (Howley, 1918; Hatch 1921) near Goose Brook , Howley Basin (Figure 3.13). Average dip/dipdirection corrected for magnetic declination for the region in 1920.

Using the results of these exploration boreholes in the Goose Brook area, the authors made several interpretations of the geological structure of the region. Pointing to a drastic increase in depth of overburden encountered in BH-08-02, BH-08-03 and BH-09-01 compared to those to the east (Table 3.1; Figure 3.13), and broken and slickensided core at the top of bedrock in BH-08-02 (Appendix A), Howley (1918i) inferred a fault to occur just to the west of BH-08-02. This argument is further supported by a coal seam "doubled up in a sharp fold," discovered in a trench along the rail bed (Howley, 1918d; Figure 3.13).

From the strata intersected in a series of boreholes running along the length of Goose Brook to the northwest into the center of the basin, Howley (1918i) interpreted the presence of a long-wavelength syncline 'or trough' to underlie this region. He interpreted that the syncline folded into an anticline by BH-09-05, stating a reversal in dip to the northwest (Figure 3.13). He further concluded that continued exploration in this direction would unveil another coal trough. As stated before it is unclear how he could have determined dip directions from these cores. Dips of bedding intersected in core is not given these drill logs.

Hatch (1921) tested Howley's theory of another coal trough occurring to the northwest by sinking a series of boreholes in 1919 (BH-19-01 to BH-19-06) along a line extending close to 3 km northwest from Howley's BH-09-05 (Figure 3.13). In the drill logs from this field season, Hatch (1921) gives the average strike and dip of bedding for each borehole. These strikes have been corrected for the magnetic declination for the region in 1919 and placed on Figure 3.13. Because of the uncertainty in their validity they

have been given in red. The results of this boring operation, led Hatch (1921) to believe that this area of the basin formed a large synclinal structure plunging to the northeast (Figure 3.13). He correctly stated the uncertainty in these interpretations, but thought that this part of the Howley Basin held a high prospectivity for economic coal measures. In 1920, Hatch (1921) sunk boreholes along the plunge of his interpreted syncline, along with several close to BH-08-05, which had intersected thick coal seams (Figure 3.13; Appendix A). He was unable to correlate strata between boreholes, even over very short distances. This led Hatch (1921) to believe that "during the coal forming period, subsidence and upheavals occurred at frequent intervals" causing periodic inundation, depositing coal seams between thick shale beds. He further suggested that subsidence and uplift occurred heterogeneously over a considerable area.

Regardless of the uncertainty in the quality of orientation data ascertained from the authors' interpretation of core from these boreholes, or their consequential structural interpretations, these logs are important in the evaluation of Howley Basin. Drill logs of these boreholes (Table 3.1; Appendix A) show that the Howley Formation in the center of the basin is dominated by thick beds of fine-grained strata, or shales (some over 10 m thick). This is much different than what is observed in exposures of the Howley Formation along the basin's western and eastern margins and has significant consequence for both lithofacies distributions analysis and potential-field modeling (see Chapters 5, 6).

3.3.4 Northeast Brook

Extending to the northwest from the junction of the most northerly cross fault and the Grand Lake Fault, the Howley Formation is exposed in an unnamed brook (assigned as Northeast Brook for this study) to where it enters northeast Sandy Lake (Map A; Figure 3.14). The northwest section of the brook was traversed, but high water made accessing the southeast section difficult. Hyde's (1979b) bedding measurements in the eastern part of the brook were used for cross-section construction (Figures 3.14, 3.15). The Howley Formation along Northeast Brook forms a moderately steep to vertical northwest dipping and younging homocline with dip domains folding around shallow to moderately steep southeast dipping axial planes, giving a very poorly constrained calculated beta axis of 35-266 (Figures 3.14, 3.15). The vertical cross-section in Figure 3.15 was oriented slightly oblique (344°) to the calculated beta axis to give more realistic apparent dips in section. In the northwestern part of the section, a minor trust fault with a hanging wall flat geometry was observed in outcrop (Figure 3.14 B), indicating southeast directed reverse slip across the western portion of the homocline. This trust fault was extended to depth with a hanging wall flat geometry, bending around the most northwesterly axial plane (Figure 3.15), offering a possible, but poorly constrained geometry. The strike of the most southeasterly exposure of the Howley Formation in Northeast Brook (Hyde, 1979b) diverges from the rest of the population of bedding planes to a more westerly dip (Figures 3.14, 3.15).

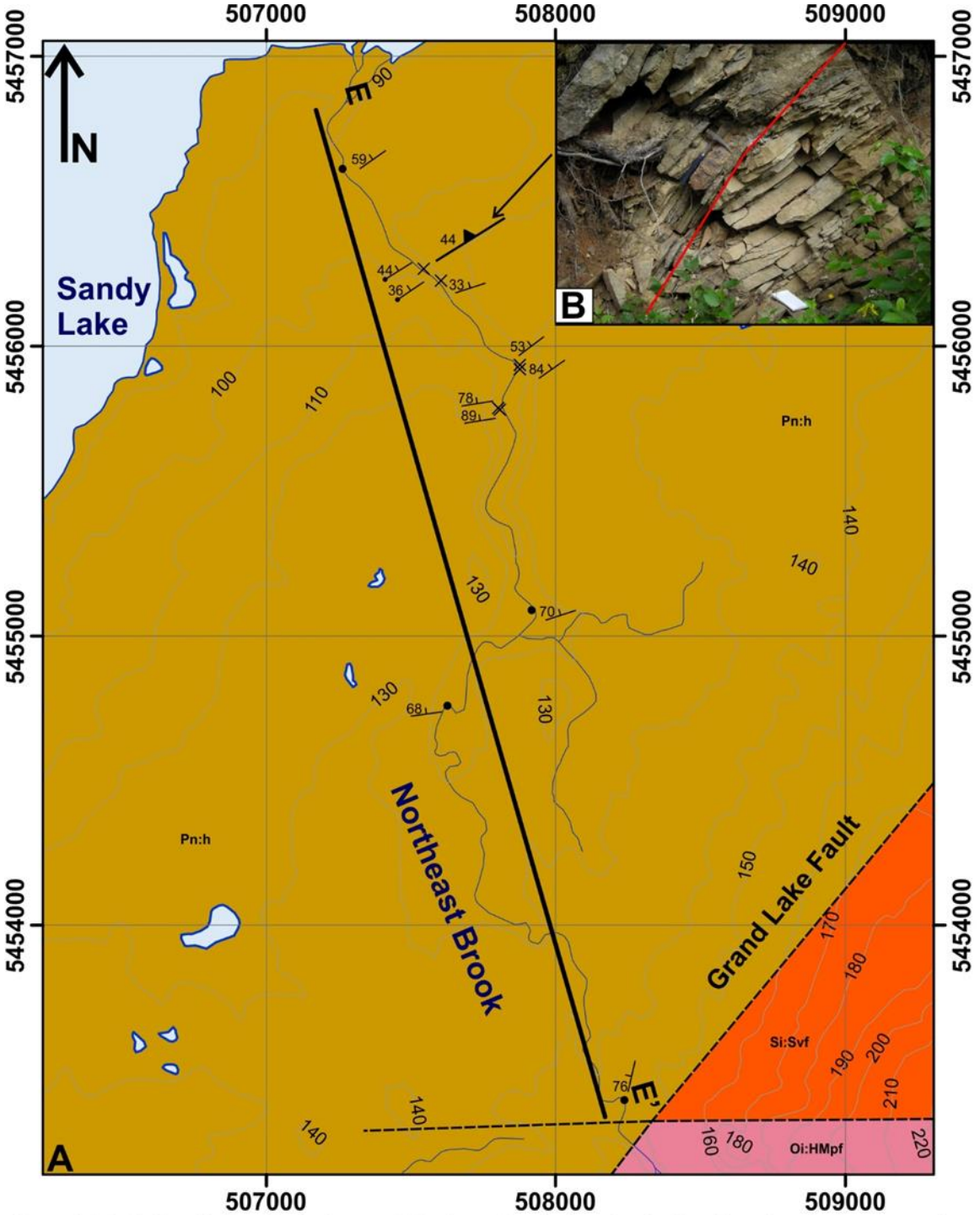

Figure 3.14: A) Detailed geological map of Northeast Brook showing the location of vertical cross-section E to E', trending at 164°. Map scale at 1:22,000. Lithological units, map symbols, and location of map given on given on Map A. **B)** Photograph looking northeast of minor thrust fault (red) with hanging wall flat/footwall ramp geometry. Hammer is 28 cm in length.

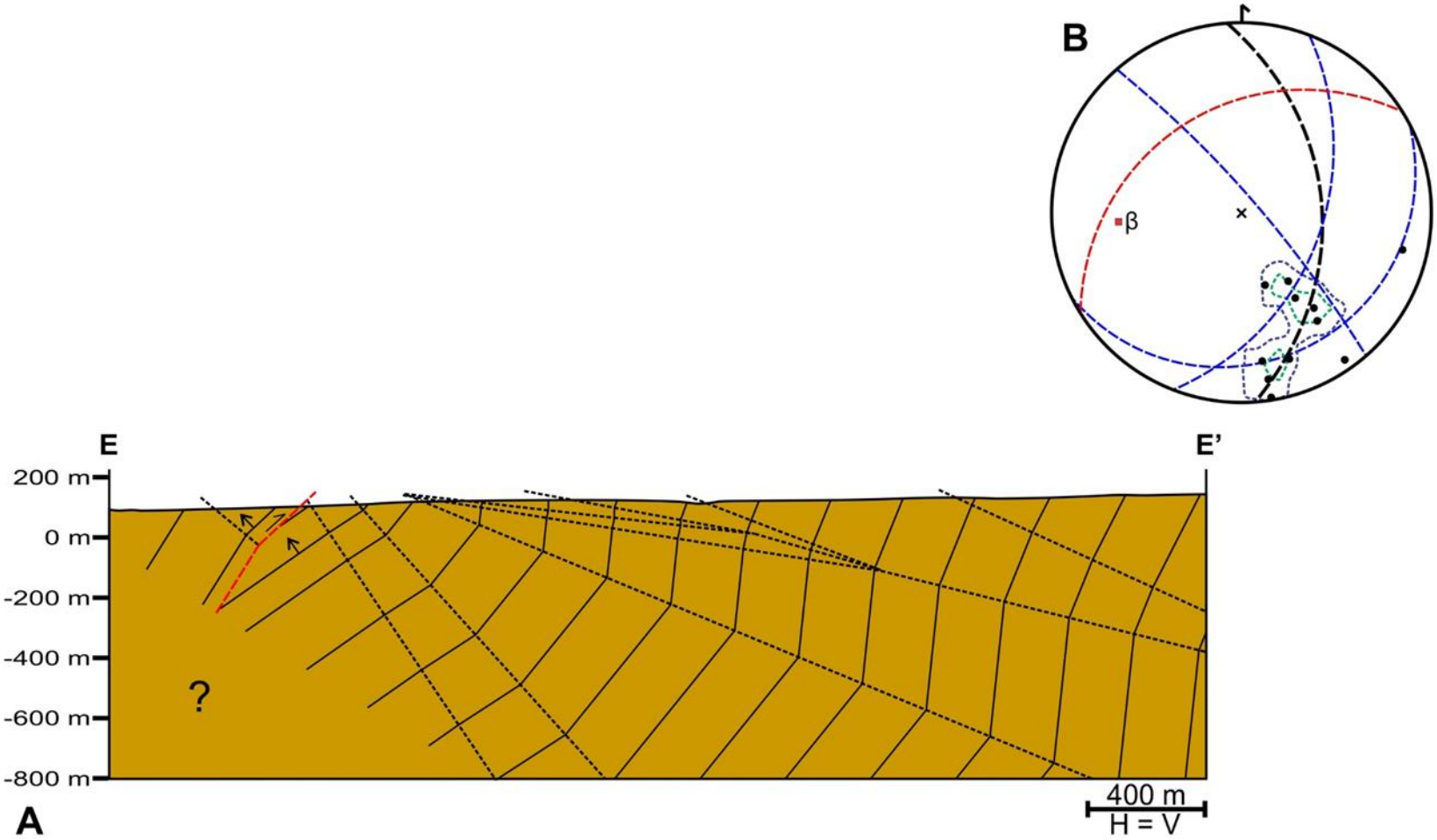

Figure 3.15: A) Vertical cross-section E to E' through Northeast Brook. Location of cross-section given on Figure 3.14. No vertical exaggeration. Legend for cross-section symbols given on Map A. **B)** Lower-hemispere, equal area stereographic projection plot of structural elements at Northeast Brook; number of poles = 11; calculated beta axis is 35-266; calculated girdle is 086/55; contour intervals at 10%, 20% with a maximum of 27.27%. Legend for plot symbols given on Map A.

Calculated axial planes along Northeast Brook do not contain the beta axis (Figure 3.15), and thus represent a separate set of structures unrelated to the dispersal of the bedding pole partial girdle; the beta axis reflects bending over an east-west axis, while the axial planes reflect kinking over southwest axes. This discontinuity between axial planes and the beta axis is interpreted to represent localized polyphaser deformation of the Northeast Margin of the Howley Basin.

Assuming that structural repetition is minor southeast of the observed thrust, an estimated average stratigraphic thickness for the Howley Formation through Northeast Brook can be calculated. Using the same methods as applied earlier to the Alder Brook and Coal Brook sections, i.e., taking an average strike and dip for the section (62/332), and correcting for changes in topography (55 meters to the southeast), the minimum stratigraphic thickness for the Howley Formation in the northeastern part of the basin is approximately 2.5 kilometers.

3.3.5 Northeast Ultramafic Thrust Slice

A further 3.3 kilometers northeast, the Grand Lake Fault is offset by another east-southeast trending cross fault (Map A). Hyde and Alexander (1979b) interpreted this cross fault to have a sinistral strike separation of 800 meters (Map A). The Howley Formation is not exposed in proximity to this cross-fault.

North of this cross-fault, a thrust (?) slice of unnamed serpentinized ultramafic rock of Late Cambrian to Ordovician age (Whalen and Currie, 1988) is exposed along the western flank of the Grand Lake Fault (Map A), and is thought to be an extension of the

BBL (Dawson and Mersereau, 1989). The high magnetic anomaly and positive electromagnetic results (Adams, 1981) associated with the ultramafic slice have enticed several exploration companies to perform reconnaissance mapping, detailed geophysical and geochemical surveying, and light drilling over the area, in hopes of delineating a zone of economical asbestos mineralization within the ultramafics. A ground-based magnetic survey was interpreted to show that the ultramafic body dips steeply to the east (Adams, 1981). Three closely spaced (within 1 km of each other) diamond drill holes (DDH-80-BL-001, 002, 003; locations of drill holes unseparated on Map A) were sunk on the ultramafics as part of an exploration program by Minorex in 1980 (Adams, 1981). These holes were drilled at an angle of 45^0 from vertical with two at azimuths of 146^0 and one at an azimuth of 326^0 reaching a maximum hole depth of 120 m. However, none of the drill holes intersected Howley Formation.

3.3.6 Structure of the Northeast Margin

The poorly populated pole plot for bedding along the Northeast Margin of the Howley Basin shows a bedding population distribution with a predominance of moderate to steep northwest dipping beds (Figure 3.16 B). Three gently east to southeast dipping beds in the southern portion of the Northeast Margin strongly influence a calculated shallowly southwest plunging beta axis (09-247) and a very steep northeast dipping pi girdle (067/81) (Figure 3.16 B). These three outliers are isolated from each other and are in close proximity to the Grand Lake Fault; the orientation of these beds could represent faulted blocks and not folded strata. Thus, their impact on regional fold geometry – as depicted in the pole plot (Figure 3.16 B) – is likely not accurate. Overall the bedding in

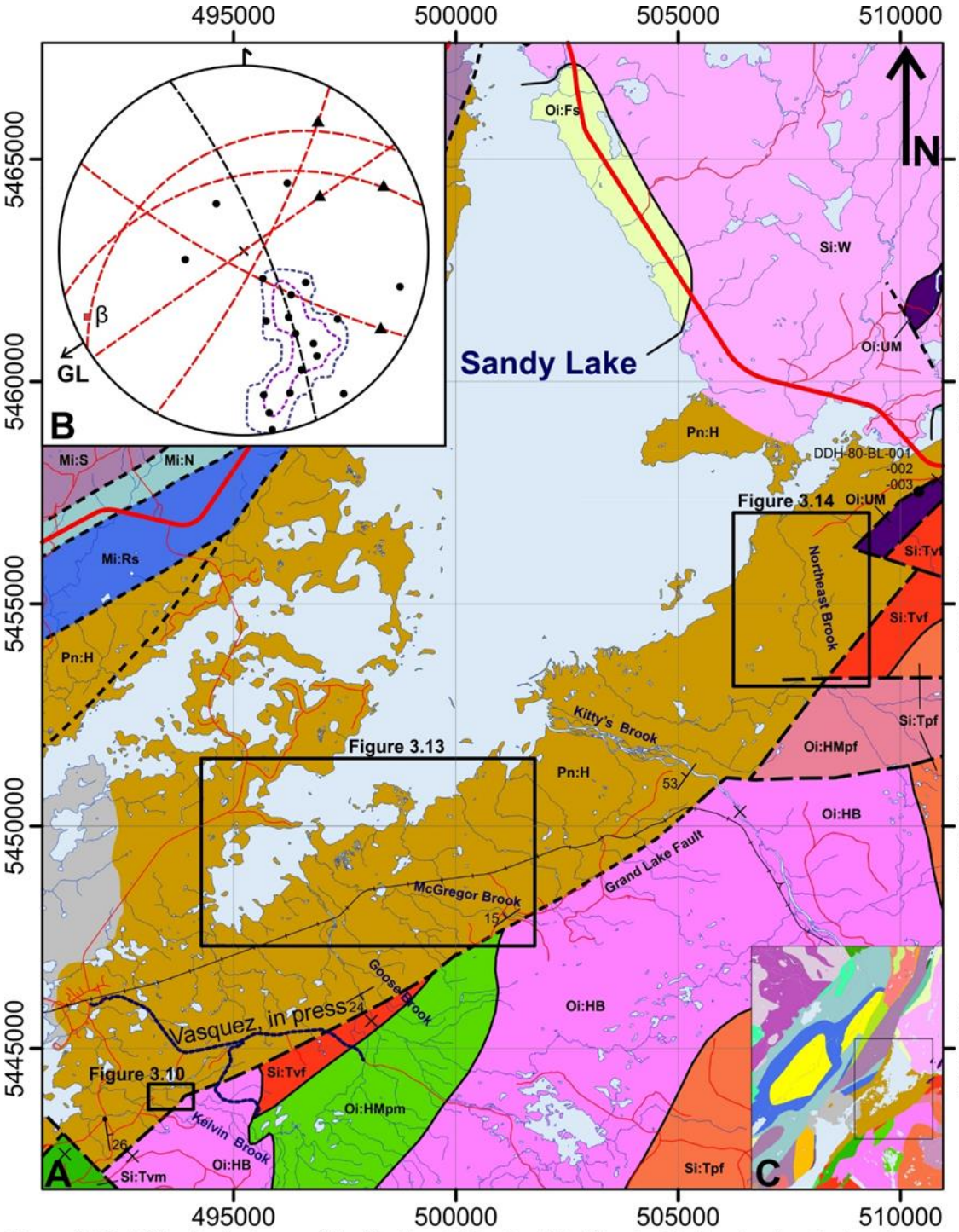

Figure 3.16: A) Geological map of the Northeast Margin of the Howley Basin, showing the locations of detailed subareas. Map scale, 1:135,000. Lithological units and map symbols Given on Map A. **B)** Lower-hemispere, equal area stereographic projection plot of bedding planes and faults along the Northeastern Margin of the Howley Basin; number of poles = 19; beta axis is 09-247; pi girdle is 067/81; contour intervals at 6%, 12%, with a maximum of 15.79%. Legend for plot symbols given on Map A. Average strike of Grand Lake Fault (GL) at 240^0. **C)** Insert showing location of map.

the Northeast margin is too sparse and occur at too great of a distance from each other to draw any conclusions on potential fold geometry in this region.

Bedding orientations of the Howley Formation in the Northeast Margin are enigmatic. Strikes of bedding close to the Grand Lake Fault are nearly parallel with its map trace, but further west, towards the center of the basin, the dip directions of beds diverge to a more north-easterly trend. This is particularly evident in Northeast Brook (Figure 3.14), where the whole section has a very consistent dip direction to the northeast, with the exception of the most easterly outcrop which dips to the east-northeast (Hyde and Alexander, 1979; Figure 3.14). The rotation of bedding orientations to more north-easterly trends may represent the superposition of later compressional folding onto earlier developed tilted sections, possibly developed during initial extension.

Although the orientations of dips documented in drill logs of boreholes sunk along Goose Brook and west of it are speculative, the consistently shallow dips observed in core are continuous over large distances (Hatch 1921; Figure 3.13; Table 3.1; Appendix A). Overall, clearly both the Southeast and Northeast Margins show a dominance of steep beds, dipping both into and away from the inferred sub-vertical basin bounding fault in close proximity to it compared to exposures towards the centre of the basin. This may reflect dissipating deformation towards the center of the basin, producing large wavelength very open macroscopic folds.

The lack of, and large distances between, exposures in the Northeast Margin of the Howley Basin limits any definitive interpretation of structures within. However,

where exposed, bedding and fault orientations suggest that this region experienced a transpressional event post- Howley Formation deposition. Steep to upright bedding of the Howley Formation occurs in both Kelvin Brook (Figure 3.10) and Northeast Brook (Figure 3.14). Faults in Kelvin Brook are steep to vertical with typically shallowly plunging slickenlines and strike from nearly parallel to almost perpendicular to the trace of the Grand Lake Fault, suggesting a predominance of strike-slip deformation (Figures 3.10, 3.16). A single southeast verging thrust fault observed in Northeast Brook (Figures 3.14, 3.16) indicates local contractional deformation.

As interpreted by Howley (1918b), the possible presence of Rocky Brook Formation directly under overburden in BH-93-01 and Howley Formation in BH-79-01 to the west (Map A) suggests that the Rocky Brook Formation underlies the Howley Formation on the eastern margin of the basin, and at this location occupies a structural high relative to the east margin of the Howley Basin. Either the Rocky Brook Formation is in an eroded core of a high-amplitude anticline, or has been thrusted over the Howley Formation. Alternatively, BH-93-01 may have penetrated an eroded horst of Rocky Brook Formation. Without further drilling or seismic reflection geophysics no other conclusions can be made about the structure in this now flooded area.

3.4 Northern Margin

The Howley Formation is not exposed along the Northern Margin of the Howley Basin (Map A). Early to late Silurian post-kinematic granites of the Wild Cove Pond Igneous Complex and early Ordovician siliciclastic schists of the Fleur de Lys

Supergroup (Hibbard et al., 1980) are exposed along the northeastern shores of Sandy Lake (Map A). Hyde and Alexander (1979b, 1982) suggested that perhaps the Howley Formation underlies a low-lying peninsula in the northeast corner of Sandy Lake (Map A); however, there is no clear geological or geophysical evidence to support this interpretation. This peninsula rises only a few meters above the level of Sandy Lake and is covered by a thick flat peat bog with no exposures of bedrock (Maps A, B). In lieu of bedrock exposure, aeromagnetics are the best representative of near-surface geology. Known exposures of the Wild Cove Pond granites to the north of the peninsula form a topographic high and have a relatively positive, short wavelength, magnetic signature, and appear to be continuous over the peninsula (Maps C, D). Also, a small isolated magnetic high occurs just to the east of the peninsula (Maps C, D), and given the numerous exposures of ultramafic enclaves in the Wild Cove Pond Igneous Suite, it is likely that another occurs at this location. Therefore, it is likely that the peninsula is underlain in the near-surface by the Wild Cove Pond Igneous Suite. Both the siliciclastic schists of the Fleur de Lys Supergroup and the Howley Formation have very low measured magnetic susceptibilities (Section 5.3). If either of these units underlie the peninsula, they are predicted to form a thin veneer overlaying the Wild Cove Pond Igneous Suite.

3.5 Western Margin

The Western Margin of the Howley Basin is here considered to extend for nearly 30 km from the beginning of Junction Brook, at the northwestern corner of Grand Lake, to northwestern tip of Sandy Lake (Map A). Exposure along this margin is very poor;

much of the land on the western shores of Sandy Lake and northwestern Grand Lake are covered by extensive bogs or thick spruce forests. Outcrops of the Howley Formation along this margin are limited to a few streams that flow southeasterly off of Birchy Ridge into Grand Lake and Sandy Lake, namely Boot Brook and Mary Ann Brook (Map A). Further north, along the western shore of Sandy Lake, presence of the Howley Formation is solely constrained by the interpretations of intersections of Howley-like strata in shallow drill cores (O'Sullivan, 1979a, b, c; Map A). Core from these holes are stored at the NLGS's Core Storage Facility in Pasadena, Newfoundland, but were left exposed outside over winter allowing the cores to be degraded to the point that they are of no value to examine (O'Sullivan, 1979a, b, c) Drill-logs of these holes (Appendix A) have been reviewed and are reported on below.

Viséan Deer Lake Group formations, notably the North Brook Formation and Rocky Brook Formation, are exposed in the northwestern reaches of Boot Brook, berms of the TCH and adjacent logging roads, and in a new quarry near the intersection of the TCH and Route 401 (Map A). Hyde (1982) interpreted these units, along with the Howley Formation, to occupy three northeast-southwest trending fault panels, bounded by splays of the Hampden Fault (Map A). From northwest to southeast, these splays enclose and bring to surface fault panels of the North Brook, Rocky Brook, and Howley formations, along the southeastern flank of Birchy Ridge (Map A). The interpreted splays are not exposed, but are assumed to separate different lithologies and structural trends between them. The southwestern extent of these splays is unknown due to a lack of exposure, but

if continued along their inferred trend they would branch northeastward from the Fisher Hills-Birchy Ridge Fault near Junction Brook (Map A).

The fault panels along the western margin of the Howley Basin are not readily expressed in topographic (Map B) or magnetic (Map C) maps. This is likely due to an overshadowing by Birchy Ridge, which is associated with strong topographic relief and a consistent linear increase in magnetic signature to the northwest (Maps, A, B, C).

Mapping along the Western Margin for this project concentrated on traversing the streams and road cuts where exposures are known to occur – as documented on geological maps of Hyde et al. (1980) and Hyde and Ware (1981). Some of these outcrops were not located, and unfortunately, increased precipitation during the latter part of the field season raised the water level of the streams and prevented access to certain sections with known exposures at low water levels. The following geological maps and cross-sections are a combination of observations made in this study and the data and interpretations of Hyde et al. (1980) and Hyde and Ware (1981).

3.5.1 North Brook Fault Panel

The North Brook Fault Panel is interpreted as the narrow northeast-southwest trending strip of fine-grained, thick interbedded, locally rippled and laminated, muddy-red and grey/green sandstones exposed along the northern berm of the TCH and adjacent logging roads (Map A). Hyde (1982) interpreted that this strip of North Brook Formation is in fault contact along a northeast-southwest trending fault with the Saltwater Cove Formation in the north, and the Rocky Brook Formation in the south. Its eastern extent is

terminated by the inferred map trace of the Hampden Fault which juxtaposes it with the Howley Formation to the east (Hyde, 1982; Map A).

Bedding orientations within the fault panel are highly variable. Along the TCH and in Boot Brook, going from south to north, bedding of the North Brook Formation switches from dipping and younging to the east-southeast to southeast to south, with an overall trend of shallowing dips to the northeast (Map A). Within the most southern exposures in the North Brook Fault Panel, bedding is cut by a moderately south-southeast dipping fault with sub-horizontal lineations and a sub-vertical north-northwest dipping quartz vein (Map A). Further to the northeast, along a logging road north of the TCH, Hyde et al. (1980) interpreted beds of the North Brook Formation to young and dip very steeply to vertical to the east-southeast and west-southwest, defining an isoclinal vertical fold with a fold axis plunging to the southeast (Map A). This fold geometry implies that polyphased deformation has affected the North Brook Formation within the fault panel.

Two diamond drill holes (DDH-79-04 and DDH-79-01; Map A) were collared along the northeastern contact of the North Brook Fault Panel, where it is interpreted to branch from, or is cut by, the Hampden Fault (Map A). Hyde et al. (1980) and Hyde (1982) placed these drill holes within the North Brook Formation; however, O'Sullivan (1979a, c) – author of the exploration reports for North Gate Exploration – placed these drill holes within the Howley Formation, east of the Hampden Fault. It would appear that this discrepancy of geological units in which these drill-holes are collared has arisen from Hyde's (1982) interpretation of the Hampden Fault's map trace being further east than shown on the geological map of Baird (1960); the drill hole locations were originally

projected by O'Sullivan (1979a, c) on Baird's (1960) map. For this reason, the locations of these drill-holes – as given by the NLGS's GeoAtlas – are believed to be accurate with respect to UTM grids and therefore have not been adjusted in the following figures.

The log for hole DDH-79-04 (Appendix A; Map A) describes very steeply dipping, pale grey, medium- to very fine-grained sandstones, that are 'the most coherent of all the units intersected within the drill holes along this margin' (O'Sullivan, 1979c), persisting until 35 m depth. This succession is followed by steeply dipping, friable, poorly cemented, locally micaceous, brown silty mudstone until the end of the hole at 68 m depth (O'Sullivan, 1979c; Appendix A). Three kilometers to the north-northeast, situated very close to the interpreted location of the Hampden Fault, DDH-79-01 (Map A) is described as intersecting poorly consolidated, pale green/grey to black to red/brown, locally micaceous, interbedded silt to mudstones until the end of the hole at 41.5 m depth. Bedding in core varies from dipping 50° to vertical, and at 27.4 m depth the core is reported as being highly sheared (O'Sullivan, 1979a; Appendix A).

The indurated sandstones and steep dips in the top of DDH-79-04, may suggest that the Saltwater Cove Formation was intersected and not North Brook Formation, as both North Brook Formation and Howley Formation are typically friable. Also, the change to poorly cemented and friable mudstone down hole may indicate that this drill hole encountered a geologic contact, perhaps a faulted contact with the Howley Formation. If this is the case, then the Saltwater Cove Formation would need to be thrust over the Howley Formation on a west-dipping reverse fault. This interpretation is in agreement with the suggestion that the vertical fold in the northern North Brook Fault

Panel is the product of high strain poly-deformation and is more suited to structures mapped in the Saltwater Cove Formation (Section 3.6). The poorly consolidated mudstone with changing dips and sheared intersections of DDH-79-01 is interpreted to be the Howley Formation and supports an argument that the orientation and locations of the splays in the Western Margin may be misrepresented on Map A (Hyde, 1982).

3.5.2 Rocky Brook Fault Panel

The Rocky Brook Fault Panel trends parallel to the North Brook Fault Panel and extends from the Hampden Fault to the south (Map A). To the south, the extent of the Rocky Brook Fault Panel is uncertain because of extensive bogs preventing observable exposure. The contact between these two fault panels was first considered a geological contact by Hyde and Ware (1981), but was later re-interpreted to be a faulted contact by Hyde (1982). Exposure within the Rocky Brook Fault Panel is limited to abundant outcropings in the streambed of Boot Brook (Figure 3.17), and in a newly developed quarry, near the junction of the TCH and Route 401 (Map A). Boot Brook exposes sections of the Saltwater Cove Formation, North Brook Formation, Rocky Brook Formation, and Howley Formation on its southerly course from its headwaters on Birchy Ridge to its mouth on the channel connecting Sandy Lake and Grand Lake (Map A). The section of Boot Brook south of the TCH, which exposes Rocky Brook Formation and Howley Formation lithologies, was traversed for this study.

Rocky Brook Formation lithologies along this section of Boot Brook consist of predominately blue/grey and red very fine-grained sandstones (color changes a product of

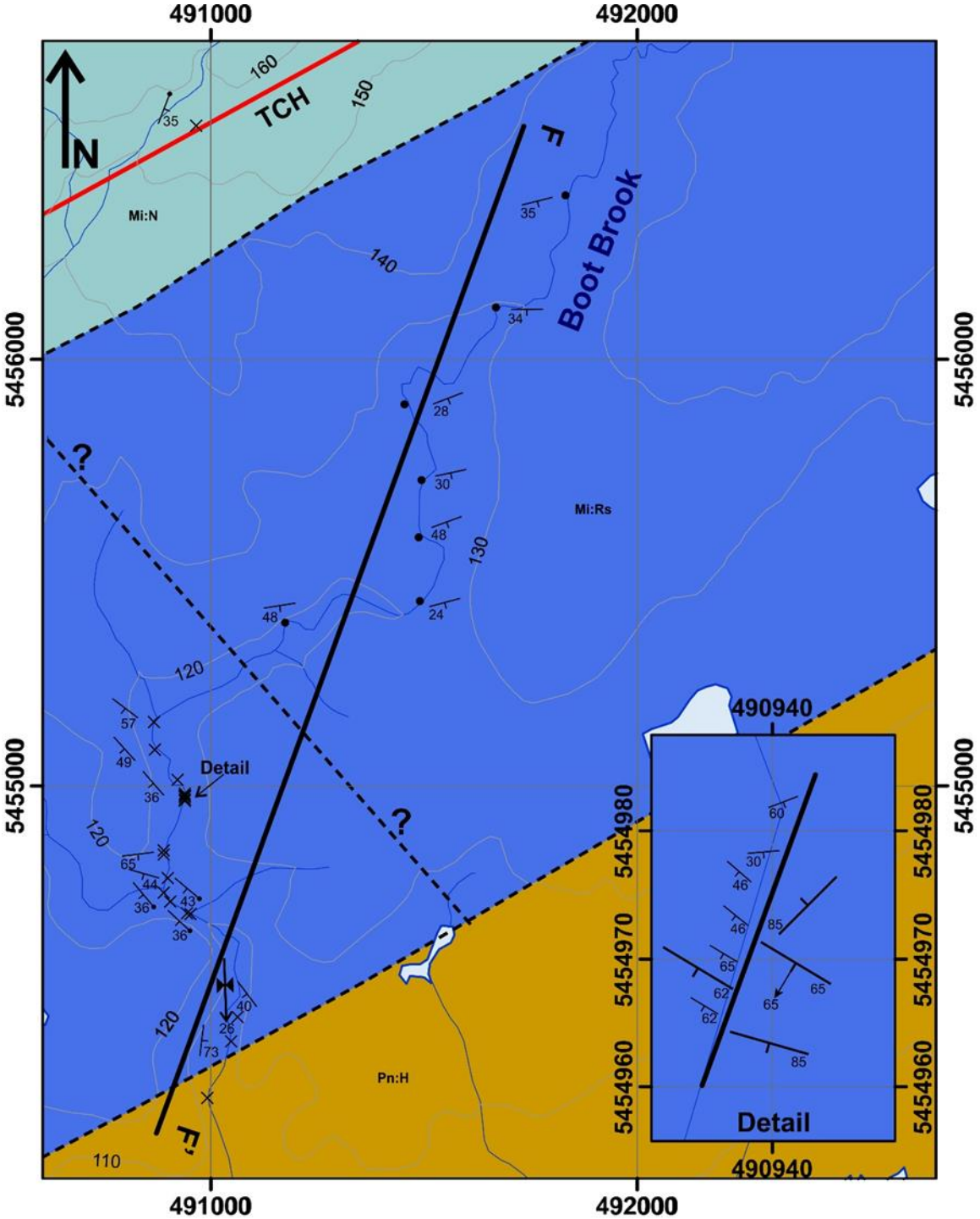

Figure 3.17: Detailed geological map of Boot Brook showing the location of vertical cross-section F to F', trending at 200°. Map scale, 1:15,000. Lithological units, map symbols, and location of map given on Map A.

redox reactions) with subordinate thin beds of laminated fine-grained sandstones that locally form lenses and are crossbedded. At the southernmost part of the section, limey-tan weathered, light grey limestone beds with wavy black laminations are exposed.

For the first 1.5 km, south of the TCH and the inferred fault contact with North Brook Formation, Boot Brook winds through a low-lying alder forest with no exposure. The lack of exposure along this section could possibly be due to the presence of predominately easily weathering lithologies, such as shale and limestone. The location of the panel's southerly inferred faulted contact with the Howley Formation is spatially constrained by a sub-crop of very coarse-grained pebbly sandstone 150 m downstream from an outcrop of limestone (Figure 3.17). Angular boulders of quarts-pebble conglomerates at this location show slickensided surfaces, indicating that a fault is nearby, and this is likely a faulted contact.

In Boot Brook, bedding planes of the Rocky Brook Formation form two dip domains with varying strikes between them (Figures 3.17, 3.18). In the north, moderately steep south-southwest dipping bedding planes form long open folds along moderately steep north-northwest dipping axial planes. In the south, beds face and dip moderately to steeply to the southwest with dip variations forming long open folds around moderately steep northwest dipping axial planes (Figures 3.17, 3.18). Combined, these two dip domains give a moderately inclined beta axis plunging due south (39-180; Figure 3.18). This is, however, not likely a true portrayal of fold geometry; maintaining bed thickness between these two dip domains with flexural slip folding is not geologically feasable, and a fault has been inferred to separate the two dip domains (Figures 3.17, 3.18). This

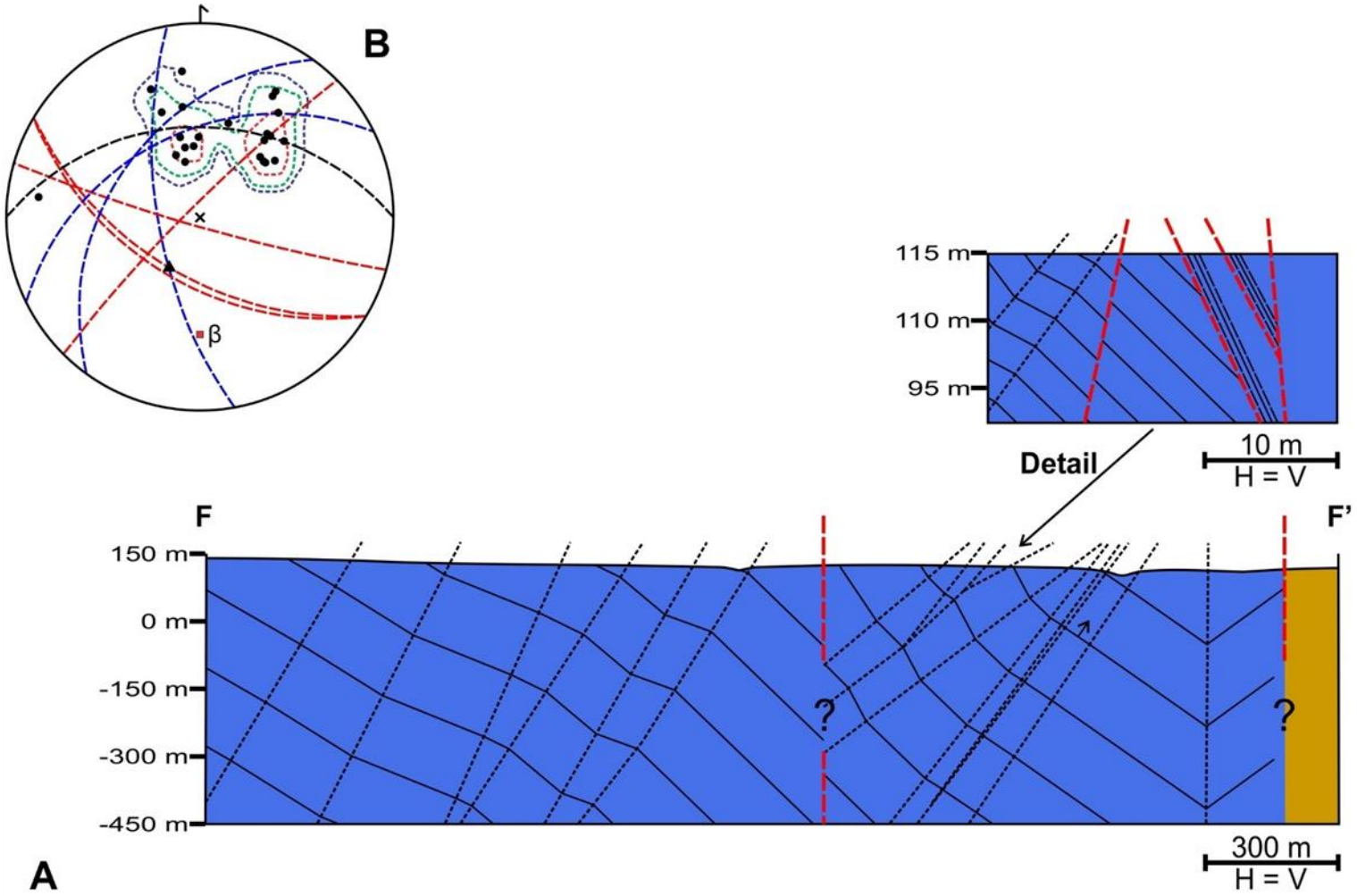

Figure 3.18: A) Vertical cross-section F to F' through Boot Brook. Location of cross-section given on Figure 3.17. No vertical exaggeration. Legend for cross-section symbols given on Map A. **B)** Lower-hemispere, equal area stereographic projection plot of structural elements at Boot Brook; number of poles = 23; calculated beta axis is 39-180; calculated girdle is 51/100; contour intervals at 5%, 10%, 20% with a maximum of 34.78%. Legend for plot symbols given on Map A.

inferred fault was given a southeast-northwest trend in keeping with trends of faults observed further south in Boot Brook (Figure 3.17).

A well-exposed section in the southern dip domain displays various lithologies, bedding orientations, and faults over a short interval (Figures 3.17, 3.18). Here, from north to south, a sharp contact between medium- to coarse-grained sandstones and muddy-red fine-grained sandstones dips steeply to the south-southeast, and is followed by very fine-grained laminated muddy- red sandstones that dip moderately to the south. These beds then fold to dip more steeply to the southwest. A sub-vertical northwest dipping fault crosscuts these beds, but lineations are weathered out and offsets were not observed. To the south of this fault, the same very fine-grained laminated muddy-red sandstones continue to dip moderately to the southwest and are followed by a steep southwest-dipping fault with a hanging wall flat geometry and downdip slickenlines. A few meters to the south, coarse arkosic sandstones with abundant mud chips are exposed. This unit is then cut by another steeply southwest dipping fault that is parallel to bedding of a thin shale bed (5 to 10 cm thick). Another 5 meters to the south, a sub-vertical southerly dipping fault is located in very fine-grained sandstones to shaley beds, with unknown dips, before exposure is lost (Figures 3.17, 3.18).

At the southernmost, part of the section – close to its faulted contact with the Howley Formation – bedding in limestone outcrops form a close syncline with a steeply west dipping axial plane (260/72) and a gently south- plunging calculated fold axis (26-178; Figures 3.17, 3.18). This fold is not well represented on cross-section F to F' because its limbs strike at a large angle to the trend of the cross-section, and its projection

does not depict true fold geometries (Figures 3.17, 3.18). This syncline is also notably oblique to the inferred trace of the faulted contact with the Howley Formation, just to the south (Figure 3.17). Alternatively, the rapid change in dip directions of the limestone beds may represent the presence of an unexposed fault. However, a fold is favored at this location because limestone beds in the Rocky Brook Formation are thin and rare, and given the proximity of the two outcrops of limestones combined with their drastic contrast in dip directions, a fault-induced change in dip direction with such little offset is unlikely.

To the northeast of Boot Brook, a newly developed quarry – not documented on Hyde and Ware's (1981) map – just to the west of the intersection of the TCH and Route 401, exposes a 100 m east-west vertical section of the Rocky Brook Formation (Map A). Flooding of the quarry prevented examination of the entire quarry wall, but bedding is easily recognized from afar and a consistent steep dip to the west was observed across its entirety (Figure 3.19). On the western edge of the quarry, medium- to coarse-grained, parallel laminated and cross-bedded arkosic sandstones with thin beds containing pebble clasts, overlie a brecciated horizon with dark brown to black rip-up clasts (Figure 3.19). The rest of the quarry, to the east, is dominated by dark gray/blue shale. The change in lithologies along the western edge of the quarry may expose an interfingering of North Brook Formation with the Rocky Brook Formations, or the base of the Humber Falls Formation; coarse- to medium-grained arkosic sandstones are not present in the Rocky Brook Formation (Hyde, 1995). All lithologies dip and face moderately steep to the west (Figure 3.29). These dip directions are nearly perpendicular to those of the Rocky Brook

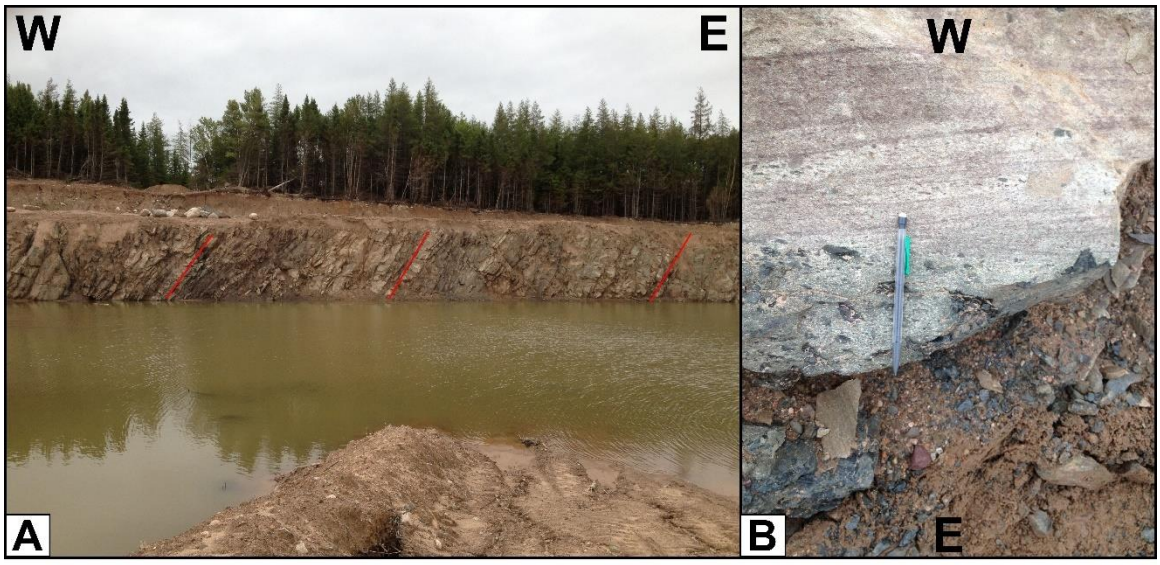

Figure 3.19: A) Photograph looking north at the northern wall of a new quarry near the junction of the TCH and Route 401(Map A). Bedding of Rocky Brook Formation is seen to dip steeply to the west (red lines). **B)** Photograph of medium- to coarse-grained arkosic cross-bedded sandstone with thin beds of pebble clasts overlying a breccia horizon of rip-up clasts. Picture taken on west quarry wall.

Formation observed in the northern section of Boot Brook (Figure 3.17) and indicate that folding and/or faulting must occur between these exposures.

The Boot Brook Fault Panel is internally strongly deformed and shows contractional structures. Observed faults within the fault panel dip steeply to sub-vertical to the southwest and northwest, parallel to and cross-cutting bedding, respectively. The strikes of the southwest faults are nearly perpendicular with the inferred map traces of bounding faults, whereas the northwest dipping fault is nearly parallel (Figures 3.17, 3.18). These geometries would suggest that these faults developed as conjugate synthetic and antithetic shears (southeast- and northwest-dipping, respectively) during dextral displacement along the bounding faults. However, the downdip lineations observed on one of the steep southeast-dipping faults in a shale horizon, with a hanging wall flat geometry, is enigmatic (Figures 3.17, 3.18). Another ambiguous structure is the close

syncline that gently plunges to the south at the top of the succession; its fold axis – albeit poorly constrained - makes a very large angle to the map trace of the bounding fault just to the south (Figure 3.17). During dextral strike-slip deformation, fold axes are predicted to form at 45º to master faults, with their acute angle in the direction of displacement, and progressively rotate towards parallelism with the master fault (e.g., Harding (1988)). The angle between the fold axis and the inferred strike of the fault is too large for the fold to have developed from either dextral or sinistral strike-slip movement along this fault. This fold axis orientation relative to bounding faults may be evidence of polyphase deformation within the Rocky Brook Fault Panel. Moreover, the calculated beta axis does not lie on the calculated axial planes and indicates bending of already tilted/folded beds. Together, these observations are strong evidence that the Rocky Brook Fault Panel has a polyphased deformation history.

3.5.3 Howley Fault Panel

Exposure of the Howley Formation to the east of the Rocky Brook Fault Panel is limited to a few localities in the southerly reaches of Boot Brook and Mary Ann Brook (Hyde, 1982; Map A). Exposures of the Howley Formation in Boot Brook are interpreted to be located in a fault panel, bounded by the Hampden Fault to the south and a splay that juxtaposes Howley Formation with Rocky Brook Formation to the north (Hyde, 1982). If these bounding faults continue with their inferred trend to the south, they would enclose the exposures of the Howley Formation in Mary Ann Brook as well (Map A).

Bedding of the Howley Formation in Boot Brook is documented as dipping gently to the west for the northerly exposure and very steeply to the southeast for the southerly exposure (Map A). On Hyde and Ware's (1981) original map, they put the more southerly, steeply dipping bed of Howley Formation, to the east of the Hampden Fault, but on Hyde's (1982) compilation map both exposures are included in the fault panel. If these beds are not separated by a fault and represent folding within the fault panel, they would produce an open synclinal structure with a sub-horizontal fold axis plunging to the southwest (06-217; Map A). This fold axis is speculative because it is based on only two bedding measurements, one of which is very gently dipping, and the error in the calculation is large (i.e., the gently dipping bedding could easily represent the hinge region of a fold). If, however, the predicted fold axis is true and the inferred map trace of the Hampden Fault is accurate, then their relative geometries may suggest dextral transpression along the Hampden Fault.

Further to the southwest, in the streambed of Mary Ann Brook, Hyde and Ware (1981) documented several bedding measurements and assigned the rocks to the Howley Formation (Map A). This stream was traversed during this study, but exposure of bedrock was not found. The bedding measurements of Hyde and Ware (1981) dip sub-horizontally to gently to the southeast, south, and east over a short interval, and presumably lie inside Howley Fault Panel (Map A).

3.5.4 Howley Formation Drill Holes in the Western Margin

North of Boot Brook, the Howley Formation is interpreted to lay to the east of the Hampden Fault, along the western shore of Sandy Lake all the way to its northwest extremity (Hyde, 1982; Map A). This area is however low-lying and underlain by boggy terrain with no bedrock exposure. The presence of Howley Formation along this section of the Western Margin is solely constrained by intersections of Howley-like strata in shallow drill holes (DDH-79-02, DDH-79-03, and DDH-79-05; O'Sullivan 1979a, b, c; appendix A), in close proximity to the Hampden Fault (Hyde, 1982; Map A).

O'Sullivan (1979c) reported that DDH-79-05 intersected interbedded red/brown laminated siltstone, green-grey friable sandstone, unconsolidated siltstone, and green-grey medium-grained sandstone to the end of the hole at 121 m (Appendix A). Bedding/core angles are not given in this drill log. DDH-79-02, 4 km to the north of DDH-79-05 and 1 km east of DDH-79-01 (Map A), is described as intersecting frequently alternating of lithologies over short intervals, ranging from poorly consolidated brown micaceous siltstone to white coarse-grained sandstone. Dips of bedding also frequently alternate and range from horizontal to 40º with no clear trend over the 100 m of core (O'Sullivan 1979a; Appendix A). Continuing north 5 km, DDH-79-03, shown to be collared in Saltwater Cove Formation on Map A, intersected a suite of friable and poorly cemented lithologies, that notably has the most fine-grained rocks of all of the western Howley Basin drill holes. This drill hole is also unique in that many of the fine-grained lithologies have quartz pebbles throughout, as well as angular clasts of talc and schist. No bedding core angles are given. Because of the friable character of lithologies intersected in this

hole, it is interpreted to be collared in the Howley Formation and not the Saltwater Cove Formation. Bituminous material is reported at 45 m (O'Sullivan 1979b; Appendix A) and was used in Langdon and Abrajano's (1994) and Hamblin's (1997) studies of source rock and migration of hydrocarbons. It should be noted that in Hamblin's (1997) report the location of DDH-79-03 is erroneously placed approximately 22 km to the southwest.

These drill holes show a wide-range of friable and poorly consolidated lithologies with varying dips. This suggests that the Howley Formation in the Western Margin was deposited during episodic tectonic activity and that its variable lithologies reflect detritus of proximal sources. Post-deposition deformation has sheared and folded the Howley Formation in the Western Margin.

3.5.5 Junction Brook

Junction Brook begins at the northwest extremity of Grand Lake, near the southwest corner of the Howley Basin, west of the inferred continuation of the Fisher Hills-Birchy Ridge Fault (Map A). The river is dammed and is now dry unless the spillway is open, revealing excellent exposures of the North Brook Formation, Rocky Brook Formation (Spillway Member), and Humber Falls Formation, on its northwesterly course to the Humber River (Hyde, 1982; Map A). Because the rocks exposed along Junction Brook are west of the Fisher Hills-Birchy Ridge Fault, they are considered part of the Humber Basin and not the Howley Basin. However, it was decided to traverse Junction Brook because it is situated in an interesting position with regards to the structure of the western margin of the Howley Basin: if continued south along their

inferred trends, the splays that enclose the fault panels east of Birchy Ridge would meet the Fisher Hills-Birchy Ridge Fault at or near Junction Brook (Hyde, 1982; Map A). The section of Junction Brook that exposes the North Brook Formation was traversed and is reported on.

From southeast to northwest, the North Brook Formation quickly progresses from thick sequences of red, coarse- to medium-grained sandstones with thin beds of trough-filling pebble to cobble conglomerates into thick beds of very fine-grained, laminated, red sandstones that are locally cross-bedded and internally fining upwards. Overall the North Brook Formation through Junction Brook forms a steep, quickly changing to gentle, westerly dipping and younging homoclinal panel in a fining upwards sequence. Slight variations in dips produce steeply east dipping axial planes and a poorly constrained shallowly southwest plunging beta axis (06-202; Figures 3.20-3.23).

Along the most southeasterly section of Junction Brook, near the presumed location of the Fisher Hills-Birchy Ridge Fault, the North Brook Formation is highly deformed. Here, steep coarse-grained sandstone beds are crosscut by numerous very steep to sub-vertical faults (Figures 3.20-3.23). A group of these faults strike roughly east-west, nearly perpendicular to the map trace of the Fisher Hills-Birchy Ridge master fault, with shallowly west plunging lineations (Figures 3.20-3.23). One such fault, exposed on the floor of the dry riverbed, displaces an identifiable sandstone bed that displays a fault drag structure, giving a sinistral kinematic movement indicator (Figure 3.24). Two other sub vertical faults strike northeast-southwest with moderate southwest plunging lineations, and one fault, closest to the presumed map trace of the master fault, has nearly down-dip

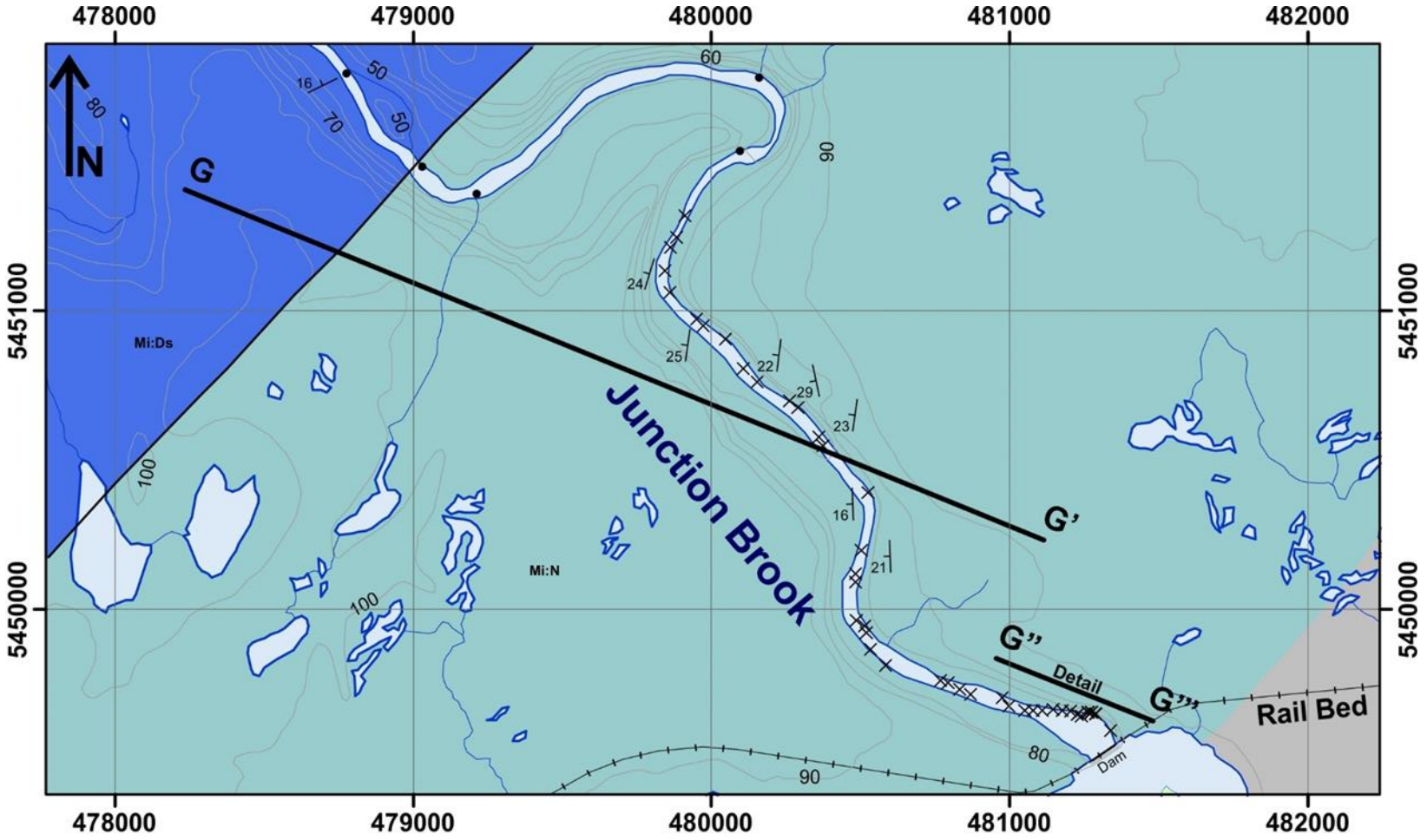

Figure 3.20: Detailed geological map of Junction Brook showing the location of vertical cross-section G to G' and G'' to G''', trending at 112°. Map scale 1:22,000. Lithological units, map symbols, and location of map given Map A.

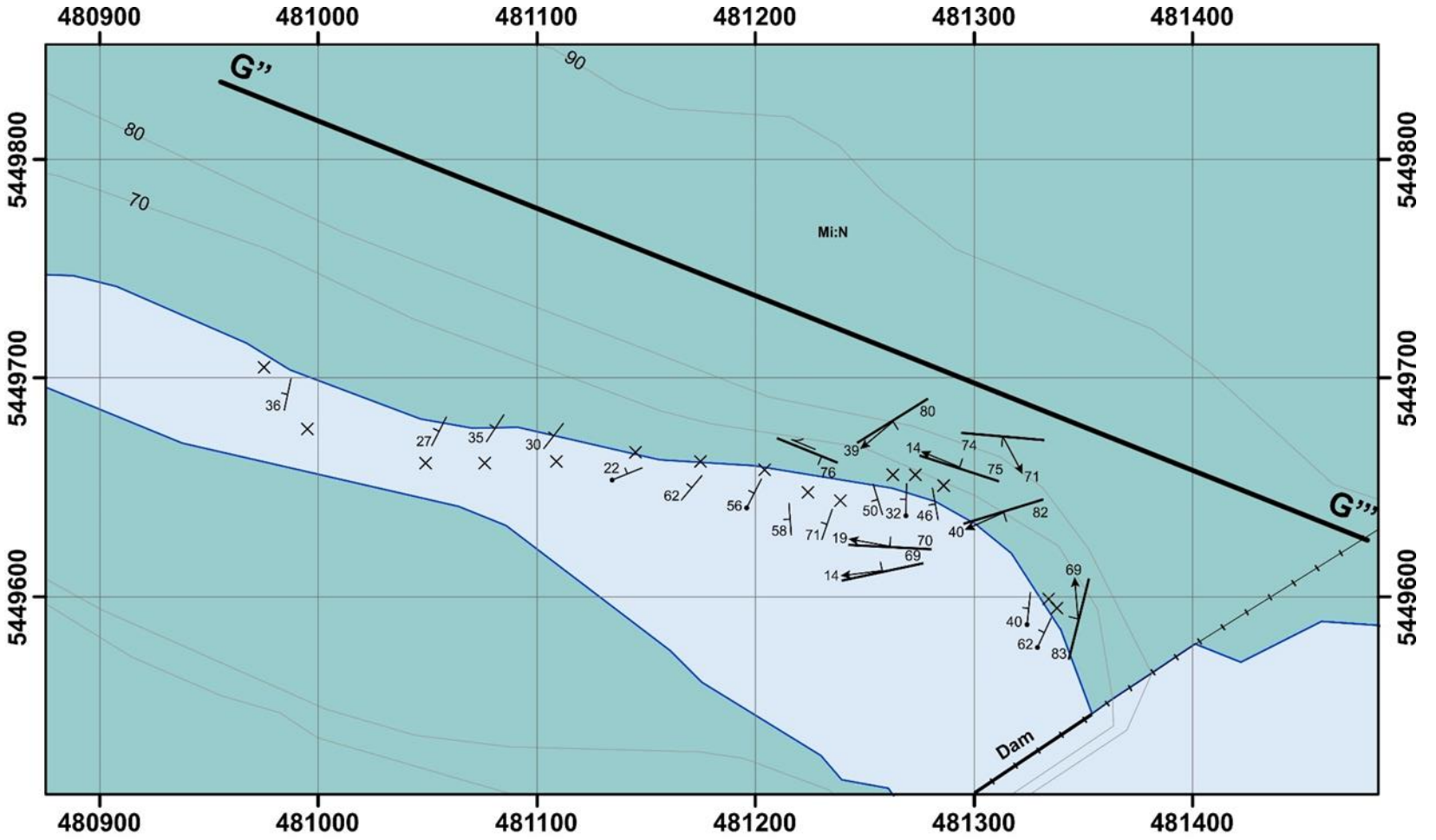

Figure 3.21: Detailed geological map of Junction Brook showing the location of vertical cross-section G''to G''', trending at 112°. Map scale at 1:3,000. Lithological units, map symbols, and location of map given on Map A.

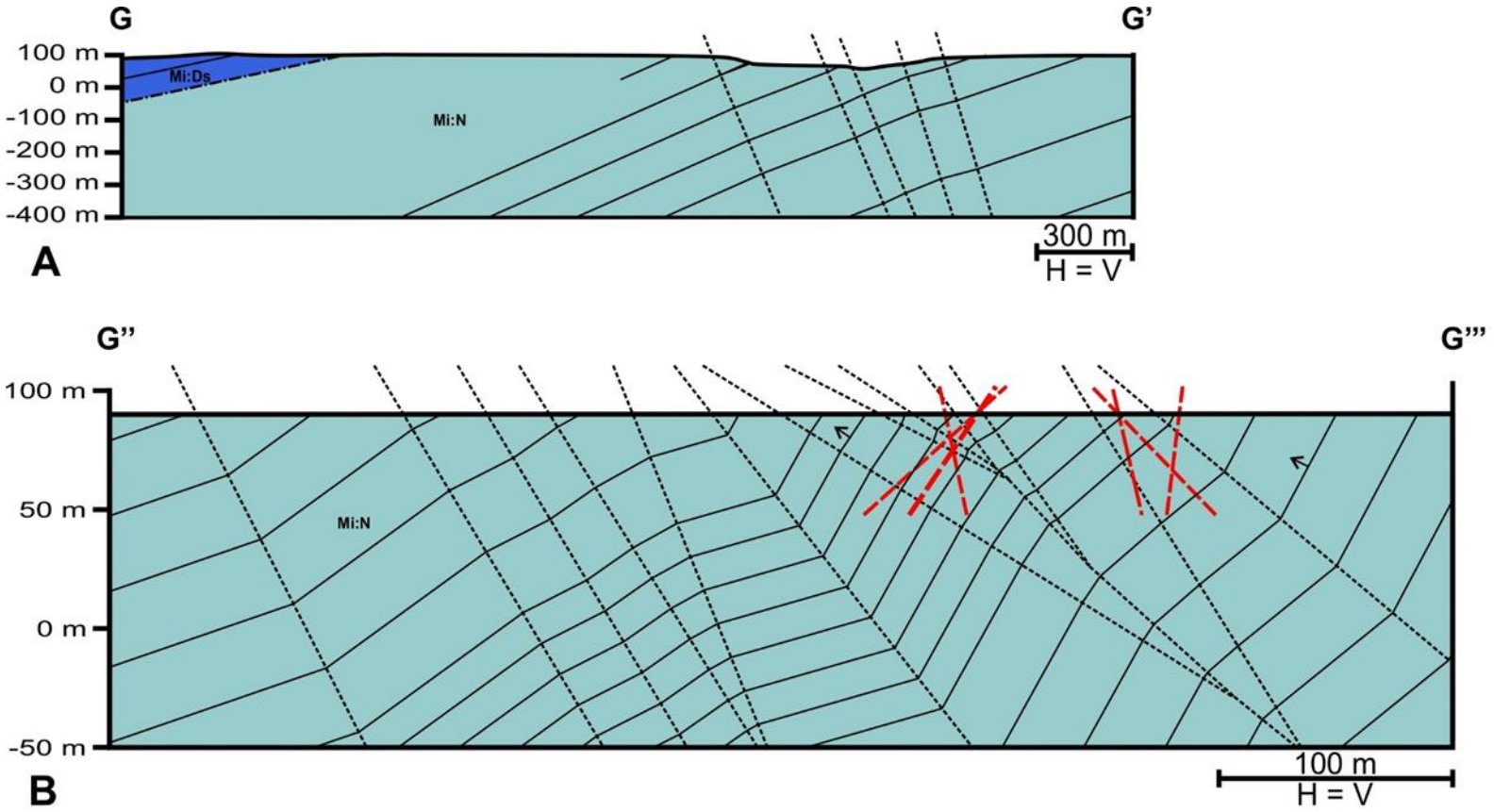

Figure 3.22: A) Vertical cross-section G to G' through northwestern Junction Brook, trending at 112°. Location of cross-section given on Figure 3.20. No vertical exaggeration. Legend for cross-section symbols given on Map A. **B)** Vertical cross-section G'' to G''' through southeastern Junction Brook. Location of cross-section given on Figure 3.21. No vertical exaggeration. Legend for cross-section symbols given on Map A.

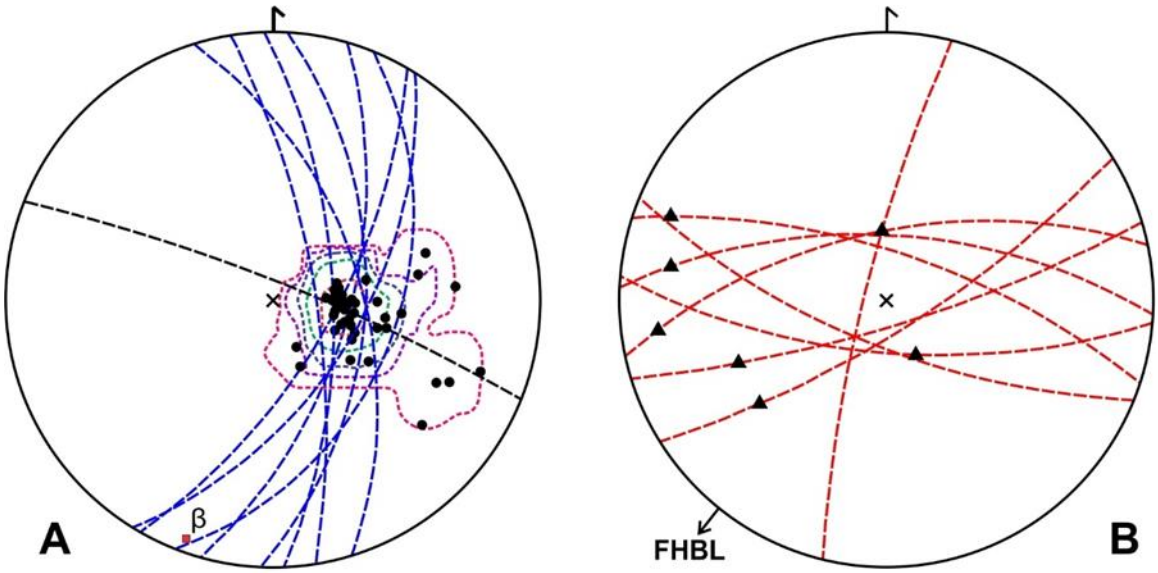

Figure 3.23: A) Lower-hemispere, equal area stereographic projection plot of bedding planes along Junction Brook; number of poles = 46; calculated beta axis is 06-202; calculated girdle is 84/022; contour intervals at 3%, 16%, 12%, 24%, 48% with a maximum of 67.39%. Legend for plot symbols given on Map A. **B)** Lower-hemisphere, equal area stereographic projection plot of faults and lineations at Junction Brook. FHBR is projected fault trace of Fisher Hills-Birchy Ridge Fault. Legend for plot symbols given on Map A.

Figure 3.24: Photograph looking north along the base of Junction Brook at sinistral sense fault drag fold of finely laminated sandstone bed (highlighted in black) along steeply south-southwest dipping fault (highlighted in red). Hammer is 28 cm in length.

lineations (Figures 3.20-3.24). Because a lot of these faults occur at high angles to bedding, they give poor apparent dips in section (Figure 3.22). Faults with very shallowly exaggerated apparent dips in section were omitted.

3.5.6 Structure of the Western Margin

The Deer Lake Group formations and Howley Formation, enclosed by inferred northeast trending splays of the Hampden Fault, form fault panels along the Western Margin of the Howley Basin (Hyde, 1982). The panels internally all show significant contractional deformation structural features. Steeply dipping bedding, tight folds, and steep to sub-vertical internal faults, suggest strike-slip transpressional deformation. Given the fault panels' location along southeast Birchy Ridge, which has compelling structural evidence for dextral strike slip transpression (e.g., Hyde et al., 1994 and many others; Section 3.6), a dextral strike-slip origin of structures observed within the fault panels would be logical. However, some geometries of structures with thoroughgoing faults are not predicted in strike-slip transpressional theory (e.g., Harding, 1985). First, strain partitioning between the Fisher Hills-Birchy Ridge Fault and the Hampden Fault along the connecting splays would produce a transtensional step-over geometry with inferred dextral displacement. Also, both fold axes of tight folds and steep faults with dip slip lineations with the fault panels, make large angles to the strikes of bounding splays (Figures 3.17; Map A). The above arguments require the splays to have their map traces as inferred by Hyde (1982) and may suggest that they may have different orientations and do not branch from the Fisher Hills-Birchy Ridge Fault. This argument is presently speculative and for this reason the fault map traces as Hyde (1982) has inferred have been

left on Map A. The splays may also be an over simplification of a complex network of connecting faults that have undergone polyphased deformation with significant fault block rotation. The lack of exposed kinematic indicators within the fault panels has not allowed for structural interpretations into the exact nature or deformational history of these fault-bounded units.

The Howley Formation mapped along the Western Margin of the basin (Hyde, 1982) is only exposed in a few localities, and based on core from shallow drill holes (O'Sullivan, 1979a, b, c; Map A). Without any palynological control or exposure/ intersections of coal, there is some skepticism that the drill holes along the Western Margin of the basin in fact intersected true Howley Formation; both Humber Falls Formation and Little Pond Brook Formation were shown by Gall (1984) to be petrologically very similar. For clarification as to which formation underlays the western Howley Basin, a palynological investigation is advised. However, once again, without further supporting geoscience, the Howley Formation will remain assumed to underlie the Western Margin and all following interpretations will be based on this assumption.

Deformation along Junction Brook is concentrated at the head of the river and quickly dissipates to the west (over a few hundred meters) to a gently west dipping homocline of un-deformed sandstone beds (Figures 3.20-3.22). The steeply west-dipping bedding and suite of steep to sub-vertical faults with shallowly plunging lineations are interpreted to reflect strike-slip deformation. The exposed fault with a sinistral kinematic indicator (Figure 3.23) suggests that this suite of faults are antithetic strike-slip shears. If deformation at the head of Junction Brook is the product of strain associated with the

Fisher Hills-Birchy Ridge Fault, the quickly dissipating deformation would suggest that fault-induced strain is very localized and reflect strike-slip rather than regional contractional deformation.

Structural mapping of the Western Margin of the Howley Basin clearly shows that all formations experienced post-depositional deformation. The fault panels show a large compressional component with structures that suggest poly-deformation, whereas Junction Brook is dominated by localized strike-slip. Episodes of post-Westphalian, but likely beginning in the Namurian, dextral strike-slip transpression is favored, with lateral growth of the Birchy Ridge manifested as predominately steep reverse-dextral faults migrating to the east. The Fisher Hills-Birchy Ridge Fault is interpreted as the master through-going strike-slip fault accommodating lateral dextral displacement.

3.6 Birchy Ridge

Birchy Ridge forms a northeast-southwest trending topographical high from the headwaters of Junction Brook into White Bay, separating the Howley Basin in the east from the Humber Basin to the west (Maps A, B). It is fault bounded along its length by the north-northeast trending Fisher Hills-Birchy Fault to the west and the Hampden Fault to the east (Map A). Birchy Ridge is not imaged well magnetically; a very long wavelength, consistent, magnetic gradient increasing to the northwest into a pronounced high over the Taylor Brook Gabbro over shadows any features in this area (Map C). However, the first vertical derivative magnetic (Map D) has a very strong continuous

signal associated with the Fisher Hills-Birchy Ridge Fault, but the Hampden Fault remains invisible.

Within the ridge the Saltwater Cove Formation of the Anguille Group is well-exposed in a network of logging roads and incised stream beds. Characteristic lithologies of the Saltwater Cove Formation consist of indurated arkosic pebble to coble conglomerates and sandstones forming fining upwards sequences, interbedded with black to grey-green shale with rare cleavage.

Much greater exposure than other Carboniferous lithologies in the map area allowed for two regional cross-section constructions, giving good control of structural style, and two small quarries permitted detailed inspection of fold geometries. No drill holes have been collared in the Saltwater Cove Formation along Birchy Ridge in the map area.

3.6.1 Southern Quarry

A small quarry next to a logging road in east-central Birchy Ridge, a kilometer west of the Hampden Fault, exposes two long (~100 m) vertical sections of typical Saltwater Cove Formation lithologies (Map A; Figure 3.25). The southern wall of the quarry exposes very steep to upright southeast dipping beds of very fine-grained grey sandstone (Figure 3.25). Immediately to the southeast a massive, very coarse-grained, thick arkosic sandstone bed overlays a 2 m thick shale bed, together younging and dipping shallowly to the southwest (Figure 3.25). Marker beds were not observed crossing this sharp change in orientations over a short length; thus there are two options

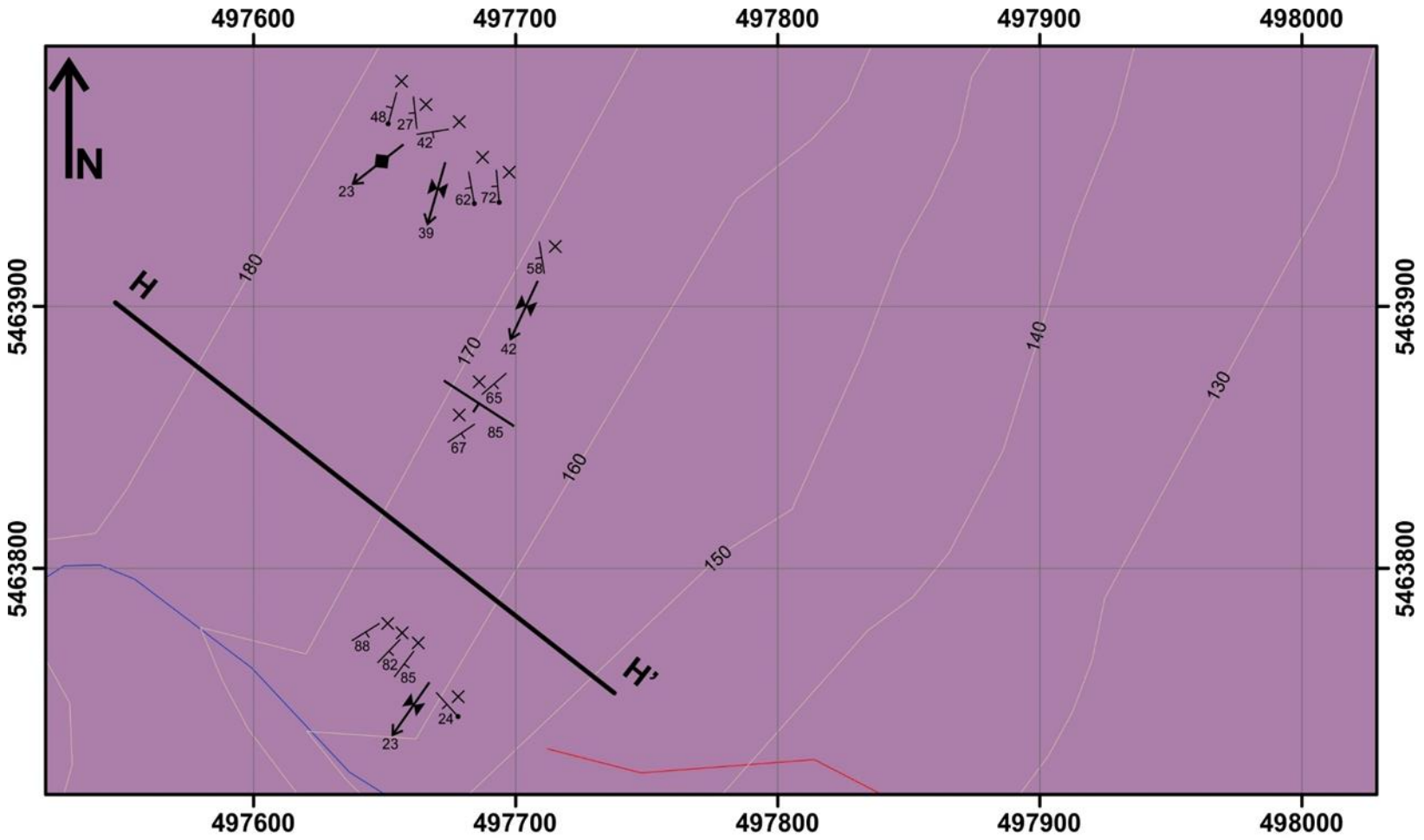

Figure 3.25: Detailed geological map of the Southern Quarry in Birchy Ridge showing the location of vertical cross-section H to H', trending at 128°. Map scale at 1:2,500. Lithological units, map symbols, and location of map are given on Map A.

to account for this type of geometry: there is a fault separating the two almost perpendicular dips; or the shallowly dipping massive arkosic bed sits in the core of a shallowly southwest plunging syncline, and the upright fine grained beds to the northwest lay underneath and the marker is not exposed on the west limb. If the latter is the case, strata would kink around a moderately steep westerly dipping axial plane into a shallowly southwest dipping orientation, with a gently southwest plunging (23-215) calculated fold axis (Figures 3.25, 3.26).

In the northern quarry wall, thick bedded fining upward sequences of arkosic conglomerates, laminated blue-grey sandstones, and black shales are exposed in an upward facing anticline-syncline pair that fold around steep southeast-dipping axial planes, with calculated fold axes plunging gently to moderately to the southwest (Figures 3.25, 3.26).

An outcrop in the center of the quarry revealed a sub-vertical southwest dipping 1.5 m fault zone of brecciated fault gouge, cutting steeply southeast dipping rippled siltstone and sandstone packages (Figure 3.27). Kinematic indicators or offsets were not observed within the fault zone. It is unknown how much offset has occurred on this fault, but assuming only minor, both structures on the northern wall and southern wall are projected into cross-section (Figure 3.26). The fault was omitted because of its near parallelism with the cross-section (Figure 3.25). Together, the sparse dataset of bedding planes forms a moderately cylindrical fold plot with a calculated beta axis of 36-218 (Figure 3.26). Folding in the Southern Quarry appears to show a weak easterly directed sense of asymmetry (Figure 3.26).

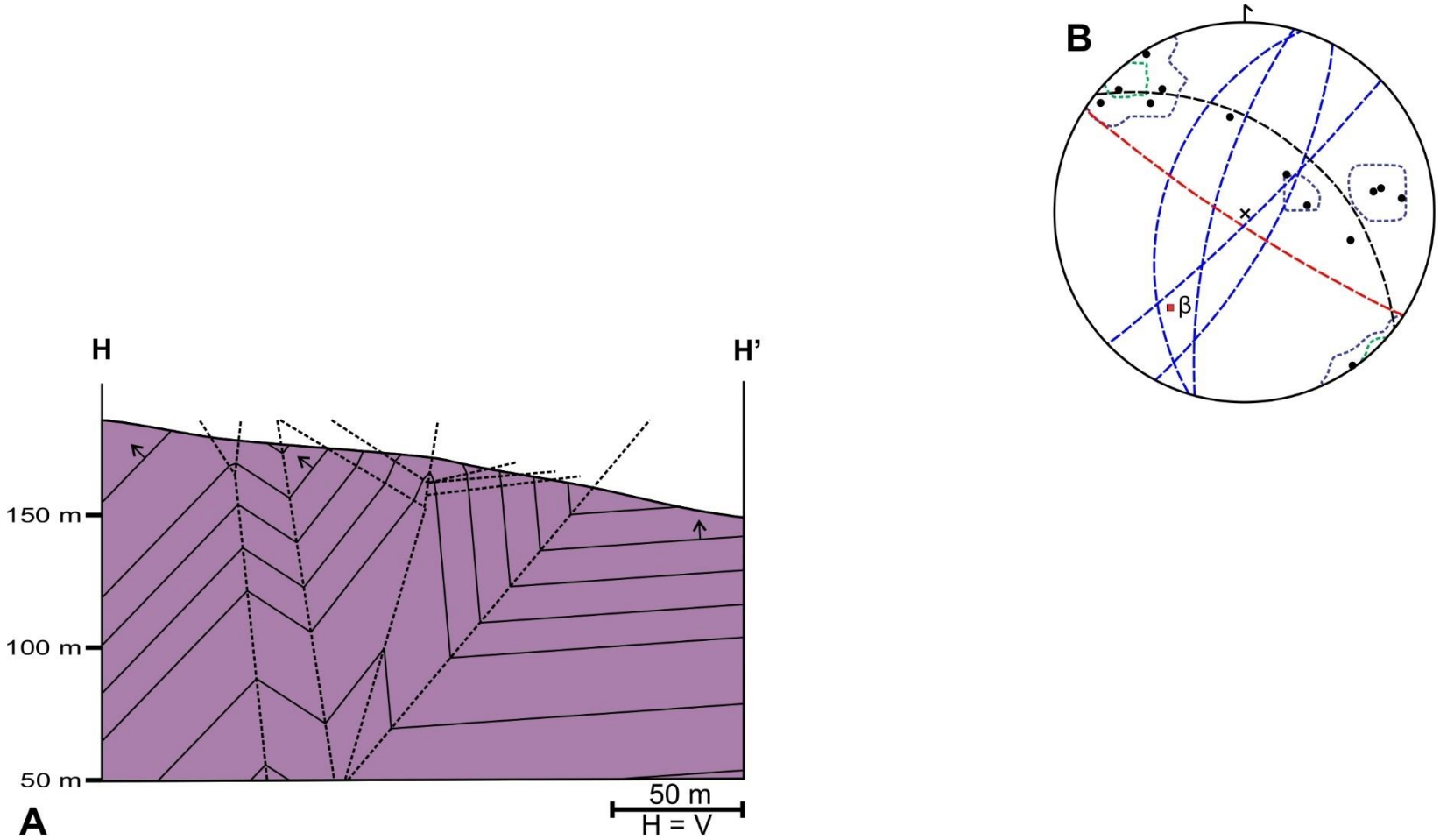

Figure 3.26: A) Vertical cross-section H to H' through the Southern Quarry in Birchy Ridge, trending 123°. Location of cross-section given on Figure 3.25. No vertical exaggeration. Legend for cross-section symbols given on Map A. **B)** Lower-hemispere, equal area stereographic projection plot of structural elements at the Southern Quarry; number of poles = 13; calculated beta axis is 36-218; calculated girdle is 54/038; contour intervals at 8%, 16% with a maximum of 23.08%. Legend for plot symbols given on Map A.

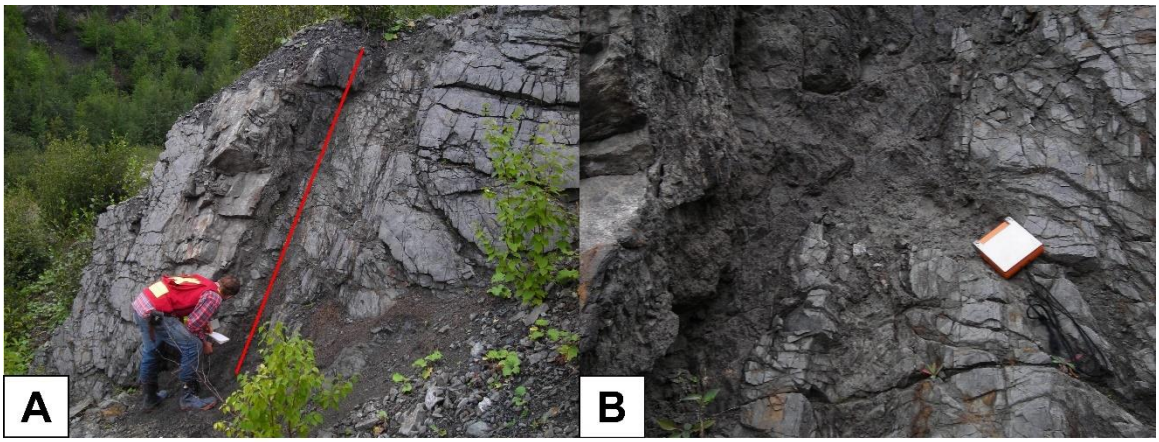

Figure 3.27: A) Photograph looking northwest at steeply southeast dipping rippled siltstone and sandstone beds cut by a 1.5m wide, very steeply southwest dipping, brecciated fault zone (red). **B)** Photograph of brecciated fault zone. Compass is 7.0 cm in length.

3.6.2 Southern Birchy Ridge

From well-exposed sections along the berms and clear-cuts of an unnamed logging road, and outcrops documented along McIsaacs Brook on Hyde and Ware's (1980) 1:50,000 geological map, a detailed cross-section through the central region of Birchy Ridge was constructed (Map A; Figures 3.28, 3.29). The Saltwater Cove Formation along this section forms fining upward packages of sub-angular, arkosic, pebble to cobble conglomerate beds, sandstones, and shales. These lithologies form non-cylindrical, steep to sub-vertical asymmetrical trains of tight, upward facing anticlines and synclines that, at depth, bend around sub-vertical axial planes trending north-south (Figures 3.28, 3.29). Fold axes plunge moderately to the north-northeast for the eastern folds, and moderately to the south-southwest for the western folds (Figure 3.28). Together, these bedding planes give a moderately well-defined beta axis (34-190)

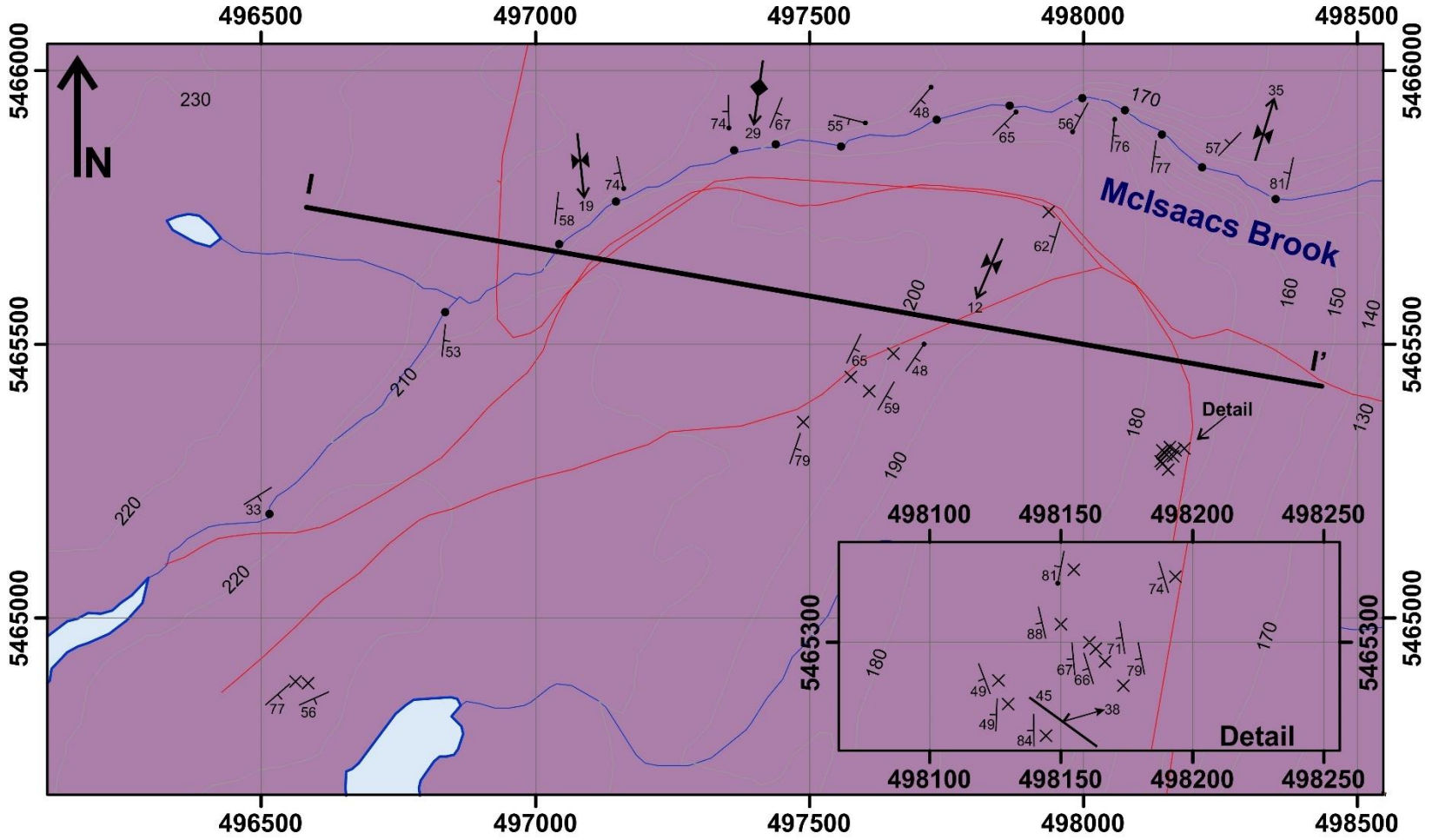

Figure 3.28: Detailed geological map of McIsaacs Brook showing the location of vertical cross-section I to I', trending at 080°. Map scale 1:12,000. Lithological units, map symbols, and location of map given on Map A.

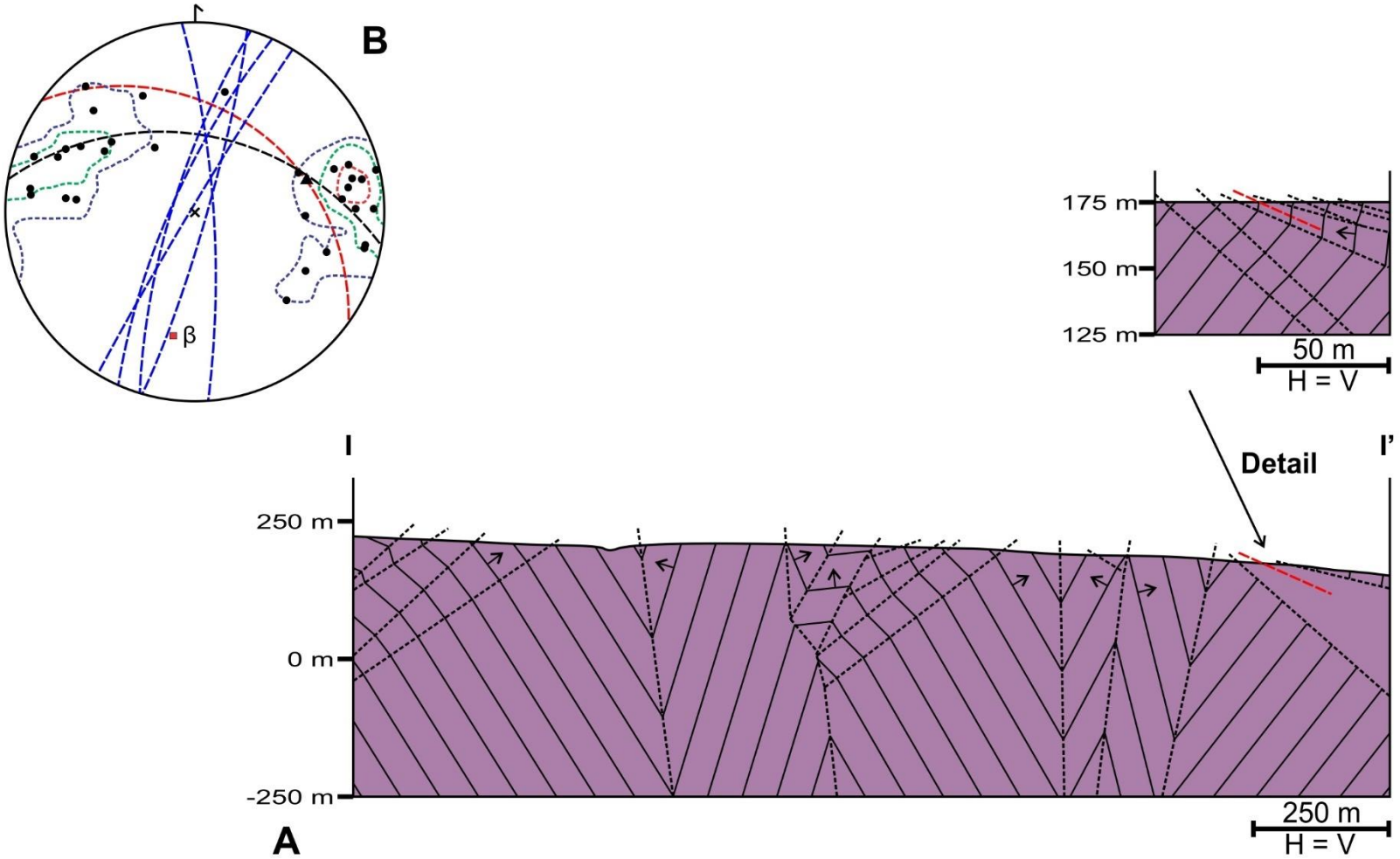

Figure 3.29: A) Vertical cross-section I to I' through Southern Birchy Ridge, trending 100°. Location of cross-section given on Figure 3.28. No vertical exaggeration. Legend for cross-section symbols given on Map A. **B)** Lower-hemispere, equal area stereographic projection plot of structural elements along Southern Birchy Ridge; number of poles = 31; calculated beta axis is 34-190; calculated girdle is 56/010; contour intervals at 4%, 8%, 16% with a maximum of 22.58%. Legend for plot symbols given on Map A.

Figure 3.30: Photograph looking northwest at new showing in landing of logging road south of McIassics Brook, showing overlying conglomerate bed creating load structures in underlying shale. Hammer is 28 cm in length.

plunging moderately to the south-southwest (Figure 3.29). Overall, folding through southern Birchy Ridge is asymmetric with an east vergence (Figure 3.29).

A well-exposed group of showings on the berm of a new logging road in the eastern part of Figure 3.28, display a faulted section on the most easterly limb of a close syncline. Here, fining upwards packages of black organic shale beds (2 cm to 1.0 m thick) and fine- to medium-grained, laminated and fractured grey sandstones are overlain by massive medium- to coarse-grained grey sandstones and pebble conglomerates. Conglomerates overlie shales to the north, creating spectacular load structures (Figure

3.30). The section forms a sub-vertical to moderately west dipping limb that shallows to the west. A moderately inclined slickensided fault surface concentrated in a shale bed separates the northern section from the southern section. This fault dips to the northeast with lineations plunging (38-074) moderately to the east-northeast (Figures 3.28, 3.29).

3.6.3 Northern Birchy Ridge

Approximately 1 km to the north, exposures along Route 422 and Flights Brook (from Hyde and Ware's (1980) 1:50,000 geological map) provide well-constrained data for a cross-section through northern Birchy Ridge (Map A; Figures 3.31, 3.32). Lithologies examined here are similar to those exposed to the south, but with greater amounts of sandstones and siltstone exposed. Fining upwards packages are typically on the order of several meters. In northern Birchy Ridge, these rocks form very steep to upright, tight, upwards facing asymmetrical anticlines and synclines that fold around very steep to upright axial planes that dip to the east and south east (Figures 3.31, 3.32), quite similar to folding observed through McIsaacs Brook (Figures 3.28, 3.29); however, in this cross-section the overall sense of fold asymmetry appears to be west-directed. Fold axes along this section predominately plunge moderately to the south with a single shallowly southwest plunging and a moderately north plunging fold axis in the eastern part of the section (Figure 3.31). A single occurrence of steep east dipping cleavage was observed in a mica-rich fine-grained sandstone and has a moderate southeast dip, roughly parallel axial planes of the folds (Figures 3.31, 3.32). Together, bedding planes form non-cylindrical folds with a gently plunging beta axis (23-192) to the south (Figure 3.32).

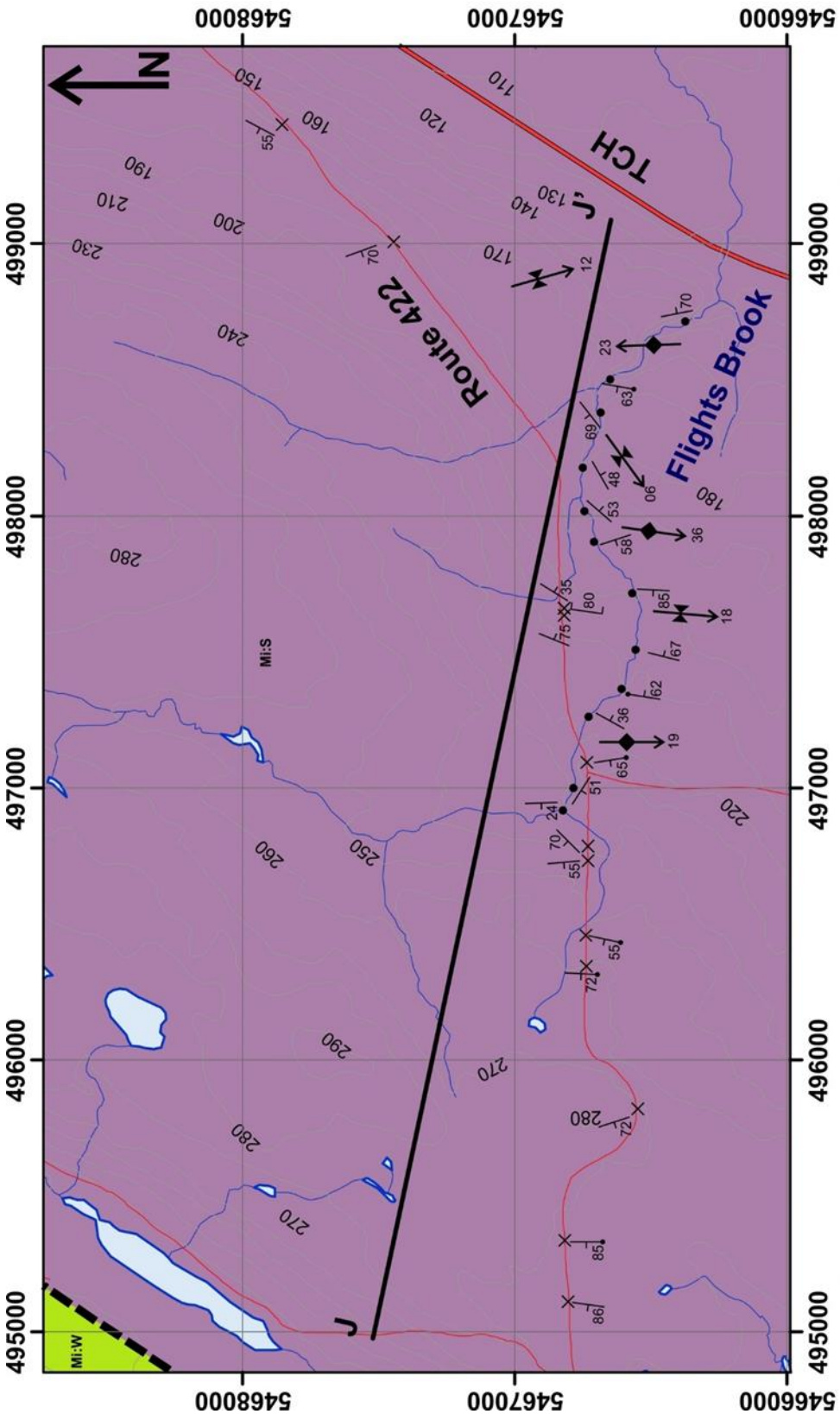

Figure 3.31: Detailed geological map of Northern Birchy Ridge showing the location of vertical cross-section J to J', trending at 102°. Map scale 1:24,000. Lithological units, map symbols, and location of map given on Map A.

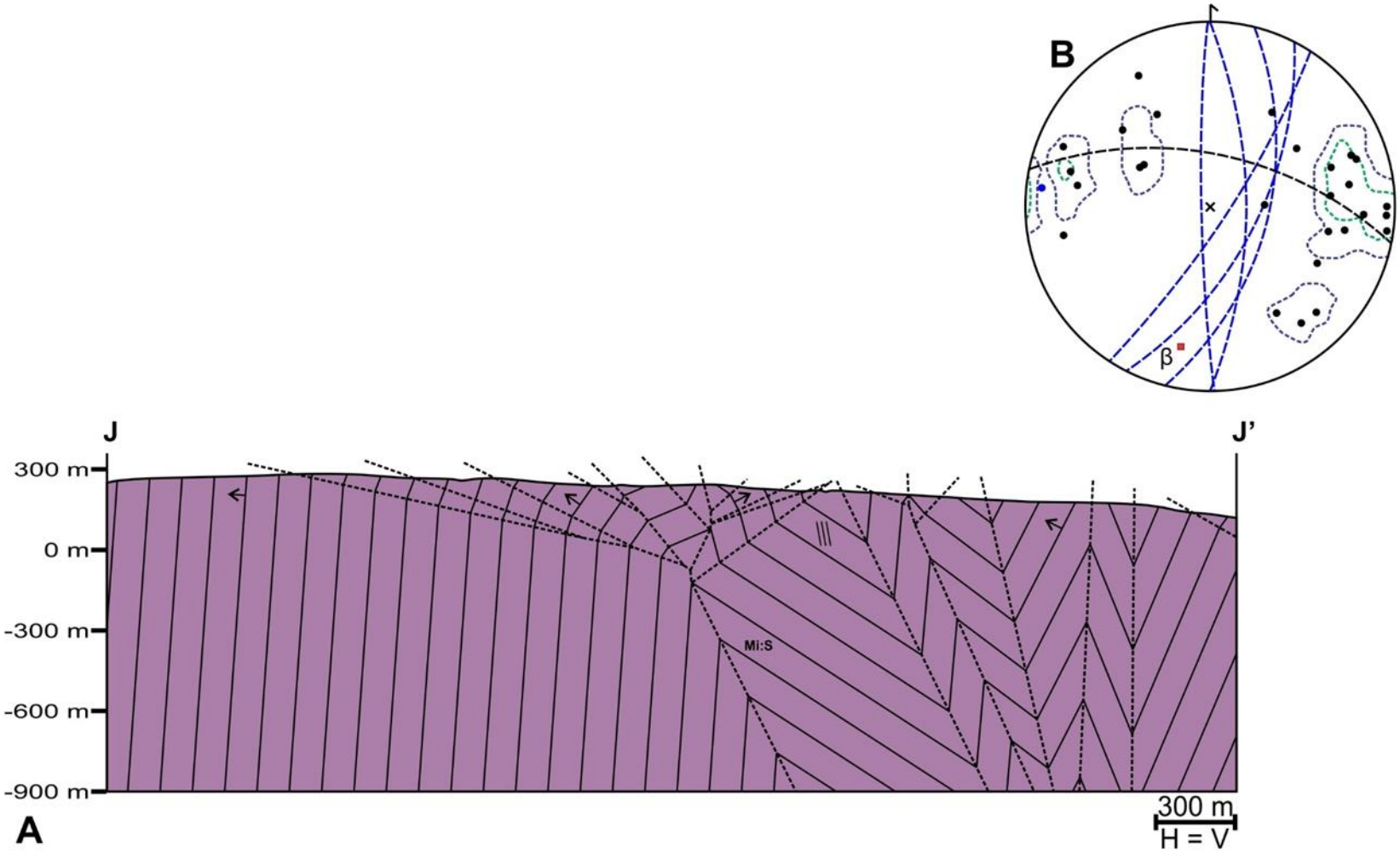

Figure 3.32: A) Vertical cross-section J to J' through Nouthern Birchy Ridge, trending 102°. Location of cross-section given on Figure 3.31. No vertical exaggeration. Legend for cross-section symbols given on Map A. **B)** Lower-hemispere, equal area stereographic projection plot of structural elements along Southern Birchy Ridge; number of poles = 27; calculated beta axis is 23-192; calculated girdle is 67/012; contour intervals at 5%, 10% with a maximum of 16.67%. Legend for plot symbols given on Map A.

3.6.4 Northern Quarry

Approximately 3 km north of McIsaacs Brook, in another small quarry, thick packages of medium grained arkosic sandstones and dark grey-black shale, with thin bedded siltstone are exposed in two vertical walls (Map A; Figure 3.33). In the northwestern wall (K to K'), an open anticline-syncline pair folds around steeply west-dipping to upright axial planes before folding into a steep close, partly broken, anticline with a very steeply west-dipping axial plane (Figures 3.33, 3.34). Cleavage in the steep forelimb of the anticline dips steeply to the west-southwest. To the east of the broken anticline, an open syncline is cut by a steep east-northeast dipping fault with near down-dip lineations (Figures 3.33, 3.34).

The southeast quarry wall (K'' to K''') displays thick bedded, medium- to coarse-grained arkosic sandstones interbedded with dark grey shales that form an open, upward facing, syncline (Figures 3.33, 3.34). Slaty cleavage in the shale beds through this fold dip moderately to steeply to the west, forming steep to near parallelism intersection angles with bedding (Figures 3.33, 3.34). The cleavage bedding relationship in this fold is near axial planar with cleavage in the west limb and the core of the syncline, but diverges to moderately southwest-dipping in the eastern limb (Figure 3.34). This anomalous cleavage measurement may reflect late-stage refolding. To the east, a steep east dipping fault within sheared along a shale bed, separates the syncline from a non-cylindrical open syncline anticline pair that projects to form an anticline folding around a steeply west dipping axial plane at depth (Figures 3.33, 3.34). On the steeply southeast dipping limb, steep east dipping cleavage is present in a shale bed (Figures 3.33, 3.34). Further to the

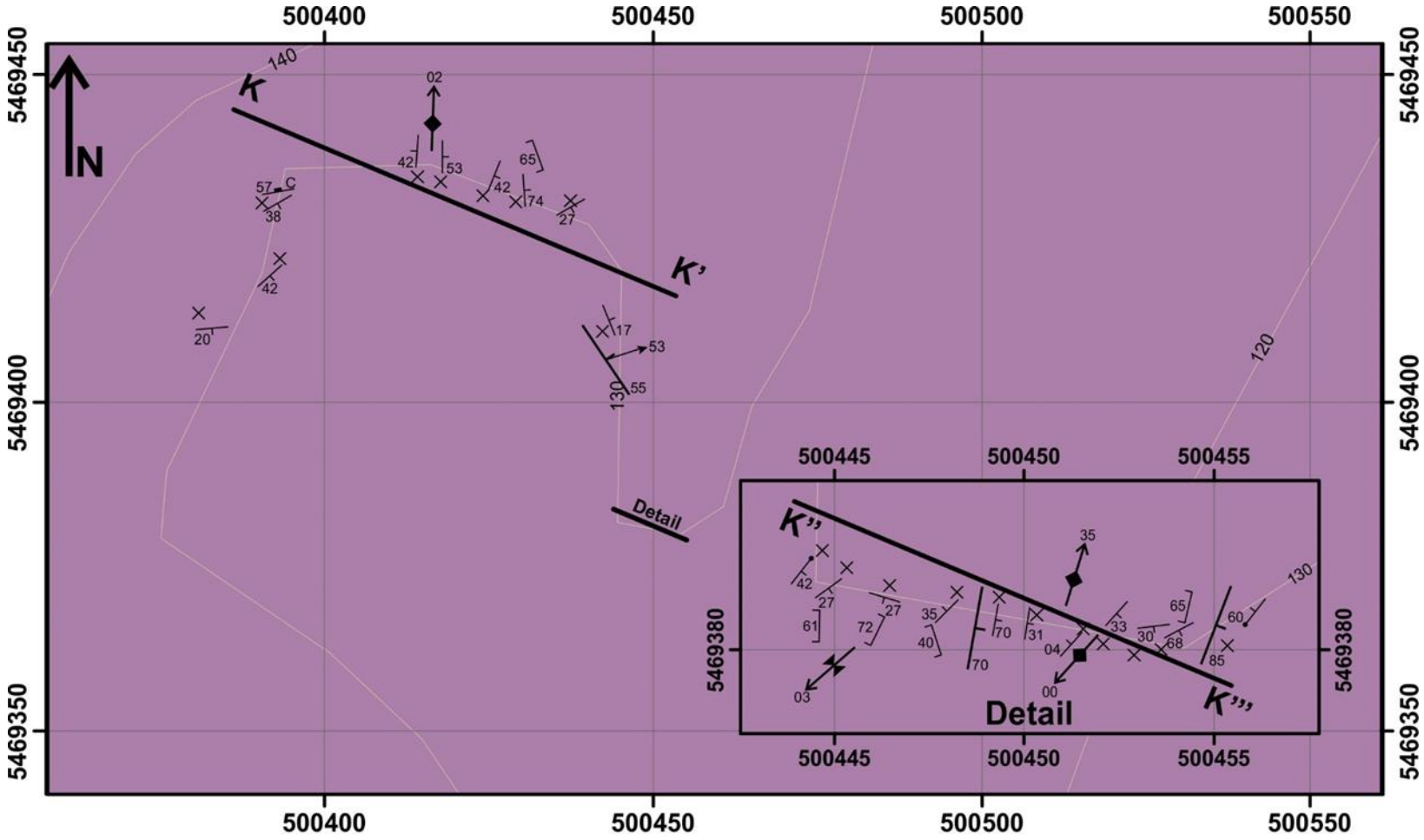

Figure 3.33: Detailed geological map of the Northern Quarry in Birchy Ridge showing the location of vertical cross-section K to K' and K" to K"', trending at 112°. Map scale 1:600. Lithological units, map symbols, and location of map given on Map A.

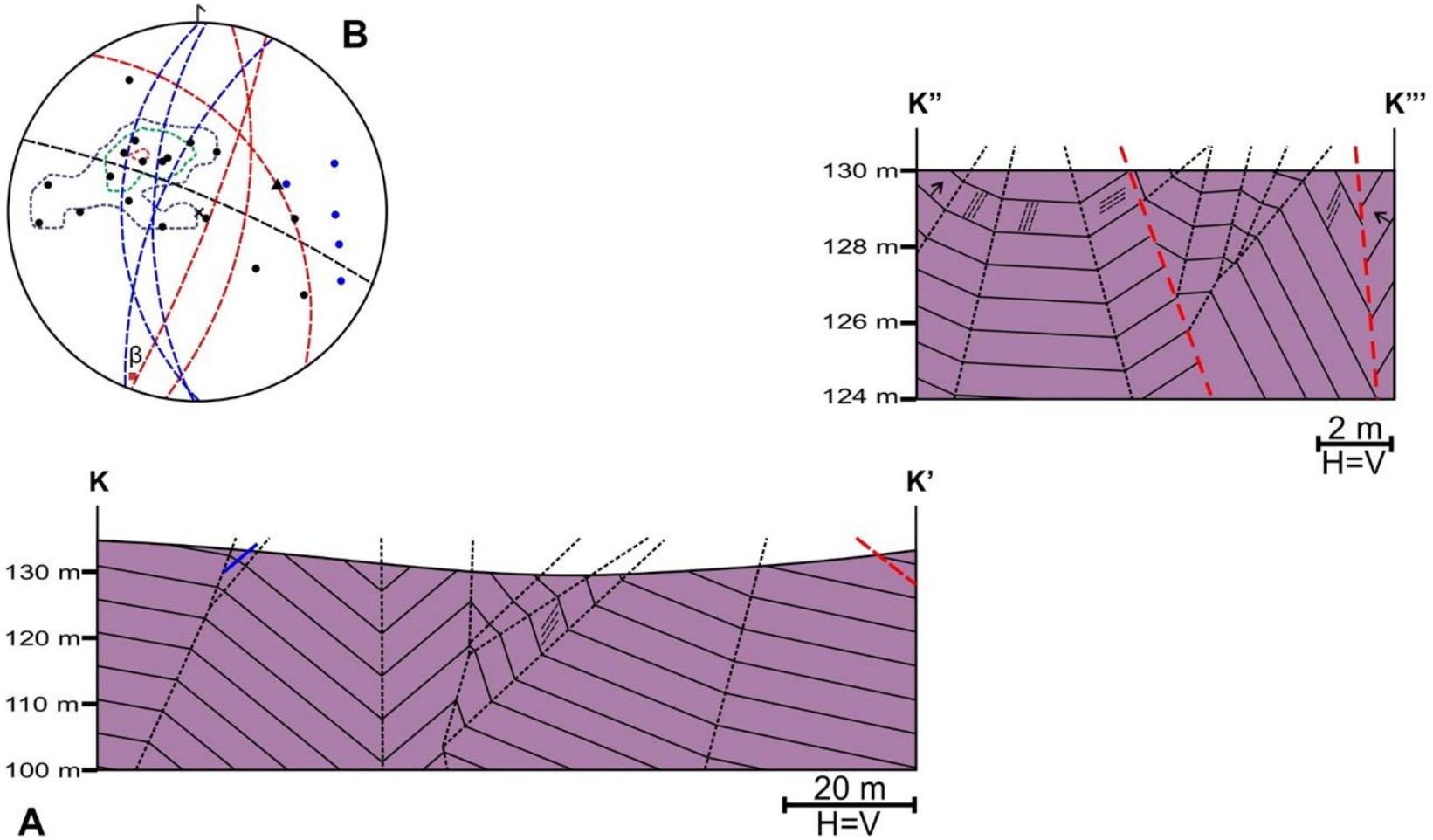

Figure 3.34: A) Vertical cross-section K to K’ and K” to K”’ through the Northern Quarry, trending 112°. Location of cross-sections given on Figure 3.33. No vertical exaggeration. Legend for cross-section symbols given on Map A. **B)** Lower-hemispere, equal area stereographic projection plot of structural elements at the Northern Quarry; number of poles = 18; calculated beta axis is 07-200; calculated girdle is 83/202; contour intervals at 6%, 12%, 24% with a maximum of 27.78%. Legend for plot symbols given on Map A.

east, a sub-vertical east dipping fault separates the eastern limb of the anticline with steep northwest dipping and younging beds before exposure is lost (Figures 3.33, 3.34).

Non-cylindrical folds along this section give shallow to moderately north-northeast and shallow southwest plunging fold axes (Figure 3.33). Together, bedding produces a very poorly constrained shallowly south-southwest plunging (07-200) beta axis, with fold geometry showing good sense of east-directed vergence (Figure 3.34).

3.6.5 Structure of Birchy Ridge Structures

The Saltwater Cove Formation exposed throughout Birchy Ridge is in a highly deformed state; mesoscopic and macroscopic folds are frequent, often with close to tight (near locking angle) interlimb angles, and steep faults are common that both cut and shear bedding planes. Lithologies are the most indurated of all of the Carboniferous units, with slaty cleavage forming in the more incompetent beds. Overall the fold system in Birchy Ridge displays an easterly sense of vergence.

Folding within Birchy Ridge, albeit predominately non-cylindrical, consistently produces en echelon fold axes that form oblique angles with bounding master faults' map traces (Fisher Hills-Birchy Ridge and Hampden faults). This is in agreement with previous workers observations and interpretation that dextral transpressional strain along these faults produced deformation of the Saltwater Cove Formation in Birchy Ridge (e.g., Hyde, 1982, 1984; Hyde et al., 1994). Internal steep northwest trending faults with near downdip lineations are interpreted to be reverse, and the sub-vertical north-northeast trending faults, synthetic strike-slip shears. Reclined to vertical folds, folded cleavage,

and curvilinear fold limbs, all suggest that the Saltwater Cove Formation has endured at least two episodes of high strain dextral transpression.

Chapter 4: Geophysical Analysis of the Howley Basin

4.1 Introduction

The lack of exposure and limited shallow drilling in the Howley Basin leaves its structural and stratigraphic architecture elusive. Geophysical surveying can be a very cost-effective method of predicting subsurface features, basin geometry and depth; all of which are critical for proper evaluation of hydrocarbon generation, migration, and trapping scenarios. A government funded, high-resolution aeromagnetic survey was collected over the Howley Basin in 2009 (Cook and Kilfoil, 2009; Section 4.5). Gravity data collection has not been carried out regionally over the basin since 1983 (Miller and Wright, 1984). Since that time there have been substantial advances in gravity collecting and processing technologies.

One of the primary objectives of this study is to supplement the high-resolution aeromagnetic data with a modern land-based gravity survey (Section 4.4). Because much of the Howley Basin is overlain by Sandy Lake – which is the largest area not sampled by previously acquired gravity surveys (Miller and Wright, 1984) – a thorough coverage of the basin required surveying over the frozen surface of the lake. In order to arrive at geologically meaningful gravity data for locations over Sandy Lake, a detailed bathymetry map (Section 4.2.5) was created in order to remove the anomalous mass of the water column (Section 4.4.4) in the complete Bouguer (terrain and bathymetry corrected) anomaly map (Map E). To accomplish this, a Ground Penetrating Radar (GPR)

was used to survey the depth of Sandy Lake along transects that traversed gravity station locations on the lake (Section 4.2).

The largest contributor to the uncertainty in gravity measurements is the accuracy and precision of the gravimeter's elevation. Advances and availability of GPSs have allowed for field-based units to reach very high and reliable resolutions. A Real Time Kinematic (RTK) GPS survey was run in conjunction with gravity surveying to reach sub-decimeter resolution at each station location (Section 4.3). This is a significant advance from previous gravity surveys collected over the Howley Basin.

Two governmentally funded high-resolution aeromagnetic surveys and several recently acquired industry aeromagnetic surveys (available in the public domain), flown in the area around the Howley Basin, have been knit together (Section 4.5) to create a regional magnetic map (Map C). Coverage of the recent surveys is not complete, and the lower-resolution GSC's regional aeromagnetic map (Kilfoil and Bruce, 1990) was used to fill in the gaps (Section 4.5).

Final compilations of gravity (Map D) and aeromagnetics (Map C) are used, along with geological interpretations and assumptions, to execute several 2 ¾ D forward modeling profiles of the Howley Basin (Chapter 5).

4.2 Ground Penetrating Radar (GPR) – Bathymetry Data

GPR systems use a transmitter of high frequency radio waves with a separate receiver at fixed geometry to image the subsurface through reflections of "lossy"

dielectric material (Jol, 2009). By moving the transmitter and receiver over an area of interest, reflections are processed to create a two-dimensional profile of dielectric property contrasts in the subsurface medium. This geophysical technique is well suited to image the interface between freshwater and soft sediments at the bottom of a lake because of their contrasts in dielectric properties (Jol, 2009). The results of this survey were used to create a bathymetry map of Sandy Lake (Section 4.2.5) for the purpose of removing the anomalous mass created by the water column (Section 4.4.4), from the Bouguer gravity map (Map D).

4.2.1 Sensors and Software GPR System

A GPR system was rented from Sensors & Software, Mississauga, Canada to collect the bathymetry data. The system consists of two 50 MHz antennas, a Digital Video Logger (DVL), and a control module. The two antennas are each powered by two 12 Volt batteries, mounted on the antennas, and are connected to the control module via fiber optic cables. The control module is mounted onto the back of the DVL and is powered by an external 12 Volt battery. The DVL allows the user to see reflections in real-time and is the interface in which parameters for data collection are set. A Garmin hand-held GPS was connected to the control module to georeference data as it was stored in the control module's internal memory.

4.2.2 GPR Surveying

Prior to GPR surveying, the approximate maximum depth of Sandy Lake (100 feet) was obtained through discussions with residents of Howley, who had observed lake

depths with recreational depth finders while boating on the lake. This information plus an initial survey of the conductivity of the lake water (Appendix B) led to the choice of renting 50 MHz antennas in order to image the deepest portions of the lake with the highest resolution.

The GPR surveying was done over Sandy Lake to measure the depth of the water column under gravity stations taken on the ice. This was completed by attaching the GPR transmitter and receiver on two parallel toboggans with a 1.4 m horizontal separation and towed behind a sleigh attached to a snow machine (Figure 4.1). The snow machine was driven at approximately 22 km/h along transects over gravity station locations while the GPR collected GPS referenced data (Figure 4.2).

Figure 4.1: Photograph of Dr. Alison Leitch displaying the setup used to collect GPR data over Sandy Lake. Antennas are attached to the toboggans at the rear with fibre optic wires running along the tow-bar connecting to the control module and the DVL in the sled. Dr. Alison Leitch monitored data collection on the DVL from the sled while the snow machine was in motion.

4.2.3 Bathymetry

Georeferenced GPR reflection data collected over Sandy Lake (Appendix C) was uploaded into Sensors & Software's EKKO_Project 2 software platform. Each transect was plotted with a velocity of 0.033 m/ns – the speed of electromagnetic waves in fresh water (Jol, 2009) – to give the depth of the water column (e.g., Figure 4.3A). Each transect was then interpreted for reflections of the bottom of the lake with EKKO_Project 2 Polyline Interpretation Tool in the LineView screen (e.g., Figure 4.3B). The nodes used to make the polyline interpretations were exported into Microsoft Excel as georeferenced depth files, recorded as Eastings and Northings, UTM Zone 21N, NAD83, and depth in meters (Appendix C). An ArcGIS shape file of the shoreline and islands of Sandy Lake was exported as a .csv file, with each node used to create the polyline of the lake assigned a depth value of zero (Appendix C). This file was then added to the bathymetry Excel file (Appendix C) and loaded into Oasis Montaj as a database. The shoreline point data was used to more accurately represent the true depth of the lake by interpolating only to the shore of the lake and assigning that point a value of zero meters. GPR and shoreline point data were gridded in Oasis Montaj with a 50 m minimum curvature cell size and linear color scheme, and then windowed with the outline of Sandy Lake polygon file (Figure 4.4; Appendix C). This grid was used to correct for the mass of the water column beneath each gravity reading taken on the lake (Section 4.4.4).

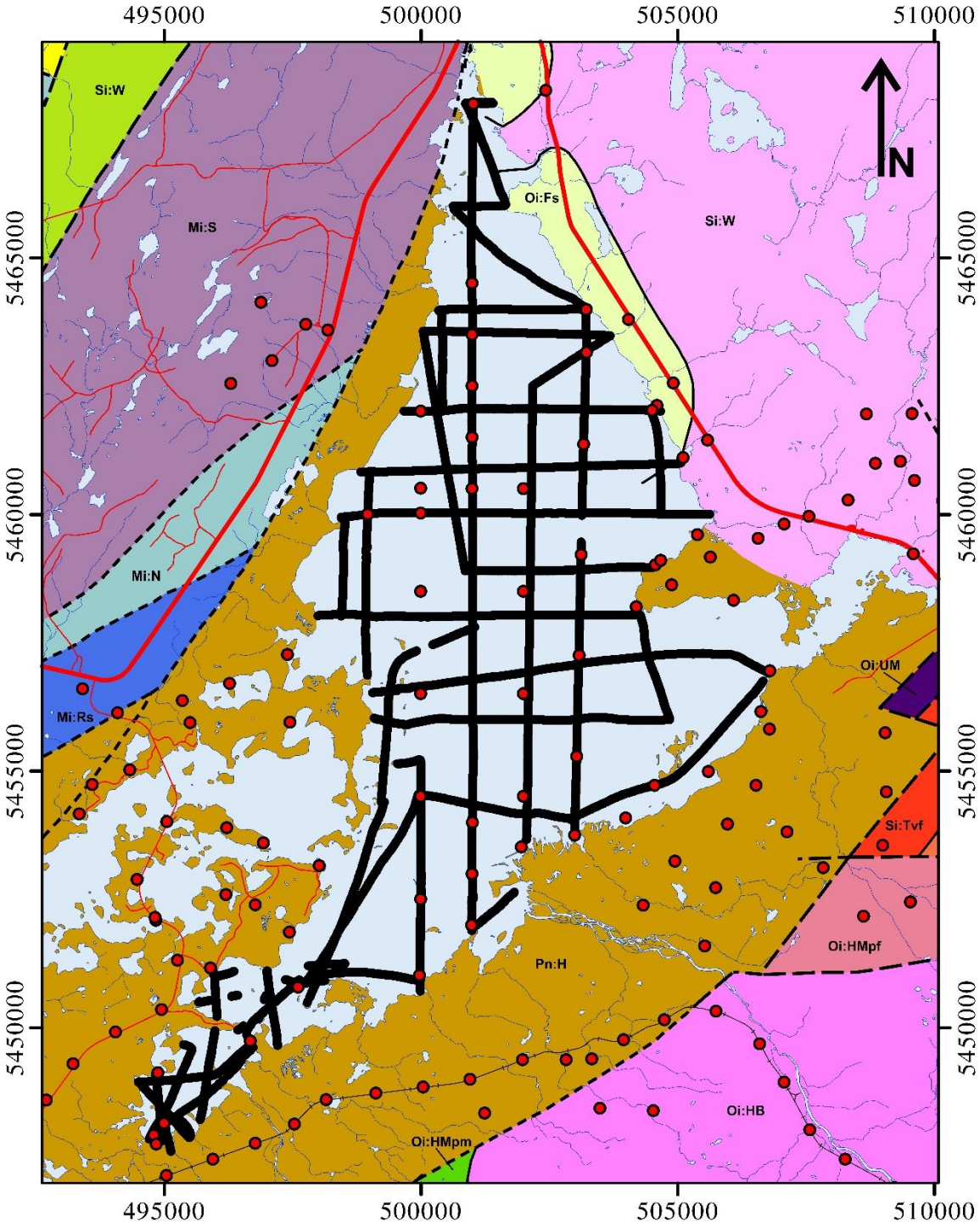

Figure 4.2: Map of GPR transects (black lines) over Sandy Lake, with gravity station locations collected during this study shown as red dots. Map scale, 1:125,000. Map symbols given on Map A.

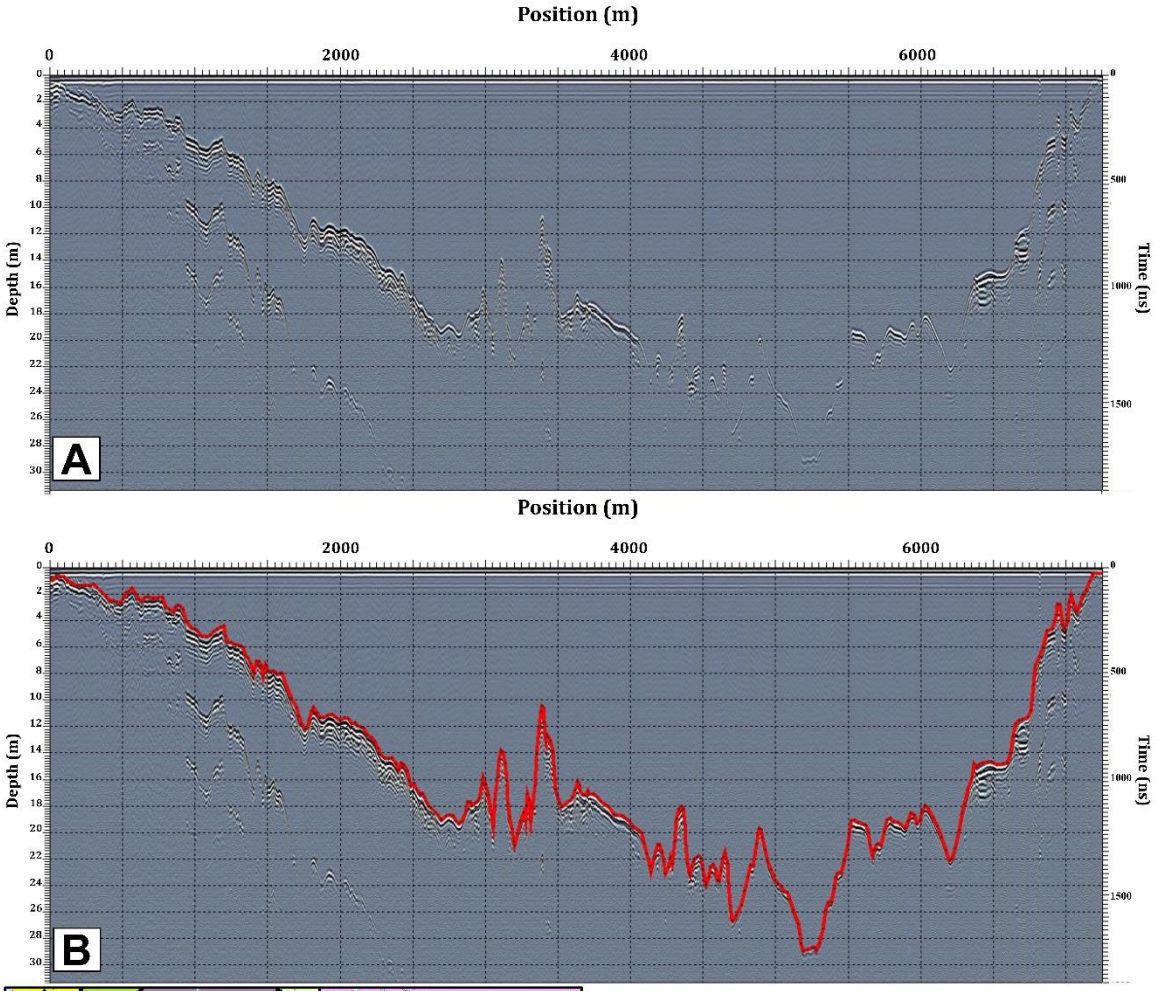

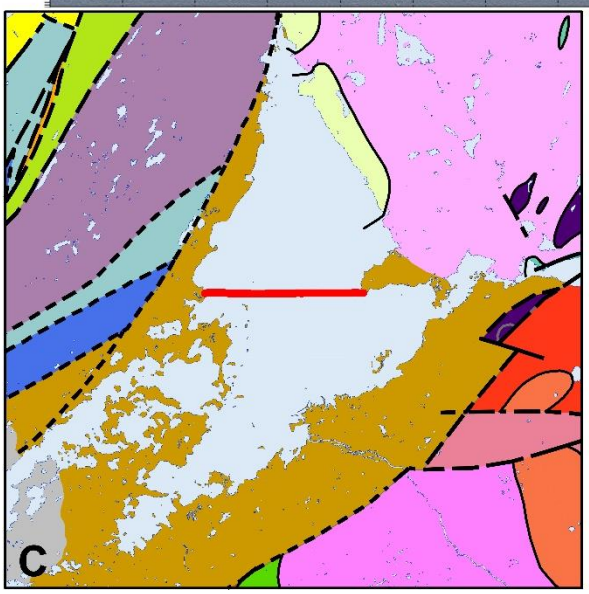

Figure 4.3: A) Example of a GPR transect plotted in Sensors & Software's EKKO_Project 2 Line View menu with 0.033 ns/m velocity; depth in meters is on the left vertical and reflection time is on the right vertical. **B)** Same image as Figure 3.1A with interpretation of lake bottom traced in red with the Polyline Interpretation Tool. **C)** Location of the above transect over Sandy Lake.

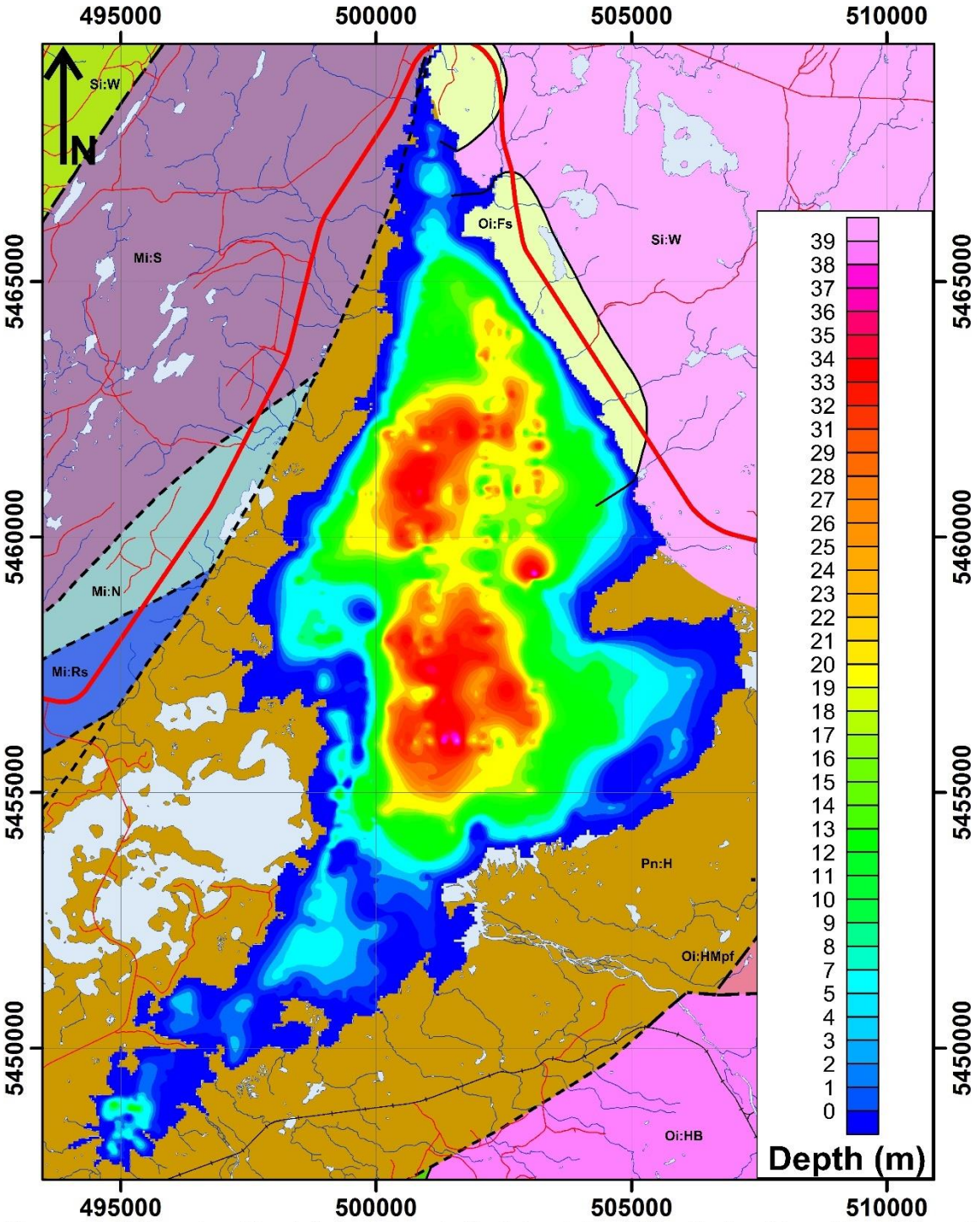

Figure 4.4: Bathymetry of Sandy Lake, interpreted by interpolating GPR reflection data, with a polyline of Sandy Lake's shoreline set to zero meters depth, in Oasis Montaj; cell size set to 50 m, gridded with minimum curvature, plotted with a linear color scheme. Map scale, 1:125,000. Map symbols given on Map A.

4.3 Real Time Kinematic (RTK) Global Positioning System (GPS)

A GPS survey was conducted in conjunction with the gravity surveys to accurately determine each gravity station's exact planimetric and vertical location, referenced to the GRS80 ellipsoid. The accuracy and precision of the vertical component is particularly important in gravity surveying because of the inverse squared relationship gravity has with distance to mass (Section 4.4).

An RTK survey was selected as the most practical survey method for this study because of the speed at which sub-decimeter accuracy is achieved in both the planimetric and vertical. The RTK method uses two receivers, a stationary receiver (the base station) and a roving receiver. The base station is set up to calculate its approximate location by averaging satellite signals, for an unspecified amount of time, as determined by the user. Once the base's location has been approximated it is then locked at this specific location. It uses this approximate location, along with satellite ephemeris, to calculate the differential corrections (atmospheric and orbital errors and counteract anti-spoofing signals put on by the United States Department of Defence (DoD)). The approximate location of the base and correction code is sent to the roving receiver via radio signal. If the roving receiver shares multiple common satellites with the base, it is able to use this data to determine its location to within a few centimeters relative to the base's location in real-time. Detailed description of the theory and algorithms used in RTK surveying are beyond the scope of this study and the interested reader is referred to Hofmann-Wellenhof and Moritz (2006).

4.3.1 Topcon HiPer Lite+ GPS

The Topcon Positioning HiPer Lite+ system uses two dual-frequency receivers that are capable of receiving and processing L1 and L2 signals from both GPS satellites, DoD, and Global Navigation Satellite System (GLONASS) satellites, Russian Federation Ministry of Defence. This capability allows for more satellites to be in view at any one time, increasing accuracy in position and decreasing the Dilution of Precision (DOP) – a function of the geometric arrangement of satellites, as they are presented to the receiver, which can enhance or reduce location resolution depending on degree of clustering and position of satellites on the horizon. The ability of the HiPer Lite+ receivers to process both frequencies of GPS and GLONASS satellites, allows them to remove almost all ionospheric effect from the code and carrier phases, and requires less observation time to achieve the same precision as single frequency receivers (Topcon, 2004).

Both receivers are equipped with 915 MHz spread radio modems that enable communication between themselves. The 1 Watt transmitter on the base is only able to transmit a relatively short distance of 1-2 km, and is dependent on line-of-sight and atmospheric conditions. A Topcon RE-S1 1 Watt 915 MHz spread radio repeater was purchased and used for surveys conducted after March, 2013, effectively doubling the range of communication between the base and roving receivers (Topcon, 2006). The receivers also use an internal Bluetooth transmitting and receiving module to communicate with other devices with Bluetooth wireless technology (Topcon, 2004). A Topcon FC-200 data collector was used in conjunction with Topcon's TopSURV

integrated controller survey software to record rover measurements and configure receivers in the field.

4.3.2 GPS Surveying

During RTK surveying, the base receiver was set to record 'static' observations. Satellite observations and estimation steps were recorded every 1.0 seconds with a 10.0º elevation mask cut-off. Typical static observations were taken for two hours or greater. The raw data was then uploaded to a computer and post processed with a publically available application (Section 4.3.3). After post processing, the base's location is determined to within a few centimeters. The difference between the approximate location of the base and its post-possessed location is used to perform a three-dimensional shift to all of the roving receiver's stations associated with that base, giving their precise location relative to the preferred ellipsoid.

The receivers record the position of their Antennas' Phase Center (APC), which is located inside the receiver. The receivers are either placed on a leveled tripod, which stands an unfixed height above the surface of the Earth (base receiver), or on a 2 m stake (roving receiver). In order to determine the ellipsoidal height of each gravity station's location to the desired accuracy, both receivers' heights above the surface of the Earth must be known. Before a base receiver is set to its approximate its location, the slant height of the receiver, measured with a measuring tape from a point directly under the receiver – located with a scope attached to the tripod - and its *Slant Height Measure Mark* (SHMM) (Topcon, 2004). The slant height was recorded in both a notebook and

internally in the FC200 within TopSurv survey software. The fixed vertical height of the roving receiver was recorded in TopSurv as 2.0 m.

To insure that only measurements with the desired accuracy were taken with the roving receiver, survey parameters were set in TopSURV to allow station locations to be recorded only if the roving receiver had a fixed solution (sharing multiple satellites with and was receiving corrections from the base) and had an uncertainty of less than 3.0 cm in the vertical.

On the first survey (February 14th to March 3rd, 2013) we were unable to collect raw satellite ephemeris data with the base receiver due to technical issues. This meant that all of the roving stations had the same uncertainty in position as their base station's initial approximation. To overcome this, all roving stations were tied back to the first base station's approximation. This was done by re-occupying a point common within both the current base station's radio transmitting range and that of the previous base station. The difference between the two roving receiver locations, at the same point, was then applied in a three-dimensional shift to all of the roving stations associated with that particular base. Upon resolving the technical issue with the base receiver, raw data was collected and processed on the following fieldtrip (July 18th to 23rd, 2013) for a base station with a rover measurement at precisely the same location of a previously occupied rover station from the winter survey (marked with flagging tape and in a flat, unique location). This allowed for one three-dimensional shift be applied to all of the winter survey's stations, bringing their precise locations relative to the accuracy of position of the later base.

Another method used during the winter survey was to consider the ice surface overlaying Sandy Lake to be at the same elevation everywhere. Using this assumption, day surveys that were conducted too far away from the original base station, but within transmitting range of the lake, used the lake as a defined vertical reference point. That is, each base station would have at least one rover measurement on the lake surface. This allowed us to tie in stations vertically to the original base station by treating the entire lake as a common vertical point. A vertical shift was then applied to the roving stations for each base station to bring them to a common survey datum. This method introduced large errors (several meters) into these peripheral surveys' horizontal resolution, but kept the vertical to within a few centimeters. Great care was taken to record all of the common points and shifts during the winter survey and we feel that the resulting data is in good standing.

4.3.3 Post-processing of GPS Static Observations

Base stations' static observations were uploaded to a PC from the receiver using Topcon's PC-CDU software, which places observations in a .tps format. These files were then translated into Receiver Independent Exchange Format (RINEX) observation (.??O format) files using Topcon's Topcon Link v.7.5 software application. The slant height of each base station was recorded within Topcon Link and the plum line was internally calculated and placed within its respective RINEX file. Each RINEX file was post-processed using NRCan's CSRS-PPP online application (Natural Resources Canada, c). Processing parameters were static observations, NAD83 Epoch 2010 Newfoundland with the CGDV28 vertical datum. Results of the post-processing were received by email.

Ellipsoid heights were returned in WGS84; however, WGS84 and GRS80 have the exact same value for their semi-major axis, and their semi-minor axes only differ by less than a millimetre, thus transformations from WGS84 to GRS80 are not needed (Neacsu, 2011).

Final vertical uncertainties in post-processed base stations' static observations range from 1.0 centimeter to 15.7 centimeters, with an average of 3.1 centimeters (Table 4.1). The 15.7 centimeter uncertainty is an outlier. Removing it from the others gives an average uncertainty of 1.9 centimeters and brings the maximum uncertainty to 2.5 centimeters. Fortunately, the base associated with this large vertical uncertainty was only used for one gravity station (#22133; Section 4.4). This gravity station was not omitted from the database because a high uncertainty in the vertical does not necessarily mean inaccuracy in the measurement.

Base Name	Log File	Northing (m)	Easting (m)	Ellipsoidal Height (m)	Uncertainty in height (m)
HB130718	log0199t	5448373.828	492140.525	115.835	0.014
HB130719E	log0200u	5460990.872	508856.070	140.850	0.017
HB130720	log0201s	5451190.618	495057.643	98.585	0.025
HB130719C	log0200n	5459526.082	506575.748	98.639	0.011
HB130720A	log0201u	5454725.381	493558.682	103.938	0.025
HB130721B	log0202u	5452349.333	511567.151	392.226	0.157
HB130721	log0202n	5452161.357	508585.012	234.359	0.012
HB130722DD	log0203w	5443426.697	494328.466	197.013	0.025
HB130721B-130722	log0203n	5453479.297	497021.288	88.941	0.010
HB130723A	log0204n	5448475.861	503969.785	239.790	0.019
HB130901	log0244s	5443112.140	492267.041	120.887	0.025
HB130902	log0245t	5453791.199	505914.306	128.053	0.022
HB130723B	log0204q	5447649.818	496512.847	104.925	0.019

Table 4.1: Results of processed RTK static base station locations, including uncertainty in ellipsoidal height. Eastings, Northings, and Ellipsoidal Height are all reference to NAD83(CSRS).

4.4 Gravity

Gravity surveying is a geophysical method that measures the gravity field at a series of specific locations to record spatial differences. Spatial differences (or anomalies) are then related to subsurface geology, based on contrasts in densities of lithological units.

Geophysical interpretations of gravity surveys are based on Newton's law of gravitational force. This law, given by Equation (4.1), states that there is a mutual attractive force between two masses, m_1 and m_2, which is proportional to the product of the masses and inversely proportional to the square of the separation between their centers of mass:

$$\overrightarrow{F_{21}} = G\frac{m_1 m_2}{r^2}\hat{r} \tag{4.1}$$

Here, $\overrightarrow{F_{21}}$ is the force on m_2 due to m_1, $\hat{r}$ is a unit vector directed from m_2 towards m_1, r is the distance between m_1 and m_2, and G is the universal gravitational constant, which in SI units is equal to 6.672 x 10^{-11} Nm^2/kg^2 (Telford, 1990). The force $\overrightarrow{F_{12}}$ on m_1 due to m_2 is equal and opposite to $\overrightarrow{F_{21}}$. If we consider the force exerted on a mass at the surface of the Earth, and Newton's second law of motion (i.e., $\vec{F} = m\vec{g}$), then by dividing Equation (4.1) by m_2 and substituting in the mass of the Earth (m_e) and radius of the Earth (r_e), we arrive at Equation (4.2), where g is the force per unit mass, which is equivalent to acceleration (Mishra, 2011).

$$g = G\frac{m_e}{r_e^2} \tag{4.2}$$

The mass of an object is a function of its volume and density. If an object is not of uniform density, then its gravitational acceleration is a vector product of the density and distance to the point of measurement integrated over the volume. Consequently, the gravitational attraction of a non-homogenous body will vary from point to point, in response to its density distribution (Seigel, 1994); thus, gravity measurements taken over lithological units with varying densities will show spatial differences.

The gravity surveying geophysical method is of particular interest in the Howley Basin because the less dense sediments within the basin will give an anomalously low gravity signal. The amplitude of the relative gravity low can be related to the thickness of sediments, and a depth estimate for the basin can be made.

4.4.2 Scintrex CG-5 Autograv Gravimeter

A Scintrex CG-5 Autograv gravimeter was used to measure the gravity field for this survey. The Scintrex CG-5 Autograv Gravimeter is a microprocessor-based automated gravimeter that uses a fused quartz spring system to give relative gravity measurements over an 8000 mGal range with ± 0.001 mGal precision. The system operates by balancing the gravitational force the proof mass applies to the spring with an electrostatic restoring force. The position of the mass is read by a capacitive displacement transducer to within 0.02 nm and an automatic feedback circuit applies DC voltage to capacitor plates to produce an electrostatic force, bringing the mass back to a null

position. This feedback voltage is a measure of the relative gravity field. Voltage is then converted to a digital signal and stored in the machine's data acquisition system for processing. Measurements are obtained by continuously averaging a series of readings at a 6 Hz sampling rate (Scintrex, 2009). The readings are displayed graphically or numerically on its screen in real-time along with running calculations of error and standard deviation, allowing for on-site assessment of data accuracy/noise.

The CG-5 Autograv uses an onboard computer and numerous sensors to make several internal calculations to correct for external effects on the gravity field, including: an automated tidal accelerating calculation; drift correction; tilt correction; temperature correction; along with an auto rejection filter (see Scintrex, 2009 for more details). The CG-5 is equipped with a manual adjustable leveling tripod to ensure the machine is level and sturdy during gravity readings.

The CG-5 Autograv also benefits from a durable shock mount system, which is reported to be able to withstand up to 20 G shocks with tares of less than 0.005 mGals (Scintrex, 2009). This feature makes the CG-5 Autograv an attractive gravimeter for field-based surveys in which transportation over rough terrane is unavoidable, such as this one.

4.4.3 Gravity Surveying

Gravity measurements were collected at a total of 202 unique gravity stations over the Howley Basin and adjacent formations on four separate fieldtrips: February 14th to

March 3rd, 2013; July 18th to 23rd, 2013; February 17th to 18th, 2014; and June 19th to 22nd, 2014.

During the first fieldtrip, emphasis was put on collecting gravity over Sandy Lake, because during the winter the lake's frozen surface was stable enough (Section 4.4.4) for the gravimeter to achieve accurate readings. Fluctuations in the water level with time required all gravity readings taken over the lake to be done during this fieldtrip – in order to keep all stations on the lake at the same elevation. Transportation during winter surveys was done with snowmobiles along a network of trails, old railway tracks, and over frozen lakes and bogs. Subsequent fieldtrips concentrated on collecting gravity stations along transects that extended beyond the basin's boundaries and filling in gaps from previous surveys. Access was via truck, ATV, and foot.

Before gravity measurements were collected in the field, instrument drift and X and Y tilt offsets and sensitivities were measured. This was done before each field trip to correct for minor adjustments in the gravimeter's spring relaxation and sensitivity to tilt, which can change with time and environmental factors i.e., vibration during transport.

Once the gravimeter was properly calibrated, a field base station was created. The field base station was chosen to be located in an un-occupied dairy barn (-57.106824° W, 49.156262° N) because it provided a sheltered location, with a concrete slab, and was isolated from varying anthropogenic noise. To ensure the gravimeter was at exactly the same location and elevation for each reading, tape was placed on the floor and the leveling tripod was set to its lowest level.

To obtain absolute gravity measurements, the field base station was tied in to a secondary station of the Canadian Gravity Standardization Network (CGSN), station number 2307, located at the Visitor's Information Centre in Deer Lake (-56.982948º W, 49.187866º N), absolute gravity value of 981000.4700 mGal (Natural Resources Canada, d). By reading the relative gravity, with the CG-5, at the Visitor's Centre and then at the field base station, the absolute gravity value at the field base station could be determined. This was done by adding the difference between the relative gravity reading made at the CGSN station and its known value to the relative gravity readings at the field base station. Ties between the CGSN station in Deer Lake and our field base station were made each field trip and resulted in a calculated averaged absolute value of 980967.893 mGal with a standard deviation of 0.014 mGal (Appendix D). This field base station was denoted as station number 90001 for later processing purposes (see Section 4.4.4).

All of the relative gravity readings taken in the field during this study were tied to a base station of known absolute gravity before and after each day. For the initial three fieldtrips all of the field readings were tied into the field base station (90001), but during the June 19th to 22nd, 2014 field trip, field readings were directly tied to CGSN stations in Deer Lake (described above) or in Springdale, station number 9221-1977, located at the Green Bay Information Centre (-56.190833^{0} W, 49.481111^{0} N), absolute gravity value of 981031.2100 ± 0.0310 mGal (Natural Resources Canada, d). These two CGSN stations were given survey station numbers 90002 and 90003, respectively.

Gravity readings were collected throughout the Howley Basin with several transects crossing the basin's boundaries (Map E). The surveying was completed in a

non-traditional format (i.e., without grids) because densely forested areas and large bogs made transportation along grids difficult. However, a series of logging roads and old rail beds provided good coverage over the basin and were the main locations of gravity readings. In some instances, where a hole in the spatial coverage persisted, bogs were traversed by foot or snowmobiles to obtain gravity readings.

Gravity station locations were selected mainly by their distance from a previous station along a transect line. If the ground was unsuitable because of instability of the ground (see below) or excessive topographic undulation within approximately 50 meters of the proposed gravity station site, a better suited location was sought within as close proximity as possible to the proposed location. After each gravity measurement, the gravimeter displayed: station number or latitude and longitude, the average relative gravity measurement, the standard deviation of the individual readings, X and Y tilts, internal temperature of the spring, earth tide correction, duration of the measurement, number of rejected readings, and time and date. All of the above data were recorded in the gravimeter's internal computer and later uploaded to a computer. These data plus geographical references were also recorded in field notebooks as a safeguard from loss. Each gravity station was marked with a unique station number recorded on flagging tape. This was done so that repeat measurements could be taken at the exact same location, either on the same day or subsequent days.

Surface stability proved to be an issue with collecting gravity readings over both frozen surfaces and bogs. The frozen surface of Sandy Lake was in particular noisy due to surface vibration. Several factors were postulated as to why this occurred: diurnal

fluctuations in temperature causing cracks in the ice would create vibrations that would reflect off of the shoreline, which could last for hours; changes in barometric pressure and wind would create contrast in pressure over the lake and produce waves in the ice; and anthropogenic noise from people on snowmobiles traveling over the lake. In an effort to remove noise caused by vibrations in the ice, the seismic filter on the gravimeter was used during the first fieldtrip (February 14th to March 3rd, 2013). For all other surveys, the regular auto-rejection filter was used.

Another issue that arose during the winter surveys was that the metal feet of the leveling tripod would slowly melt into an icy layer that covered much of the ground under the snow or on the frozen lake. This would cause the gravimeter to tilt during a recording. To fix this problem, three small wooden blocks with dimensions of approximately 3.5 cm x 8.5 cm x 12 cm, laid on their widest face, were placed under the tripod feet while taking gravity readings in the winter (Figure 4.5). The additional height of the gravimeter's sensing unit caused by placing the wooden blocks under the tripod (3.5 cm) was recorded and compensated for during processing (see Section 4.4.4)

Taking gravity recording in bogs during the summer surveys also had complications: soft unstable ground produced tilting problems and wave-like fluctuations in the gravity signal – observed in real-time on the gravimeter's interface. Several methods were tried to reduce noise caused by the un-stable surfaces of bogs: holes were dug through the top layer and the leveling tripod placed on more stable peat, or onto gravel or clay (Figure 4.5); or a one meter stake with threads that fit into the bottom of the gravimeter's leveling tripod was sunk into the peat with the gravimeter attached. It was

found that the least noisy readings were acquired when holes were dug close to substantial vegetation (i.e., spruce tree stands), which typically coincided with gravel or clay under a shallow layer peat, which produced a more stable platform. When available, vegetation was sought to dig holes next to, for gravity readings taken in bogs during the summer surveys. Wind was also a factor for noisy gravity readings. To limit the amount of wind-induced vibration on the gravimeter, an umbrella was used to block the prevailing winds (Figure 4.5).

Winter surveying required shoveling pits in the snow to reach the ground. These pits were dug with a telescoping avalanche shovel and were made only big enough to allow the gravimeter to be placed inside and operated. The bottom of the pit was scraped vigorously to remove all snow and achieve a stable surface, typically on iced-over ground, for the gravimeter to take a reading on. No depth measurements of snow pits were made, and the gravitational effect of the surrounding snow mass was considered to be negligible.

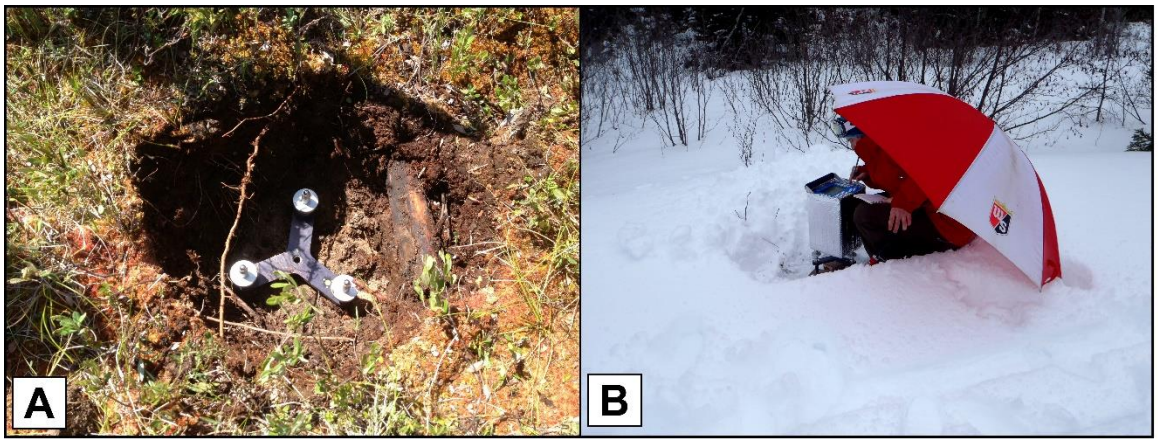

Figure 4.5: Photographs of methods in gravity surveying to keep the gravimeter stable. **A)** Showing levelling tripod in a hole dug through moss and peat in a bog to reach more stable sandy ground. **B)** Gravity measurement being taken in the winter, showing hole dug through snow, wooden blocks under the levelling tripod to prevent it from melting the ice underneath, and an umbrella to help keep wind vibrations down.

4.4.4 Gravity Corrections

In order to arrive at geologically meaningful gravity anomalies, certain 'corrections' need to be applied to the observed gravity, as measured in the field. These corrections are adjustments for known temporal and spatial variations in the observed gravity that can overshadow the effects of subsurface density distributions in the observed gravity field. The corrections applied to this data set follow Hinze et al., (2005) – *New standards for reducing gravity data: The North American gravity database*. This was done so that gravity readings collected during this dissertation would be easily transferred to publically available databases (e.g., Canada Geoscience Data). Oasis Montaj's Gravity and Terrain Correction Extension program was used to execute these reductions.

Data recorded with the gravimeter were uploaded to a computer for each day survey, or loop, and formatted to be edited in Microsoft Excel. This data was then placed in an Oasis Montaj .raw file format, to be uploaded into Oasis Montaj. Each .raw loop contains station numbers, relative gravity readings, date and time of measurements (in GMT), instrument height above the ground (Section 4.4.3), and units of measurement for distance and elevation (Appendix D). The location of each station – recorded with the Topcon HiperLite+ GPS and post processed with PPP (Section 4.3.3) – was placed in .csv format and uploaded to Oasis along with corresponding gravity station numbers (Appendix D). Absolute gravity readings at base stations were placed into a .csv file and loaded into Oasis as a separate database (Appendix D). This data was then used to make the necessary corrections to the observed gravity with Oasis Montaj's Gravity and Terrain Correction Extension.

Tidal Correction

Tidal acceleration in the gravity field is caused by the temporal variations in position of the moon and the sun with respect to a specific location and time on the Earth's surface. Each of these bodies has its own gravitational force, which is proportional to its mass and distance from the location of observation. Because both the moon and the sun are in motion with respect to the Earth, their distances from a specific location on Earth vary periodically. This produces a diurnal effect on the Earth's gravitational field with a range of ±0.3mGal and an approximate period of twelve hours (Blakely, 1995).

Tidal acceleration models have been produced to calculate the theoretical value on Earth given the date, time, and longitude and latitude of a gravity station. The CG-5 Autograv uses the Longman formula (Longman, 1959) to compensate for the tidal acceleration of the moon and the sun (Scintrex, 2009); however, some mistakes were made when choosing the station designation in the gravimeter and the longitude and latitude were not properly recorded at each gravity station. This produced inaccurate tidal acceleration compensations within the gravimeter. To correct for this error, the tidal accelerations calculated by the gravimeter were removed from the observed readings and recalculated with Oasis Montaj's Gravity and Terrain Correction Extension using observation locations measured with the TopCon GPS system and the time each gravity measurement was taken, in GMT. The tidal correction formula used by Oasis Montaj is too complex to list here, but can be obtained from the Dominion Observatory of Canada.

Although not all of the field stations had erroneous longitude and latitude readings, all of the station readings had their tidal acceleration corrections removed and recalculated with Oasis to give consistency to the data set.

Instrument Height

The sensing unit in the CG-5 is an additional 8.9 cm above the instrument's base plate. The leveling tripod raises the gravimeter another 16.5 to 20.0 cm off of the ground, giving and average additional height of 27.15 cm. Because the elevations obtained with the HiPer Lite+ GPS were at the surface of the Earth, this additional height of the sensing unit in the gravimeter causes an approximately -0.084 mGal (Equation 4.2) differences in the observed gravity at each station, if not accounted for. However, since the gravimeter was at approximately the same height above the surface of the Earth at all of the absolute base station readings – used to tie in observed gravity measurements with absolute gravity – as well as all of the survey readings, this consistent off-set caused by the additional height of the sensing unit is already accounted for (Salib, 2014).

During the winter surveys (February 14th to March 3rd, 2013; February 17th to 18th, 2014) three wooden blocks were used to help stabilize the gravimeter while taking readings on frozen ground or ice (Section 4.4.2; Figure 4.5). These wooden blocks elevated the gravimeter an extra 3.5 cm off the surface of the Earth, which was not accounted for during base station readings. To correct for this additional height of the sensing unit during winter gravity surveys, an instrument height of 0.035 m was placed into the .raw files (Appendix D) and were calculated in Oasis Montaj's Gravity and

Terrain Extension with Equation 4.2: where Rh is the height corrected reading; Rt is the tide corrected reading; and Hi is the instrument height in meters.

$$Rh = Rt + 0.308596Hi \quad \textbf{(4.2)}$$

Instrument Drift

Although the CG-5 has an internal drift correction program, it needs to record periodical measurements at a stable location for over twelve hours with the tidal acceleration removed to perform an accurate calculation of the linear trend. But, during the first field trip to Howley (February 14th to March 3rd, 2013), the tidal acceleration was erroneous, resulting in an improperly calculated instrument drift by the gravimeter. This happened because the time difference between local time and GMT, which is used in the tidal acceleration calculation, was put into the gravimeter as -3.5 hours when the convention used is +3.5 hours. Fortunately, Oasis Montaj's Gravity and Terrain Correction Extension has an instrument drift correction programed into the software. It uses the closure error in the base readings to calculate instrument drift (Equation 4.3), where: D is the instrument drift in mGal/hour; Rb1 is the relative gravity reading at base 1 with the tidal acceleration and instrument height corrected, at time Tb1; Rb2 is the relative gravity reading at base 2 with the tidal acceleration and instrument height corrected, at time Tb2; Gb1 and Gb2 are the absolute gravity and base 1 and 2, respectively.

$$D = \frac{(Rb2 - Rb1) - (Gb2 - Gb1)}{Tb2 - Tb1} \quad \textbf{(4.3)}$$

Absolute Gravity

The CG-5 is a relative gravimeter, in that it is capable of measuring differences in the gravitational field very accurately, but it is unable to determine the absolute gravity. To determine the absolute gravity of field stations, a relative gravity measurement is taken at a location where the absolute gravity is known before and after each day survey, creating a loop. The difference in the relative gravity reading and the known absolute gravity measurement at the base station is then applied to all of the field readings for that loop. Equation 4.4 was used in Oasis Montaj to determine the absolute gravity and apply instrument drift to field readings, where: Ga is the absolute gravity value; Gb1 is the absolute gravity value at base station 1; Rh is the height corrected, relative gravity value from Equation 4.2; Rb1 is the relative gravity value at base station 1; T is the time of field reading; Tb1 is the time of base station 1 reading; and D is the calculated instrument drift in mGal/hour from Equation 4.3.

$$Ga = Gb1 + (Rh - Rb1) - (T - Tb1)D \quad \textbf{(4.4)}$$

Latitude Correction

The theoretical or normal value of gravity – the value that would be observed if the Earth had no geological or topographical complexities – varies on the Earth's surface, primarily with latitude. This is because the Earth's surface is best approximated by an ellipsoid, with a greater radius at the equator than the poles. The difference in radii (approximately 21 km) has two effects on the gravity field: the distance to the center of the Earth, and the centrifugal force varies with latitude (Blakely, 1995). To correct or

normalize absolute gravity measurements made in the field, the theoretical gravity value at the location's latitude is removed.

Because the Earth's surface is best represented by a smooth ellipsoid, defined by a semi-major axis at the equator and a semi-minor axis at the poles, the effect of changing radii and centrifugal force on the gravity field with latitude is calculable. Using the Somigliana (1930) closed-form formula, with constants derived from the GRS80 reference ellipsoid (Moritz, 1980), gives Equation 4.5: where Ge is the normal gravity at the equator, 978032.67715 mGal; k is a derived constant, with a value of 0.001931851353; *e* is the first numerical eccentricity, with e^2 equal to 0.0066943800229; L is latitude in decimal degrees; and Gl is the theoretical gravity in mGals (Hinze et al., 2005). This revised theoretical gravity equation was placed into Oasis Montaj's "Gravity_Formulas.lst" and used to remove the theoretical gravity value from the absolute gravity (Equation 4.4) for each field station.

$$Gl = \frac{Ge(1 + k \sin^2 L)}{(1 - e^2 \ \sin^2 L)^{1/2}} \qquad \textbf{(4.5)}$$

Free-air Correction

Field-based gravity surveys are often collected over regions with significant topographical relief, generating gravity stations collected at different elevations. Because gravity varies with distance from the center of the Earth (Equation 4.1), gravity stations at higher elevations will have considerably lower observed gravity values, which are not a

reflection of density contrasts in the subsurface. The first-order approximation of the effect of increasing elevation is 0.3086 mGal/m (Blakely, 1995); therefore, to achieve the desired accuracy needed in a geologically motivated gravity survey, the elevation of each station, from a vertical datum, must be precisely measured and compensated for.

Elevations of gravity stations, collected with the HiPer Lite+ GPS (Section 4.3), were used to calculate the free air correction, relative to the GRS80 ellipsoid. To increase accuracy and keep with standardizations recommended by Hinze et al. (2005), the second-order approximation of Heiskanen and Moritz (1969) was used with the GRS80 ellipsoid parameters, to give Equation 4.6: where, Gf is the free-air anomaly in mGals; Ga is the absolute gravity value from Equation 4.4; Gl is the latitude correction from Equation 4.5; L is latitude; and Hs is the elevation above the ellipsoidal, in meters. This equation was placed into Oasis' Gravity_Free_Air.lst file to be run with the GRFREEAIR GX script. Results are given in Appendix D.

$$Gf = Ga - Gl + (0.3087691 - 0.0004398 \sin^2 L)Hs + 7.2125 \times 10^{-8} Hs^2 \quad \textbf{(4.6)}$$

Bouguer Correction

The free-air correction compensates for the effects of increased elevation above the ellipsoid, but does not account for the additional mass of rocks existing between the level of observation and the ellipsoid. The simple Bouguer correction accounts for this additional mass by assuming an infinitely extendable slab, of homogenous density, with thickness equal to the height of observation above the ellipsoid; however, the Earth is not

flat and does not extend to infinity. To correct for the curvature of the Earth, the Bouguer slab is replaced by a spherical cap that extends to 166.7 km (see LaFehr, 1991), termed the Bullard B correction.

The Bouguer correction, used in Oasis Montaj (Equation 4.7), includes the removal of the anomalous density void in the Bouguer slab caused by the mass of the water column for stations taken over Sandy Lake. This was accomplished by sampling the bathymetry grid (Section 4.2; Appendix C) with the locations of gravity stations using Oasis Montaj's GRIDSAMP GX script, giving the predicted water depth in meters below each station. The water depth was then included into Equation 4.7: where, Gb is the Bouguer anomaly in mGal; Gf is the Free Air correction from Equation 4.6; D is the density of the Bouguer slab (2.67 g/cm^3); Dw is the density of water (1.00g/cm^3); Hs is the station's elevation above the ellipsoid; Hw the water depth in meters; and Gc is the Bullard B correction.

$$Gb = Gf - 0.0419088[D\ Hs + (Dw - D)Hw] - Gc \qquad \textbf{(4.7)}$$

Terrain Corrections

Gravity readings taken at the Earth's surface, in areas of moderate to strong topographic relief, need to be corrected for the additional mass, or lack thereof, caused by hills or valleys, not compensated for by the Bouguer slab. Both hills and valleys reduce the value of g_z – what the gravimeter measures – and the terrain correction needs to be added to the observed gravity value (Blakely, 1995).

To calculate the terrain correction, information about the surrounding topography is needed. DEMs were downloaded from the Canadian Digital Elevation Database (Natural Resources Canada, d) in .dem formats, and loaded into Oasis Montaj to be plotted as grids. Two separate DEM grid files were created: a local DEM, from 1:50,000 National Topographic System (NTS) map sheets with 0.75 arc second horizontal resolution; and a regional DEM, from 1:250,000 NTS map sheets with 3 arc second horizontal resolution. Both the local and regional DEMs are projected in the NAD83 (GRS80) horizontal datum in decimal degrees, with the Canadian Geodetic Vertical Datum of 1928 (CGVD28) as a vertical datum. The vertical positional accuracy is approximately 3.0 m, for both the local DEM and approximately 50 m for the regional DEM (Natural Resources Canada, e).

Once loaded into Oasis Montaj as grid files, both DEMs were reprojected from latitude and longitude to meters, referenced to UTM Zone 21 NAD83, with the local DEM and the regional DEM having cell sizes of 18.8 m and 77.9 m, respectively (Appendix D). This was done for the regional DEM as well – even though it spans both UTM zones 21 and 22 – because the regional correction grid needs to be referenced to the same false Eastings and Northings as the survey data.

There is a difference in vertical datums between the gravity station location data (GRS80 ellipsoid height) and the DEMs (CGVD28 orthometric height). However, Oasis Montaj's terrain correction utility automatically assigns each station an elevation value that is on the surface of the DEM, so that during computation of the terrain corrections

none of the gravity stations are placed above or below the predicted surface of the Earth at that location.

Terrain corrections in Oasis Montaj are calculated using a combination of the methods described by Nagy (1966) and Kane (1962). Three different zones (Figure 4.6) are defined by the user: the near zone – Zone 0, centered on the gravity station and extending a distance of one cell (0 to 111.88 m); the intermediate zone – Zone 1, extending from cells one to eight (111.88 to 895 m); and the far zone – Zone 2, extending from the eighth cell to a Regional Correction Distance (895 m to 166.7 km). The number of cells in each zone is defined by the terrain corrections script in Oasis Montaj (GRTERAIN GX) and the user defines the boundary between Zones 1 and 2, and the Regional Correction Distance. An intermediate zone extending to 895 m and a far zone extending to 166.7 km was chosen as the input parameters to comply with recommendations by Hinze et al. (2005).

In each of these zones the effect of the topography on the gravity signal is calculated by different approach of averaging the actual topography, based on distance from the station. In the near zone, four sloping triangular sections are summed together using Equation 4.8 (Figure 4.6A), which describes a surface defined by the gravity station and the elevations of the four diagonal corners. In the intermediate zone, the terrain effect for each point is calculated by the flat topped square prism approximation of Nagy (1966), using Equation 4.9 (Figure 4.6B). The terrain effect, in the far zone (beyond eight cells), is derived based on the annular ring segment approximation to a square prism as described by Kane (1962) (Equation 4.10; Figure 4.5C). In all of the below terrain

correction equations (Equations 4.8 – 4.10): $g_{1\text{-}3}$ is the gravity attraction caused by topography within the respected segments; G is the gravitational constant; D is the assigned density of topography (2.67 g/cm^3); and the remaining variables are geometric constants relating to distance to topography, shown in Figure 4.6. The gravitational attraction calculated for each zone for each station is summed together and added to the Bouguer corrected gravity value (Equation 4.7) to give the Complete Bouguer correction (Equation 4.11).

$$g_1 = GD\emptyset\left(R - \sqrt{R^2 + H^2} + \frac{H^2}{\sqrt{R^2 + H^2}}\right) \quad \textbf{(4.8)}$$

$$g_2 = -GD\left|\begin{matrix}z_2\\z_1\end{matrix}\right|\left|\begin{matrix}y_2\\y_1\end{matrix}\right|\left|\begin{matrix}x_2\\x_1\end{matrix}\right| x \cdot ln(y + R) + y \cdot ln(x + R) + Zarctan\frac{Z \cdot R}{x \cdot y}\Bigg|\Bigg|\Bigg| \quad \textbf{(4.9)}$$

$$g_2 = 2GDA^2\frac{\left(R_2 - R_1\sqrt{R_1^2 + H^2} - \sqrt{R_2^2 + H^2}\right)}{(R_2^2 - R_1^2)} \quad \textbf{(4.10)}$$

$$Gcb = Gb + Gt(g_1 + g_2 + g_3) \quad \textbf{(4.11)}$$

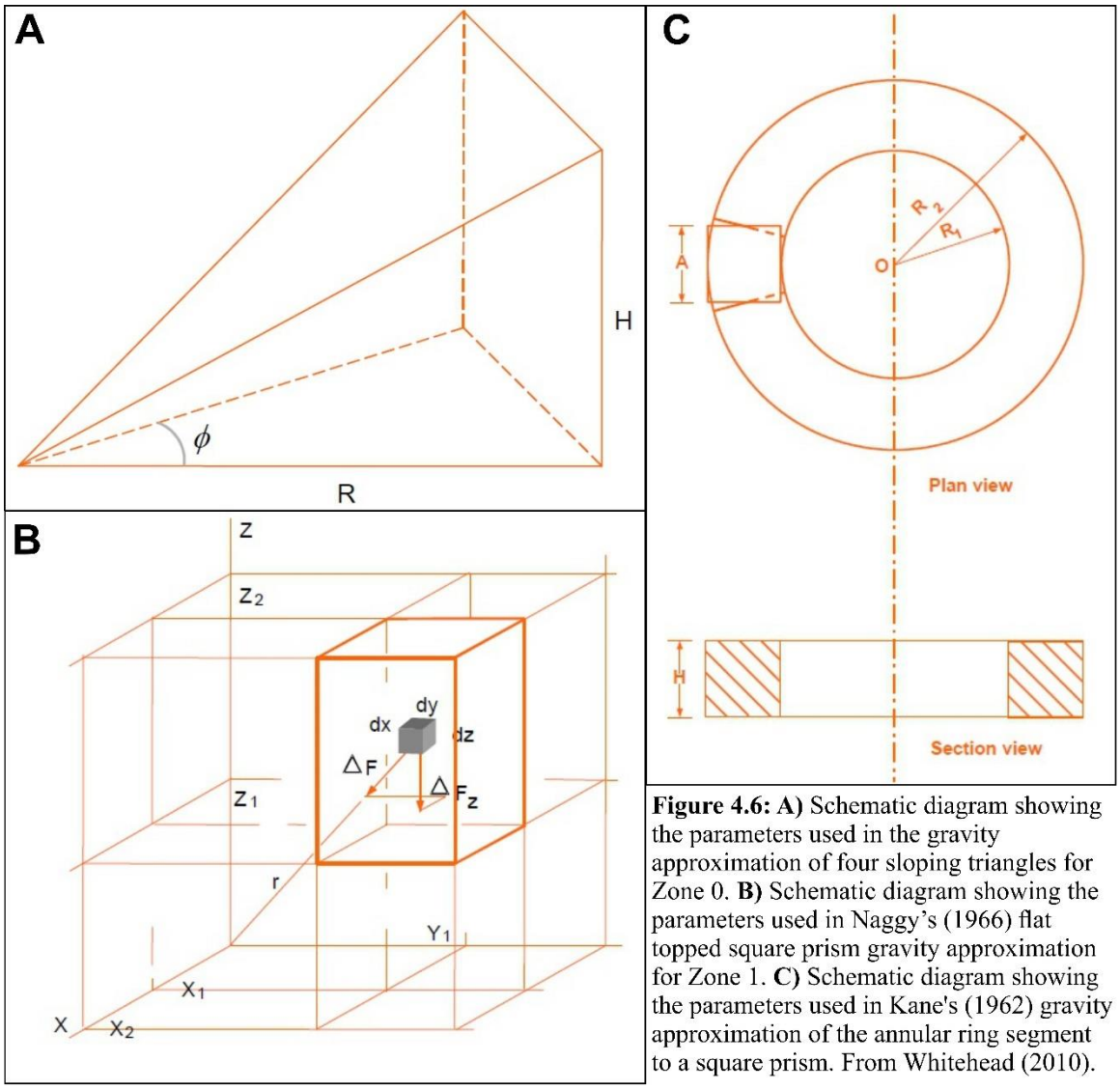

Figure 4.6: A) Schematic diagram showing the parameters used in the gravity approximation of four sloping triangles for Zone 0. **B)** Schematic diagram showing the parameters used in Naggy's (1966) flat topped square prism gravity approximation for Zone 1. **C)** Schematic diagram showing the parameters used in Kane's (1962) gravity approximation of the annular ring segment to a square prism. From Whitehead (2010).

4.4.5 Repeatability – Gravity Data Quality

As a measure of gravity data quality, select gravity stations were reoccupied. Many gravity stations were re-measured immediately after the initial reading was taken, whereas others were re-measured later the same day (or loop) or on subsequent days (different loops) (Appendix D). This method of assessing gravity data quality introduces issues: does the immediate re-measurement of the gravity field at a location skew the

repeatability towards a smaller average and standard deviation, or is it a better assessment of repeatability – and hence gravity data quality – because errors introduced by reoccupying a station at a later time (i.e., not precisely being at the exact same location or elevation, changes in atmospheric pressure) are removed? Although great care was taken to ensure that repeated gravity measurements were taken at stations that were easily locatable with unique features, adverse weather (the peril of any Newfoundland-based geophysical survey) could change ground conditions between days. This was especially a factor for winter surveys.

Analysis of the absolute value of differences between repeated absolute gravity measurements and the average gravity value for that particular station, reveals favorable results: all repeated measurements (taken immediately after as well as at a later time or date) gives an average difference of 0.008 mGals and a standard deviation of 0.014 mGals; isolating just the repeated measurements taken a different time or another day gives an average difference of 0.021 mGals and a standard deviation of 0.021 mGals (Appendix D). The actual degree of repeatability likely lies somewhere between these values. Regardless, the higher endmember, which is likely overestimated because of reasons stated above, is still a very good value for repeatability – especially for a survey designed to capture such large amplitude anomalies – and is deemed of high quality.

4.4.6 Existing Gravity Datasets Over the Howley Basin

There are three publicly available ground-based gravity datasets that include stations over the Howley Basin: LITHOPROBE East transects 89-2 and 89-3 (project

number 1989107); Miller and Wright (1984) (project number 1985291); and Weaver (1967) (project number 1964010). Selected areas of these gravity surveys that cover and extend several kilometers beyond the Howley Basin's boundaries were downloaded as point data from NRCan's Geoscience Data Repository for Geophysical Data (Natural Resources Canada, f), and processed to be used with gravity data collected during this study. This was done to assist with modeling of the Howley Basin and help delineate regional trends.

In order to combine (or level) the pre-existing datasets with gravity data collected during this study, the data was reprocessed with the same parameters (Section 4.4.4) as applied to the present gravity survey. That is, they were reprocessed from their absolute gravity values (tied to the International Gravity Standardization Network 71) with newly calculated latitude and terrain corrections, to give new free-air and complete Bouguer values. It should be noted that all previous interpretations of the older gravity datasets in the Deer Lake area (e.g., Miller and Wright (1984) and Wiseman in Langdon (1993)), were completed without terrain corrections applied. Thus, the newly processed datasets better represents the true response of the gravity field due to subsurface features and are less obscured by mass associated with topographic relief in the surrounding area.

To complete the reprocessing of the pre-existing gravity data, locations of stations were projected into the NAD83 (CSRS) UTM Zone 21N horizontal datum – to comply with the present study and the DEMs used for terrain corrections (Section 4.4.4) – and elevations were converted from orthometric heights (CGVD28) into ellipsoid elevations (GSR80), with NRCan's GPS·H v3.2 application.

Because the older datasets were collected before the advent of field-based GPSs, planimetric locations of gravity stations were likely located by referencing geographic features on topographic maps, and elevation data was acquired with barometric altimeters and sling psychrometers for temperature and humidity information (Miller and Wright, 1984; Weaver, 1967). Planimetric uncertainties reported for these datasets are 20 m, 20 m, and 100 m, with uncertainties in elevations of 1.0 m, 3.0 m, and 3.0 m for the LITHOPROBE, Miller and Wright's (1984), and Weaver's (1967) datasets, respectively. The error in the quantitative measurement of gravity station locations is evident for these datasets when they are overlaid onto digital topographic maps; some of Miller and Wright's (1984) gravity stations that were collected near waterbodies plot within the waterbodies – even though their survey did not include gravity measurements over lakes. As a measurement of location data quality, the pre-existing datasets' gravity station locations (reprojected in NAD83 (CSRS) UTM Zone 21N) were used to sample the DEM grid to get expected elevations for each station's location. These values were then compared to elevations reported during the collection of the gravity data. This exercise returned undesirable results: Miller and Wright's (1984) dataset has 37 stations (10.0% of the dataset) and Weaver's 8 stations (7.5% of the dataset) with differences between the sampled DEM elevations and reported elevations of greater than 20 meters, with maximum and average differences of 153 m and 9.6 m, and 90 m and 7.9 m for Miller and Wright's (1984) and Weaver's (1967) datasets, respectively (Appendix D). In comparison, the same exercise on the data collected in this study (after converting from ellipsoid elevations (GRS80) to orthometric heights (CGVD28)) gave a maximum difference of 6.98 m and an average of 1.74 m. The LITHOPROBE gravity survey had

better results with a maximum difference of 9.86 m and an average of 1.58 m (Appendix D).

The increased differences between elevations reported in Miller and Wright's (1984) and Weaver's (1967) and their sampled DEM elevations could be caused by: uncertainties in their planimetric locations, which could cause the sampled elevations from the DEM to have been sampled at a location not precisely where the actual gravity station was; error within the measurement of elevations themselves; human error; or any combination of the above. To test the theory of error in the planimetric locations causing the increased differences between sampled and recorded elevations in the historic datasets, a slope map was created from the DEM, and the gravity stations with the greatest differences in elevations (greater than 20 m) were overlaid onto it (Figure 4.7). If the differences between the sampled and reported elevations are due to the planimetric uncertainties, then the stations with the greatest differences should be located in areas with a steep gradient (100% and 20% slope for Miller and Wright's (1984) and Weaver's (1967) datasets, respectively). Figure 4.7 shows that although many of the stations with large discrepancies between elevation values are near areas of steep gradients, the vast majority of them are not (note: because of the scale of Figure 4.7 and the size of station location markers, many of the stations that appear to plot in areas of steep topographic gradient in fact plot off of slopes greater than 20%). Thus, there must have been additional errors included in the measurement of elevations for some of the historic gravity stations. It should be stated that because of the planimetric resolution of the DEM (18.8 m; Section 4.4.4), there exists a possibility that large isolated undulations in

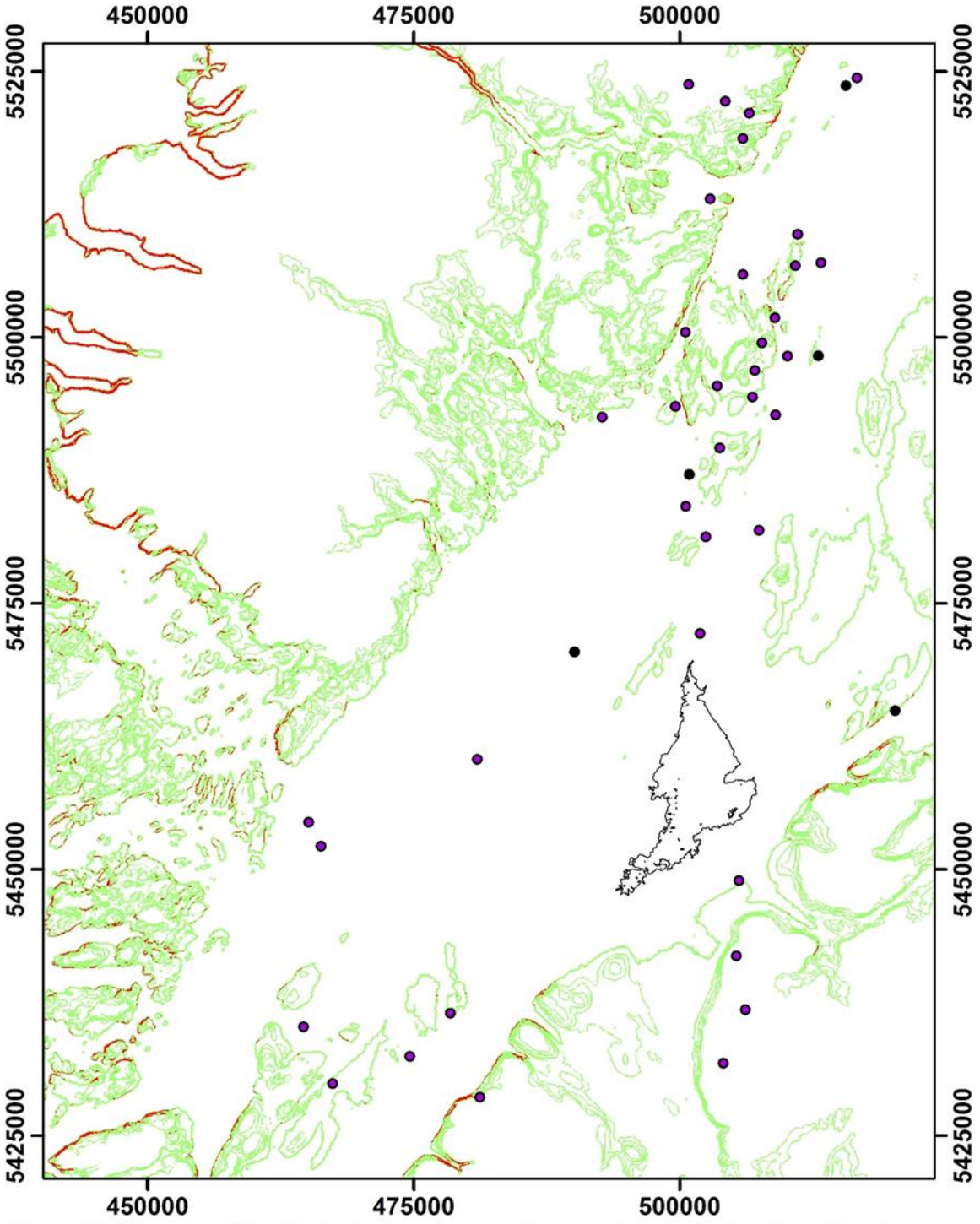

Figure 4.7: Slope map of the Howley Basin and surrounding area, showing the locations of gravity stations with greater than 20 m difference between reported elevations and DEM sampled elevations. Slopes between 20% and 60% are shown in green, and slopes greater than 60% are in red. Miller and Wrights' (1983) stations are given in purple, and Weaver's (1967) stations are in black. The shoreline of Sandy Lake is given for a geographical reference. Map scale 1:600,000.

topography could be aliased by undersampling. However, after traveling through much of the basin, it is the writer's opinion that topography of this nature is non-existent within the study area. Furthermore, the magnitude of some of the differences between sampled and recorded elevations are too great to be a function of uncertainties in planimetric location or accuracy of elevation measurements and must have a degree of human error involved. One such station – Miller and Wright's (1984) station number 2038 – has a difference in elevation between the sampled DEM and the reported elevation of 153 m. This station's gravity value is also anomalously high compared to surrounding values and does not agree with the gradient of the gravity field in the area, and therefore must be of human error. This station does not appear on Miller and Wright's (1984) published map of the gravity survey over the Deer Lake Basin. It is quite possible that because Miller and Wright's (1984) survey took place before the wide use of field-based computers to record data in real time, there was a point when hand-written data were transferred to digital form, which could have easily introduced errors by misreading hand-written numbers.

Upon the discovery of this anomalous value in Miller's (1984) dataset, his published paper copy of the gravity survey was scanned, georeferenced, and then overlaid with downloaded gravity stations from his survey (Natural Resources Canada, f). This exercise revealed that several gravity stations that appear on the downloaded dataset were not used in Miller's (1984) published gravity maps of the Deer Lake Basin. It is unknown why there is this discrepancy in the number of stations between Miller and Wright's (1984) report and data from their survey available on Natural Resources Canada (f). It

should be noted that the paper map in Miller and Wright's (1984) report does not cover the full extent of their gravity survey, and gravity stations beyond its boundaries were not able to be checked for errors in the same manner.

An attempt to reoccupy some of the previously recorded gravity station locations was done to compare values between gravity surveys to see if they produce similar values. However, because there are no permanent monuments of the historic gravity station locations, and given their planimetric uncertainties, we were unable to exactly reoccupy historic gravity stations. Table 4.2 displays the coordinates, distances between neighbouring stations, and the absolute differences between their absolute gravity values and calculated complete Bouguer anomaly values for the different surveys. Despite not being able to precisely reoccupy the historic gravity stations, differences in values between surveys were generally low relative to the scale of the complete Bouguer gravity anomaly over the Howley Basin (> -10 mGal): mean difference for absolute gravity is 0.699 mGal and 0.685 mGal for the complete Bouguer gravity anomaly (Table 4.2). This shows that the re-processed existing gravity datasets agree to within acceptable resolution for combining them with the present survey datasets and will assist with gravitational modeling of the Howley Basin.

Station	Easting	Northing	dDistance	AbsGrav	dAbsGrav	C_Bouguer	dC_Bouguer
P-21911	504201	5458196		980989.809		1.903	
M-20035	504269	5458268	99	980989.56	0.249	1.85	0.053
P-12718	506804	5456945		980986.920		-0.143	
M-20037	506925	5457048	159	980986.69	0.230	0.01	0.153
P-21934	507566	5459960		980988.505		4.475	
M-20142	507454	5460068	156	980989.000	0.495	4.212	0.263
P-22203	496275	5456701		980984.126		-1.999	
M-20020	496303	5456545	159	980984.13	0.004	-2.240	0.241
P-11918	507078	5448936		980950.795		-12.477	
W-3822	507226	5448951	149	980952.8	2.005	-12.6	0.123
P-11514	496678	5449744		980967.677		-13.403	
M-20022	496699	5449874	131	980967.63	0.047	-13.50	0.097
P-22309	494848	5447734		980967.265		-12.163	
M-20023	494901	5447781	71	980966.56	0.705	-11.88	0.283
W-2459	494840	5447837	104	980967.3	0.035	-12.4	0.237
M-20164	501526	5470070		981011.44		18.49	
W-5577	501392	5470070	133	981013.0	1.56	17.9	0.59
M-20070	495765	5435998		980932.50		12.629	
W-2460	495802	5435979	42	980932.9	0.40	9.7	2.93
L-5207	468342	5446769		981001.50		7.82	
M-20114	468414	5446741	77	981001.50	0.00	7.75	0.07
M-20152	527919	5468288		980990.75		0.55	
W-5579	527895	5468288	24	980991.1	0.35	-1.6	2.15
P-41904	500892	5469542		981010.071		14.909	
W-3802	501029	5469700	209	981013.3	3.23	16.6	1.69
P-11923	509229	5446887		980941.912		-12.743	
M-20041	509270	5446879	42	980943.00	1.09	-11.90	0.84
P-21934	507565	5459959		980988.505		4.475	
M-20142	507454	5460069	156	980989.00	0.49	4.76	0.29
M-20161	504556	5477762		980998.69		14.96	
W-5576	504532	5477669	96	980998.4	0.29	14.0	0.96
Mean					0.699		0.685

Table 4.2: Comparison of closely spaced gravity stations from different surveys. Station numbers are given with letters representing surveys: P - PEEP, or this study; L - LITHOPROBE; M - Miller and Wright (1984); W - Weaver (1967). Eastings and Northings (NAD 83 CSRS UTM Zone 21N), in meters; dDistance - distance between stations relative to the first listed, in meters; AbsGrav - absolute gravity value in mGals; dAbsGrav - absolute difference of absolute gravity values between stations relative to the first listed, in mGals; C_Bouguer - complete Bouguer gravity values, in mGals; dC_Bouguer - absolute difference of complete Bouguer gravity values between stations relative to the first listed, in mGals.

4.4.7 Composite Complete Bouguer Anomaly Map

To keep erroneous gravity values from entering the current gravity database, all gravity stations that have large differences between the sampled DEM elevations and reported elevations (greater than 20 m) – for both Miller and Wright's (1984) and Weaver's (1967) stations – and/or stations that do not appear on Miller and Wright's (1984) gravity map were removed. Also, where multiple gravity stations from different surveys occur within close proximity to each other, the most recent survey's value was kept and the older survey's removed. This was done because given the advance in technology, especially with GPS development, the newer survey's gravity values are likely more reliable. A list of gravity stations removed from the downloaded databases, with reasons for doing so, is given in Appendix D.

Once all of the erroneous gravity stations were removed, the datasets were combined into a single, simplified, database (Appendix E), and uploaded in Oasis Montaj for interpolating. Map E is the resulting composite complete Bouguer gravity anomaly map with geological contacts and faults overlaid onto it. A 250 m grid cell size was used to keep high resolution in areas of greater gravity station density (i.e., in the Howley Basin), but the blanking distance needed to be increased to 12000 m so that interpolations would extend between gravity stations with greater sampling intervals (i.e., in areas where Weaver's (1967) stations are the only data points). A minimum curvature gridding algorithm with a histogram equalization color zoning method was used. The resulting grid is available in Appendix D.

4.5 Aeromagnetics

Several high-resolution aeromagnetic surveys cover areas within and around the Deer Lake region that are all available in the public domain through the NLGS's airborne geophysical database (Newfoundland and Labrador Geological Survey, d), including both governmentally funded and industry acquired surveys. Coverage of high-resolution aeromagnetic surveys is not complete, and gaps exist outside of the margins of the Howley Basin, noteably over the Notre Dame arc to the east and over the Wild Cove Pond Igneous Suite to the north (Map C). In these regions the only available aeromagnetic data is that of the GSC's composite 200 m gridded magnetic map (Kilfoil and Bruce, 1990; DN09898; Appendix E).

All of the aeromagnetic surveys used are available as Oasis Montaj .grd files through the NLGS's airborne geophysical database (Newfoundland and Labrador Geological Survey, d). However, each survey was flown at different elevations, and each grid has been interpolated with different cell sizes (Appendix E). Some of the aeromagnetic surveys are only available as available as residual grids. In order to combine all of the aeromagnetic surveys into one composite grid, each grid needed to be leveled before combining. A method of leveling and stitching was chosen that keeps all individual grids with their original interpolation parameters, as not to introduce processing artifacts through blending of overlap points (Kilfoil pers. comm., 2018). The Deer Lake aeromagnetic survey (Kilfoil and Cook, 2009; DN09907; Appendix E) covers all of the Howley Basin and is the best representation of the magnetic signatures within it. All other grids were leveled to this grid.

To accomplish the leveling process, first each grid was re-gridded with a 50 m cell size in Oasis Montaj in order to allow each grid to be compared with a grid that shares common survey points, so as to reflect true values that are not skewed by cells, or interpolated survey points, not lining up. Once re-gridded, each grid was compared to the Deer Lake grid (Cook and Kilfoil, 2009; DN09907; Appendix E) along shared survey areas to determine its mean difference in nT. The mean difference was then added or subtracted from the grid to level it with the Deer Lake grid. However, because not all surveys share large areas with the Deer Lake survey, first the regional GSC compilation grid (Kilfoil and Bruce, 1990; DN09898; Appendix E) was leveled to the Deer Lake grid, combined into a composite grid, and then used as the base for each subsequent grid to be leveled to. This allowed for each high-resolution survey to be leveled from the mean difference calculated over the entire area of its survey, giving a much larger number of cells to calculate from. After each grid was leveled and stitched with the composite aeromagnetic map, the process was redone with the original Deer Lake grid for final leveling and to keep the entirety of the Deer Lake survey. Below is the stepwise process that was used, which will hopefully clarify the rational and methods used to level all of the aeromagnetic grids to the Deer Lake grid.

(1) Re-grid each grid to a 50 m cell size. (2) Use the Boolean And utility in Oasis Montaj grid utilities to isolate the area of the low-resolution regional GSC grid that is shared with the Deer Lake grid. (3) Subtract the isolated GSC grid (product of step 2) from the Deer Lake grid with the grid math utility. (4) Use the grid properties menu to find the mean value of the difference grid (the product of step

3). (6) Use the grid math utility to add the mean difference, in nT, to the GSC grid (leveling it with the Deer Lake survey/grid). (7) Use the Boolean XOR function to remove the area within the GSC grid that the Deer Lake grid occupies. (8) Use the Boolean OR utility to add (or stitch together) the cut GSC grid (product of step 7) and the Deer Lake grid to make a leveled composite grid. (9) Repeat steps 2-8 for the rest of the survey/grids, with the exception of finding the mean difference between it and the now composite grid and leveling the additional grid to the composite grid. (10) Repeat steps 2- 8 for the Deer Lake grid.

After the leveling and stitching process, the composite grid was windowed to a smaller size, and the first vertical derivative was derived. The resulting grids were then overlaid with geological contacts and faults for geological interpretation (Maps C, D; Appendix E).

4.6 Qualitative Interpretations of Gravity and Magnetic Maps

The Howley Basin is associated with a large negative gravity anomaly (up to -13.5 mGal) that is centered along the southeastern shore of Sandy Lake and is elongated northeast-southwest parallel to the Grand Lake Fault map trace (Map E). The negative anomaly extends to the west-southwest over the basin with a moderate gradient increasing towards the Fisher Hills Ridge. A large positive gravity anomaly high over Proterozoic basement rocks in the northwest of the map leaves the Humber Basin dominated by a consistent gradient increasing in that direction. To the north, the Howley Basin also has a consistent gradient increasing to a localized anomalous gravity high situated over the

most western exposure of the Wild Cove Pond Igneous Suite. Along the southeastern margin of the Howley Basin, the negative gravity anomaly has a very sharp gradient over the Grand Lake Fault with a relative high over the Notre Dame arc rocks, including over the Hinds Brook Granite. In contrast, the assumed map trace of the Grand Lake Fault is not well defined over the Hinds Brook Granite in the region between Kitty Brook and Northeast Brook (Maps A, E). In fact, the Bouguer gravity map shows a negatively anomaly, with magnitudes on par with that associated with the Howley Basin, to the east over the Hinds Brook Granite. This anomaly has been well-sampled by this survey, as well as 9 stations of Miller and Wright (1984) (Map E). All gravity measurements agree to acceptable values. This anomalous gravity low over the Hinds Brook Granite has sharp gradients to high gravity values to the north, south, and east, indicating that the source of the anomalous low gravity signal is manifested in the upper crust. However, these sharp gradients do not agree with mapped contacts of igneous bodies in the area (Whalen and Currie, 1988; Map A). Unfortunately, the gradients have not been sampled densely (Map E).

The possibility that the Hinds Brook Granite forms basement to the Howley Basin, and the low gravity response associated with part of it, could have a significant contribution to the gravity signal of the Howley Basin, has not been addressed by previous geophysical modelers (e.g., Miller and Wright, 1984; Wisemen in Langdon, 1993). This seems like an oversight on their behalf. Without knowledge of basement rock properties, it is difficult to make conclusions on this potential overshadowing by low density basement rocks. However, there is very little to no strike-separation of this

anomalous low over the Grand Lake Fault, and if any it would have an apparent sinistral offset. The CFS is predicted to have experienced more than 140 km dextral strike-slip displacement during the Carboniferous alone (Stockmal et al., 1990). If the Hinds Lake Granite underlays the Howley Basin, and is contributing to the low gravity response, then the Grand Lake Fault has had little to no lateral displacement along it in the late Carboniferous to Permian.

The residual composite aeromagnetic map (Map C) and the complete Bouguer gravity map (Map E) agree many ways. The sediments in the Humber Basin are obscured by a magnetic high, with very high values associated with Proterozoic basement to the northeast, and the Silurian Taylor Brook Gabbro to the north. A localised magnetic high appears over the western portion of the Wild Cove Igneous Suite, although with a more northwest increasing gradient than the gravity field. The southwestern Howley Basin margin is delineated along the Grand Lake Fault, where mafic igneous rocks of the Topsails Igneous Sweet and Hungry Mountain Complex have large short wavelength magnetic signatures. And the anomalous gravity low over the northern portion of the Hinds Brook Granite, is mirrored by a strikingly similar low magnetic signal, extending into plutonic felsic units of the Topsails Igneous Complex to the south (Map C). It is unfortunate that this area of the Notre Dame arc is only covered by the much lower-resolution regional aeromagnetic survey (Kilfoil and Bruce, 1990).

One feature of the magnetic data that is not represented in the gravity map is that of a large, smooth, ellipsoidal shaped magnetic high, centered on the northern fringes of the Howley Basin gravity low (Maps C, E). With the abundance of ophiolites in the

region, and with the remnants of the BBL predictably lying beneath the basin, an ophiolite source is logical; however, the disconnect between gravity and magnetic signals, suggest that the source of the high magnetic anomaly is of low density rock, or does not have a great depth extent. Given the diverse pre-Carboniferous geology along the basin's margins, there are many possibilities for the source of the magnetic anomaly.

The first vertical derivative of the magnetic data (Map D), reveals many of the same features as the magnetic map (Map C); exposures of pre-Carboniferous igneous rocks are expressed as high amplitude, short-wavelength gradients, clearly outlining the map trace of the Grand Lake Fault.

A feature highlighted in the first vertical derivative map is a sharp consistent gradient associated with the Fisher Hills-Birchy Ridge Fault, that clearly shows its map trace continuing through the head of Junction Brook (Maps A, D). Within the Howley Basin, the magnetic first vertical derivative reveals a blotchy expression that appears to form northeast trending lineations (Map D). The source of these lineations is unclear.

Chapter 5: Potential-field Modeling

5.1 Introduction

Forward modeling of gravity and magnetic databases aims to match measured values to computer predicted gravity and magnetic responses of the geometry assigned densities and magnetic susceptibilities of constructed geology. This method relies heavily on a priori knowledge of geology and physical properties to constrain the model (i.e., potential-field modeling is non-unique and there are many models that can fit the observed data). Pre-Carboniferous basement geology and internal stratigraphy are not constrained in the Howley Basin and pose a significant hurdle in the modeling process. Several assumptions and tactics that are used to simplify basement geology in order to arrive at a geologically reasonable model of the Howley Basin are discussed in this chapter.

5.2 Regional-Residual Separation of Gravity Data

The observed gravitational response is a complex combination of fields generated from multiple source bodies, of various geometries and depths (Telford et al., 1990). In any particular investigation, any number of sources may be considered ‘noise’ in delineating the extent of a geological body of interest. The regional-residual separation aims at removing the gravitational field caused by geological bodies of noninterest from the observed field to highlight the response of bodies of interest.

As a result of the gravitational field of a mass being a function of the reciprocal of distance squared (Section 4.4), sources at deeper depths produce a gravitational response with a larger wavelength than shallowly buried sources (Telford et al., 1990). This relationship provides a means for separating deep sources from shallow sources: waveform filtering. Ideally, by removing the long wavelength spectra from the observed gravity field, the signal from the regional (or basement rocks) can be removed, leaving the gravitational response of the shallow sources, and allowing for better modeling of geometries and depth extents of these geological bodies. However, the wavelength of a shallow geological body also depends on the lateral extent of the body. In the Howley Basin, this becomes an issue for wavelength filtering; the anomalous gravity low associated with sedimentary units within the basin is laterally extensive (10s of kms). Therefore, a regional separation based on long wavelength removal will also potentially remove aspects of the gravity field associated with the basin. This is unfortunate because the gravitational low over the Howley Basin extends east of the Grand Lake Fault into the Notre Dame arc (Map E; Section 4.6), and any attempt to remove the low gravity anomaly associated with potential basement rocks to the east will inadvertently remove part of the gravity signal associated with the Howley Basin.

Previous interpretations of the depth of the Howley Basin from gravity data (Miller and Wright, 1984) were completed after a 5^{th}-order polynomial trend was removed, stating it was statistically the best fit. These authors offered no geological rationale for this approach, and may have potentially removed part of the gravity anomaly

associated with the Howley Basin's sedimentary pile. For this reason a regional residual separation was not conducted on the gravity data before geophysical modeling.

5.3 Potential-field Properties of Lithologies

During structural field mapping, rock samples of lithologies in the map area were collected and brought back to Memorial University of Newfoundland to ,measure their densities and magnetic susceptibilities for the geophysical modeling process. Unfortunately the sample survey concentrated on Carboniferous units and some of the igneous lithologies encountered at the basin's margins were not sampled. This was because access to exposures in this area is very limited and the terrain is long and difficult to traverse.

Density measurements of the samples were made using Archimedes Method, which states that the difference in weights of the rock in air and the totally submerged rock is equal to the weight of the displaced volume of water (Equation 4.12). Rearranging Equation 4.12 gives Equation 4.13, and substituting V_r into the density formula (Equation 4.14), allows the density of a rock to be determined with Equation 4.15; where M_r is the weight of the rock in air, M_s is the weight of the submerged rock, M_{dw} is the weight of water displaced by the submerged rock, V_r is the volume of the rock, ρ_r is the density of the rock, and ρ_w is the density of the water.

$$M_r - M_s = M_{dw} = \rho_w V_r \qquad \textbf{(4.12)}$$

$$V_r = (M_r - M_s)/\rho_w \quad \textbf{(4.13)}$$

$$\rho_r = M_r/V_r \quad \textbf{(4.14)}$$

$$\rho_r = M_r\rho_w/(M_r - M_s) \quad \textbf{(4.15)}$$

Rock samples were submerged in fresh water for several days before measurement to yield water saturated or *in situ* densities. Samples were allowed to dry for half an hour to allow surface water to evaporate, weight measured with an electronic scale, and then submerged in a pail of fresh water and weighed with the same electronic scale via a net of fishing line attached to a wooden rod placed over the electronic scale. The results of the density calculations are given in Table 5.1.

Magnetic susceptibility of the rock samples were measured with a Terraplus K-10 v2 handheld magnetic susceptibility meter set to 5 cm dimeter core reading. Each sample was measured ten times at various angles and then averaged. The results of the magnetic susceptibility measurements are given in Table 5.1

As expected, the Carboniferous sedimentary rocks are essentially magnetically invisible, with a slightly elevated value for the Saltwater Cove Formation. Silurian basalts of the Topsails Igneous Suite have the greatest magnetic susceptibility value and variation, with more hematized samples, typically occurring near faults, being less magnetic. Both Ordovician plutonic felsic formations are considerably magnetic, but the Hinds Lake Granite has more variation than the Hungry Mountain Complex, although not enough samples were taken to draw any robust conclusions (Table 5.1).

Formation (n)	Min ρ	Max ρ	Mean ρ	Min χ	Max χ	Mean χ
Howley (13)	2.31	2.63	**2.48**	0.01	0.24	**0.08**
Rocky Brook (4)	2.51	2.67	**2.58**	0.01	0.12	**0.06**
North Brook (5)	2.47	2.58	**2.51**	0.02	0.09	**0.04**
Saltwater Cove (4)	2.56	2.65	**2.61**	0.09	0.25	**0.15**
TS volcanic mafic (6)	2.65	2.76	**2.71**	0.38	52.01	**12.5**
TS volcanic felsic (2)	2.57	2.66	**2.61**	0.11	0.17	**0.14**
HLG plutonic felsic (4)	2.57	2.67	**2.63**	0.44	15.35	**7.14**
HMC plutonic felsic (2)	2.61	2.64	**2.62**	7.07	16.24	**11.66**
WCP plutonic felsic (3)	2.64	2.66	**2.65**			**3.64**
FDL psammiteschist(4)	2.67	2.73	**2.71**	0.03	0.23	**0.09**
Fine-grained Howley (Pn: H')			**2.55**			
Miller and Wright (1984)						
Humber Falls (26)			**2.42**			
North Brook (22)			**2.47**			
Rocky Brook (22)			**2.53**			
Saltwater Cove (14)			**2.59**			
Howley (11)			**2.37**			
Hunt et al. (1995)						
HMC plutonic mafic			**2.80**			**35.0**
Ophiolite			**3.00**			**150.0**
Proterozoic basement			**2.80**			**15.0**

Table 5.1: Measured densities and magnetic susceptibilities of hand samples collected during this study, those of Miller and Wright (1984), and un-sampled lithologies from Hunt et al. (1995). Density (**ρ**) is given in g/cm^3; magnetic susceptibility (**χ**) is given in SI units x10^{-3}. (n) is the number of samples; TS is Topsails Igneous Suite; HLG is Hinds Lake Granite; HMC is hungry Mountain Complex; WCP Wild Cove Pond Igneous Suite; FDL is Fleur de Lys Supergroup.

Comparing calculated densities of Carboniferous hand samples collected during this study to those used by Miller and Wright (1984) (Table 5.1) shows that they are in general agreement with a slightly increase in mean density for all of the formations than Miller and Wright's (1984), except for the Howley Formation, for which Miller and Wright (1984) report a value 0.1 g/cm^3 lower. Along the margins of the basin the Howley Formation is often represented by poorly indurated pebble to cobble conglomerates and coarse-grained sandstones, which give considerably lower density values. It has come

into question as to how much of the Howley Formation is actually represented, away from the basin margins and at depth, by the coarse-grained beds; looking at the drill logs of the early coal explorers (Murray and Howley, 1918; Hatch, 1921; Section 3.3.3; Appendix A), it appears that shales constitute a large portion of the Howley Formation towards the center of the basin to ~150 m depth. These fine-grained rocks would likely yield a greater density. The fine-grained Howley Formation (Pn:H'), has been modeled to prevail at depth and towards the center of the basin, has been assigned a higher density (2.55 g/cm^3; Table 5.1).

5.4 Geological Constraints for Geophysical Modeling

The Howley Basin has very few geological constraints to assist with geophysical modeling. A lack of exposure in the center of the basin and low density of shallow drill holes along the basin's margins leaves the internal stratigraphy of the Howley Basin at depth unknown. Basement geology is unknown as well. The Taconic BBL (the tectonic boundary between the Humber Margin and the Notre Dame arc) lies somewhere beneath the sediments of the Deer Lake Basin, thus it is unknown whether Grenvillian basement, Taconic allochthons, or arc related igneous rocks form the basement to the Howley Basin. Also, post-Ordovician magmatic rocks that have intruded over the BBL are both diverse and complex. This lack of definitive geological constraints leaves the modeler in the position that there could be any number of models to fit the geophysical data, with extreme endmembers.

One opportunity presents itself in the geophysical data to overcome the lack of geological constraints for modeling: if the assumption is made that the source of the magnetic high in the center of the Howley Basin (Map C; Section 4.6) is produced by a magnetic source in basement rocks, then determining the depth to the top that source body would reveal the depth of the Carboniferous-basement contact. By using this depth point as an anchor, and assuming that there is a limited lateral variation of basement rock density over the basin, the depth and geometry of the basin can be modeled without knowing the specific basement rock type or its properties. This is the best approach to arriving at a viable basin model without introducing many assumptions.

To determine the depth of the magnetic source, the magnetic high was isolated by windowing it out of the grid (Map C; Figure 5.1A), and applying a radial average power spectrum with the MagMap application in Oasis Montaj. The slope of the log of the power spectrum is proportional to the depth of magnetic source populations (see Spector and Grant, 1970). The isolated high magnetic anomaly in the center of the Howley Basin is an ideal signal for this method of depth determination (see Spector and Grant, 1970). This method of depth estimation predicts that the magnetic source, assumed to be isolated in potential basement rocks, is at 2 km depth (Figure 5.1B).

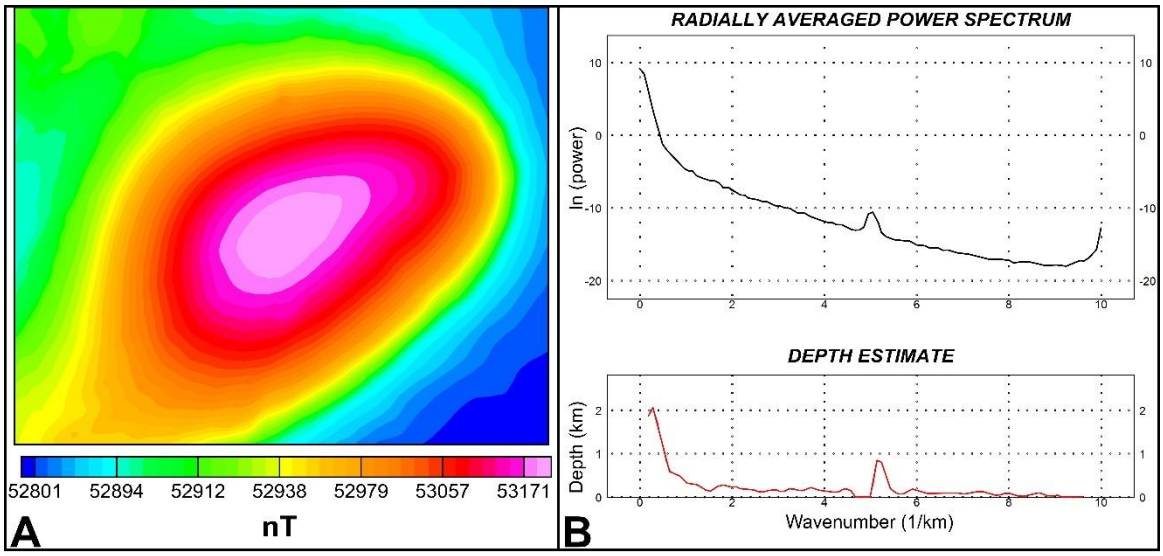

Figure 5.1: A) Windowed magnetic anomaly from the center of the Howley Basin. **B)** Radially averaged power spectrum of the magnetic anomaly shown in A, giving a depth to source of 2 km.

5.5 Methods and Results

Potential-field modeling of the Howley Basin was completed with the GM-SYS extension in Oasis Montaj and is presented in Profile X to X'. The composite complete Bouguer gravity dataset (Appendix D) and the Total Magnetic Field Deer Lake aeromagnetic survey (Cook and Kilfoil, 2009; Appendix E) were used in for the modeling process. A magnetic field of 53957.4 nT with an inclination of 69.2º and a declination of -19.1º was used for the Earth's field parameters. The magnetic station locations were set to 90 m elevation, to account for the nominal terrain elevation of the Deer Lake aeromagnetic survey (Cook and Kilfoil, 2009; Appendix E). Gravity stations were left at ground-level. Topography was not included because the gravity data has already been terrain corrected (Section 4.4.4).

The first step in the modeling process was to use the magnetic data to model the high magnetic anomaly in the middle of the basin at 2 km depth. Its large amplitude (~ 450 nT) with short strike and width (~6 km x 5 km) required a very magnetically susceptible body to fit the observed field. A steeply east-dipping ophiolite was determined to be the most geologically reasonable solution. Given the numerous ophiolite xenoliths in the Silurian Wild Cove Pond Igneous Suite to the north (Hibbard et al., 1990; Map A), granites of this formation were used to model the pre-Carboniferous basement in the Howley Basin.

Once the geometry of the ophiolite was modeled, 2 km of Carboniferous sedimentary rocks were placed on top of it. DC shifts (a static shift applied to the whole data set) were then performed on both the magnetic and gravity profiles to level them with the observed values at station 54, centered on the magnetic high (Profile X to X'). This made the rest of the model relative to the known depth point.

Outside of view of Profile X to X', a rough Humber Basin (2.5 g/cm^3) was modeled with Proterozoic basement (with properties given in Table 5.1) extending from the western edge of the Humber Basin, dipping to the east, to a depth of 10 km under the center of Birchy Ridge (Map A). Below 10 km, Proterozoic basement is modeled to underlie the entire region.

All mapped faults and geological contacts were located along the profile. When applicable, the strike lengths of pre-Carboniferous geological bodies were limited to their mapped extent or geophysical expression (e.g., the ophiolite was assigned a strike length

of 3 km into and out of the profile). All Carboniferous units were left at the default strike length of 30 km.

Stratigraphic thicknesses of the North Brook Formation and Rocky Brook Formation are not constrained in the Howley Basin from geological mapping, as they sit in deformed fault panels in the Western Margin (Section 3.5). These units, however, are expected to underlie the Howley Formation (see Section 3.3). Deer Lake Group subsidence models in the Howley Basin are not full understood, and these formations have been modeled with homogeneous thicknesses throughout the basin (Profile X to X'). The remaining accommodation space, predicted from the low gravity signal over the basin, was filled with Howley Formation. Fine-grained constituents of the Howley Formation are expected to comprise a large portion of the Howley Formation at depth and towards the center of the basin (Section 3.3.3), and a higher density has been assigned for these rocks for the modeling process (Pn:H'; Table 5.1).

Profile X to X' shows the Howley Basin to form an asymmetric half-graben deepening to the east, to a maximum depth of 4.3 km. Subsidence is predicted to have been rapid during Howley Formation deposition, in a tectonically active basin. Coarse-grained and fine-grained Howley Formation members are shown to interfinger towards the center of the basin to reflect this tectonic activity on facies during deposition. The model presented in Profile X to X' is based on reasonable geological assumptions and interpretations, but many other models may fit the observed gravity and magnetic fields. Further supporting geoscience investigations are needed to constrain and refine potential-field modeling of the Howley Basin.

Chapter 6: Discussion and Conclusions

6.1 Geophysical Modeling

Basement geology in the potential-field model of the Howley Basin (Profile X to X') needed to be simplified due to the lack of geological constraints for the modeling process. The model presented is one of many that could fit the observed data. The Deer Lake Group is shown to underlie the Howley Formation. This interpretation is based on their exposure in the Western Margin fault panels, as well as Howley's interpretation of BH-93-01, located in the on the Eastern Margin, intersection of bituminous shales that he correlated to exposures that have since been dated to Viséan and are considered Rocky Brook Formation (Howley 1918b; Hyde, 1982; Map A; Appendix A). Without further knowledge of stratigraphic thicknesses of the Deer Lake Group in the Howley Basin, or evidence for Viséan subsidence models, they have been modeled as isopachous.

Granite of the Wild Cove Pond Igneous Suite has been interpreted to form the pre-Carboniferous basement to the Howley Basin. This interpretation is based on a relatively consistent magnetic signal along the strike of the Howley Basin (Map C), suggesting basement lithologies do not vary laterally. This combined with the presence of numerous ophiolite xenoliths in the Wild Cove Pond Igneous Suite and the large magnetic anomaly in the center of the basin, which best fits a very magnetically susceptible steeply dipping body, made choosing the Wild Cove Pond Igneous suite a reasonable choice. The pre-Carboniferous geology of the area is diverse and there are many possible lithologies that could underlie the Howley Basin.

Using the radially averaged spectrum of the magnetic anomaly (Section 5.2.3) and the assumption that the magnetic source is in pre-Carboniferous basement, the Howley Basin is predicted to be 2 km deep over the magnetic anomaly. Assuming the anomalous gravity low over the Howley Basin (Map E) is the product of increased sedimentary fill, the model shows that the Howley Basin forms an asymmetric half-graben, deepening to the east to a depth of 4.3 km (Profile X to X').

The potential-field model presented in Profile X to X' is in general agreement with the seismic (Vasquez, 2017) and magnetotelluric (Livada, 2014) imaging of the eastern margin of the Howley Basin (Map A), in that this part of the basin is relatively shallow (1-1.5 km), Deer Lake formations underlie the Howley Formation, and major faults dip steeply to the west. Both the seismic and magnetotelluric surveys were unable to transect the entire basin perpendicular to strike, missed the large negative gravity anomaly associated with it (Map A, Map E), and likely did not image the deepest part of the basin. The inverted magnetotelluric profile predicts that the Howley Basin reaches a maximum depth of 2.5 km to the southwest (Livada, 2014). Interpolating between the magnetotelluric and potential-field models suggests a sharp lateral depth change along the strike of the Howley Basin, supporting a pull-apart subsidence model.

6.2 Structural Synthesis

Geological contacts in the Howley Basin were not observed during this study, precluding definitive kinematic indicators of basin development. Through distribution of lithofacies and inferred or assumed contacts (Hyde et al., 1988; Hyde, 1995),

palynological dating (Barss 1980, 1981; Hamblin et al., 1997), structural deformation, and regional tectonic considerations, the Howley Basin is interpreted to have been affected by several episodes of transpression (TP) and transtension (TT) throughout the Carboniferous. These phases of subsidence and deformation have been overlaid onto the X to X' potential-field modeling profile (in pocket) to help depict the proposed deformational history of the Howley Basin.

Tournaisian (possibly late Devonian; Hyde et al., 1988) structural development of the 'Anguille Basin' is obscured by its present state of deformation as exposed in the Fisher Hills and Birchy Ridge. Regionally, wide-spread Anguille Group (or Horton Group) basin development is considered to have occurred along reactivated Acadian thrusts in extension (Gibling et al., 2008). The elongated northeast-southwest extent (extending all the way to Conche (~250 km); Figure 2.3; Hamblin et al., 1995) of the Anguille Group favors subsidence facilitated by normal faulting on east-dipping Acadian tectonic structures and not a pull-apart origin; releasing bends in strike-slip systems produce short-lived, localized subsidence, as continued displacement straightens master faults (e.g., Zhang et al., 1989). Extension to produce the Anguille basin may have been rooted to the BBL in the south but must have continued with a north-northeast trend into White Bay (Map A; Hamblin et al., 1995). Thinning of the crust along the Anguille basin likely would have promoted subsequent strike-slip faulting to occur along the same path.

The Saltwater Cove Formation in Birchy Ridge is strongly deformed and bound by prominent northeast trending faults (Map A). Aside from a tentative interpretation that the Saltwater Cove formation is thrust over Howley Formation on a west-dipping fault in

DDH-79-04 (Section 3.5.1; Map A; O'Sullivan 1979c; Appendix A), observations of bounding-faults were not made during this study. Cleavages and highly indurated lithologies indicate that the Anguille Group was deeply buried before becoming inverted to their current state. Tight fold trains are interpreted as contractional structures with orientation patterns indicating sustained poly-phase dextral transpressive strike-slip (Section 3.6). Structures observed in this study agree with previous workers (e.g., Hyde et al., 1988; Langdon 1996) that Birchy Ridge forms a positive flower structure. The overall east-verging asymmetry of fold geometries of the Saltwater Cove Formation in Birchy Ridge (Section 3.6) indicate that the flower structure is rooted to the Fisher Hills-Birchy Ridge Fault, to the west (Map A).

Initiation of transpression of the Saltwater Cove Formation can not be determined by mappable structures; however, clast lithologies of the Wigwam Brook Formation suggest that uplift began by the late Tournaisian (TP1; Hyde et al., 1988). Growth of the Saltwater Cove Formation as a positive flower continued into the Viséan, or the basin experienced another phase of transpression (TP2). This interpretation is based on the stratigraphic relationship with unconformable offlapping of the North Brook Formation in the Fisher Hills, which indicates that Viséan basin initiation (TT1) was coeval with tectonic growth of the Anguille Group (Hyde, 1982; Hyde et al., 1988).

Structural evidence for Viséan basin development was not obtained in this study. Regionally, Viséan accommodation space has been attributed to thermal subsidence, with localized thickening in active fault zones (Gibling et al., 2008). In the Deer Lake Basin Viséan subsidence was, at least in part, fault controlled. It is postulated that dextral

transtension (TT1) produced steep normal faults linked to Acadian tectonic structures developing on the flanks of the growing Anguille ridges. There is no evidence that this phase of basin development is of pull-apart origin (i.e., there are no documented strike-slip faults in the western Humber Basin and the Grand Lake Fault in the south is interpreted to have only minor Carboniferous offset (Cawood and van Gool, 1998).

A regional, erosive, unconformity and sedimentary hiatus in the Namurian is well-imaged in marine seismic lines over the CFS (Langdon, 1996; Pascucci et al., 2000). This unconformity separates the Deer Lake Group and Howley Formation in the Deer Lake Basin. Gondwana glaciation has been purposed for this time period; however, faults cutting Mississippian formations are observed to not affect overlaying Pennsylvanian formations (Gibling et al., 2008). These observations, combined with the onset of the Alleghanian Orogeny, clearly indicate that the region experienced another episode of tectonism (Gibling et al., 2008). Vasquez (2017) also interpreted seismic profiles in the eastern Howley Basin to show sub-vertical faults terminating at the Rocky Brook Formation – Howley Formation contact, greatly supporting that the basin was tectonically active in the Namurian.

The Howley Formation is presently deformed and inverted (Chapter 3), with no preservation of structures related to basin initiation or development. Two palynological dates of Westphalian A have been interpreted for samples of exposures in the Southeast Margin (Section 3.2; Barss, 1981; Hyde, 1982); however, clear evidence of tectonism in the Namurian suggests that Howley Formation deposition began in the Namurian. Given the large low gravity anomaly and the predicted asymmetric half-graben shown in the

geophysical model (Profile X to X'; Section 5.3), it is reasonable to assume that the Howley Basin formed as a dextral transtensional pull-apart basin (TT2), with extension focused on the Grand Lake Fault. With the locus of extensional subsidence located along the Grand Lake Fault, it is clear that temporally and spatially, regional tectonic strike-slip activity migrated from west to east across the region. The Grand Lake Fault is likely a major splay in the CFS PDZ and is interpreted to form a listric west-dipping fault linked to the BBL root at depth.

It is predicted that dextral transpressional growth of the Anguille flower structures (TP3) coincided with Howley Basin evolution. A west to east migration of strike-slip faulting from the Fisher Hills-Birchy Ridge Fault to Hampden Fault during TP3 would have incorporated the Deer Lake Group fault panels into the growing positive flower structure.

In this model of Howley Basin deposition, substantial and rapid subsidence is predicted to have occurred during active strike-slip faulting along bounding faults. This argument is supported by a minimum of 2.5 km measured stratigraphic thickness along Northeast Brook (Section 3.3.4) and the bore holes of Hatch (1921) that show thick packages of shale interbedded with sandstones and minor coal. Potential-field geophysical modeling also predicts up to 4 km of Carboniferous sediments in the Howley Basin, much of which could be the Howley Formation (Profile X to X').

The Howley Formation is clearly presently inverted in both the Eastern and Western Margins, with steep bedding, close folds, and varying fault orientations and

lineations where exposure permits examination. In the Southeast Margin gently plunging fold axes make small angles to the Grand Lake Fault and are not traceable between nearby sections with good exposure (Section 3.2.4), suggesting a component of post-Howley Formation dextral transpressional (TP4) deformation. This phase of deformation, however, shows a large compressional factor and is interpreted to have reactivated extensional structures into steeply dipping reverse faults. Post-Howley deformation may have been concentrated on the margins of the basin as the basin remains in net extension and, when reported, logs of bore holes towards the center of the basin show consistently shallow dips of bedding (Section 3.3.3; Hatch 1921).

Sub-cylindrical folds mapped throughout the Eastern Margin, with fold axes not contained in calculated axial planes (Sections 3.2, 3.3), suggest a syn- to post-Howley Formation poly-phased, predominately contractional, deformation history. The kinematics of these phases of deformation are unclear.

6.3 Hydrocarbon Potential

Active oil seeps and bitumen in shallow core (Langdon, 1993, 1994; Hamblin et al., 1997; Hyde et al., 1994), clearly show that oil has been generated and migrated east of the Anguille positive flower structures. Albeit limited in extent of study, Langdon (1993) showed the Howley Formation, along it's western extent, to have good porosity and represents potential reservoir rocks. Distribution and deformation of both source and reservoir rocks in the Howley Basin present both potential stratigraphic and structural traps for migrated hydrocarbons. Structural analysis and geophysical modeling presented

in this study show that the Howley Basin may have several attributes favorable for hydrocarbon production, migration, and trapping.

Source Rock:

Organic rich mudstones and shales of Rocky Brook Formation have been identified as the primary source rock for conventional hydrocarbon plays in the Deer Lake Basin (Hyde et al., 1988; Hamblin et al., 1997; Burden et al., 2014). Exposure of the Rocky Brook Formation has been well documented east of the Anguille positive flower structures (Hatch, 1919; Hyde, 1982; Section 3.5.2); however, the question as whether Rocky Brook Formation underlies the Howley Basin has been a topic of debate among researchers (e.g., Hyde et al., 1994).

A review of historic boring operations on the Eastern Margin of the Howley Basin and Howley's (1918b) interpretations place the Rocky Brook Formation at shallow depth (Section 3.3; BH-93-01; Map A; Appendix A), provides good evidence that this targeted source rock underlies the Howley Formation with significant lateral extent. With confidence, the Rocky Brook Formation has been modeled to underlie the Howley Basin (Profile X to X').

Coal boring operations along Goose Brook (Section 3.3.3; Murray and Howley, 1918; Hatch 1921) revealed that at shallow depths (maximum of 150 m), a large portion of the Howley Formation is comprised of very thick black shale beds (many over 10 m). These shale packages present another potential source rock in the Howley Basin. Rapid subsidence in the Howley Basin's pull-apart model, may have created a stratified anoxic

lacustrine setting with good organic material accumulation and preservation, similar to what has been suggested for basal Rocky Brook Formation (e.g., Hamblin et al., 1997; Kelly and Burden, 2011). These interbedded shales and sandstones could also represent potential seals and reservoirs for hydrocarbon traps.

Hydrocarbon Maturation:

The Howley Basin has a conventional hydrocarbon play exploration depth of 2-3 km (Hamblin et al., 1997). Potential-field geophysical modeling (Profile X to X') predicts that the Howley Basin forms an asymmetric half-graben deepening to the east, to a depth of 4.3 km. This places Carboniferous sediments in the Howley Basin well into the predicted oil window. Stratigraphic thicknesses of formations within the Howley Basin can not be determined with the presently available datasets. In the model presented in Profile X to X', subsidence in the Howley Basin was focused in the Namurian to Westphalian. With sedimentation and burial continuing into the early Permian (Ryan and Zentilli, 1993), hydrocarbon maturation is expected to have peaked in the late Pennsylvanian to early Permian.

Migration and Traps

Trap preservation is the greatest uncertainty in estimating the hydrocarbon potential in the Howley Basin and is dependent on relative timing of hydrocarbon generation and migration with basin deformation. Structural mapping of the Howley Basin has shown that the Howley Formation experienced at least one phase of post-depositional transpressional deformation (Sections 3.2, 3.3). If oil generation predates

inversion of the basin, then initial migration oil into stratigraphic reservoirs may have been breached by faults, potentially leading to a secondary migration of oil into newly formed structural traps, if present and not breached. On the other hand, if oil generation was syn- to post-transpressional inversion the likelihood of trap preservation is greater, with both stratigraphic and structural traps prospective targets.

The degree of deformation in the center of the Howley Basin is critical in evaluating the potential of the basin to have preserved hydrocarbons in reservoirs. If deformation associated with the last transpressional phase was focused on the basin's margins, leaving the center of the basin remained relatively unaffected, then the probability of oil migration into sealed traps is greatly increased. Whereas, if the center of the Howley Basin experienced strong compressional stresses causing faulting and tight folding, as observed along the margins of the basin, then traps have a higher probability of being breached and/or being much smaller. Geophysical imaging of the structure of the center of the Howley Basin is strongly recommended before further evaluation.

6.4 Recommended Future Work

As discussed in the previous section the Howley Basin possesses several attributes of a promising hydrocarbon play, what it lacks is a systematic basin-wide evaluation scheme to mitigate risk associated with exploration in a poly-phased strike-slip dominated basin. This has been obviously hampered by a lack of exposure within the basin.

Many of the kinematic structural arguments presented in Section 6.2 are based on palynologic dates of the Howley Formation, of which there are only two from outcrops in

the Southeast Margin (Barss, 1981; Hyde, 1982). It is recommended that a basin-wide assessment of the timing of deposition of the Howley Formation through palynological dating be conducted. This is particularly important for the Northeastern and Western Margins of the basin.

Gravity data collection during this study, greatly increased the station density within the Howley Basin, especially over Sandy Lake, and is of good quality. The modeling process, however, is restricted in certainty and offers too much freedom in model possibilities due to limited knowledge of stratigraphy at depth towards the center of the basin and unknown pre-Carboniferous basement geology. A deep exploration well drilled towards the center of the Howley Basin would most certainly aid in basin assessment and would help refine and expand geophysical models.

Structural mapping of the Howley Basin has been exhausted. Any future structural interpretation will need to rely heavily on high-resolution geophysics. A basin-wide seismic survey would greatly enhance all aspects of Howley Basin assessment.

References

Adams, K., 1981. Report on geological and geophysical surveys of the Birchy Lake prospect on Reid lot 45, Newfoundland. Reid Newfoundland Company Limited and Minorex Limited, Newfoundland and Labrador Geological Survey, Assessment File 12H/07/0697, 27 p.

Anderson, S. D., Jamieson, R. A., Reynolds, P. H. and Dunning G. R., 2001. Devonian Extension in Northwestern Newfoundland: 40Ar/39Ar and U-Pb Data from the Ming's Bight Area, Baie Verte Peninsula. The Journal of Geology, vol., 109, p. 191–211.

Baird, D. M., 1960. Sandy Lake, west half, Newfoundland. Geological Survey of Canada, Preliminary Map 47-1959.

Blakely, R.J., 1995. Theory in Gravity and Magnetic Applications. Cambridge University Press, New York, p. 441.

Bradley, D. C., 1982. Subsidence in Late Paleozoic basins in the Northern Appalachians. Tectonics, vol. 1, no. 1, pp. 107-123.

Barss, M. S., 1980. Palynological analyses of samples submitted for age determinations. Geological Survey of Canada, Internal Paleontological Report No. EPGS-PAL, 3-80 MSB, 2 p.

Barss, M. S., 1981. Palynological analyses of samples from Deer Lake and Rainy Lake map areas, Newfoundland. Geological Survey of Canada, Internal Paleontological Report No. EPGS-PAL, 4-81 MSB, 3 p.

Brem, A. G., Lin S. and van Staal C. R., 2003. Structural Relationships South of Grand Lake, Newfoundland. Current Research Newfoundland Department of Mines and Energy Geological Survey, Report 03-1, pp. 1-13.

Burden, E., Burden, D. and Parsons G., 2014. Finding the Parts: A Searchable Database and Report of Petroleum Geology and Geophysics Literature for Paleozoic Basins of Newfoundland and Labrador. OmniChron Associates Inc., St. John's, NL, 198 p.

Cawood, P. A. and Suhr G., 1992. Generation and obduction of ophiolites: constraints from the Bay of Islands Complex, western Newfondland. Tectonics, vol. 11, pp. 884-897.

Cawood, P. A. and van Gool, J. A. M., 1998. Geology of the Corner Brook-Glover Island Region, Newfoundland. Geological Survey of Canada Bulletin 427, 96 p.

Cawood, P.A. and Williams, H., 1988. Acadian basement thrusting, crustal delamination, and structural styles in and around the Humber Arm allochthon, western Newfoundland. Geology, vol. 16, pp. 370-373.

Cawood, P.A., Dunning, G.R., Lux, D. and Van Gool, J.A.M., 1994. Timing of peak metamorphism and deformation along the Appalachian margin of Laurentia in Newfoundland: Silurian, not Ordovician. Geology, vol. 22 no. 5, pp. 399-402.

Colman-Sadd, S. P., Hayes, J. P., and Knight, I., 2000. Geology of the Island of Newfoundland (digital version of Map 90-01 with minor revisions). Newfoundland Department of Mines and Energy, Geological Survey, Map 2000-30.

Cook, L.A. and Kilfoil, G., 2009. Aeromagnetic survey - Deer Lake area, Newfoundland (parts of NTS map areas 12A/13, 12A/14, 12H/02, 12H/03, 12H/04, 12H/06, 12H/07, 12H/10). Newfoundland and Labrador Geological Survey, Open File NFLD/3075.

Dawson, M.E. and Mersereau, T.G., 1989. First year assessment report on geological, geochemical and geophysical exploration for the Birchy Lake project for licence 3233 on claim blocks 5593-5594 in the Birchy Narrows area, northwestern Newfoundland, 2 reports. Bay Roberts Resources Limited, Newfoundland and Labrador Geological Survey, Assessment File 12H/1072, 65 p.

Devereaux, A., O'Reilly, D., Churchill, R., Thurlow, J. G., Jackson, R. G., Kennedy, C. and Sweet, K., 2009. Sixth year supplementary, seventh year and eighth year assessment report on geological, geophysical, and geochemical exploration for licences 7897M, 10141M and 16050M-16052M on claims in the Rocky Brook area, western Newfoundland, 4 reports. JNR Resources Incorporated and Altius Resources Incorporated, Newfoundland and Labrador Geological Survey, Assessment File 12H/1962, 328 p.

Durling, P.W. and Marillier, F. J. Y., 1990. Structural trends and basement rock subdivisions in the western Gulf of St. Lawrence, northern Appalachians. Atlantic Geology, vol. 26, p. 79–95.

Froude, T. and Metsaranta, R., 2009. First year assessment report on compilation and geological, geochemical and trenching exploration for licences 8913M, 10668M, 11809M, 11830M-11831M, 12375M, 12600M, 12636M, 12713M, 12733M, 12850M, 12883M, 12914M, 13254M, 15638M and 15718M on claims in the Deer Lake and Turners Ridge areas, western Newfoundland, 2 reports. Delta Uranium Incorporated and Spruce Ridge Resources Limited, Newfoundland and Labrador Geological Survey, Assessment File 12H/2023, 102 p.

Froude, T., Mouge, P., D'Amours, I. and Largeaud, J., 2008. First year assessment report on prospecting and geophysical, geochemical and diamond drilling exploration for licences 12374M, 12565M-12566M, 12583M-12584M, 12600M, 12636M, 12705M,

12712M, 12714M, 12733M, 12737M-12742M, 12849M-12850M, 13254M and 13513M-12514M on claims in the Deer Lake area, western Newfoundland, 2 reports. Spruce Ridge Resources Limited, Newfoundland and Labrador Geological Survey, Assessment File 12H/1955, 198 p.

Gall, Q., 1984. Petrography and Diagenesis of the Carboniferous Deer Lake Group and Howley Formation, Deer Lake Subbasin, Westen Newfoundland. Unpublished M.Sc. Thesis, Memorial University of Newfoundland, 242 p.

Gall, Q. and Hyde, R.S., 1989. Analcime in lake and lake-margin sediments of the Carboniferous Rocky Brook Formation, western Newfoundland, Canada. Sedimentology, vol. 36, p. 875-887.

Gibling, M. R., Culshaw, N., Rygel, M. C. and Pascucci, V., 2008. Chapter 6: The Maritimes Basin of Atlantic Canada: basin creation and destruction in the collisional zone of Pangea. In A. D. Miall (Ed.), Sedimentary Basins of the World, Volume 5: The Sedimentary Basins of the United States and Canada (pp. 211-244). Elsevier Science, Amsterdam; Oxford, U.K.; Boston, Mass.

Gibling, M. R., Saunders, K. I., Tibert, N. E. and White, J. A., 2004. Chapter 8: Sequence sets, high-accommodation events and the coal window in the Carboniferous Sydney Basin, Atlantic Canada. In Pashin, J. C. and Gastaldo, R. A. (Eds.), Sequence stratigraphy, paleoclimate, and tectonics of coal-bearing strata (pp. 169–197). American Association of Petroleum Geology Studies in Geology 51.

Hall, J., Langdon, G., Roberts, B., Hawkins, D., Fagan, A., Knight, I. and Kilfoil, G., 1992. Reflection seismic imaging of the Carboniferous Bay St. George Subbasin, onshore western Newfoundland: a reappraisal of Paleozoic stratigraphic thickness. Bulletin of Canadian Petroleum Geology, vol. 40, pp. 321–334.

Hall, J., Marillier, F. and Dehler, S. A., 1998. Geophysical studies of the structure of the Appalachian orogen in the Atlantic borderlands of Canada. Canadian Journal of Earth Sciences, vol. 35, no. 11, pp.1205-1221.

Hamblin, A. P., Fowler, M. G., Utting, J., Hawkins, D. W. and Riediger, C. L., 1995. Sedimentology, palynology and source rock potential of Lower Carboniferous (Tournaisian) rocks, Conche area, Great Northern Peninsula, Newfoundland. Bulletin of Canadian Petroleum Geology, vol. 43, no. 1, pp. 1-19.

Hamblin, A. P., Fowler, M. G., Utting, J., Hawkins, D. W. and Riediger, C. L., 1995. Sedimentology, palynology and source rock potential of Lower Carboniferous (Tournaisian) rocks, Conche area, Great Northern Peninsula, Newfoundland. Bulletin of Canadian Petroleum Geology, vol. 43, no.1, pp. 1-19.

Hamblin, A.P., Fowler, M.G., Utting, J., Langdon, G.S. and Hawkins, D., 1997. Stratigraphy, palynology and source rock potential of lacustrine deposits of the Lower Carboniferous (Visean) Rocky Brook Formation, Deer Lake Subbasin, Newfoundland. Bulletin of Canadian Petroleum Geology, vol. 45 no. 1, pp. 25-53.

Harding, T.P., 1985. Seismic characteristics and identification of negative flower structures, positive flower structures, and positive structural inversion. American Association of Petroleum Geologists Bulletin, vol. 69, pp. 582-600.

Hardy, S. and McClay, K., 1999. Kinematic modelling of extensional fault-propagation folding. Journal of Structural Geology, vol. 21, no. 7, 695-702.

Hatch, H.B., 1919. Geological report on Deer Lake, Humber River and Grand Lake Shale areas, Newfoundland. Reid Newfoundland Company Limited, Newfoundland and Labrador Geological Survey, Assessment File 12H/03/0003, 38 p.

Hatch, H.B., 1921. Report on Coal boring operations in the Sandy Lake River-Goose Lakes Basin, central Carboniferous area, west coast of Newfoundland. Reid Newfoundland Company, Newfoundland and Labrador Geological Survey, Assessment File 12H/03/0052, 25 p.

Haworth, R.T., Poole, W.H., Grant, A.C. and Sanford, B.V., 1976. Marine geoscience survey northeast of Newfoundland. Geological Survey of Canada, Paper 76-1A, p. 7-15.
Hayes, A.O. 1949: Coal possibilities of Newfoundland. Newfoundland Geological Survey, Information Circular no. 6, 39 p.

Heiskanen, W. A. and Moritz, H., 1969. Physical geodesy: W. H. Freeman Co.
Hibbard, J., Muggridge, W. and Gagnon, J. 1980: Sheffield Lake, Newfoundland. Government of Newfoundland and Labrador, Department of Mines and Energy, Mineral Development Division, Map 80-010.

Hinze, W. J., Aiken, C., Brozena, J., Coakley, B., Dater, D., Flanagan, G., … Winester, D., 2005. New standards for reducing gravity data: The North American gravity database, Geophysics vol. 70, no. 4, J25-J32.

Holcombe, R., 2011. "GEOrient ver 9.5.0 Stereographic Projections and Rose Diagram Plots software." Last update: January 2011. https://www.holcombe.net.au/software/georient.html. [downloaded September 2013].

Holcombe, R., 2013. "GEOcalculator ver 4.9.8 Geological Structural Calculator." Last update: July 2013. https://www.holcombe.net.au/software/geocalculator.html. [downloaded September 2013].

Howley, J. P., 1907. Map of Newfoundland. Geological Survey of Newfoundland?. Memorial University of Newfoundland Map Library, local call no. G 3435 1907 H6 MAP.

Howley, J. P., 2009. Reminiscences of Forty-Two Yeas of Exploration in and About Newfoundland. Kirwin, W. J., O'Flaherty P.A. and Hollet R. C. (Eds.), Memorial University of Newfoundland, 2158 p.

Howley, J.P., 1881. Chapter 19: Report for 1879 - boring operations near the Grand Pond - survey of the west branch of the Humber River. In Geological Survey of Newfoundland, By A. Murray and J. P. Howley, 1881, pp. 512-531.

Howley, J.P., 1918a. Chapter 11: report for 1891 and 1892, on the Humber Valley and central Carboniferous area of the Island and continuation of coal exploration near Grand Lake. In Reports of Geological Survey of Newfoundland from 1881 to 1909, By A. Murray and J. P. Howley, pp. 171-218.

Howley, J.P., 1918b. Chapter 13: report for 1893, coal boring operations at the head of Grand Lake. In Reports of Geological Survey of Newfoundland from 1881 to 1909, By A. Murray and J. P. Howley, pp. 258-274.

Howley, J.P., 1918c. Chapter 15: report for 1895, coal exploration near Goose Brook. In Reports of Geological Survey of Newfoundland from 1881 to 1909, By A. Murray and J. P. Howley, pp. 317-319.

Howley, J.P., 1918d. Chapter 26: report for 1904, exploration and boring operations in the central Carboniferous basin near Grand Lake. In Reports of Geological Survey of Newfoundland from 1881 to 1909, By A. Murray and J. P. Howley, pp. 548-558.

Howley, J.P., 1918e. Chapter 28: report for 1905, the continuation of the coal boring operations in the central Carboniferous area near Goose Brook, Humber Valley. In Reports of Geological Survey of Newfoundland from 1881 to 1909, By A. Murray and J. P. Howley, pp. 571-577.

Howley, J.P., 1918f. Chapter 30: report for 1906, coal boring operations near Goose Brook. In Reports of Geological Survey of Newfoundland from 1881 to 1909, By A. Murray and J. P. Howley, pp. 588-596.

Howley, J.P., 1918g. Chapter 31: report for 1907, coal boring operations near MacGregor, Grand Lake, Carboniferous area. In Reports of Geological Survey of Newfoundland from 1881 to 1909, By A. Murray and J. P. Howley, pp. 597-602.

Howley, J.P., 1918h. Chapter 33: report on coal boring operations for the year 1908. In Reports of Geological Survey of Newfoundland from 1881 to 1909, By A. Murray and J. P. Howley, pp. 608-615.

Howley, J.P., 1918i. Chapter 34: report for 1909, coal boring operations near Goose Brook. In Reports of Geological Survey of Newfoundland from 1881 to 1909, By A. Murray and J. P. Howley, pp. 616-625.

Howse, A. and Fleischmann, J., 1982. Coal assessment in the Deer Lake Carboniferous Basin. In C. F. O'Driscoll and R. V. Gibbons (Eds.), Current research, Government of Newfoundland and Labrador (pp. 208-213). Department of Mines and Energy, Mineral Development Division, Report 82-01.

Howse, C. F., 1947. Assorted reports and correspondence re. Howley coal area. Unpublished report, Anglo Newfoundland Development Co. Ltd., 28 p.

Hunt, C. P., Moskowitz, B. M., and Banerjee, S. K., 1995. Magnetic properties of rocks and minerals. In T. J. Ahrens (Ed.), Rock Physics and Phase Relations, A Handbook of Physical Constants, Ref. Shelf, vol. 3, (pp. 189–204), AGU, Washington, D. C.

Hyde, R.S., 1978. Howley area coal deposits-history of exploration and new information on the geology of the region. 1978, 37 p.

Hyde, R.S., 1979a. Hampden, Newfoundland. Government of Newfoundland and Labrador, Department of Mines and Energy, Mineral Development Division, Open File 012H/0551, Map 79-02.

Hyde, R.S., 1979b. Sheffield Lake, Newfoundland. Government of Newfoundland and Labrador, Department of Mines and Energy, Mineral Development Division, Open File 012H/0551, Map 79-03.

Hyde, R.S., 1982. Geology of the Carboniferous Deer Lake Basin. Government of Newfoundland and Labrador, Department of Mines and Energy, Mineral Development Division, Map 82-007.

Hyde, R. S., 1984. Geologic history of the Carboniferous Deer Lake Basin, west-central Newfoundland, Canada. In H. H. J. Geldsetzer, W. W. Nassichuk, E. S. Belt and R. W. Macqueen (Eds.), Ninth International Congress of Carboniferous Stratigraphy and Geology (pp. 85-104). Southern Illinois University Press, Carbondale, Illinois.

Hyde, R.S., 1989. The North Brook Formation: a temporal bridge spanning contrasting tectonic regimes in the Deer Lake Basin, western Newfoundland. Atlantic Geology, 25, pp. 15-22.

Hyde, R. S., 1995. Upper Paleozoic rocks, Newfoundland. In H. Williams (Ed.), Geology of the Appalachian-Caledonian Orogen in Canada and Greenland (pp. 523-552). Geological Survey of Canada, Geology of Canada Series 6.

Hyde, R.S. and Ware, M.J., 1981. Deer Lake and Rainy Lake (west half). Government of Newfoundland and Labrador, Department of Mines and Energy, Mineral Development Division, Open File NFLD/1152, Map 81-017.

Hyde, R. S., Langdon, G. S., Tuach, J. and Wilton. D. H. C., 1994. The Last Frontier -A Field Conference to The Deer Lake Basin, Newfoundland, September 30-October 2, 1994. Geological Summary and Fieldtrip Guidebook. Center for Earth Resources Research (CERR) Report No. 1, 74 p.

Hyde, R.S., Miller, H.G., Hiscott, R.N. and Wright, J.A., 1988. Basin architecture and thermal maturation in the strike-slip Deer Lake Basin, Carboniferous of Newfoundland. Basin Research, 1, pages 85-105.

Hyde, R.S., Ware, M., Bradley, P. and Connor, W., 1980. Cormack and part of Silver Mountain, Newfoundland. Government of Newfoundland and Labrador, Department of Mines and Energy, Mineral Development Division, Open File 12H/0713, Map 80-011.

Jol, H. M., 2009. Ground Penetrating Radar: Theory and applications (1st edition). Elsevier Science, Amsterdam; Boston Mass., 524 p.

Kalkreuth, W. and MacAuley, G., 1989. Organic petrology and rock - eval studies on oil shales from the Lower Carboniferous Rocky Brook Formation, western Newfoundland. Bulletin of Canadian Petroleum Geology, vol. 37 no. 1, pp. 31-42.

Kane, M. F., 1962. A comprehensive system of terrain corrections using a digital computer: Geophysics, vol. 27, pp. 455-462.

Keats, K. and Smith, G., 2006. First, second and fourth year assessment report on geophysical exploration for licences 8913M, 10668M, 11809M, 11830M-11831M and 12375M on claims in the Turners Ridge area, White Bay, Newfoundland, 2 reports. Spruce Ridge Resources Limited, Newfoundland and Labrador Geological Survey, Assessment File 12H/1848, 46 p.

Kelly, M. L. and Burden, E. T., 2011. Atlas of strata and source rock characteristics for the Rocky Brook Formation, Deer Lake Group, Newfoundland and Labrador. Petroleum Exploration Enhancement Programme (PEEP), 144 p.

Kilfoil, G. J. and Bruce, P. A., 1990. Regional aeromagnetic data grids (200m grid cell), in digital form, for all of insular Newfoundland, version 1.0. Newfoundland Department of Mines and Energy, Geological Survey Branch, Open File NFLD (2063), 24 p.

Kilfoil, G.J. and Cook, L.A., 2009. Aeromagnetic survey - Corner Brook Newfoundland (NTS maps areas 12A/12, 12A/13, 12B/09, 12B/16, 12G/01, 12H/04, 12H/05). Government of Newfoundland and Labrador, Department of Natural Resources, Geological Survey, Open File NFLD/3058.

Knight, I., 1983. Geology of the Carboniferous Bay St. George Subbasin, western Newfoundland. Department of Mines and Energy, Mineral Development Division, Government of Newfoundland and Labrador, Memoir, vol. 1, 358 p.

Knight, I., James, N.P. and Lane, T.E., 1991. The Ordovician St. George Unconformity, northern Appalachians: the relationship of plate convergence at the St. Lawrence Promontory to the Sauk/Tippecanoe Sequence Boundary. Geological Society of America Bulletin, vol. 103 no. 9, pp. 1200-1225.

LaFehr, T. R., 1991. An exact solution for the gravity curvature (Bullard B) correction. Geophysics, vol. 56, pp. 1179–1184.

Landell-Mills, T., 1954. Report on the Oxley oil and oil shales in the Deer Lake area, Newfoundland. Oxley, J. J., Newfoundland and Labrador Geological Survey, Assessment File 12H/0365, 8 p.

Langdon, G. S., 1993. A Study of Petroleum Potential and Regional Petroleum Prospsectivity of The Deer Lake Group and Howley Formation on Permits 93-1 03 and 93-104, Deer Lake Basin. Center for Earth Resources Research (CERR) Report. Dept of Earth Sciences, Memorial University of Newfoundland, 36 p.

Langdon, G.S., 1996. Tectonics and basin deformation in the Cabot Strait area and implications for the Late Paleozoic development of the Appalachians in the St. Lawrence Promontory. Unpublished Ph.D. thesis, Memorial University of Newfoundland, 330 p.

Langdon, G. S. and Abrajano, J., 1994. Geochemical correlation study of degraded oils and Rocky Brook source rocks, Deer Lake Basin. Memorial University of Newfoundland, Centre for Earth Resources Research (CERR), Report EL 94-105-01-EC, 11 p.

Langdon, G. S. and Hall, J., 1994. Devonian–Carboniferous tectonics and basin deformation in the Cabot Strait area, eastern Canada. American Association of Petroleum Geologists, Bulletin, vol. 78, no. 11, pp. 1748-1774.

Lavoie, D., Pinet, N., Dietrich, J. R., Hannigan, P. K., Castonguay, S., Hamblin, A. P. and Giles, P. S., 2009. Petroleum Resource Assessment, Paleozoic successions of the St. Lawrence Platform and Appalachians of eastern Canada. Geological Survey of Canada, Open File 6174, 275 p.

Livada, T., 2014. Magnetotelluric study of Howley Basin, Newfoundland. Unpublished MSc thesis, Memorial University of Newfoundland, 181 p.

Longman I. M., 1959. Formulas for Computing the Tidal Accelerations Due to the Moon and the Sun. Journal of Geophysical Research, vol. 64, pp. 2351–2355.

Marillier, F., Keen, C. E., Stockmal, G. S., Quinlan, G., Williams, H., Colman-Sadd, S. and O'Brien, S., 1989. Crustal structure and surface zonation of the Canadian Appalachians: implications of deep seismic reflection data. Canadian Journal of Earth Sciences, vol. 26, pp. 305–321.
Marshak, S., and Mitra, G., 1988. Basic methods of structural geology. Englewood Cliffs, N.J: Prentice Hall. 446 p.

Miller, H.G. and Wright, J.A., 1984. Gravity and magnetic interpretation of the Deer Lake Basin, Newfoundland. Canadian Journal of Earth Sciences, vol. 21 no.1, pp. 10-18.

Mishra, D., 2011. Gravity and magnetic methods for geological studies: Principles, integrated exploration and plate tectonics. BS Publications, Hyderabad, India, 938 p.

Moritz, H., 1980. Geodetic Reference System 1980. Bullet in Geodesique, vol. 54, no. 3, pp. 395-405.

Mukhopadhyay, P. K., 2010. Preliminary evaluation of shale gas/oil shale resources of the Werner Hatch #1 well and leased area of the Deer Lake Oil & Gas Inc. within the Deer Lake Basin, western Newfoundland. Revised Final Report Submitted to Deer Lake Oil & Gas Inc., 95 p.

Murray, A. and Howley J. P., 1918. Reports of Geological Survey of Newfoundland from 1881 to 1909. Robinson & Company. Limited, Press, St. John's, NF., 725p.

Murray, A., and Howley J. P., 1881. Geological Survey of Newfoundland. Edward Stanford, London, Eng., 536 p.

Nagy, D. 1966: The gravitational attraction of a right rectangular prism. Geophysics, vol. 31, pp. 362–371.

Natural Resources Canada a. National Topographic Data Base. Retrieved from: http://ftp.geogratis.gc.ca/pub/nrcan_rncan/vector/ntdb_bndt/50k_shp_en/.

Natural Resources Canada b. Magnetic Field Calculator. Retrieved from: http://geomag.nrcan.gc.ca/calc/mfcal-en.php.

Natural Resources Canada c. Precise Point Positioning. Retrieved from: https://webapp.geod.nrcan.gc.ca/geod/tools-outils/ppp.php.

Natural Resources Canada d. Gravity Network (CGSN). Retrieved from: http://webapp.geod.nrcan.gc.ca/geod/data-donnees/cgsn-rncg.php.

Natural Resources Canada e. Index of /pub/nrcan_rncan/elevation/cdsm_mnsc. Retrieved from: http://ftp.geogratis.gc.ca/pub/nrcan_rncan/elevation/cdsm_mnsc/.

Natural Resources Canada f. Geoscience Data Repository for Geophysical Data. Retrieved from: http://gdr.agg.nrcan.gc.ca/gdrdap/dap/search-eng.php.

Neacsu, M., 2011. What is the difference between WGS84 and NAD83. Retrieved from: https://www.uvm.edu/giv/resources/WGS84_NAD83.pdf.

Newfoundland and Labrador Geological Survey a. Detailed Bedrock Geology. Newfoundland and Labrador GeoScience Atlas OnLine. Last update: January 2013. http://geoatlas.gov.nl.ca. [downloaded September 2013].

Newfoundland and Labrador Geological Survey b. "Detailed Contacts." Newfoundland and Labrador GeoScience Atlas OnLine. Last update: January 2013. http://geoatlas.gov.nl.ca. [downloaded September 2013].

Newfoundland and Labrador Geological Survey c. "Detailed Faults." Newfoundland and Labrador GeoScience Atlas OnLine. Last update: January 2013. http://geoatlas.gov.nl.ca. [downloaded September 2013].

Newfoundland and Labrador Geological Survey d. "Index of Airborne Geophysical Surveys." Newfoundland and Labrador GeoScience Atlas OnLine. Last update: April 2014. Retrieved from: http://geoatlas.gov.nl.ca.

O'Sullivan, J., 1979a. Report on geological, geochemical and geophysical surveys for project 724 for licence 1306 on claim block 1574 in the Sandy Lake area, Newfoundland. Northgate Exploration Limited, Newfoundland and Labrador Geological Survey, Assessment File 12H/06/0592, 24 p.

O'Sullivan, J., 1979b. Report on geological, geochemical and geophysical surveys for project 724 for licence 1304 on claim block 1572 in the Sandy Lake area, Newfoundland. Northgate Exploration Limited, Newfoundland and Labrador Geological Survey, Assessment File 12H/06/0590, 25 p.

O'Sullivan, J., 1979c. Report on geological, geochemical and geophysical surveys for project 724 for licence 1307 on claim block 1575 in the Sandy Lake area, Newfoundland. Northgate Exploration Limited, Newfoundland and Labrador Geological Survey, Assessment File 12H/06/0593, 24 p.

Owen, J.V., 1991. Geology, Long Range Inlier, Newfoundland. Geological Survey of Canada, "A" Series Map no. 1764A.

Pascucci, V., Gibling, M. R. and Williamson, M. A., 2000. Late Paleozoic to Cenozoic history of the offshore Sydney Basin, Atlantic Canada. Canadian Journal of Earth Sciences, vol. 37, pp. 1143–1165.

Plint, A. G., 1985. Possible earthquake-induced soft-sediment faulting and remobilization in Pennsylvanian alluvial strata, southern New Brunswick, Canada. Canadian Journal of Earth Sciences, vol. 22, pp. 907–912.

Popper, G. H. P., 1970. Paleobasin analysis and structure of the Anguille Group, west-central Newfoundland. Unpublished PhD thesis, Lehigh University, Bethlehem, Pennsylvania, 297 p.

Quinlan, G., Hall, J., Williams, H., Wright, J. A., Colman-Sadd, G., O'Brien, S. J., Stockmal, G. S. and Marillier, F., 1992. LITHOPROBE onshore seismic reflection transects across the Newfoundland Appalachians. Canadian Journal of Earth Sciences, vol. 29, pp. 1865-1877.

Ramsay, J. G. and Huber, M. I., 1987. The Techniques of Modern Structural Geology, Vol. 2: Folds and Fractures. Pergamon Press, London, Eng., 392 p.

Reid, W., Greenwood, R. and Largeaud, J., 2008. First, second and sixth year assessment report on geophysical exploration for licences 9074M, 12902M-12908M, 12994M-12995M, 12999M, 13007M-13008M, 13034M, 13040M, 13052M, 13072M-13078M, 13978M, 14088M, 14289M and 14411M on claims in the Sops Arm, Baie Verte Junction and Sheffield Lake area, western Newfoundland, 2 reports. Metals Creek Resources Limited, Quinlan, E and Quinlan Prospecting, Newfoundland and Labrador Geological Survey, Assessment File 12H/1898, 61 p.

Rosenfeld, J. and Gordon, T., 2010. First, second, third, fifth, seventh and eighth year assessment report on prospecting and geochemical, geophysical and trenching exploration for licences 8296M, 9253M-9256M, 10499M, 13026M, 14370M and 15880M on claims in the Hinds Brook area, western Newfoundland, 2 reports. Aspect Canada Mining Company, Newfoundland and Labrador Geological Survey, Assessment File 12H/03/2035, 68 p.

Ryan, R. J. and Zentilli, M., 1993. Allocyclic and thermochronological constraints on the evolution of the Maritimes Basin of eastern Canada. Atlantic Geology, vol. 29, pp.187-197.

Sanford, B. V. and Grant, A. C., 1990. Bedrock geological mapping and basin studies in the Gulf of St. Lawrence, Geological Survey of Canada (Paper 90-1B), pp 33-42.

Scintrex, 2009. CG-5 Scintrex Autograv System Operation Manual (revision 5). Scintrex Limited, Concord, ON., 312 p.

Seigel, H. O., 1994. A Guide to High Precision Land Gravimeter Surveys. Scintrex Limited, Concord, ON., 122 p.

Smyth, W.R. and Schillereff, H.S., 1981. Hampden southwest 12H/10SW. Government of Newfoundland and Labrador, Department of Mines and Energy, Mineral Development Division, Open File 12H/10/0747, [Map 81-112].

Somigliana, C., 1930. Geofisica — Sul campo gravitazionale esterno del geoide ellissoidico: Atti della Accademia nazionale dei Lincei. Rendiconti. Classe di scienze fisiche, matematiche e naturali, vol. 6, pp. 237-243.

Spector, A. and Grant, F. S., 1970. Statistical Models for Interpreting Aeromagnetic Data. Geophysics, vol. 35, pp. 293-302.

St. Peter, C. ,1993. Maritimes Basin evolution: key geologic and seismic evidence from the Moncton Subbasin of New Brunswick. Atlantic Geology, vol. 29, pp. 233-270.

T'Railway., Newfoundland T'Railway Bridges/Trestles. Retrieved from: http://www.trailway.ca/bridges.php.

Thurlow, J.G., Churchill, R. and Smith, G., 2007. Assessment report on geophysical exploration for 2006 submission for Mining Lease 60 and for second year, second year supplementary, fourth year, fourth year supplementary, fifth year and sixth year supplementary assessment on licences 7897M, 8647M, 8878M, 8913M, 9287M, 10141M, 10727M and 10935M on claims in the Rocky Brook and White Bay areas, western Newfoundland, 2 reports. Altius Resources Incorporated, Bidgood, R, Spruce Ridge Resources and JNR Resources Incorporated, Newfoundland and Labrador Geological Survey, Assessment File 12H/1850, 41 p.

Topcon, 2004. HiPer Lite & HiPer Lite+ Operator's Manual.
Topcon 2006: RE-S1 915+ Spread Spectrum Radio Operator's Manual.

van de Poll, H. W. 1995: Upper Paleozoic rocks: NewBrunswick, PrinceEdwardIsland and Iˆles de la Madeleine. In H. Williams (Ed.), Geology of the Appalachian-Caledonian Orogen in Canada and Greenland. Geological Survey of Canada, Geology of Canada Series no. 6, pp. 455-492.

van der Velden, A. J., van Staal, C. R. and Cook, F. A., 2004. Crustal structure, fossil subduction and the tectonic evolution of the Newfoundland Appalachians: Evidence from a reprocessed seismic reflection survey. Geological Society America Bulletin, vol. 116, pp.1485-1498.

van Staal, C. R. and Barr, S. M., 2012. Lithospheric architecture and tectonic evolution of the Canadian Appalachians and associated Atlantic margin. In J. A. Percival, F. A. Cook, and R. M. Clowes (Eds.), Tectonic Styles in Canada: the LITHOPROBE Perspective. Geological Association of Canada, Special Paper 49, pp. 41-95.

van Staal, C.R., Whalen, J.B., McNicoll, V.J., Pehrsson, S., Lissenberg, C.J., Zagorevski, A., van Breemen, O., and Jenner, G.A., 2007. The Notre Dame arc and the Taconic orogeny in Newfoundland. In Hatcher, R.D., Jr., Carlson, M.P., McBride, J.H. and Martínez Catalán, J.R (Eds.), 4-D Framework of Continental Crust. Geological Society of America Memoir 200, pp. 511–552.

Vasquez, O. E., 2017. Interpretation of Gravity and Seismic Data and Assessment of the Performance of the MUN SWEPT Impact Seismic Source in the Howley Basin, Howley, Newfoundland. Unpublished MSc thesis, Memorial University of Newfoundland, 118 p.

Waldron J. W. F. and Stockmal G. S., 1991. Mid-Paleozoic thrusting at the Appalachian deformation front: Port au Port Peninsula, western Newfoundland. Canadian Journal of Earth Sciences, vol. 28, no. 12, pp. 1992-2002.

Waldron J. W. F. and Stockmal G. S., 1994. Structural and tectonic evolution of the Humber Zone, western Newfoundland; 2, A regional model for Acadian thrust tectonics. Tectonics, vol. 13, no. 6, pp. 1498-1513.

Waldron, J. W. F., 2004. Anatomy and evolution of a pull-apart basin, Stellarton, Nova Scotia. Geological Society of America Bulletin, vol. 116, pp. 109-127.

Waldron, J. W. F. and Rygel, M. C., 2005. Role of evaporite withdrawal in the preservation of a unique coal-bearing succession: Pennsylvanian Joggins Formation, Nova Scotia. Geology, vol. 33, pp. 337-340.

Waldron, J. W. F. and van Staal, C. R., 2001. Taconian orogeny and the accretion of the Dashwoods block:A peri-Laurentian microcontinent in the Iapetus Ocean. Geology, vol. 20 no. 9, pp. 811-814.

Waldron, J. W. F., Anderson, S. D., Cawood, P. A., Goodwin, L. B., Hall, J., Jamieson, R. A. and Williams, P. F. 1998: Evolution of the Appalachian Laurentian margin: Lithoprobe results in western Newfoundland. Canadian Journal of Earth Sciences, vol. 35, no. 11, pp. 1271-1287.

Waldron, J. W. F., S. M. Barr, Park, A. F., White, C. E. and Hibbard, J., 2015. Late Paleozoic strike-slip faults in Maritime Canada and their role in the reconfiguration of the northern Appalachian orogen. Tectonics, vol. 34, pp. 1661-1684.

Weaver, D.F., 1967. A Geological Interpretation of The Bouguer Anomaly Field of Newfoundland. Publications of the Dominion Observatory, Ottwa, ON., vol. 35, no. 5, pp. 916-926

Wellenholf, H. and Moritz H., 2006: Physical Geodesy (second, corrected edition). Springer Wien New York, Austria, 403 p.

Whalen, J.B. and Currie, K.L., 1988. Geology, Topsails Igneous Terrane, Newfoundland. Geological Survey of Canada, "A" Series Map 1680A.

Whalen, J. B., Mcnicoll, V. J., van Staal, C. R., Lissenberg, C. J., Longstaffe, F. J., Jenner, G. A. and van Breemen, O., 2006. Spatial, temporal and geochemical characteristics of Silurian collision-zone magmatism: An example of a rapidly evolving magmatic system related to slab break-off. Lithos, vol. 89, pp. 377-404.

Wilkinson, R.I., 1982. Report on the geological, geochemical and geophysical surveys for licences 1818-1830, 1837-1840, 1987-1988, 1482 and 1872-1873 on the Howley and Kittys Brook claims areas, Newfoundland. Westfield Minerals Limited, Memorial University of Newfoundland, Shell Canada Resources Limited and Northgate Exploration Limited, Newfoundland and Labrador Geological Survey, Assessment File 12H/0774, 41 p.

Williams, H., 1979. Appalachian Orogen in Canada. Canadian Journal of Earth Sciences, vol. 16 no. 3, pp. 792-807.

Williams, H., 1995. Temporal and spatial divisions. In H. Williams (Ed.), Geology of the Appalachian-Caledonian Orogen in Canada and Greenland. Geological Survey of Canada, Geology of Canada Series no. 6, pp. 21-44.

Williams, H. and Cawood, P.A., 1989. Geology, Humber Arm Allochthon, Newfoundland. Geological Survey of Canada, "A" Series Map 1678A.

Williams, H. and St Julien, P., 1982. The Baie Verte-Brompton Line: Early Paleozoic continent-ocean interface in the Canadian Appalachians. In Major structural zones and faults of the northern Appalachians. Edited by P. St - Julien and J. Beland, Geological Association of Canada, Special Paper no. 24, pp. 177-207.

Williams, H., Colman-Sadd, S.P. and Swinden, H.S., 1988. Tectonicstratigraphic Subdivisions of Central Newfoundland. In Current Research Part B. Geological Survey of Canada, Paper 88-01B, pp. 91-98.

Wright, J. A., Hoffe, B. H., Langdon, G. S. and Quinlan, G. M., 1996: The Deer Lake basin, Newfoundland; structural constraints from new seismic data. Bulletin of Canadian Petroleum Geology, vol. 44, no. 4, pp. 674-682.

Zagorevski, A. and van Staal, C.R., 2011. The record of Ordovician arc-arc and arc-continent collisions in the Canadian Appalachians during the closure of Iapetus. In Arc Continent Collision; Frontiers in Earth Science, pp 341-371.

Zhang, P. Z., Burchfiel, B.C., Chen, S. and Deng, Q., 1989. Extinction of pull-apart basins. Geology, vol. 17, pp. 814-817.

Appendix A – Drill Logs

In the attached folder are spread sheets of all of the borehole and diamond drill core logs collared in the Howley Basin, as described by the original authors. Many of the drill logs are from coal boring operations from the turn of the 20th century and are difficult to locate in the literature, were continued in following field seasons, are mislabelled, and have been erroneously placed on previous authors' maps. This appendix aims at providing an easily accessible and accurate account of this dataset for future studies to benefit from.

Boreholes that were initiated in one field season and continued in a following one are labeled with initial year of drilling and are continued until the end of the hole. Approximate locations of boreholes, determined by the methods described in Section 3.3.3, are given in UTM coordinates (NAD83 Zone 21N).

Appendix B –Conductivity of Sandy Lake Water Samples

The GPR geophysical method uses pulses of an electromagnetic field to image the subsurface (Section 4.2). The conductivity of the subsurface limits the penetrating depth of the GPR, and can be estimated by equation: $D= 40/\alpha$ meters, where $\alpha= 0.18\sigma$ dB/m, and σ is in mS/m (Jol, 2009). Before the GPR survey was run, the average conductivity of the water in Sandy Lake was measured to determine if the GPR method would be effective in imaging the bottom of the lake, and creating a bathymetry map.

Three 40 ml samples of water were collected and their conductivity measured. One sample was taken at the main inflow to Sandy Lake, one at its outflow, and another away from the main current. The conductivity of the samples was measured with Memorial University of Newfoundland's IQ Scientific Instrument's 180G Handheld Multiparameter Meter. A standard 10 mS/cm was measured between each sample to ensure that the instrument was properly calibrated. The mean conductivity of all of the samples was 3.21 mS/cm with a standard deviation of 0.42 mS/cm. Using the above equation, an estimated depth of penetration of 70 m was determined, and the GPR was deemed appropriate to be used for recording the bathymetery of Sandy Lake.

Appendix C – Ground Penetrating Radar Data, Interpretations, and Bathymetry Grid

The attached folder contains the raw GPR data and associated GPS data (File: GPR_Raw); georeferenced nodes of lake-bottom interpretations (File: Interpretations), in .csv format; the georeferenced nodes that make up the shoreline (including islands) of Sandy Lake, as given by NRCan (Natural Resources Canada, a) (File: Sandy_Lake_Shoreline), in .csv format; the two combined (File: Bathymetry_Point), in .csv format; and the 50 m cell size minimum curvature interpolated bathymetry grid with a linear color scheme (File: Bathymetry_Grid), in .grd format.

Appendix D – Gravity Data

The attached file contains all of the gravity data collected during this study, RTK GPS gravity station locations (NAD83 (CSRS) UTM Zone 21N) and elevations (GRS80),

all data used for the reduction of the gravity data, as well as re-processed previous gravity surveys. This data was used to create Map E – composite complete Bouguer Gravity Map.

Preprocessed gravity data collected during this survey (File: Oasis_Loops) is archived in .txt files in the Oasis gravity import format. Each .txt file corresponds to a day survey or "loop", with the title of each file as that date in DDMMYY. Within each loop file, station number (STN); Type of station (T; 0 is base; 1 is survey station); Time in GMT (Time); Relative gravity reading (Rdng) without tidal acceleration removed, in mGals; and instrument height above the ground (In_Ht), in meters. The top line in each loop files specifies the date of collection (dt=YY/MM/DD), difference in time from GMT (gt=H.h), and units of distance used for distance, elevation, and instrument height, set to meters (un=MMM).

Column descriptions for the following gravity data spreadsheets are given in File Grav_Descrp, where downloaded data follows file, Gravity_point_data_description, and any processing or collection completed in this study follows Gravitv_Key.

The gravity data used for calculating the absolute gravity of the Howley base station (Section 4.4.3) is given in File: BaseTie, in .xslx format. The absolute gravity of all base stations used in all of the loops (Section 4.4.3) is given in File: BaseStations, in .csv format.

The location of each gravity station (File: GPS_Location), as determined from the post-processed RTK GPS survey (Section 4.3), is given in.csv format, with station

number, Eastings and Northings in NAD83 (CSRS) UTM Zone 21N, and ellipsoid elevations in GSR80.

The re-projected DEMs used for the terrain correction processing (Section 4.4.4) are given in File: DEMs, in .grd format.

The final corrected gravity data collected during this study is given in File: PEEPgrav, in .xslx format.

The previously collected gravity databases, with new calculations (Section 4.4.6), are given in Files: 89Grav, 85Grav, and 64Grav, in .csv formats. The gravity stations removed from the above databases, as discussed in Section 4.4.6, are given in File: Removed_Stations, in .xlsx format.

A simplified composite gravity database of all stations used in final interpolation (Section 4.4.7) is given in File: Comp_Grav, in .xlsx format. The resulting composite interpolated composite complete Bouguer gravity grid, as discussed in Section 4.4.7, is given in File: Comp_Bouguer_Grav, in .grd format, and in GeoTIFF (.tif) format.

Appendix E – Aeromagnetic Data

The compilation aeromagnetic grids used for Maps C and D are given in .grd format and GeoTIFF (.tif) format in the folder Comp_Grids. Individual aeromagnetic surveys used in the derivation of the compilation aeromagnetic maps, with their designated Survey ID, Geofile number, and acquisition parameters is given as an .xslx file in the folder Surveys.